# INFORMATION TO USERS

UNIVERSITY OF ALBERTA

TRACE ANALYSIS OF PEPTIDES AND PROTEINS BY

CAPILLARY ELECTROPHORESIS

BY

Ⓒ

DEVANAND MICHAEL PINTO

A THESIS SUBMITTED TO THE FACULTY OF GRADUATE STUDIES AND

RESEARCH IN PARTIAL FULFILLMENT OF THE REQUIREMENTS FOR THE

DEGREE OF

DOCTOR OF PHILOSOPHY

DEPARTMENT OF CHEMISTRY

EDMONTON, ALBERTA

FALL 1998

Canada

University of Alberta

Library Release Form

Author of thesis: **Devanand Michael Pinto**

Title of thesis: **Trace analysis of peptides and proteins**
**By capillary electrophoresis**

Year this Degree Granted: **1998**
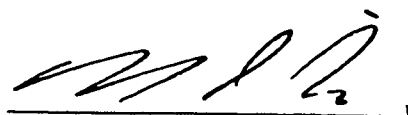
403-1991 Brunswick St.
Halifax NS B3J 2G9

August 28 1998
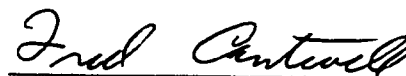
# UNIVERSITY OF ALBERTA

# FACULTY OF GRADUATE STUDIES AND RESEARCH

The undersigned certify that they have read, and recommend to the Faculty of Graduate Studies and Research for acceptance, a thesis entitled Trace Analysis of Peptides and Proteins by Capillary Electrophoresis submitted by Devanand Pinto in partial fulfillment for the degree of Doctor of Philosophy
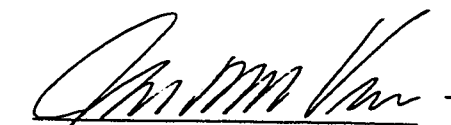
Dr. N. J. Dovichi

Dr. F. Cantwell
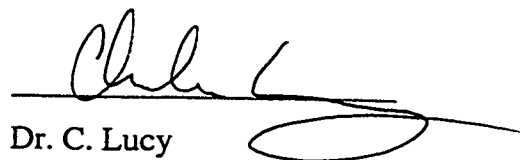
Dr. M. McDermott

Dr. J. Vederas

Dr. E. LeBlanc

Dr. C. Lucy

AUGUST 28/98

# ABSTRACT

The improvement of the detection limit is a fundamental goal of analytical chemistry. The recent achievement of a one-molecule mass detection limit in capillary electrophoresis (CE) is one instance where this goal appears to have been achieved. However, because of the small injection volume, the impressive mass detection limit of CE does not translate to concentration detection limits that are adequate for trace analysis.

This thesis presents methods that improve the concentration detection limit by using off-line and on-line concentration techniques. The first section introduces CE and presents methods for peptide analysis and the second section presents methods for protein analysis.

For peptides, two methods based on solid-phase extraction (SPE) are presented. In the first method, peptides are preconcentrated and fluorescently labelled on an SPE material and then analyzed by CE with laser-induced fluorescence (LIF) detection. This method provides nanomolar detection limits, a 1 000-fold improvement over UV absorbance detection. In the second method, peptides are preconcentrated using SPE and then analyzed by capillary isotachophoresis (CITP) with mass spectrometric (MS) detection. This method provides picomolar detection limits, an improvement of four orders of magnitude over standard CE-UV methods. SPE-CITP-MS analysis of peptides in human plasma is shown.

Proteins have many derivatizable groups; therefore, reactions between proteins and fluorescent dyes usually produce heterogeneously labelled samples. These

samples, when analyzed by CE, usually result in poor separation efficiency. This thesis presents the first application of protein labelling in which high separation efficiency is maintained. Detection limits in the in the mid-picomolar range and efficiencies of 180 000 theoretical plates are obtained. When the labelling is performed in the capillary and combined with on-capillary stacking, the separation efficiency rises to 350 000 theoretical plates and the detection limit decreases 15 fold.

These techniques bring the concentration detection limit of CE-LIF within the range required for real-world samples.

To my Mother and in memory of my Father

# TABLE OF CONTENTS

## LIST OF TABLES

# LIST OF FIGURES

CHAPTER 4

CHAPTER 5

# LIST OF ABBREVIATIONS

| | |
|---|---|
| APD | Avalanche photodiode |
| BSA | Bovine serum albumin |
| CE | Capillary electrophoresis |
| CITP | Capillary isotachophoresis |
| CZE | Capillary zone electrophoresis |
| DL | Detection Limit (S/N = 3) |
| DNA | Deoxyribonucleic acid |
| ELFSE | End-labelled free solution electrophoresis |
| EMMA | Electrophoretically mediated microchemical analysis |
| ESI | Electrospray ionization |
| FQ | 5-(furoyl)-3-benzoylcarboxyquinoline |
| LIF | Laser-induced fluorescence |
| MALDI | Matrix-assisted laser desorption and ionization |
| MECC | Micellar electrokinetic chromatography |
| MS | Mass spectrometry |
| OVA | Ovalbumin |
| PMT | photomultiplier tube |
| SDS | Sodium dodecyl sulphate |
| SIR | Selected ion recording |
| SPE | Solid phase extraction |
| TOAD | Thermo-optical absorbance detection |
| TOF-MS | Time-of-flight mass spectrometry |
| UV | Ultra violet |

# CHAPTER 1
# AN INTRODUCTION TO CAPILLARY ELECTROPHORESIS (CE)

## 1.1 GENERAL CHARACTERISTICS OF CE

In electrophoresis, a sample under the influence of an electric field separates into its various components. The separation takes places in a column, a capillary or a slab of gel. Column electrophoresis, while suitable for preparative electrophoresis, provides poor resolution and is not commonly used.[1] However, slab gel electrophoresis and capillary electrophoresis are common techniques for the analysis of biological molecules.

Slab gel electrophoresis (SGE), using cross-linked polyacrylamide, is a standard method for DNA sequencing and protein separation. In the case of protein separations, two orthogonal separations are performed on the same gel. This two-dimensional separation method provides sufficient resolution to analyze samples containing hundreds of proteins.

The gel is the source of the limitations of SGE; the technique is difficult to automate and the large volume of the gel limits the potential that can be applied. Higher potentials are desirable since they increase separation efficiency and throughput.

In contrast, CE occurs in capillaries whose inner diameters (i.d.) are a few tens of microns. The importance of the capillary dimensions to the success of CE cannot be overstated. The high surface to volume ratio of the capillary is essential to the efficient dissipation of the heat generated during the separation process. Consequently, high electric fields, which would cause excessive heating in SGE, can be used in CE. These

high electric fields provide for more efficient and more rapid separations than those obtained in SGE; CE separations are often completed within the span of a few seconds, and efficiencies of $10^6$ theoretical plates are often achieved. The small dimensions of the capillary also result in lower sample consumption; a typical injection volume is a few nanolitres. Consequently, the mass detection limit (the amount of sample that must be injected to produce a signal to noise ratio of 3) can be as low as one molecule.

While the small dimensions of the capillary provide rapid and efficient separations, they make trace analysis difficult. The small injection volume combined with the poor sensitivity of most detectors results in poor concentration detection limits. For example, UV absorbance, the most popular method of detection in CE, has mass detection limits in the order of $10^{10}$ molecules ($10^{-14}$ moles). If the injection volume is 25 nL, the corresponding concentration detection limit is approximately 0.1 $\mu M$, far from the sensitivity required for trace analysis.

There are two obvious strategies to improving the concentration detection limit of CE: increasing the amount of sample injected and increasing the detector sensitivity. Efforts to implement these strategies form the basis for this thesis.

Sample preconcentration and sample stacking increase the amount of sample injected. Sample preconcentration involves the reduction of the sample volume prior to injection. The success of the technique hinges on efficient sample handling. In stacking techniques, a large volume of sample is injected into the capillary and then the analytes are stacked into a narrow zone. The long initial plug must be converted into a narrow zone to provide a sensitive and efficient analysis.

2

The above methods will be discussed simultaneously with two high sensitivity detection methods; mass spectrometry (MS) and laser induced fluorescence (LIF) detection. Both techniques have higher sensitivity than UV absorbance detection but are more complex. The CE-MS instrument used here is commercially available and has been described elsewhere.[2,3,4] The CE-LIF instrument used is unique to this laboratory and is described later in this chapter.

1.2 BASIC INSTRUMENTATION

The simplicity of modern CE instrumentation is one of its major advantages. This simplicity is in contrast to the complexity of the first CE apparatus, the rotating tube apparatus described by Hjerten in 1958.[5] Figure 1.1 contains a schematic of the basic CE components. There are no moving parts nor are pumps or valves required. The instrument can be thought of in terms of the electrical circuit formed by its
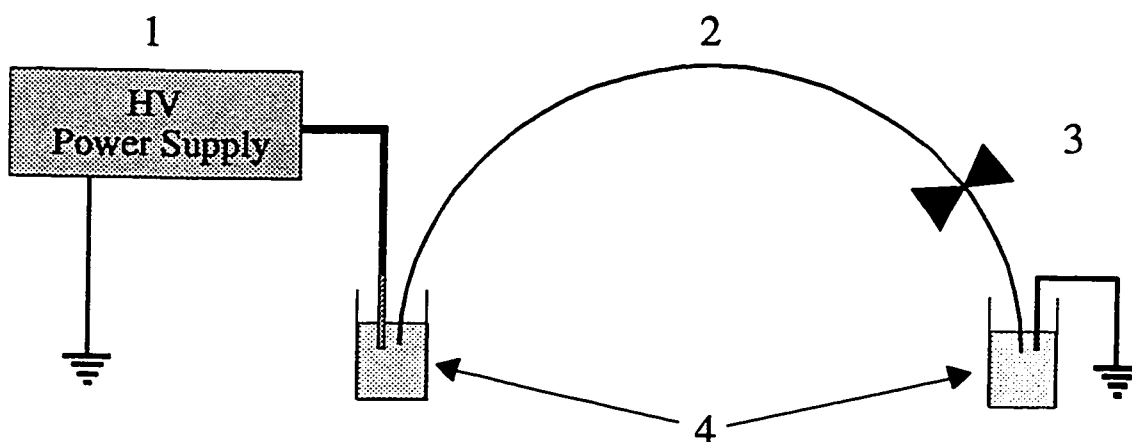


Figure 1.1 Basic CE components; (1) HV power supply with platinum electrode,

(2) separation capillary, (3) detector and (4) background electrolyte (BGE) reservoirs

components. The first component is the high voltage power supply with a platinum electrode. The electrode and the capillary inlet share a common background electrolyte (BGE) reservoir. The capillary is the second component of the circuit. The detector and the outlet BGE reservoir are the third and fourth components of the circuit respectively.

A typical CE experiment consists of an injection step followed by a separation step. A sample vial replaces the inlet reservoir during the injection step and a pressure or potential difference is placed across the capillary for a few seconds to inject the sample. After the injection, the sample vial is replaced with a BGE reservoir and the separation voltage is applied. The analytes separate as they migrate towards the detector.

The two modes of detection in CE are on-capillary detection, as depicted in figure 1.1, and post-capillary detection. On-capillary detectors are easier to construct and easier to operate since the capillary also serves as the detection cell. However, on-capillary detection is less sensitive than post-capillary detection. The majority of the data presented here is obtained using post-capillary detection.

## 1.3 BASIC PRINCIPLES OF CAPILLARY ZONE ELECTROPHORESIS (CZE)

The following equation defines the electrophoretic velocity ($v_{ep}$) of an analyte:

$$v_{ep} = \mu_{ep}E \qquad (1.1)$$

where $\mu_{ep}$ is the electrophoretic mobility in $m^2/V \cdot s$ and $E$ is the electric field in V/m, i.e. the applied voltage divided by the capillary length. The analyte's electrophoretic

4

mobility depends on its charge and the friction it experiences as it travels through the BGE. The convention used in this thesis defines migration towards the detector as positive and migration away from the detector as negative. Equation 1.1 is only valid in the absence of electroosmosis.

Electroosmosis is the bulk flow of liquid that occurs in the capillary.[6,7] An electrolyte flowing over a charged surface produces an electric potential, called a streaming potential. Conversely, a potential placed across a capillary filled with an electrolyte produces electroosmosis. The following equation defines the flow velocity ($v_{eo}$) due to electroosmosis:

$$v_{eo} = \mu_{eo}E = \frac{\varepsilon\zeta}{4\pi\eta}E \qquad (1.2)$$

where $\mu_{eo}$ is the electroosmotic mobility, $\varepsilon$ is the solution's dielectric constant, $\zeta$ is the potential at the capillary wall, $\eta$ is the solution viscosity and $E$ is the electric field. In the presence of electroosmotic flow (EOF), equation 1.1 becomes:

$$v = (\mu_{ep} + \mu_{eo})E \qquad (1.3)$$

$$v = (\mu_{ep} + \mu_{eo})\frac{V}{L} \qquad (1.3a)$$

where $V$ is the applied voltage and $L$ is the capillary length. Typical values of $\mu_{eo}$ and $E$ are $5 \times 10^{-8}$ $m^2/V{\cdot}s$ and 400 V/cm respectively, which results in a flow velocity of 2 mm/s.

5

Describing the electroosmotic mobility as a constant understates its importance; electroosmosis provides a flow of liquid eliminating the need for pumps. Electroosmosis also permits simultaneous analysis of cations and anions without changing the polarity of the applied potential. To illustrate this point, consider a sample made up of anionic and cationic components. The ions' velocities are determined by the sum of their electrophoretic and electroosmosis velocities. For cations, both velocities are toward the detector when a positive potential is applied at the inlet. However, in the case of the anions, the velocities are opposing. Therefore, an anion will only migrate towards the detector if its mobility satisfies the inequality, $|\mu_{ep}| < \mu_{eo}$. Fortunately, this is the usually the case.

In order for electroosmosis to occur, the capillary must be filled with an electrolyte and the inner surface of the capillary must be charged. Fused-silica capillaries, the type used in almost all CE applications, have silanol groups on their surface. These groups have varying acidities; therefore, the number of charged groups, and consequently the EOF, varies with the pH of the BGE. The EOF is also controlled by changing the viscosity of the BGE or by using additives that neutralize a portion of the charge on the capillary surface.

## 1.4 SEPARATION EFFICIENCY AND RESOLUTION IN CZE

Band broadening is the widening of the sample zones. Band broadening and zone separation occur simultaneously and their relative magnitudes determine the quality of the separation.

Diffusion and the initial sample width are the main sources of band broadening

in typical CZE separations. The variance in peak width due to diffusion ($\sigma_D^2$) is given

by Einstein's law of diffusion:

$$\sigma_D^2 = 2Dt_m \tag{1.4}$$

where D is the analyte's diffusion coefficient and $t_m$ is the migration time of the

analyte,

which the following equation defines;

$$t_m = \frac{L}{E(\mu_{ep} + \mu_{eo})} \tag{1.5}$$

By substituting equation 1.5 into equation 1.4 we obtain;

$$\sigma_D^2 = \frac{2DL}{(\mu_{ep} + \mu_{eo})E} = \frac{2DL^2}{(\mu_{ep} + \mu_{eo})V} \tag{1.6}$$

In CZE, broadening due to diffusion is unavoidable and is the main source of band

broadening under ideal conditions. In practice, broadening due to the initial plug

width, despite being avoidable, is often the dominant source of band broadening.

Equation 1.7 describes the variance in peak width due to initial plug width ($\sigma_{inj}^2$);

$$\sigma_{inj}^2 = \tau^2/12 \tag{1.7}$$

where $\tau$ is the length of the sample injected. These last two equations can be used to

calculate the separation efficiency (N);

$$N = \frac{L^2}{\sigma^2} = L^2 \left( \frac{2DL^2}{(\mu_{ep} + \mu_{eo})V} + \frac{\tau^2}{12} \right)^{-1} \qquad (1.8)$$

$$\approx \frac{(\mu_{ep} + \mu_{eo})V}{2D} \qquad (1.8a)$$

where $\Delta v$ is the difference in analyte mobility and $\overline{v}$ is the average analyte velocity.

For CZE, equation (1.8a) holds if the sample volume is less than 1% of the capillary volume. In practice, however, the insensitivity of the detector often necessitates a large injection volume.[8]

Equation 1.8 indicates that the efficiency increases with electroosmotic mobility. While this is true, efficiency is only one of the factors that affects resolution. Resolution is a more useful measure of the quality of a separation. A brief discussion on resolution demonstrates that high electroosmotic mobility actually degrades resolution. We start with the general equation for resolution of two analytes:

$$R = \sqrt{N} \; \frac{\Delta v}{4\overline{v}} \qquad (1.9)$$

If we substitute equations 1.8a and 1.3a into equation 1.9 we obtain;

$$R = 0.18 \sqrt{\frac{V}{D}} \; \frac{\Delta\mu_{ep}}{\sqrt{(\overline{\mu_{ep}} + \mu_{eo})}} \qquad (1.10)$$

where $\Delta\mu_{ep}$ is the difference in the analytes' electrophoretic mobilities and $\overline{\mu_{ep}}$ is the average electrophoretic mobility.

Equation 1.10 shows that the resolution increases as electroosmosis decreases, at the cost of an increase in analysis time. Equation 1.10 also demonstrates that the resolution increases with the root of the applied voltage. However, band broadening due to Joule heating begins to degrade the resolution at high electric fields. Joule heating is discussed below.

Band broadening due to electromigration dispersion, analyte-wall interactions or Joule heating is occasionally encountered. For completeness, these sources of band broadening are discussed below:

(i)   Differences in mobility between the analyte and the BGE cause band broadening due to electromigration dispersion.[9] Analytes with a lower mobility than the BGE display tailing and analytes with a higher mobility than the BGE will front. Ensuring that the ionic strength of the BGE is at least 100 times higher than the ionic strength of the sample eliminates this source of band broadening. Typical BGE concentrations are greater than $10^{-2}M$ so band broadening due to electromigration dispersion is usually negligible.

(ii)   Proteins, peptides and other analytes possessing cationic moieties are prone to band broadening due to analyte-wall interactions. This is especially true when fused-silica capillaries are used. These capillaries have fixed negative charges that interact with the analytes' basic moieties. Coating the inner surface of the capillary with neutral or cationic materials reduces this interaction.[10,11]

(iii)     As in most electrical circuits, the flow of current through the capillary

generates heat. The power generated during electrophoresis is given by the following

equation:

$$P = EI/S = I^2/\kappa S \qquad (1.11)$$

Where $P$ is the power in W/m$^3$, S is the capillary cross-section in m$^2$, $I$ is the current, $E$

is the electric field and $\kappa$ is the conductivity of the BGE in $\Omega^{-1}$. The capillary wall

dissipates heat efficiently; therefore, the BGE at the capillary wall remains cool

relative to the BGE in the center of the capillary. This temperature gradient results in a

gradient in solution viscosity. Analytes in the lower viscosity region experience less

friction than analytes in the higher velocity region. This difference in velocity leads to

band broadening. The amount of band broadening due to Joule heating is only

significant when the current is high. A high current results from the use of a high ionic

strength BGE, a large i.d. capillary or a high electric field.

As mentioned above, the poor sensitivity of UV absorbance detection

necessitates the use of large injection volumes. In these cases, the separation

efficiency is well below the efficiency obtained under ideal conditions. However, high

sensitivity detection methods allow for the use of small injection volumes thereby

providing high efficiency. Laser induced fluorescence is such a method and is the

detection method used for the majority of the work presented. Therefore, a brief

description of LIF detection is warranted.

## 1.5 LASER-INDUCED FLUORESCENCE DETECTION

Laser-induced fluorescence detection (LIF) is the most sensitive detection method available for capillary electrophoresis. In our laboratory, we have achieved detection limits of one molecule using an LIF detector based on a sheath flow cuvette.[12-15] The optics are designed to collect as much sample fluorescence as possible and reject as much background light as possible.

Figure 1.2 contains the basic components of LIF detector used here. The most important component of the detector is the sheath flow cuvette. A comparison with on-capillary LIF detection demonstrates the advantage of the sheath flow cuvette over other detection methods. In on-capillary detection, the capillary serves as the detection cell. This arrangement is rugged and uncomplicated but the capillary is not an optimal detection cell. The reason for this is simple; the change in refractive index at the capillary/buffer interface produces a large amount of light scatter. The scattered light is responsible for the majority of the noise encountered in on-capillary fluorescence detection. The sheath flow cuvette eliminates this source of scattered light by surrounding the capillary eluent with a sheath fluid of equal refractive index. The major source of noise is light scattering from the solvent, which is significantly less than the light scatter found in on-capillary detection.

Of course, there is still a change in refractive index at the cuvette/sheath fluid interface. However, unlike on-capillary detection, this region of light scatter is far
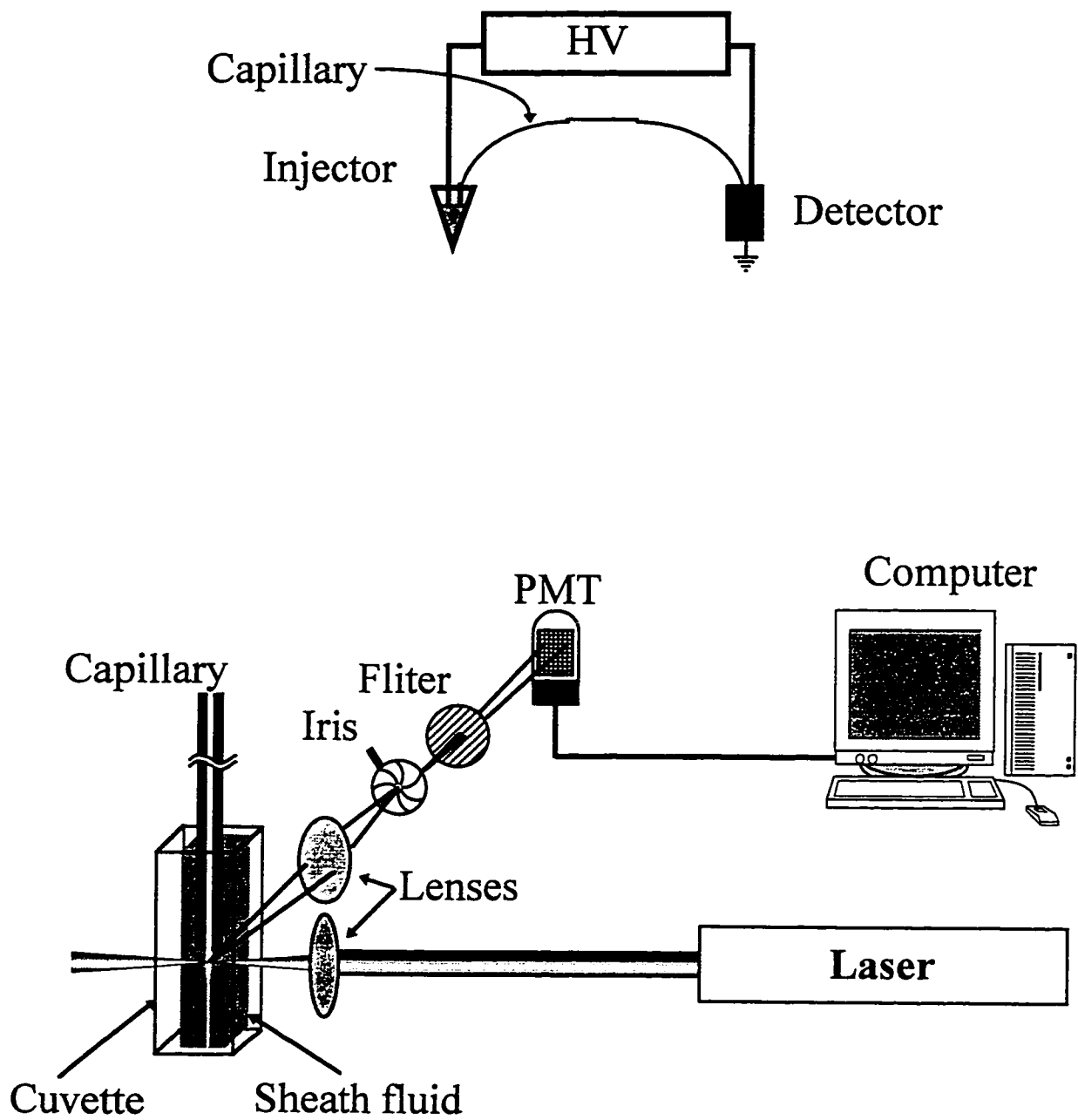
Figure 1.2 Schematic of the laser induced fluorescence detector

removed from the analyte fluorescence region and is easily discriminated from the fluorescence using confocal collection optics.

There are two focusing operations in confocal optics, the focusing of the excitation beam onto the sample and the focusing of the emission onto a point detector. This dual arrangement provides for optimal spatial resolution. However, in the case of the sheath flow cuvette the conditions of confocal optics are relaxed to maximise the S/N ratio obtained. This is achieved by matching the size of the excitation beam to the size of the capillary eluent, and by setting the detector aperture to the size of the fluorescence image. This arrangement is still able to discriminate between the analyte fluorescence and

the scatter at the cuvette/sheath liquid interface.

However, confocal optics are unable to discriminate from scatter originating in the same region as the analyte. Since this scatter is usually at a different wavelength than the analyte fluorescence it can be removed using a bandpass filter. The filter does pass 1 part in $10^6$ of light at the wavelengths it is designed to block. This scatter is the main source of noise in the LIF detector. Specifically, the shot noise from the scattered light limits the detection sensitivity.

## 1.6 THESIS SUMMARY

The next four chapters present high sensitivity techniques for the analysis of peptides and proteins.

The method presented in chapter 2 makes use of LIF detection to analyze trace amounts of insulin chain B. The key to the success of the technique is the use of a solid phase to preconcentrate the analyte and separate the labelled peptide from the interfering reaction products.

Chapter 3 also makes use of a solid phase to preconcentrate peptides followed by on-capillary sample enrichment. These two techniques each increase the sample concentration 100 fold, for a total increase in sensitivity of $10^4$. In this chapter, MS detection and MS-MS detection is used.

Chapters 4 and 5 present methods for the analysis of proteins using CE with LIF detection. These methods are the first labelling methods developed that provide both high sensitivity and high efficiency. In the first method, the proteins are labelled and then separated using an anionic surfactant as an ion-pairing reagent. In the second method, the capillary itself serves as the reaction vessel. The use of improved reaction conditions and on-capillary stacking provides higher sensitivity than the pre-capillary method.

All the methods in this thesis provide sensitivity that is orders of magnitude higher than the sensitivity provided by standard CE methods. The former methods provide sufficient sensitivity for the analysis of biological samples.

# References

[1] Porath, L., *Ark. Khim.*, 11, 1957, 259.

[2] Pleasance, S., Thibault, P. and Kelly, J., *J. Chromatogr.*, 591, 1992, 325-339.

[3] Olivares, J. A., Nguyen, N. T., Yonker, C. R. and Smith, R. D., *Anal. Chem.*, 59, 1987, 1232-1236.

[4] Kelly, J. F., Ramaley, L. and Thibault, P., *Anal. Chem.*, 69, 1997, 51-60.

[5] Hjerten, S., *Arkiv. Kemi*, 13, 1958, 151-157.

[6] Hjerten, S., *Chromatogr. Rev.* 9, 1967, 122-219.

[7] Kuhr, W. G. and Monnig, C.A., *Anal. Chem.*, 64, 1992, 389R-407R.

[8] Delinger, S. L. and Davis, J. M., *Anal. Chem.*, 64, 1992, 1947-1959.

[9] Mikkers, F. E. P., Everaerts, F. M. and Verheggen, P. E. M., *J. Chromatogr.*, 169, 1970, 1.

[10] Cobb, K. A., Dolnik, V and Novotny, M., *Anal. Chem.*, 62, 1990, 2478-2483.

[11] Huang, M., Vorkink, W. P. and Lee, M. L., *J. Microcol. Sep.*, 4, 1990, 233-238.

[12] Chen, Y-F and Dovichi, N. J., *SPIE*, 910, 1988, 112-114

[13] Dovichi, N. J., *Trends in Anal. Chem.*, 3, 1991, 55-7

[14] Zarrin, F. and Dovichi, N. J., *Anal. Chem.*, 59, 1987, 846-850.

[15] Chen, D. Y. and Dovichi, N. J., *J. Chromatogr. B*, 657, 1994, 265-269.

# CHAPTER 2

## PEPTIDE ANALYSIS BY SOLID-PHASE LABELLING AND CE-LIF

### 2.1 INTRODUCTION

Peptide separation and purification is traditionally performed by ion exchange chromatography, gel filtration, SDS-PAGE electrophoresis, or HPLC.[1] Detection methods are based on colorimetry (the ninhydrin reaction), UV absorbance, refractive index, optical rotation, mass spectrometry, and fluorescence. In most cases, these methods can detect peptides in the micromolar range.[2] Detection methods based on antigen-antibody interaction can detect as little as $10^{-15}$ moles. These methods are specific to one peptide making multiple peptide analysis difficult. In most cases, peptides of physiological importance are present at trace levels and in complex matrices. Therefore, peptide determinations often require large sample volumes and extensive sample purification.

An alternative technique for the analysis of peptides is capillary electrophoresis (CE) with laser induced fluorescence (LIF) detection. CE provides high separation efficiency and LIF detection provides high sensitivity. LIF detection provides signal-to-noise ratios that are at least 100 times greater than those obtained in UV absorbance detection.[3] Unfortunately, sample derivatization is necessary for most peptides. Native fluorescence is possible for peptides containing tryptophan, phenylalanine or tyrosine, however, the sensitivity is far from that required for trace analysis.[4-6] Another approach to the analysis of dilute peptide solutions is the use of concentration techniques. These techniques include on-column sample stacking, and isotachophoretic preconcentration.[3]

Sample derivatization often involves the use of a labeling reagent that reacts with the peptide's amino group to form a fluorescent derivative. Labeling reagents such as fluorescein

isothiocyanate and 5-carboxytetramethylrhodamine succinimidyl ester are common examples. Their use provides mass detection limits in the zeptomole range or lower for fluorescently labelled biological molecules (1 zeptomole = $10^{-21}$ moles).[7,8] These reagents require a high concentration of the labeling reagent ($10^{-2}$ to $10^{-4}$ M), and a high concentration of peptide ($10^{-3}$ to $10^{-6}$ M). The excess derivatizing reagent interferes with the signal from the derivatized peptide; therefore, these dyes are useful for preparing fluorescent biological substrates and probes but are often not suitable for derivatization at trace levels.

Another limitation to fluorescent labelling for CE is that only a few nanolitres of the sample is injected whereas a few microliters of sample are required for labeling. Clearly, the main obstacle in applying CE-LIF to trace analysis of peptides is the development of an efficient labeling method. [3,9,10]

An alternative to traditional fluorescence labeling is the use of fluorogenic reagents. Fluorogenic reagents do not fluoresce *per se*, but form fluorescent products when they react with the analyte's primary amino group. As with the fluorescent reagents mentioned earlier, fluorogenic reagent must also be present at high concentrations. Unfortunately, fluorogenic reagents also react with species other than the analyte to form secondary fluorescent products whose peaks may overlap with the peaks of interest.[10] Fluorogenic reagents have been used in the analysis of amino acids, peptides, and aminated sugars.[11-16]

This chapter describes a method for handling small volumes of dilute peptides solutions using membrane preconcentration followed by derivatization with a fluorogenic reagent. Figure 1 shows the steps used to analyze dilute solutions of peptides. An aqueous peptide solution passes over a cationic membrane and the membrane binds peptides through a combination of electrostatic and hydrophobic interactions. The fluorogenic reagent, 3-(2-furoyl)quinoline-2-
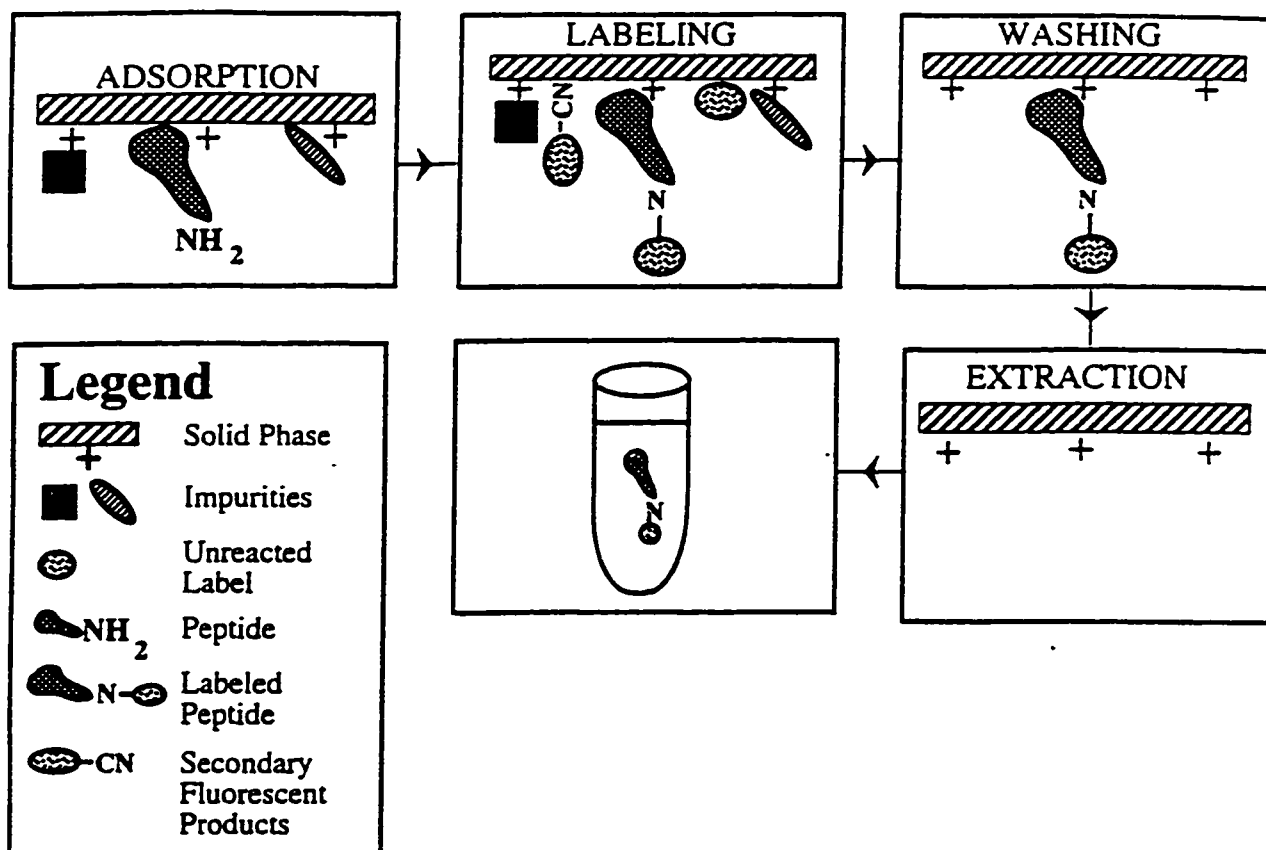
Figure 2.1: Pictorial representation of peptide labeling on Immobilon CD Membrane. The peptide is first adsorbed onto the membrane. The labeling reagents are then added to the membrane, and after the reaction, the impurities as well as any other reaction by-products are washed off the membrane. Finally the labeled peptide is extracted from the membrane.

18

carboxaldehyde (FQ), and cyanide ions react with the peptides to form a fluorescent FQ-peptide derivative.[15] The membrane is washed to eliminate secondary fluorescent products. Finally, the labeled peptide is extracted from the membrane and analyzed by CE with LIF detection. Insulin chain B (Ins B) is used as the test peptide and is labeled and detected at concentrations as low as $10^{-8}$ M.

## 2.2 EXPERIMENTAL

### 2.2.1 Materials

HPLC grade methanol and acetone were supplied by Aldrich (Milwaukee, WI). Biobrene-treated fiber disks were supplied by Applied Biosystems (Foster City, CA). Analytical grade acetic acid, n-propanol, dimethylsulfoxide (DMSO), ammonium hydroxide, sodium dodecyl sulfate (SDS) and disodium tetraborate were supplied by BDH (Toronto, ON). Analytical grade chloroform was obtained from Fisher Scientific (Nepean, ON). Immobilon CD, DEAE Ultra-free filters, and Sequelon AA were provided by Millipore (Bedford, MA). Potassium cyanide and 3-(2-furoyl)quinoline-2-carboxaldehyde (FQ) were obtained from Molecular Probes (Eugene, OR). Bovine oxidized insulin chain B (Ins B) was obtained from Sigma (St. Louis, MO).

A stock solution of $1 \times 10^{-2}$ M Ins B was prepared in 0.1 M $NH_4OH$. Aliquots of the stock solution were dried in a SC110 Speed Vac (Savant Instruments Inc., Farmingdale, NY) and stored at -20 °C. Stock solutions of FQ and potassium cyanide were prepared in methanol. BS buffer (pH 9.4) consisted of 10 mM disodium tetraborate and 10 mM SDS. Acidified BS buffer (pH 5.3) was prepared by adding 50% v/v acetic acid to BS buffer until pH 5.3 was reached.

## 2.2.2 Liquid-phase labeling reaction

Fresh dilutions ($10^{-3}$ to $10^{-6}$ M) of Ins B in 0.1 M NH4OH were prepared before each experiment. A 5-µl aliquot of the Ins B was mixed with 5 µl of 5 mM KCN. To the above mixture, 10 µl of 10 mM FQ was added, mixed and allowed to react at room temperature for one hour. Blanks were prepared using 5 µl of 0.1 M $NH_4OH$ instead of Ins B. The reaction was stopped by diluting the mixture with pH 9.4 BS buffer. The dilution was analyzed by MECC-LIF.

## 2.2.3 Solid-phase labeling reaction

After a preliminary evaluation of the compatibility and ease of the labeling reaction on several solid supports (Polybrene, DEAE and Sequelon AA), Immobilon CD was selected. The Immobilon CD membrane was cut into a wedge shape measuring 10-mm by 2-mm, similar in shape to a slice of pizza, and inserted into a 200 µl pipette tip (Fisher Scientific, Nepean, ON) to form a cone at the end of the tip. We refer to this design as the solid-phase reactor. A P2 or a P20 Gilson Pipetman (Mandel Scientific Co. Ltd., Guelph, ON) was used to load into and expel the different reagents from the solid-phase reactor. With the solid-phase reactor attached to the pipettor, reagents could be delivered in accurate and precise volumes without direct handling of the membrane. During waiting periods, the solid-phase reactor was placed in a pipette tip rack.

Once the solid-phase reactor had been constructed, the labeling reaction was performed. First, the membrane was wetted with 20 µl of distilled water and then with 20 µl of methanol. The solvents were pipetted and allowed to soak the membrane for 5 minutes and then expelled. Then 5 µl of an Ins B dilution ($10^{-3}$ to $10^{-6}$ M) containing 5 mM potassium cyanide was pipetted and allowed to stand for 10 minutes. To deliver the FQ, the solid-phase reactor was removed from the pipettor and a 10 µl aliquot of 10 mM FQ solution was added through the top to prevent contamination of the FQ stock solution. The reaction proceeded at room temperature for one hour. Midway through the reaction, 5-10 µl of methanol was added through the top to prevent drying of the membrane.

This procedure was used for Ins B concentrations ranging from $10^{-3}$ to $10^{-6}$ M. The sample volume was increased to 100 μl for the analysis of $10^{-7}$ M InsB and the sample was taken up and expelled ten times. In the case of the analysis of $10^{-8}$ M Ins B, the sample volume was 1 mL. However, the volume of the solid-phase reactor was only 200 μl; therefore, a 100-μl aliquot of the sample was pipetted and then expelled into a second vial until the entire 1-ml sample was used. This procedure was done twice, so that the entire sample was passed through the solid-phase reactor twice. In addition, for the analysis of $10^{-8}$ M Ins B, the solid-phase reactor was made up of approximately 20 circular pieces (3-5 mm diameter) of Immobilon CD. The reasons for these variations in procedure will be explained in results and discussion.

Impurities and unreacted FQ were washed away by pipetting 25 μl from 500 μl of the washing solvent and expelling it back into the same vial. This cycle was repeated ten times. Using this procedure, DMSO, methanol, n-propanol, chloroform, and acetone were evaluated as potential wash solvents. The labeled peptide was extracted with 50 μl of acidified BS buffer (pH 5.3) or BS buffer (pH 9.4). The extraction was accomplished by pipetting and expelling 25 μl of the acidified BS buffer from the same vial ten times. The extracts were analyzed by MECC-LIF.

## 2.2.4 CE separation

The CE-LIF instrument used has been described in chapter 1 and elsewhere.[17] An argon-ion laser provided excitation at 488 nm, (Model 2211-55SL, Uniphase, San Jose, CA). A 630DF55 (Omega Optical, Brattleboro, VT) bandpass filter was chosen for the detector. Separations were conducted in a 50-cm long, 30-μm i.d., 150-μm o.d. capillary (Polymicro Technologies, Phoenix, AZ) at 400 V/cm. The running buffer was BS buffer (pH 9.4).

## 2.3 RESULTS AND DISCUSSION

### 2.3.1 Liquid-phase labeling reaction

Figure 2.2 contains an electropherogram resulting from a typical liquid-phase labeling reaction. The concentration of InsB was $10^{-3}$. The FQ-Ins B derivative has an efficiency of 4.6 x $10^6$ plates and a migration time of 454.1 sec (the efficiency is defined as 5.54 x $(t_R/FWHM)^2$ where $t_R$ is the migration time and FWHM is the full width at half maximum). Secondary fluorescent products, possibly from the reaction between FQ and cyanide, produce the other peaks in the electropherogram.[10] The mass limit of detection (3 times the standard deviation of the background) for the FQ-Ins B derivative is 2.4 x $10^{-21}$ zeptomoles. This calculation assumes that 100% of Ins B has been labeled.[18] The aqueous labeling reaction is suitable for Ins B concentrations between $10^{-3}$ M and $10^{-6}$ M.

The liquid-phase labeling reaction is unsatisfactory at low peptide concentrations. Figure 3 shows an electropherogram for the labeling of $10^{-6}$ M Ins B (trace A) and a blank (trace B). The blank was diluted 10-fold prior to injection while the sample was diluted five fold. Dilution is necessary to prevent saturation of the detector. The lower dilution factor for the sample was necessary in order to maximize the FQ-Ins B derivative (peak 4). The secondary fluorescent products are the major peaks in both electropherograms. There are two obvious differences between the secondary fluorescent product peaks in electropherograms A and B; the secondary fluorescent product peaks have different migration times and different relative heights. Different migration times could result from overloading of the capillary and different compositions in the sample and blank. In figure 3, the sample contains 19% methanol while the blank contains 7.5% methanol. The difference in the relative peak height of the secondary fluorescent products has been observed previously for a labeling reaction with a similar fluorogenic reagent, 3-(p-carboxybenzoyl)quinoline-2-carboxaldehyde.[10] The different relative peak heights result from different rates of the secondary reactions in the presence or absence of primary amino groups.
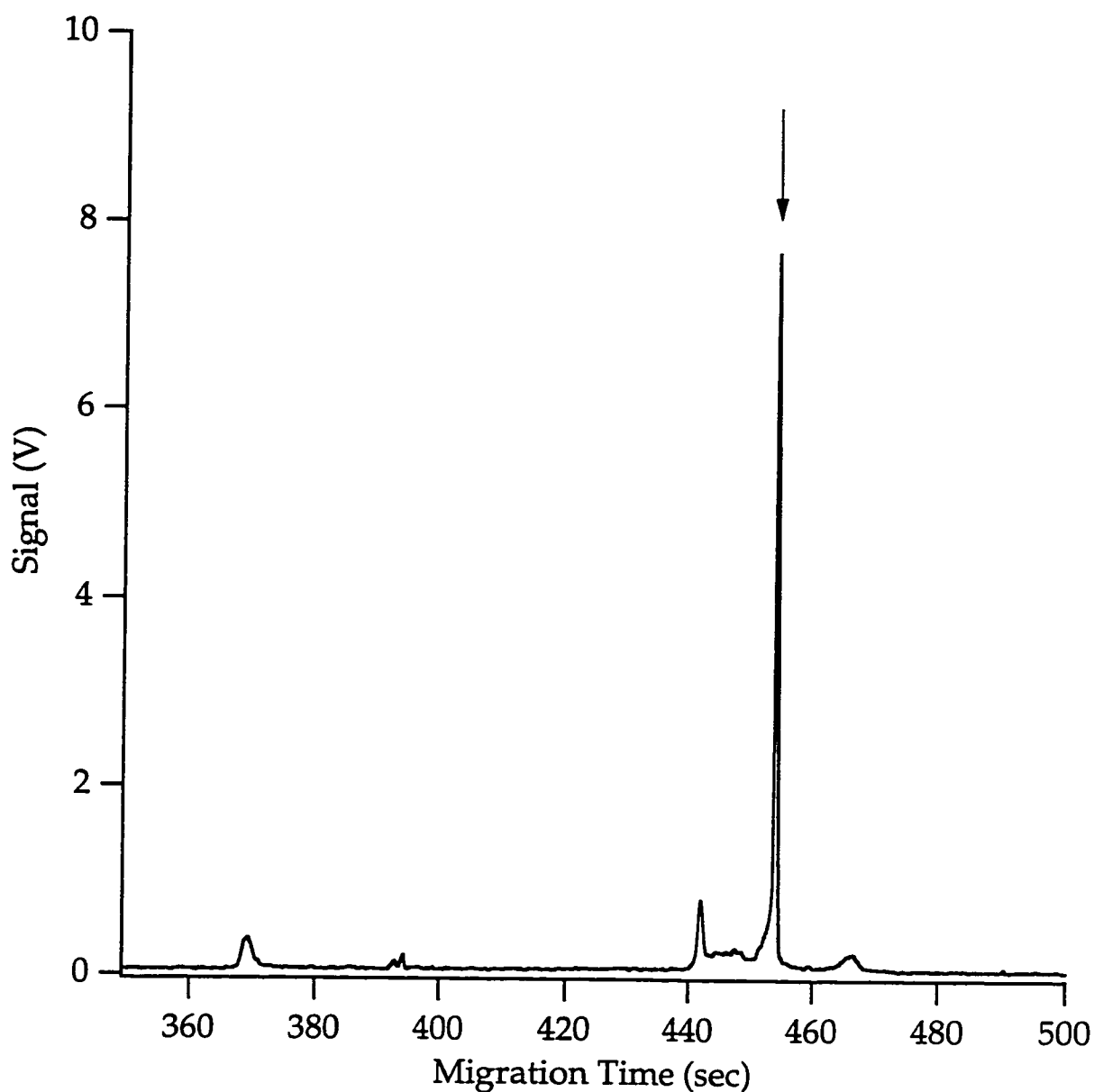
Figure 2.2 - Electropherogram of liquid-phase labeling of Ins B with FQ.

The peak corresponding to FQ-Ins B derivative is indicated by the arrow. Rxn conditions:

5 μl of 1 x 10-3 M Ins B, 5 μl of 5 mM KCN and 10 μl of 10 mM FQ; reaction time,

1 hr at room temperature; sample was diluted 1:100 in BS buffer (pH 9.4) prior to

injection. Separation conditions: 30 μm x 50 cm capillary; running buffer, BS buffer

(pH 9.4); injection 5 s at 5 kV, applied voltage, 20 kV (400 V/cm).

23
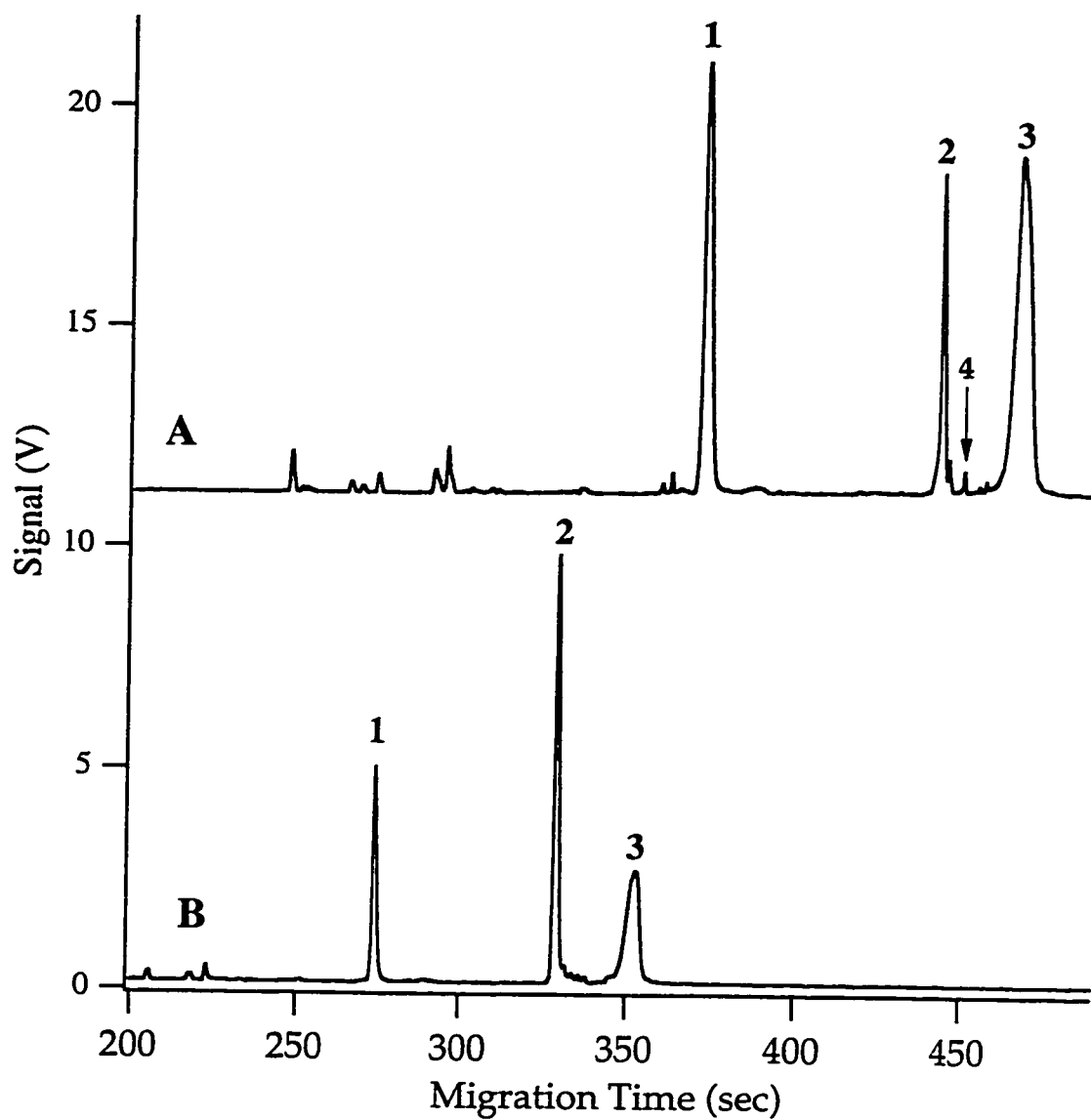
Figure 2.3 - Electropherogram of liquid-phase labeling of Ins B with FQ.

Reaction conditions: (A) sample; same as Fig. 2.1 except [Ins B] = 10-6 M. (B) blank; same as (A) except 5 μl of 0.1 M NH4OH used in place of Ins B. Peak identification: peaks 1, 2 and 3 are due to fluorescent secondary products, peak 4 is the FQ-Ins B derivative. Separation conditions: same as Fig. 2.2 except injection was 5 s at 20 kV.

24

We were fortunate that none of the peaks of the secondary fluorescent products directly overlapped the peak for the FQ-Ins B derivative. Clearly, in the case of other FQ-peptide derivatives, there is great potential for overlap with secondary fluorescent products, not to mention the potential for overlaps when mixtures of peptides are analyzed.

## 2.3.2 Selection of a membrane for solid-phase-labeling

A membrane used in solid-phase labeling must have a high affinity for peptides, a low affinity for both unreacted reagents and reaction impurities, a high recovery of peptides, as well as mechanical and chemical stability. Polybrene showed poor stability and its use resulted in broad background variations. DEAE did not exhibit sufficient affinity for Ins B. Sequelon AA forms a covalent bond with the carboxylic end of the peptide making recovery of the peptide virtually impossible. Furthermore, Sequelon AA reacts with FQ. Immobilon CD was selected because its properties closely matched the selection criteria. Immobilon CD is a cationic membrane that binds peptides via electrostatic and hydrophobic interactions. This membrane has been used in Western blot analysis and in protein sequencing analysis.[19,20]

## 2.3.3 Elimination of unwanted fluorescent products

The efficacy of DMSO, methanol, n-propanol, acetone, and chloroform to eliminate unwanted fluorescent products was evaluated. DMSO and methanol provided the best results. Methanol and DMSO were further evaluated for such parameters as the volume required for an effective wash and the number of cycles required to eliminate fluorescent peaks. Performing the washes in ten-cycle sets, with each set performed in a fresh vial of solvent, minimized the possibility of saturating the washing solvent. More than ten cycles or the use of fresh solvent did not improve the elimination of the blank peaks. Another point to consider in selecting an effective washing solvent is its inability to remove peptide from the membrane. The FQ-InsB signal was 1.80 ± 0.08 V, n = 3 for methanol versus 0.92 ± 0.18 V, n = 3 for DMSO. Thus, methanol was selected as the washing solvent.

## 2.3.4 Extraction of FQ-Ins B derivative from Immobilon CD

BS and acidified BS buffer efficiently extract the FQ-Ins B derivative from Immobilon CD. However, there is an interesting effect of using low-pH extraction buffers combined with a separation using a high-pH running buffer. Trace A in figure 2.4 shows an electropherogram of an extraction of Ins B from the solid-phase reactor using acidified BS buffer. Trace B shows the electropherogram of an extraction using BS buffer. The peak heights for FQ-Ins B derivative are 1.57 V and 0.21 V for acidified BS buffer (pH 5.3) and BS buffer (pH 9.4) respectively. The number of theoretical plates are $(5.1 \pm 0.7) \times 10^6$ and $(0.18 \pm 0.01) \times 10^6$ respectively. Thus, acidified BS buffer was chosen for the extraction procedure.

The higher signal and higher efficiency obtained when injecting a sample in acidified BS buffer is due to focusing of the FQ-Ins B derivative in the injection buffer/running buffer interface region. This effect has been reported previously for other peptides.[21] The sample plug has a lower pH than the running buffer; therefore, the derivative is positively charged while it is in the acidified BS buffer and has a relatively high mobility compared to when the derivative is in the higher pH running buffer. This causes the derivative to accumulate in the narrow interface region between the two buffer zones. The result is an extremely sharp sample zone and very high efficiency, up to $(20 \pm 3) \times 10^6$ theoretical plates. Eventually, this zone dissipates and the separation continues under CE conditions.[22]

## 2.3.5 Liquid-phase labeling reaction versus solid-phase labeling reaction

There are many advantages to using a membrane for the labeling reaction, the most obvious being the cleaner electropherograms obtained. Figure 2.5 shows an FQ-Ins B derivative peak resulting from a liquid-phase labeling reaction (trace A) and the solid-phase labeling reaction (trace B). The initial Ins B concentration was $1 \times 10^{-6}$ M for both cases. There is a complex
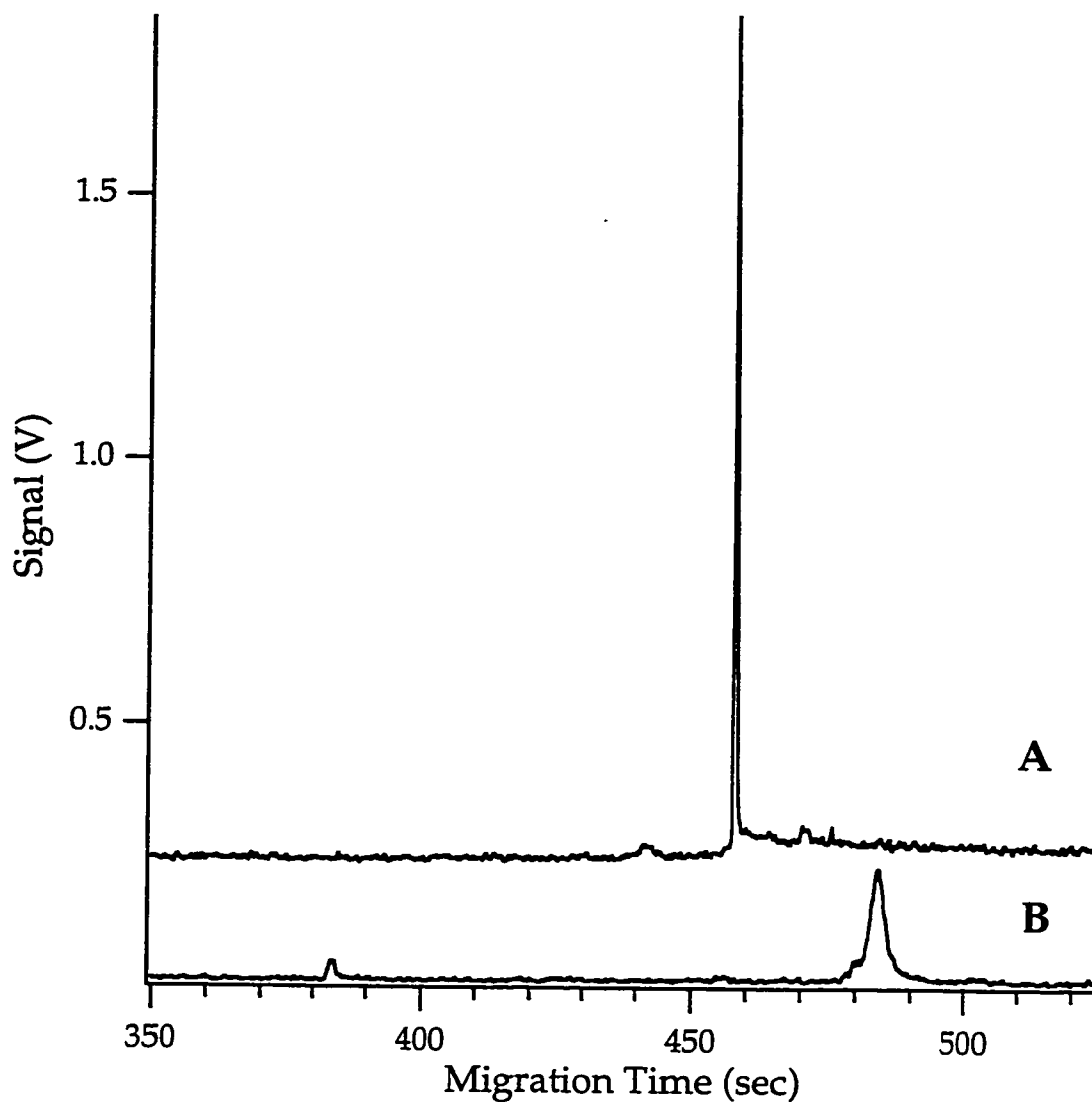
Figure 2.4 - Electropherograms of FQ-Ins B derivative injected from different sample buffers. Reaction conditions: same as Fig. 2.2, except samples were diluted 1:100 in either (A) acidified BS buffer (pH 5.3) or (B) BS buffer (pH 9.4) prior to injection. Separation conditions: same as Fig. 2.2, except injection; 5 s at 2 kV.

27
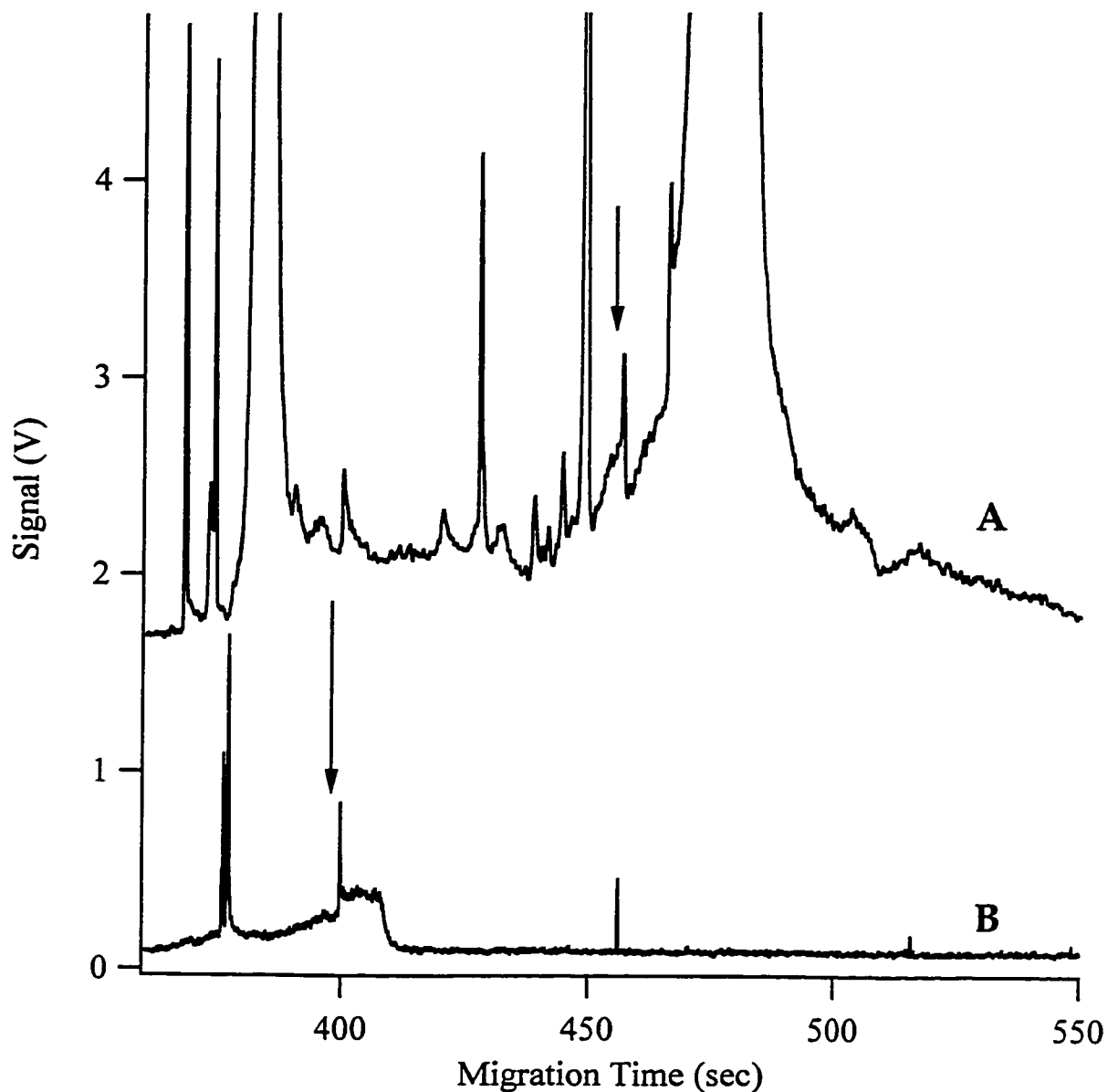
Figure 2.5 - Electropherograms of (A) liquid-phase and (B) solid-phase
labeling reactions of 10-6 M Ins B. Liquid-phase labeling reaction conditions; same as
Fig. 2, except [Ins B] = 10-6 M. Solid-phase labeling reaction conditions: 5 μl of Ins B
containing 5 mM cyanide pipetted into the solid-phase reactor followed by pipetting 10 μl
of 10 mM FQ. Washes, 10 x 25 μl of methanol; extraction, 25 μl of acidified BS buffer.
Separation conditions: same as Fig. 2 except injection was 5 s at 10 kV. FQ-Ins B derivative
peaks indicated by arrows.

28

background due to the presence of secondary fluorescent products in the electropherogram of the liquid-phase labeling reaction products. However, the secondary fluorescent products are almost completely eliminated in the case of the solid-phase reactor. Also, in the case of the solid-phase reactor, the residual methanol is expelled prior to the extraction of and does not interfere with the separation. Therefore, the solid-phase reactor allows us to produce electropherograms in which the potential overlap of sample and secondary fluorescent product peaks is minimized. In addition, detector saturation and contamination of the capillary is avoided by removing the high levels of secondary fluorescent products.

A further advantage to the use of the solid-phase reactor is the extension of the concentration range of samples that can be analyzed. Figure 2.6 shows the Ins B concentration range that can be analyzed using the solid-phase reactor. The fluorescent signal is normalized to standard injection conditions (5 sec @ 1000 V) and corrected for differences in sample dilution factors. The plot shows linearity between the log of signal and the log of [Ins B], (slope = 0.81 ± 0.08; $r^2$ = 0.98; n= 6). The RSD in peak height for the determination for Ins B at $10^{-5}$ M is 15%. By using the standard liquid-phase labeling approach, we could only label Ins B samples in the range of $10^{-3}$ to $10^{-6}$ M, while by using the solid-phase reactor, we are able to extend that range to $10^{-8}$ M.

2.3.6 Preconcentration of diluted peptide solutions

While Ins B concentrations down to $10^{-7}$ M can be easily labeled using the solid-phase reactor, this technique fails as the concentration drops below $10^{-7}$ M. An improvement in the design of the solid-phase reactor is required to allow us to analyze sample at or below concentrations of $10^{-8}$ M. Since the efficiency of the peptide transfer from the solvent to the membrane will increase with increased membrane surface area, it was found that by packing approximately 20 circular pieces (3-5 mm diameter) of Immobilon CD into a pipette tip, an efficient solid-phase reactor for the analysis of dilute solutions could be prepared. By using this new design for the solid-phase reactor, we could analyze 1 x $10^{-8}$ M Ins B samples, figure 2.7.
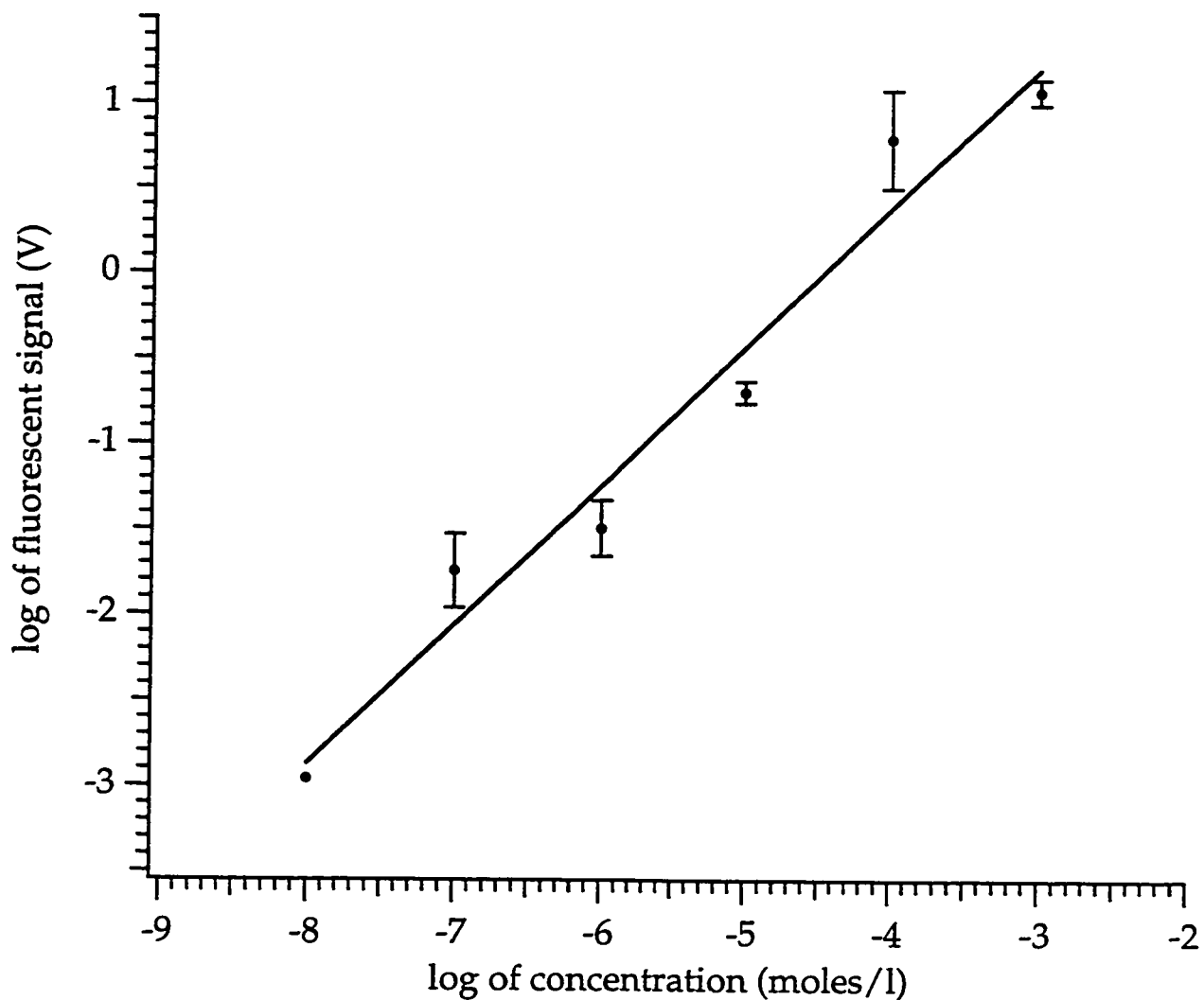
Figure 2.6 - Normalized fluorescent signals for the various dilutions of Ins B.

Solid-phase labeling reaction conditions. For 1 mM to 10 μ M Ins B same as Fig. 5; for

100 nM and 10 nM, preconcentration of 100 μl and 1 ml respectively was necessary.

Separation conditions: same as Fig. 2.2 except injections, all were for 5 s at 1 kV to 20 kV

depending on concentration. Amounts injected are not proportional to the injection electric

field for a sample in acidified BS buffer; a calibration curve based on one reaction mixture

injected at different voltages was used to normalize amounts injected to 1 kV (20 V/cm).
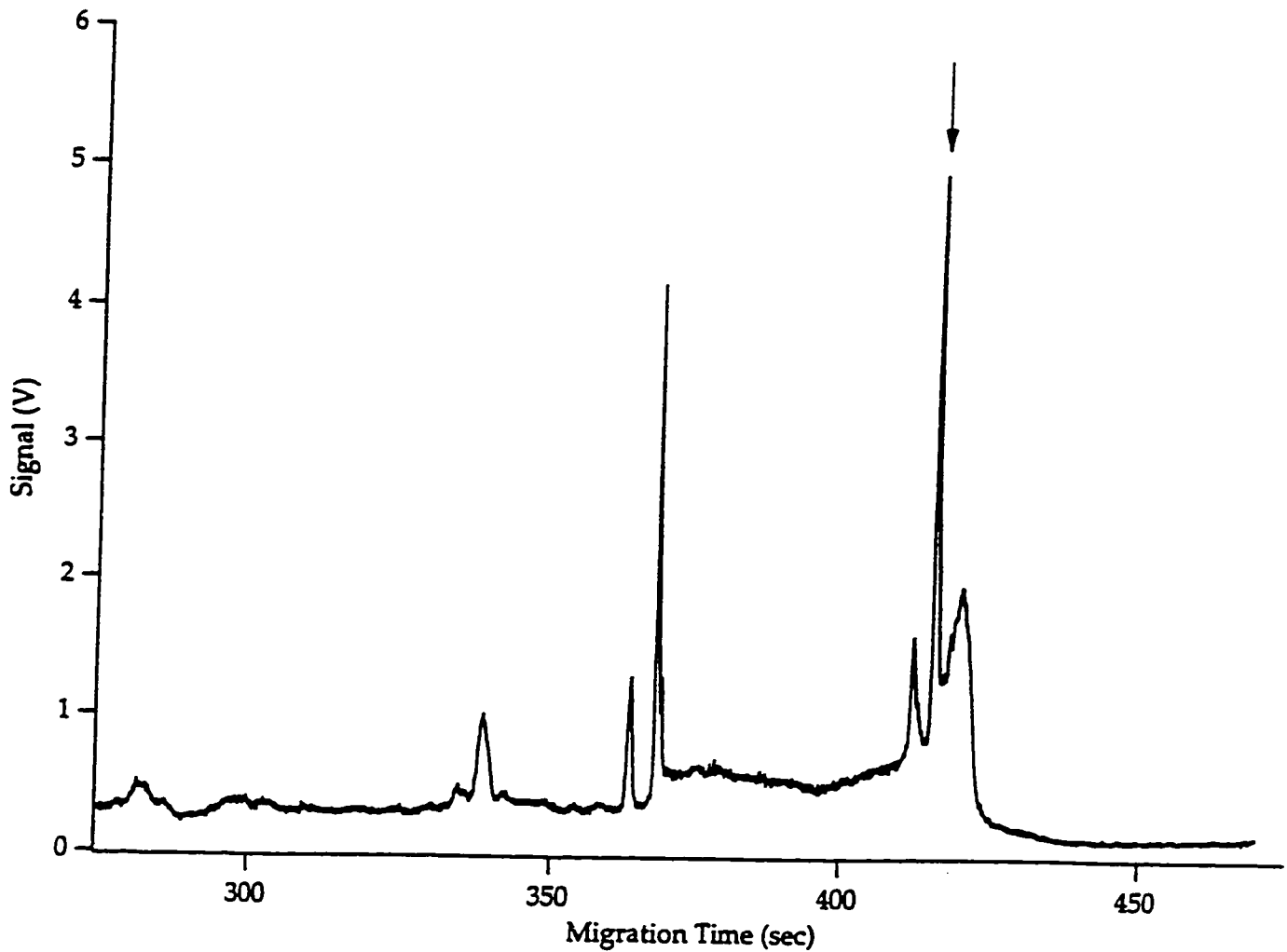
Figure 2.7 shows an electropherogram of $10^{-8}$ M Ins B which has been preconcentrated and labeled in the solid-phase reactor. Other authors have reported detection of peptide samples at similar concentrations analyzed both (a) after other preconcentration methods[23] and (b) directly by intrinsic LIF of unlabeled samples.[4-6] The high signal-to-noise ratio (S/N = 449) suggests that lower Ins B concentrations could be labeled using this approach.

## 2.4 CONCLUSIONS

This chapter presents a simple and rapid method to analyze peptides by CE-LIF. The range of concentrations analyzed extends over 5 orders of magnitude ($10^{-3}$M to $10^{-8}$ M) for the test peptide, Ins B. The concentration limits of this technique surpasses those of the traditional liquid-phase labeling technique by two orders of magnitude. Mass detection limits of 2.4 x $10^{-21}$ moles have been obtained. The high sensitivity coupled with the high efficiency of the separation (up to 20 x $10^{6}$ theoretical plates) should allow for excellent separation of peptide mixtures at very dilute levels.

The next chapter presents an alternative method to trace analysis of peptides by CE. This method also makes use of a solid phase to preconcentrate the sample. Similarly, a discontinuous buffer system is used to concentrate the sample on-line.

# REFERENCES

[1] Schöneich, C., Kwok, K., Wilson, G. S., Rabel, S. R., Stobaugh, J. F., Williams, T. D. and Vander Velde, D. G., *Anal. Chem.* 1993, 65, 67R-84R.

[2] Bailey, P. D., *An Introduction to Peptide Chemistry*, John Wiley & Sons, Chichester, 1992. Pp. 232.

[3] Szulc, M. E. and Krull, I. S., *Journal of Chromatography A* 1994, 659, 231-245.

[4] Lee, T. and Yeung, E. S., *J. Chrom.* 1992, 595, 319-25.

[5] Chan, K. C., Janini, G. M., Mushchik, G. M. and Isaaq, H. J., *Journal of Liquid Chromatography 1993*, 16, 1877-1890.

[6] Lee, T. and Yeung, E. S., *Analytical Chemistry 1992*, 64, 3045-51.

[7] Wu, S. and Dovichi, N. J., *Talanta 1992*, 39, 173-178.

[8] Zhao, J. Y., Dovichi, N. J., Hindsgaul, O., Gosselin, S. and Palcic, M. M., *Glycobiology 1994*, 4, 239-242.

[9] Novotny, M. V., Cobb, K. A. and Liu, J., *Electrophoresis 1990*, 11, 735-749.

[10] Arriaga, E., Zhang, Y. and Dovichi, N. J., *Analytica Chimica Acta* in press,

[11] Liu, J., Hsieh, Y-Z, Wiesler, D., and Novotny, M., *Anal. Chem.* 1991, 408-412.

[12] Liu, J. S., O., and Novotny, M, *Anal. Chem.* 1991, 63, 413-417.

[13] Beale, S. C., Savage, J. C., Wiesler, D. Wiestock, S. M. and Novotny, M., *Anal. Chem.* 1988, 60.

[14] Beale, S. C., Hsieh, Y-Z, Savage, J. C., Wiesler, D. and Novotny, M., *Talanta 1989*, 36, 321-325.

[15] Beale, S. C., Hsieh, Y-Z., Weisler, D., and Novotny, M., *J. Chrom.* 1990, 499, 579-587.

[16] Dolník, V. and Novotny, M. V., *Anal. Chem.* 1993, 65, 563-567.

[17] Chen, D. Y. a. D., N. J., *J. Chrom. B* 1994, 657, 265-269.

[18] Huang, X., Gordon, M. and Zare, R., *Anal. Chem.* 1988, 60, 375-377.

[19] Matsudaira, P., *Journal of Biological Chemistry 1987*, 262, 10035-10038.

[20] Patterson, S. D., Hess, D., Yungwirth, T. and Aebersold, R., *Anal. Biochem.* 1992, 202, 193-203.

[21] Krull, I. S. and Mazzeo, J. R. in: N. A. Guzman (Ed.) *Capillary Isoelectric Focusing of Peptides, Proteins, and Antibodies*, Marcel Dekker, Inc., New York 1992, pp. 795-818.

[22] Albin, M., Grossman, P. D., and Stephen, E. M., *Anal. Chem.*, 1993, 65(10), 489A-497A.

[23] Foret, F., Szökö, E. and Karger, B. L., *Electrophoresis* 1993, 14, 417-428.

# CHAPTER 3 – TRACE ANALYSIS OF PEPTIDES BY SOLID PHASE EXTRACTION AND CAPILLARY ISOTACHOPHORESIS

## 3.1 INTRODUCTION

The high separation efficiency and small sample consumption of capillary zone electrophoresis (CZE) make it an excellent method for the analysis of complex biological samples. However, the small injection volume necessitates the use of extremely sensitive detection methods or concentrated samples. The need for high detector sensitivity is a major impediment to the application of CE to biological sample analysis. Techniques such as capillary isotachophoresis (CITP),[1] electroextraction,[2] field amplification, coupled LC-CE[3], and high sensitivity detection [4,5] have been developed to increase the sensitivity of CE.

Electroextraction, field amplification and CITP are performed in the capillary. All three techniques use a high electric field in the sample region to increase sensitivity. In this chapter, field amplification will be briefly discussed, followed by a discussion on the use of CITP in conjunction with solid-phase extraction (SPE).

## 3.2 STACKING THROUGH FIELD AMPLIFICATION:

### 3.2.1 Basic theory

Field amplification is the simplest method, both conceptually and practically, for in-capillary sample concentration. In this method, the sample is dissolved in a buffer whose conductivity is lower than the conductivity of the background electrolyte (BGE). The difference in conductivity between the sample and BGE results in a concentrating effect. Chien and Burgi have reviewed the theoretical basis for the method.[6] Briefly, a large volume of sample is hydrodynamically injected into a capillary previously filled with BGE. The conductivity of the sample is low relative to

that of the BGE. The sample ($s$) fills a fraction $x$ of the capillary and the BGE fills the remainder of the capillary. The net electric field ($E$) across the capillary is given by,

$$E_{cap} = V / L_{cap} \qquad (3.1)$$

where $V$ is the applied voltage and $L_{cap}$ is the capillary length. However, $E$ is not constant throughout the capillary; the electric field in sample and BGE regions is given by,

$$E_{BGE} = \frac{E_{cap}}{x\gamma + (1-x)} \qquad E_s = \frac{\gamma E_{cap}}{x\gamma + (1-x)} \qquad (3.2a, 3.2b)$$

where $x$ is the fraction of the capillary filled with sample and $\gamma$ is the ratio of conductivivties;

$$\gamma = \sigma_{BGE}/\sigma_s \qquad (3.3)$$

This condition is analogous to the voltage drop across resistors in series. The ratio of the electric felds in the two regions, $E_s/E_{BGE}$, is also equal to $\gamma$.

Recall that the velocity of an analyte is directly proportional to $E$; therefore, an analyte molecule in the sample region has a higher velocity than an analyte molecue in the BGE region. This change in mobilities results in the accumulation of analyte at the sample/BGE boundary. Thus $\gamma$, the ratio of conductivities, determines the final concentration of the analyte ($C_{A'}$) at the sample BGE boundary, given by,

$$C_{A'} = \gamma \, C_A \qquad (3.4)$$

where $C_A$ is the initial analyte concentration.

## 3.2.2 Experimental

All peptides, as well as polybrene (1,5-dimethyl-1,5-diazaundecamethylene polymethobromide), were obtained from Sigma (St. Louis, MO). Formic acid was obtained from BDH (Toronto, ON, Canada). Stacking was performed in capillaries that were dynamically coated with polybrene. The capillary's total length was 87 cm long, the length to the detector was 80 cm, and the i.d. was 50 μm. The capillary was loaded into a Beckman capillary cartridge and coated by pushing the following solutions, in the order listed, through the capillary for 20 min: 1M NaOH, water, 5% (w/v) polybrene & 2% (v/v) ethylene glycol and finally BGE. All steps were performed using the instrument's high-pressure rinse feature, i.e. 60 psi pressure at the inlet. Between runs, the capillary was rinsed with 1 M NaOH for 1 min, water for 1 min, polybrene/ethylene glycol solution for 3 minutes and BGE for 3 minutes.

All samples were analysed with a Beckman P/ACE 2500 CE system (Beckman Instruments, Fullerton, CA) using absorbance detection at 200 nm. The BGE was formic acid at a concentration of 0.5, 1 or 2 M in water.

## 3.2.3 RESULTS

Figure 3.1 demonstrates the increase in sensitivity provided by stacking. The sample is a mixture of peptides at a concentration of 10 μg/ml and the injection volume is 190 nL or 10% of the capillary volume. In CZE, the injection volume should be kept below 1% of the capillary volume to achieve maximum resolution. As expected, the large injection volume results in poor efficiency and poor resolution in the CZE analysis. The rectangular peak shape reflects the dominance of band
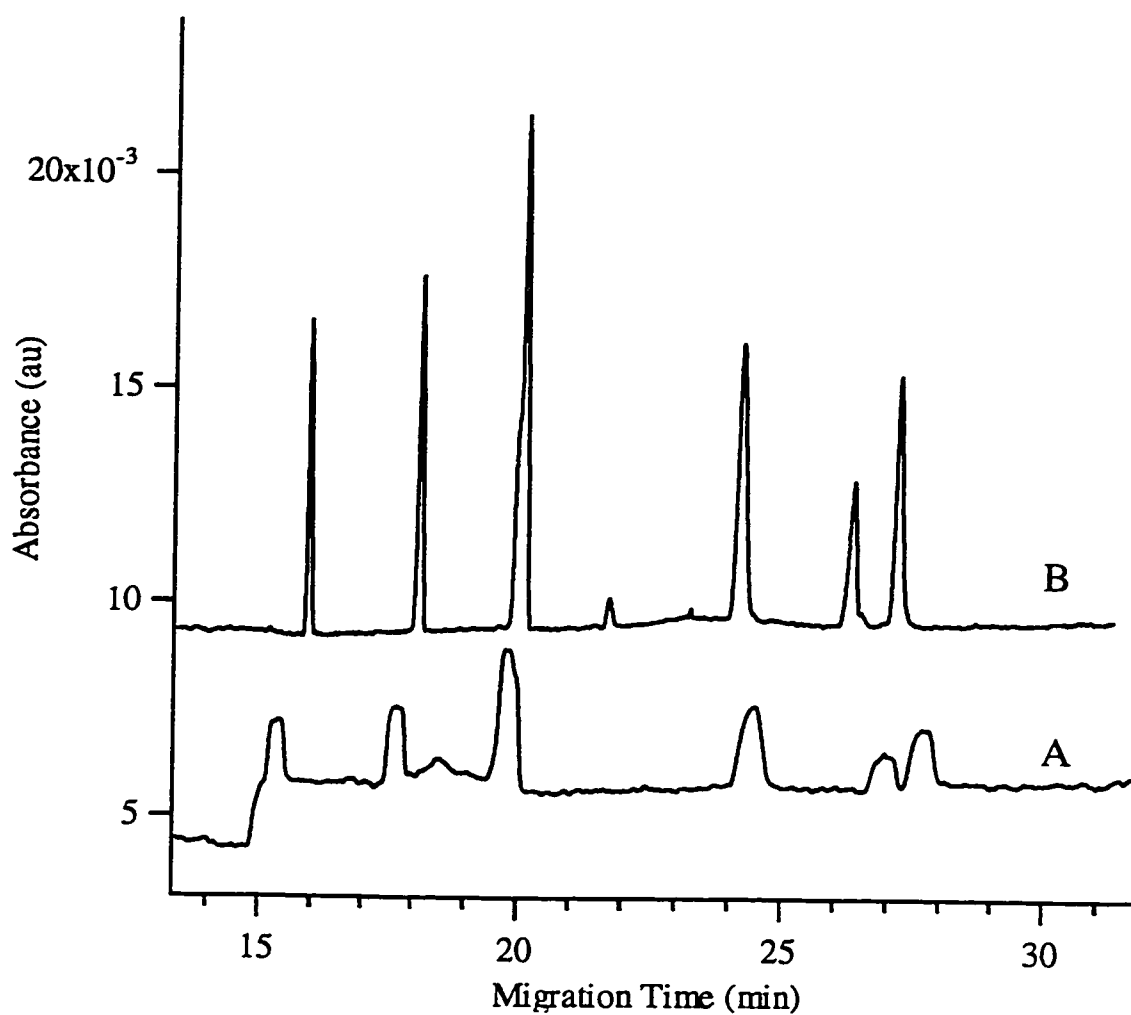
Figure 3.1 - A mixture of peptides, dissolved in (A) BGE or (B) water, were analysed by CE-UV. Conditions: 97 cm x 50 $\mu$m polybrene capillary, BGE: 0.5 M HCOOH, $V_{CE}$ = -30 kV. The peptides analysed were cholecystokinin fragment 10-20, somatostatin, leucine enkephalin, lysine bradykinin, insulin chain B and [Valine[4], Isoleucine[7]]-Angiotensin III

broadening due to initial plug width. In the case of the sample analyzed under stacking conditions, the peak efficiency ranges from 100 000 to 270 000 theoretical plates. In this example, stacking increases the sensitivity five-fold.

Figure 3.2 contains an electropherogram from the analysis of seven peptides that were dissolved in water and injected hydrodynamically. The sensitivity increases linearly with sample volume. However, as is usually the case, the increase in sensitivity is accompanied by a decrease in efficiency and resolution (see Figure 3.3). Nevertheless, this simple technique increases the sensitivity by approximately one order of magnitude. The capillary used in this example was covalently coated with quaternary amine, unlike the previous example where a dynamic coating was used. The dynamic coating provided approximately double the efficiency and was used for all further experiments.

Increasing the BGE concentration provides a modest increase in efficiency. For example, the peak at $t_m \approx 9$ min in figure 3.2 had efficiencies of 60 000, 96 000 and 120 000 theoretical plates for BGE concentrations of 0.5, 1 and 2 M respectively. This data is for a 90 s injection. Unfortunately, the increase in BGE concentration from 0.5 M to 2 M results in a doubling of the analysis time.

In stacking, the large difference between the sample and BGE conductivity results in band broadening. This band broadening limits the increase in sensitivity to one order of magnitude. However, removing the sample buffer after stacking avoids this source of band broadening and increases sensitivity by 2 orders of magnitude over CZE.[6] Unlike traditional stacking, this last technique can be used for only one polarity
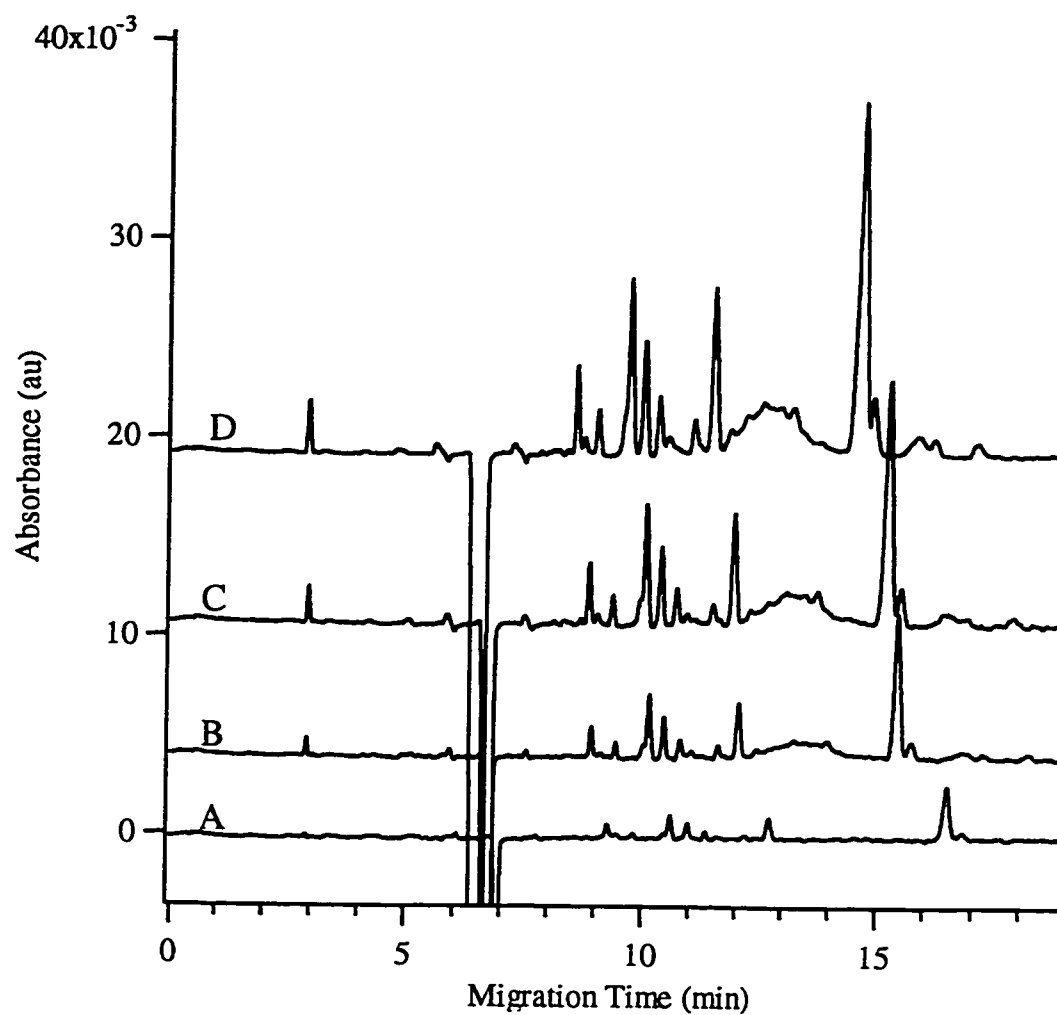
Figure 3.2. The effect of injection time on sensitivity in stacking. Injection volume:

(A) 32 μl (B) 95 μl (C) 190 μl (D) 285 μl. 87 cm x 50 μm 4° amine coated capillary,

BGE: 1 M HCOOH, sample: Angiotensin I, cholecystokinin fragment 10-20,

somatostatin, leucine enkephalin, lysine bradykinin, bradykinin and [valine[4],

isoleucine[7]]-angiotensin III at 100 μg/ml in $H_2O$.
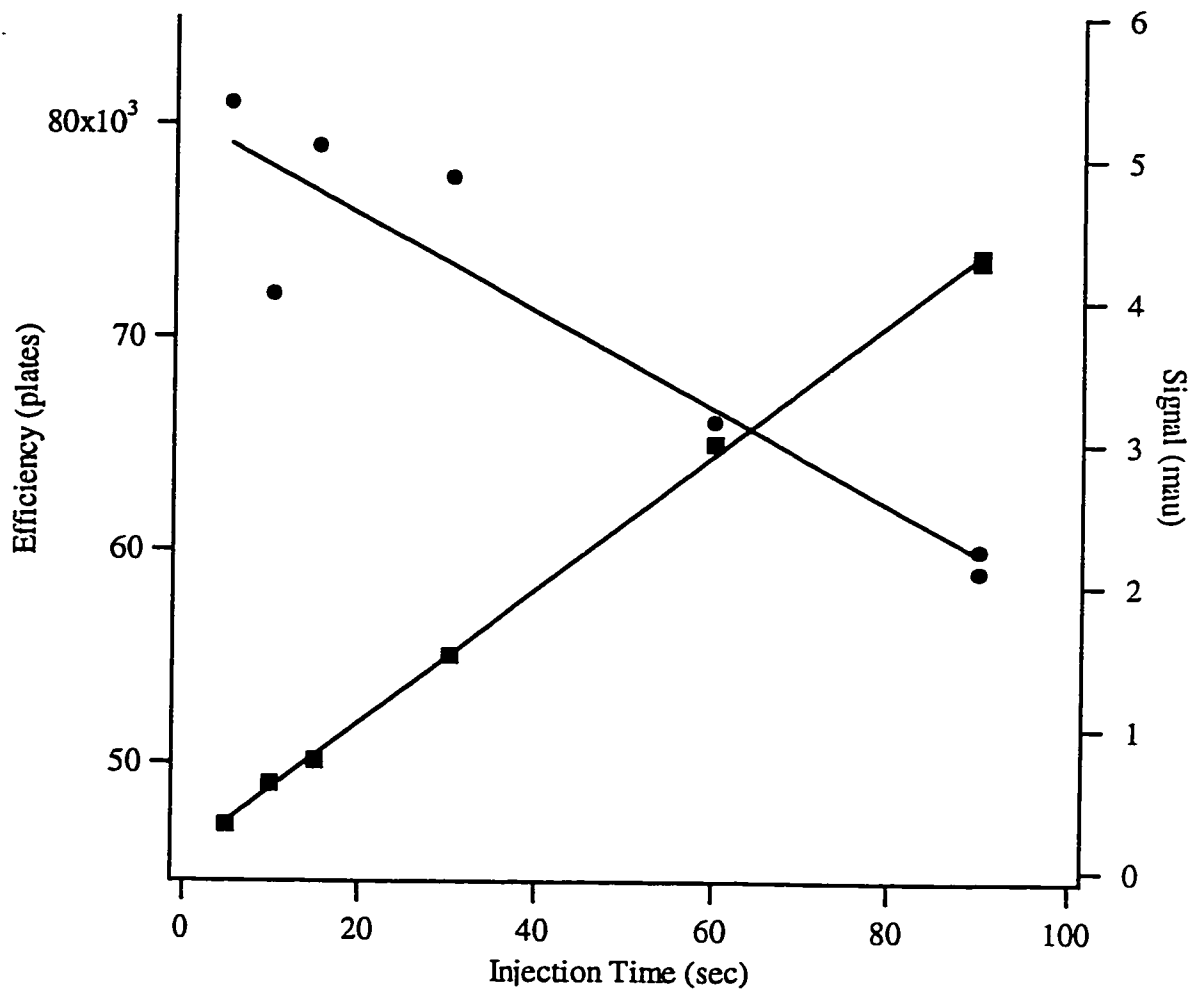
Figure 3.3: The effect of injection volume on sensitivity and efficiency in stacking.

of ions. Also, the charge on the capillary wall must be the same polarity as the ions analysed.

In the case of the analysis of peptides in plasma, sensitivity in the low ng/ml range is desirable. Simple stacking strategies do not provide this level of sensitivity. Furthermore, the complexity of plasma necessitates high efficiency or extensive sample clean up; neither of which is provided by sample stacking. Figure 3.4 illustrates these limitations of stacking. Electropherogram A corresponds to the analysis of a 100 μg/ml standard and electropherogram C corresponds to the analysis of plasma, diluted 1:4 with water. The large peaks in electropherogram C correspond to plasma proteins. The protein concentration is several orders of magnitude greater than the peptide concentration. The middle electropherogram, labelled B, corresponds to the analysis of plasma spiked with the same peptides as in electropherogram A. Despite the removal of the majority of the proteins by precipitation, the residual proteins comigrate with the peptides and ultimately limit the sensitivity. This last electropherogram also demonstrates the difficulties involved in using UV detection for the analysis of a complex sample such as plasma.

## 3.3 CAPILLARY ISOTACHOPHORESIS AND SOLID PHASE EXTRACTION

Capillary isotachophoresis (CITP) and solid phase extraction (SPE) were explored in an effort to improve the sensitivity and separation efficiency obtained through stacking. CITP and SPE are both useful for increasing the sensitivity of CE. SPE has the added benefit of allowing for sample cleanup. CITP is a relatively new
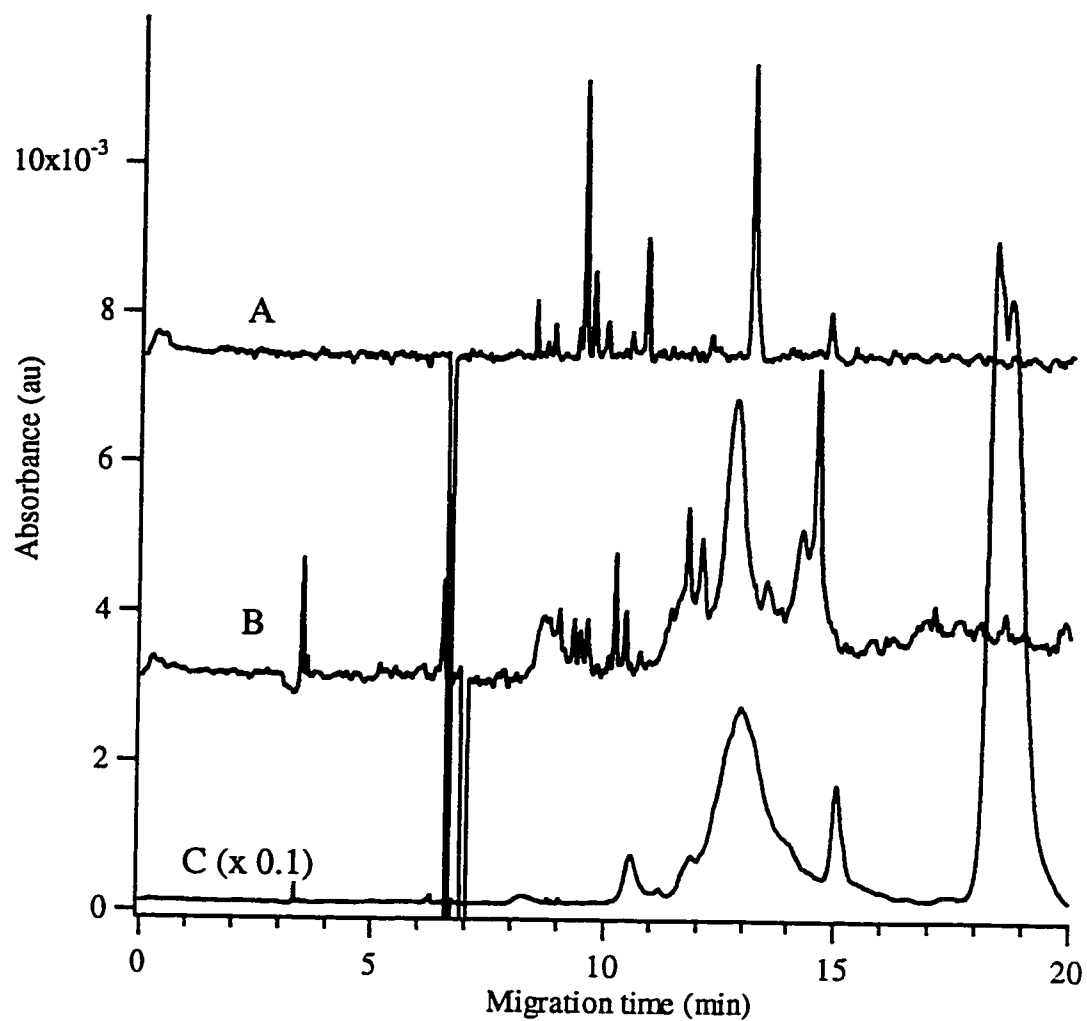
Figure 3.4 - A. 100 μg/ml peptides standard, B. Plasma, with proteins removed by

precipitation, spiked with peptides at 50 μg/ml C. Plasma diluted 1:4 with $H_2O$. 87 cm

x 50 μm BCQ coated capillary. BGE: 0.5 M HCOOH. Peptide sample: see figure 3.2.

technique; therefore, a brief introduction to CITP will be presented followed by a discussion of CITP in conjunction with SPE.

### 3.3.1 Basic theory of Capillary isotachophoresis

Capillary isotachophoresis (CITP) and capillary zone electrophoresis (CZE) are both separation methods in which the sample ions are separated according to their electrophoretic mobility. However, unlike zone electrophoresis where the buffer composition and electric field are homogeneous, isotachophoresis occurs in a capillary with a discontinuous buffer system and a heterogeneous electric field. The term isotachophoresis is derived form the Greek words ισο (equal), ταχοζ (velocity) and πορεεσθαι (to be dragged)[7].

CITP can be performed using either single or coupled capillaries. In single capillary ITP, the capillary volume limits the maximum amount of sample that can be injected. In coupled capillary ITP, a large bore capillary is placed before the separation capillary to increase the sample volume.[8] Despite its limited sample volume, the single capillary method is more popular due to its simplicity. In this work single capillary ITP is used exclusively.

There are three basic steps to isotachophoresis: sample introduction, separation into distinct zones and steady state CITP migration, as depicted in Figure 3.5. The sample, followed by the terminating electrolyte (TE), is introduced hydrodynamically. The application of an electric field separates the sample components according to their electrophoretic mobilities. The analytes continue to

A

B

C

Signal

Time
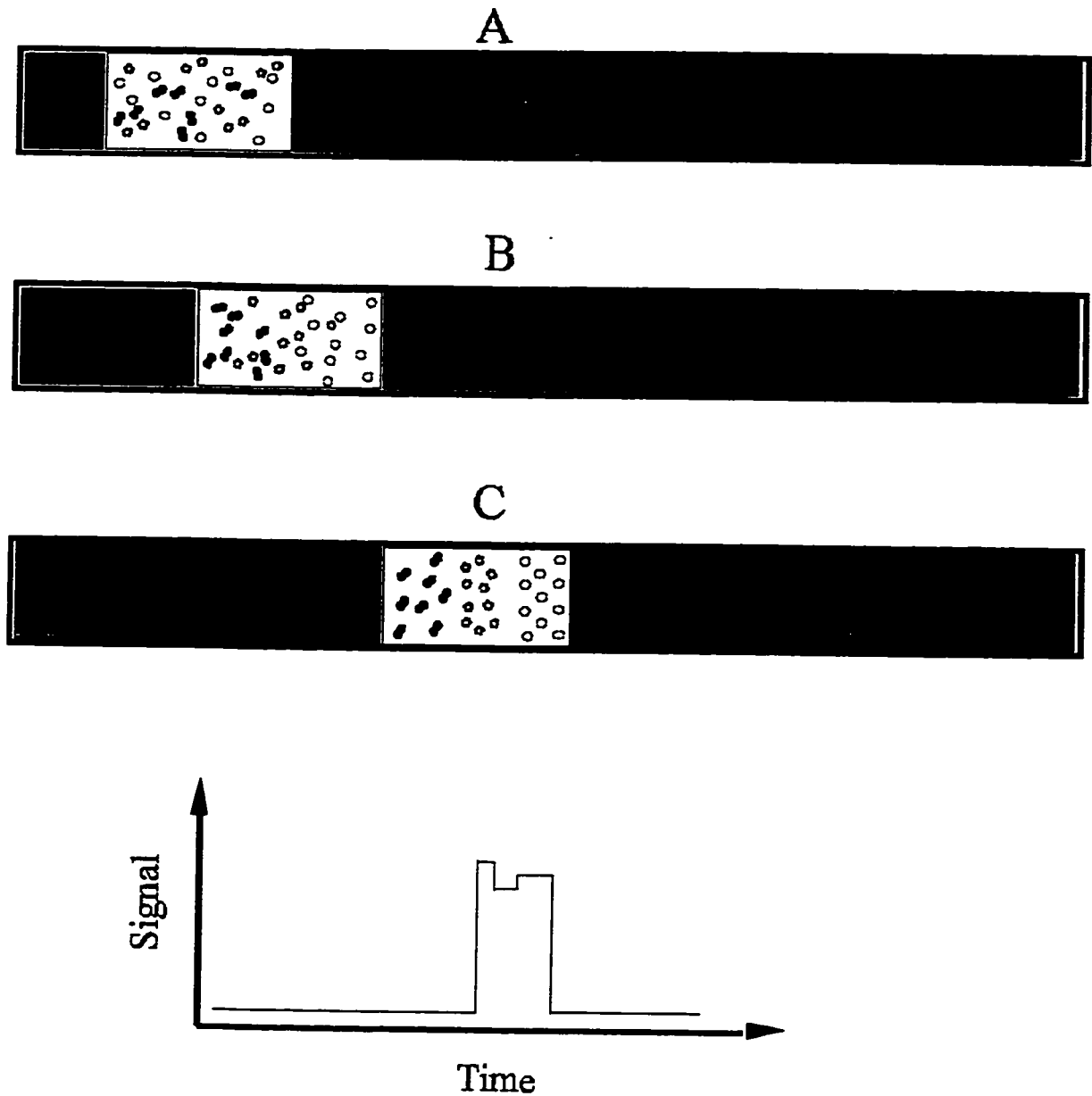
Figure 3.5 -The three steps of capillary isotachophoresis (A) sample injection between leading and terminating electrolytes, (B) separation of analytes into distinct zones, and (C) steady-state migration of zones. The bottom diagram is the expected detector response migrate at the same velocity. The separation is now complete and the zones proceed towards the detector. The ideal peak shape in CITP is rectangular.

45

separate until they form distinct zones. These adjoining zones, together with the leading and terminating electrolyte

We can now consider the differences between CITP and CZE separations. In CZE, a high ratio of BGE ionic strength to sample ionic strength is required for zones. efficient separations. However, in CITP no BGE is required. A CZE separation is complete when each sample component is baseline resolved, i.e. when a region of BGE is between the components. In CITP the separation is complete when the sample components form distinct zones which, since there is no BGE present, must be adjoining. From the point of view of sensitivity, the most important difference between CITP and CZE is the increase in concentration that occurs in the former. In figure 3.5c, we see that the length of each analyte zone is 1/3 the length of the original sample plug length in 3.5a. Therefore, the concentration of each analyte increases three-fold through the CITP process. A brief derivation serves to explain this process[1];

According to Ohm's law, the current density ($J$) in the two zones is a constant

$$J = constant = E_A\sigma_A = E_{LE}\sigma_{LE} \tag{3.5}$$

where $\sigma$ is the conductivity and $E$ is the electric field. The subscripts $A$ and $LE$ are for analyte and leading electrolyte, respectively. The conductivity of a salt AQ, where A and Q are the analyte's monovalent anion and cation respectively, is defined as;

$$\sigma = cF\left(|\mu_A| + |\mu_Q|\right) \tag{3.6}$$

Where c is the concentration, $\mu$ is the mobility and F is the Faraday constant. If we substitute equation 3.6, into equation 3.5 we obtain;

46

$$c_A(|\mu_A| + |\mu_Q|)E_A = c_{LE}(|\mu_{LE}| + |\mu_Q|)E_{LE} \qquad (3.7)$$

or

$$c_A = c_{LE}\frac{E_{LE}(|\mu_{LE}| + |\mu_Q|)}{E_A(|\mu_A| + |\mu_Q|)}$$

The analyte and leading electrolyte zones are moving at the same velocity, therefore,

$$v_{LE} = v_A \qquad (3.8)$$

or

$$\mu_{LE}E_{LE} = \mu_A E_A$$

or

$$E_{LE}/E_A = \mu_A/\mu_{LE} \qquad (3.9)$$

Substituting equation 3.9 into equation 3.7, we obtain our final result;

$$c_A = c_{LE}\frac{|\mu_A|(|\mu_{LE}| + |\mu_Q|)}{|\mu_{LE}|(|\mu_A| + |\mu_Q|)} \qquad (3.10)$$

The concentration of the analtye adjusts itself to the concentration of the leading electroylte multiplied by the quotient of mobilites term. This term is always less than unity since, by definition, $\mu_{LE} > \mu_A$. Equation 3.10 demonstrates that the increase in concentration of an analytes is proportional to its mobility. Therefore, if CITP is used for an analyte whose mobility is much lower than the mobilty of the LE, the increase in concentration and the separation efficiency obtained will be poor.

In practice, CITP can increase the sample concentraion by approximately two orders of magnitude. For trace analysis, a furthur increase of two to three orders of magnitude is required. In this work, solid phase extraction (SPE) is combined with CITP to provide high sensitivity.

47

## 3.3.2 THE USE OF SOLID PHASE EXTRACTION TO INCREASE SENSITIVITY

SPE is commonly used in conjunction with chromatography [9,10] but is not commonly used with CZE. SPE can be used for sample cleanup and sample preconcentration. These features are of particular benefit to CITP since it is susceptible to matrix effects. SPE is most often performed using $C_{18}$ based adsorbents. Alternatively, affinity SPE materials can be used for more selective analyte extraction.[11] The wide range of sorbents available and the ease of automation make SPE attractive for the analysis of biological samples.[8]

In SPE the preconcentration factor obtained is defined by the ratio of the initial sample volume to final sample volume. Analyte losses during SPE reduce the concentration factor obtained. In this study, the initial volume is typically 1 ml and the final volume after SPE is typically 10 µl, providing a concentration factor of 100. Further increases in the concentration factor are hampered by the difficulty in handling and injecting from less that 10 µl of solution. This volume is still 500 times greater than the injection volume in CZE and 50 times greater than the injection volume in CITP.

Although SPE is traditionally performed off-line, several groups have recently investigated on-line SPE-CE.[12,13,14] In this technique, a small bed of SPE material is held in the first few centimeters of the capillary. The remainder of the capillary is used for CZE or transient CITP. Capillary equilibration, sample loading and sample cleanup are performed off-line in a high-pressure device to increase throughput. The low flow rates obtained with capillaries, approximately 150 nl/min for a 25 µm i.d. capillary, necessitate the use of off-line procedures to obtain a reasonable throughput.[15] Once the

48

off-line steps are completed, sample elution, separation and detection is performed on-line. For complex samples, pretreatment using HPLC is often required prior to on-line SPE.[13] On-line SPE cartridges can be loaded off-line with microlitres of sample and then eluted on-line with nanolitre volumes of solvent thus increasing sensitivity by four to five orders of magnitude.

The method described in this chapter is based on off-line preconcentration via SPE followed by on-line concentration via CITP. When the two techniques are performed consecutively, the total concentration factor obtained is the product of the individual concentration factors. For example, if the SPE process provides a concentration factor of 100 and the CITP process provides a concentration factor of 100, the overall increase in sensitivity is $10^4$.

Performing SPE off-line makes independent optimization possible and allows for the use of the optimal sample buffer for subsequent CITP analysis. The difficulty in automation and the increased amount of sample handling are drawbacks of performing off-line SPE. Nevertheless, off-line analysis avoids the issues of compatibility between the SPE and CZE technology. Off-line SPE-CZE provides higher throughput than on-line SPE since the flow rates are higher and since multiple samples are extracted simultaneously.

UV detection was used in preliminary studies due to its simplicity and the availability of an automated CE instrument with UV detection. After the SPE and CITP conditions were optimized, MS detection was used since it provides unambiguous identification of sample components and, therefore, is well suited to the analysis of complex biological samples. MS detection also provides sequence

information and identifies post-translational modifications; this information is not provided by common detection methods such as UV absorbance.

### 3.3.3 EXPERIMENTAL

MATERIALS

All peptides, β alanine, anhydrous tetrahydrofuran (THF), ammonium persulphate (APS), and N,N,N,N-tetramethylethylenediamine (TEMED) were obtained from Sigma (St. Louis, MO). Formic acid, methanol, trifluoroacetic acid and acetic acid were obtained from BDH (Toronto, ON, Canada). Empore SDB-XC and $C_{18}$ extraction disks were obtained from 3M (St. Paul, MN), POROS R beads were obtained from PerSeptive Biosystems (Cambridge, MA) and SepPak $C_{18}$ SPE cartridges were obtained from Waters. N-acryloylaminoethoxyethanol (AAEE) was synthesized according to the method of Chiari *et al.*[16]

CAPILLARY ELECTROPHORESIS

Preparation of poly(AAEE) coated capillaries

A 5 m section of 50 μm (i.d.) capillary (Polymicro Technologies, Phoenix, AZ) was coated with a vinyl layer according to the method of Cobb et al,[17] rinsed with THF, and then filled with polymerizing solution. A capillary rinse kit (Chromatographic Specialties, Brockville, ON) was used for capillary preparation. The polymerizing solution consisted of 500 μl of 15% (w/v) AAEE in water, previously purged with nitrogen, to which 5 μl of 15% (w/v) aqueous APS and 0.5 μl of TEMED were added. The polymerizing solution was pushed through the capillary using $N_2$ at a pressure of 20 psi for 10 minutes followed by a pressure of 5 psi for 45

50

minutes. The capillary was then rinsed with water for 5 minutes and stored with the ends capped.

## CITP-UV Experiments

Preliminary studies were performed using a Beckman P/ACE 2500 CE system (Beckman Instruments, Fullerton, CA) using absorbance detection at 200 nm. Transient capillary isotachophoresis (CITP) was performed using an 87 cm x 50 μm (i.d.) x 360 μm (o.d.) poly(AAEE) coated capillary. Samples were dissolved in 0.1 M acetic acid. The background electrolyte (BGE) was 35 mM β alanine adjusted to pH 3.2 with formic acid. The transient CITP parameters were as follows: (i) capillary conditioning with BGE for 5 minutes at high pressure, (ii) hydrodynamic injection of 420 nl of sample (1/4 of the capillary volume) (iii) focusing with 50 mM formic acid at the anode (+25 kV) for 60 s (iv) CZE separation with BGE at the anode (+25 kV).

## CITP-MS Experiments

CITP-MS experiments were performed using an automated CE instrument connected, through an electrospray interface, to a triple quadropole MS (API/$III^+$, SCIEX, Concord, ON). The instrument is depicted in figure 3.6. Electrophoresis was performed using an ATI Unicam Crystal 310 CE system (Madison, WI). The transient CITP parameters were the same as those given above, with one exception; following the focusing step, a pressure of 1.4 mbar was applied for 1 minute with the BGE at the anode. This extra step was used to decrease the analysis time. The capillary measured 85 cm x 51 μm (i.d.) x 185 μm (o.d.) and was coated with poly(AAEE). A potential of +30 kV was applied at the injection end of the capillary and, since the electrospray needle was held at +5 kV, the potential drop across the capillary was +25 kV.

51

CE
+
Auto-sampler

Capillary

Electrospray
Ionization
Interface

Triple Quadropole MS
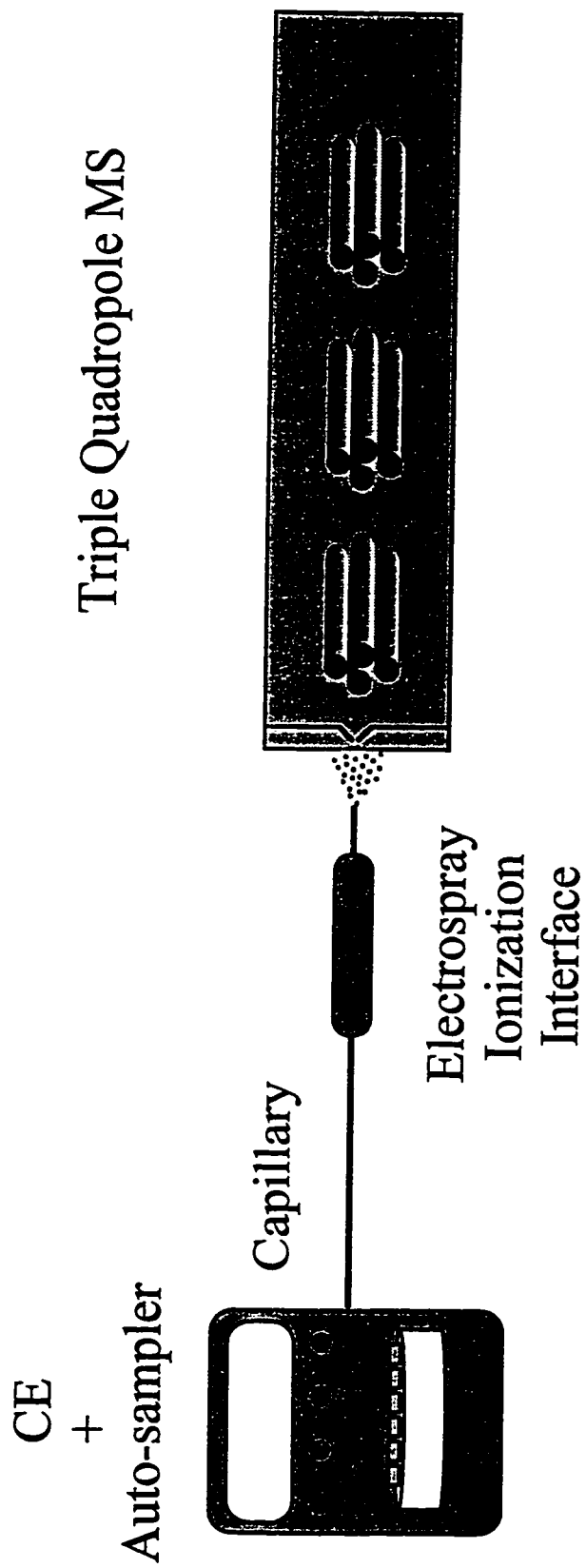
Figure 3.6 Schematic of CE-MS Instrument

52

Mass spectrometry was performed using a Perkin-Elmer SCIEX API/III+ triple quadropole mass spectrometer equipped with an atmospheric pressure ionization interface (API) operated in the pneumatically assisted electrospray (ionspray) mode.[18] Full scan MS data was collected using a step size of 1 Da and a dwell time of 5 msec. The majority of the MS spectra were collected in the selected ion recording mode, with two ions per peptide monitored and a dwell time of 30 msec, unless otherwise stated. The electrospray needle was held at +5 kV using a high power supply (Glassman EH Series, Glassman, Whitehouse Station, NJ, USA). The needle assembly contains the capillary and the inlets for the nebulizer gas (air @ ~45 psi) and the sheath liquid. In preliminary experiments, the sheath liquid was methanol, water and formic acid at a ratio 50:50:0.2; however, the electrophoretic current only stable if a 30 mbar pressure was applied during electrophoresis. If acetic acid was substituted for formic acid, the electrophoretic current was stable and pressure was not required. This observation is consistent with studies performed by Foret *et al.*[19] For all data presented here, the sheath liquid was methanol:water:acetic acid (50:50:0.2, v/v) supplied at a rate of 7 μl/min via a HPLC pump (HPLC Micro pump, Brownlee Labs, Santa Clara, CA).

Figure 3.7 contains a schematic of the two T-unions used for the interface. This interface is rugged and simple to set up. The sheath liquid maintains electrical contact between the stainless steel electrospray needle and the fused silica capillary. However, a large flow rate relative to the flow rate in the capillary is required to maintain this contact. This large flow dilutes the analyte by roughly three orders of magnitude as it passes through the interface.

Tandem mass spectrometry was performed using argon as the collision gas, at a thickness of $3.5 \times 10^{15}$ atoms/cm$^2$, and a collision energy of 25 eV in the laboratory frame of reference. Full scan MS-MS data from m/z = 150-1000 was acquired using a
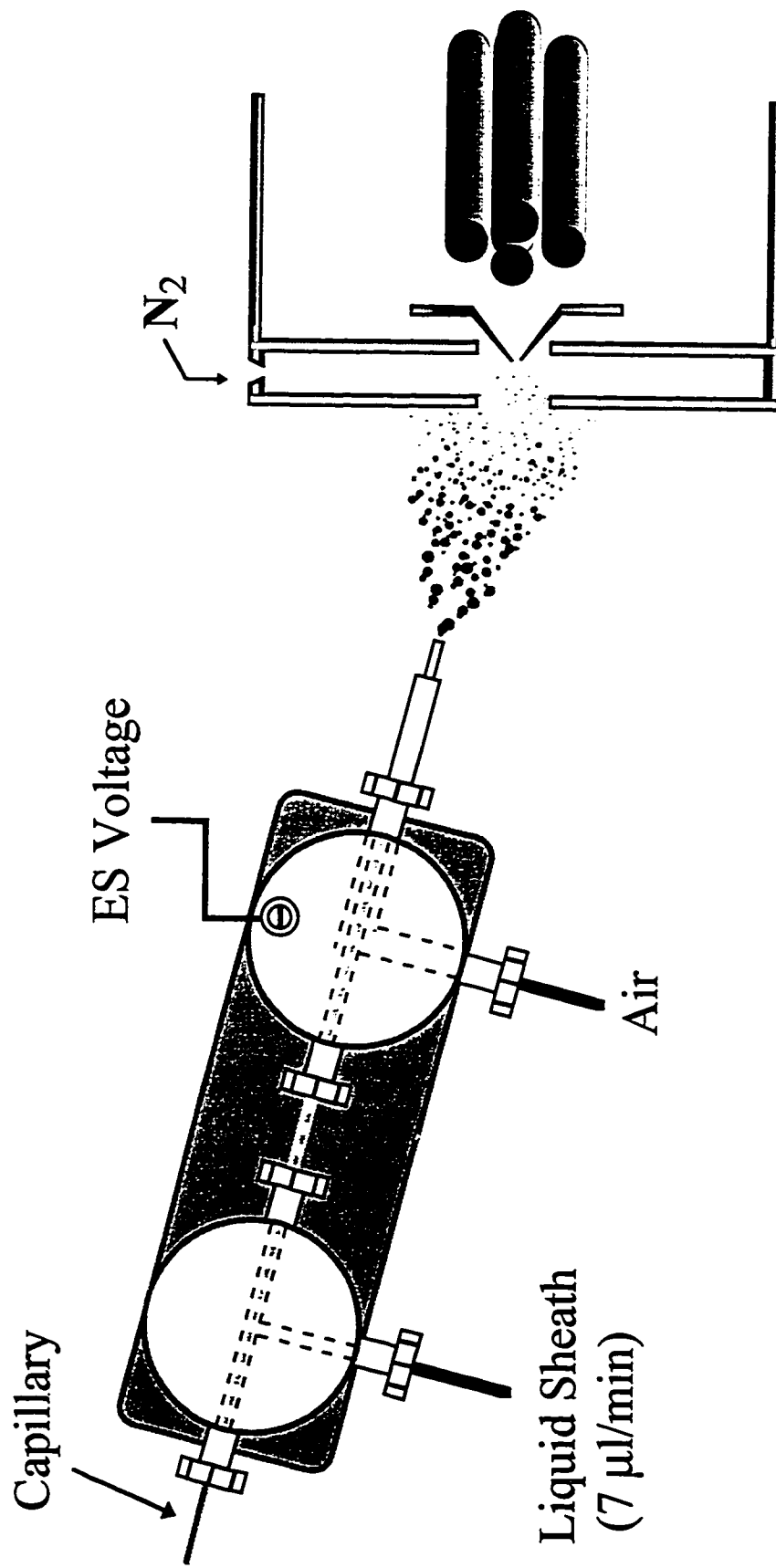
Figure 3.7 - Schematic of CE-MS Interface

Capillary

ES Voltage

Air

Liquid Sheath
(7 μl/min)

N$_2$

54

1 Da step size and a 5 msec dwell time. The scan rate under these conditions is 0.24 Hz. The separation voltage was reduced to +10 kV as soon as the leading edge of the peak of interest was detected. This technique allows us to increase the number or scans collected and, therefore, to take advantage of the S/N enhancement effect of signal averaging.

## SOLID PHASE EXTRACTION

### Preparation of SPE spin tips

SPE spin tips were constructed by placing a circular piece of SDB-XC membrane (diameter = 2 mm) into a standard 200 μl gel loading pipette tip thus forming a membrane bed whose volume was approximately 5 μl. A second piece of $C_{18}$ membrane, or a small bed (ca. 20 μl) of beads, was placed on top of the membrane. In the case of the SPE tips with POROS and $C_{18}$ beads, a second piece of SDB-XC membrane was placed on top of the beads to hold them in place. The SPE tips were placed in a centrifuge tube and then loaded into a benchtop centrifuge. Liquids, loaded via the top of the tip, were forced through using the centrifuge and collected in the centrifuge tube.

### SPE of peptides

The SPE tips were conditioned by whetting the SPE material with 30 μl of methanol followed by 30 μl of water. This step also removes from the membranes any extractables, which may interfere with CITP-MS analysis. The sample was spun through the membrane. The membrane was then washed three times with 30 μl of water to remove salts and any other non-adsorbed materials. The peptides were then extracted twice with 30 μl of methanol:water:TFA (80:20:0.1) followed by two

extractions with 30 µl of acetonitrile:water:TFA (80:20:0.1). The extraction solvent was removed under vacuum and the samples were reconstituted in 0.1 M HOAc.

Prior to the SPE of the plasma samples, the proteins were precipitated by slow addition of an equal volume of acetonitrile. In some cases, the plasma was spiked with peptide standards prior to protein precipitation. Endogenous peptides could have been analyzed but, since their concentrations vary, this would have complicated the calculation of recoveries. To remove the precipitated proteins, the plasma was centrifuged at 14 000 rpm for 10 min (Eppendorf microcentrifuge, model 5415, Madison, WI) and the supernatant was evaporated to dryness using a vacuum centrifuge (Speedvac, Savant Instrument). The plasma was reconstituted in 200 µl of water and the peptides were extracted according to the procedure given above.

3.3.4 RESULTS

OPTIMIZATION OF CITP CONDITIONS

The entire separation process used here consists of CITP followed by CZE or, as it is sometimes called, transient CITP. Transient CITP combines the sensitivity enhancing features of CITP and the high resolution afforded by CZE. In transient CITP, the terminating electrolyte is replaced with a vial of BGE after the analytes are focused into narrow, adjoining zones. This change of electrolytes results in a gradual return to a CZE regime. These parameters, as well as other parameters that are critical to transient CITP are discussed below.

The length of the initial focusing step is critical to the performance obtained.[19] A long focusing time delays the transition to a CZE regime resulting in poor resolution. However, if the focusing time is too short, the analytes with low mobilities relative to the leading electrolyte do not focus into narrow zones, resulting in poor
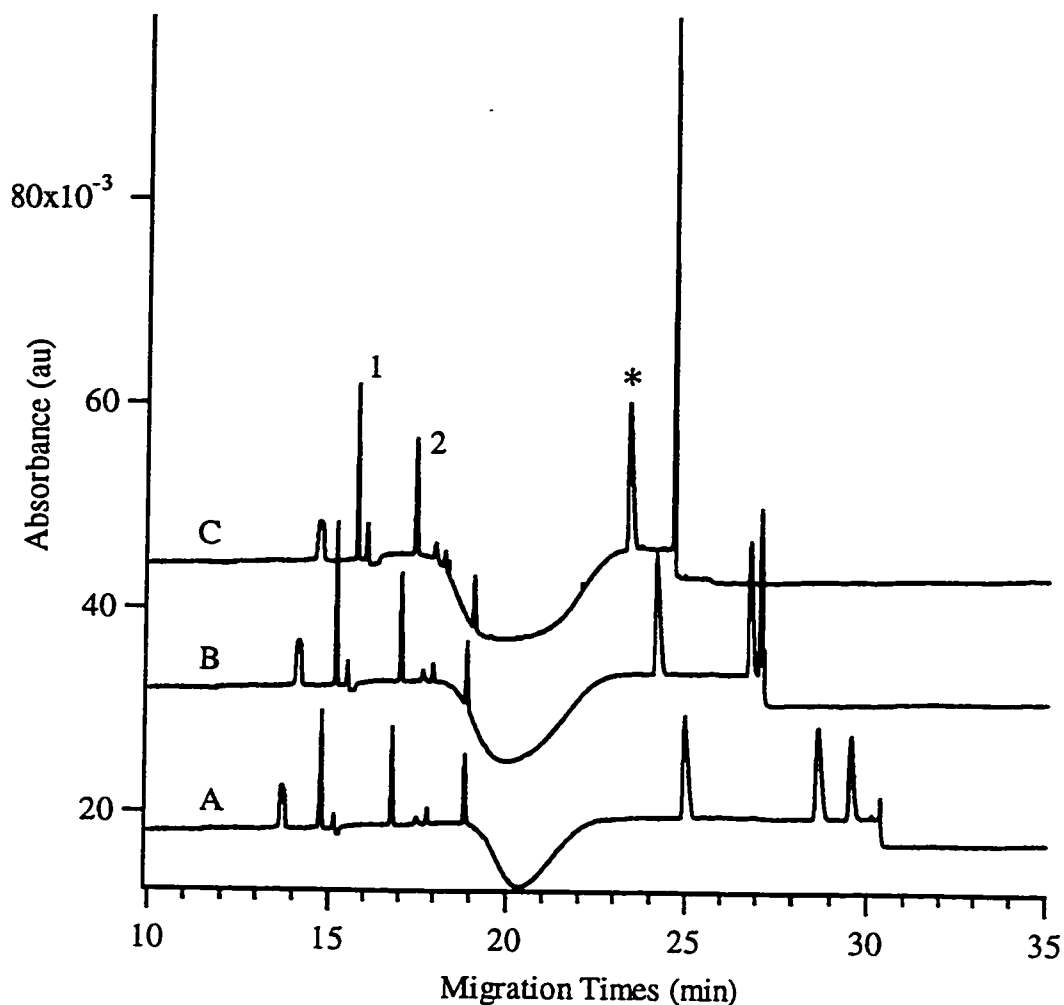
Figure 3.8 - The effect of focusing time on separation and sensitivity. Focusing times

are (A) 1.15 min, (B) 2.0 min and (C) 3 min. The resolution and efficiency for peaks 1

and 2 is given in Table 1. CITP Conditions: Sample 1 $\mu$g/ml of Angiotensin I, Insulin

chain A, insulin chain B, Kassinin, Somatostatin, Lys-bradykinin, Leu-enkephalin,

$Val^4-Ile^7$-angiotesin III and Des-Leu-$Tyr^1$-enkephalin, cap. 87 cm x 50 $\mu$m AAEE

coating, $t_{inj}$ = 20 s, BGE: 35 mM $\beta$-alanine, pH 3.17. The peaks marked 1,2 and * are

discussed in table 3.1.

sensitivity and poor efficiency. These effects are demonstrated in figure 3.8. The

separation data for the peaks marked 1 and 2 in figure 3.8 is given below;

TABLE 3.1: EFFECT OF FOCUSING TIME

| Focusing Time (min) | Efficiency (x $10^3$ plates) | | Peak Height MAU | | Resolution | Analysis Time* (min) |
|---|---|---|---|---|---|---|
| | Peak1 | Peak2 | Peak 1 | Peak 2 | | |
| 1.15 | 485 | 557 | 12 | 9.6 | 23 | 26.1 |
| 2.0 | 762 | 573 | 16 | 10.5 | 23 | 26.1 |
| 3.0 | 875 | 610 | 17 | 11 | 18 | 26.3 |

*Analysis time = (focusing time) + ($t_m$ of peak marked with an asterisk in fig. 8).

Optimization of BGE pH was performed using 35 mM β alanine in a pH range

of 2.75 - 3.5. Results, as shown in figure 3.9, were quite different even though the pH

range is quite narrow. A pH of 3.17 provided optimal resolution and efficiency and

was used for further experiments.

BGE concentrations of 35, 45 and 66 and 80 mM were used. As can be seen in

figure 3.10, the analysis time increased from 10.5 to 19.0 minutes as the β-alanine

concentration was increased from 35 to 80 mM. Figure 3.11 shows the increase in

efficiency obtained by increasing the BGE concentration. Unfortunately, in the case of

CITP-MS experiments, the increasing the electrolyte concentration from 35 mM to 66

mM resulted in a decrease in signal of approximately 50%. For all further CITP-MS

experiments, a β-alanine concentration of 35 mM was used in order to maximize

sensitivity.
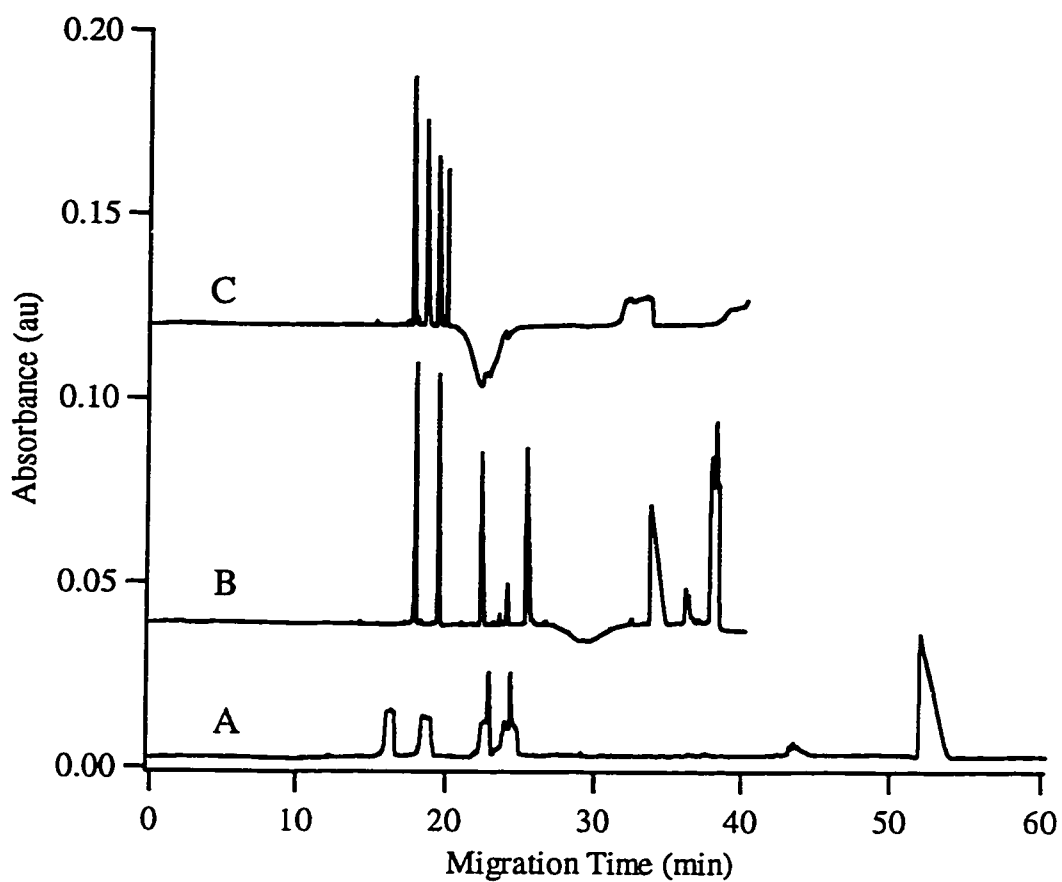
Figure 3.9 - Effect of BGE pH on separation and efficiency. The BGE pH was (A) 3.5, (B) 3.17 and (C) 2.75
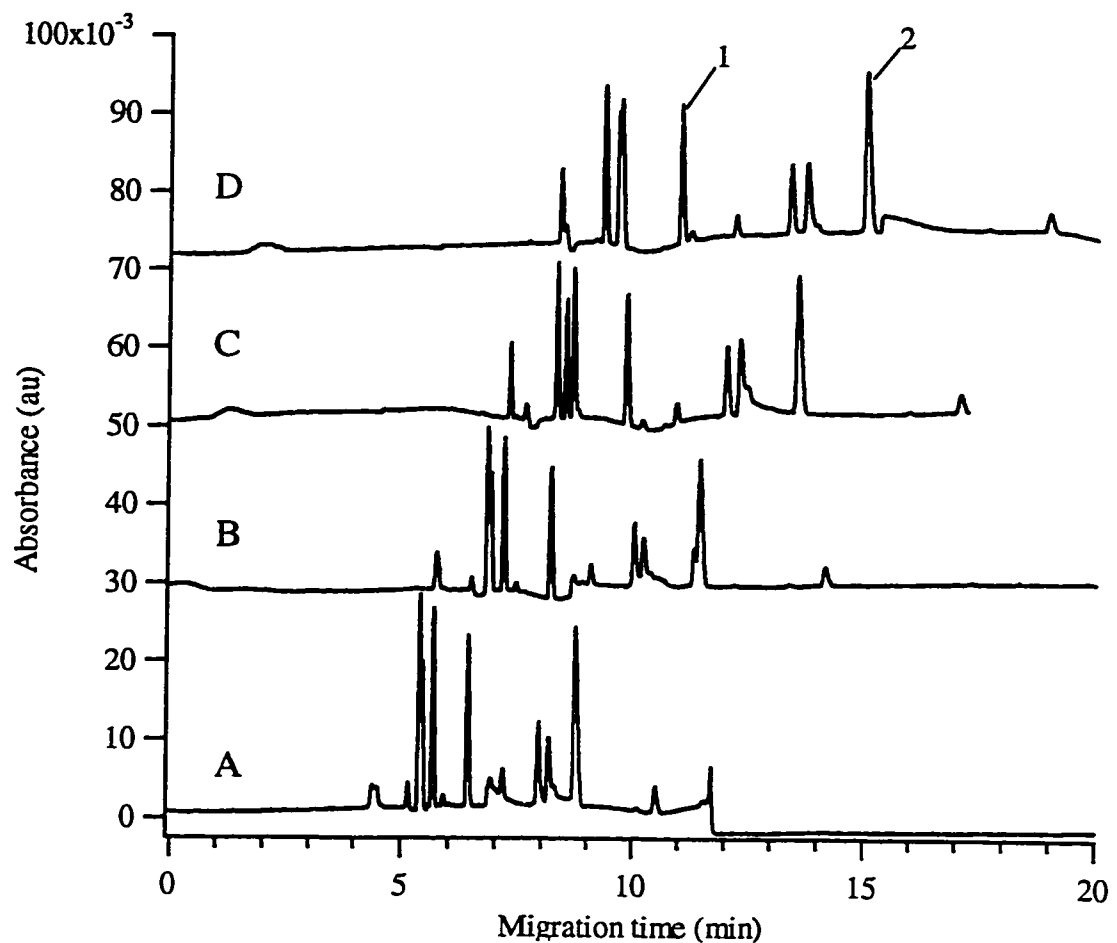
Figure 3.10 - Effect of BGE concentration on separation. The concentration of β
alanine was (A) 35, (B) 48, (C) 65 and (D) 80 mM. The separation efficiencies for the
peaks marked 1 and 2 are plotted in figure 3.11. For sample composition and peak
identities, see figure 3.13.
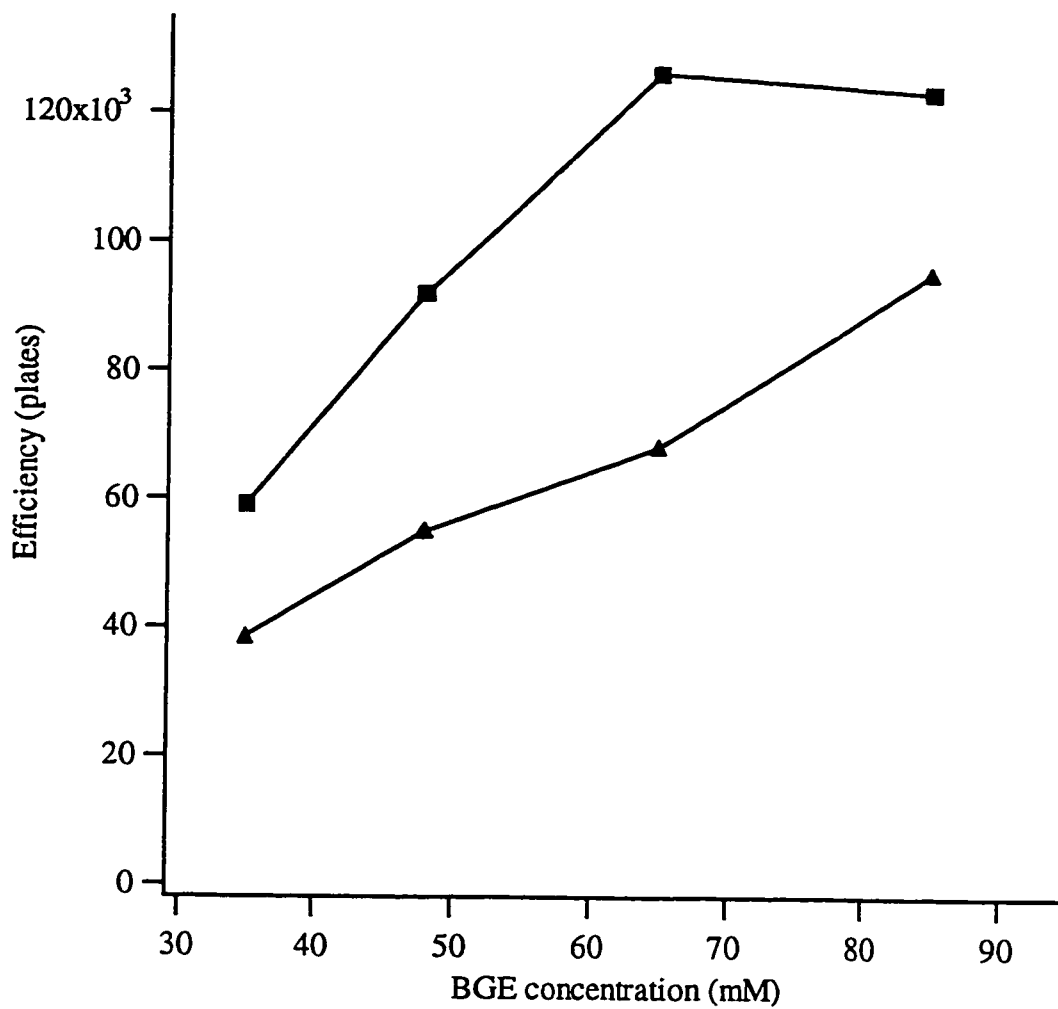
Figure 3.11 - Effect of BGE concentration of separation efficiency in CITP for (■')
Angiotensin I and (▲) Angiotensin II, which are peaks 1 and 2, respectively, in figure
3.10.
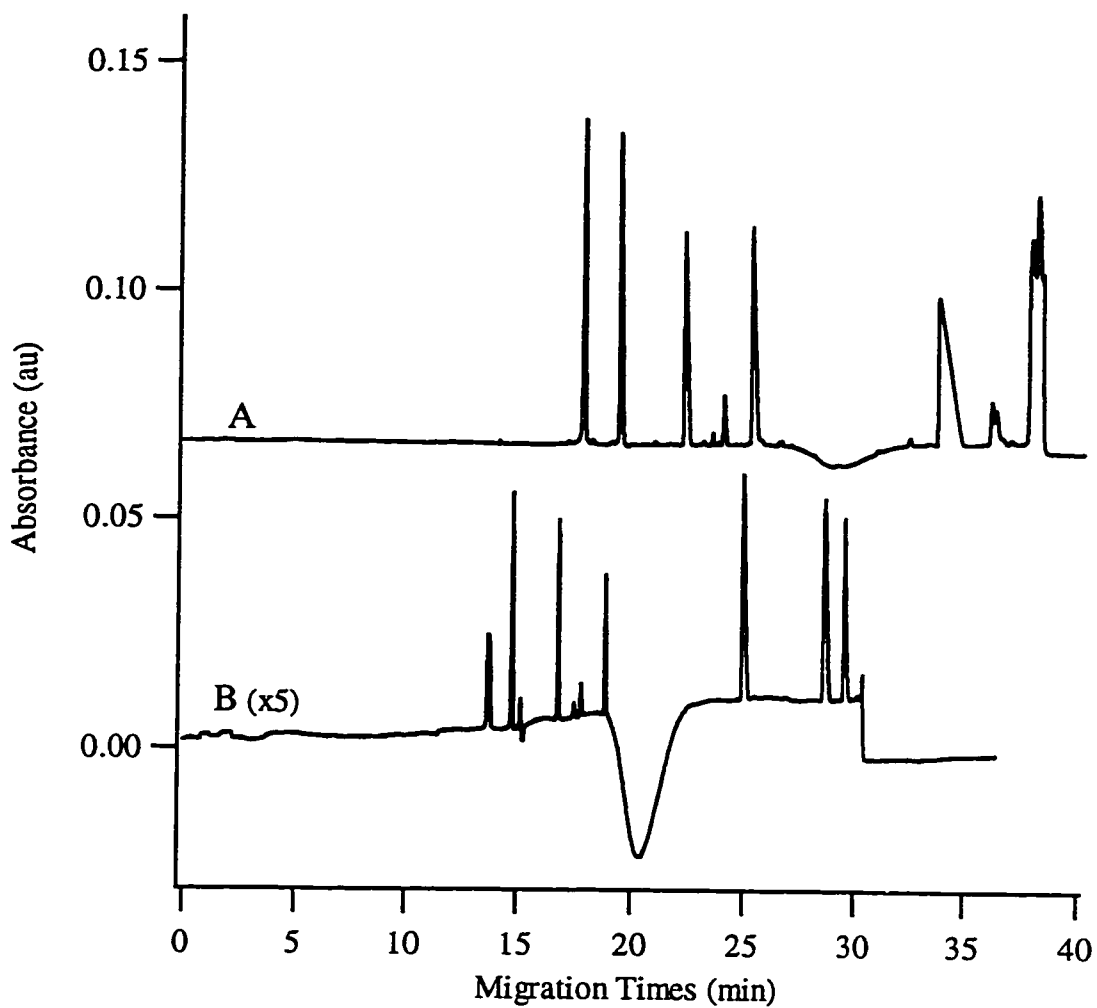
Figure 3.12 - Effect of formic acid concentration on separation and efficiency. The formic acid concentration were (A) 10 mM and (B) 50 mM.

The concentration of the terminating electrolyte must be greater than a critical

concentration (c) given by the following equation;[19]

$$c_T = \frac{\mu_T}{\mu_L} \cdot \frac{u_L + \mu_Q}{\mu_T + \mu_R} \cdot c_L \qquad (3.11)$$

Where the subscripts T, L and Q refer to the terminator, leading and counter ions and

$\mu$ refers to the mobility. Formic acid over a concentration of 10 to 75 mM was used as

a terminating electrolyte. Figure 3.12 demonstrates the improvement in efficiency

obtained when the formic acid concentration was increased from 10 mM to 50 mM.

Above this concentration, no significant change in the efficiency was observed. These

observation are consistent with equation 3.11.

The sample volume was varied from 84 to 840 nl, i.e. 5-50% of the capillary

volume. As expected, the peak height increased and the efficiency decreased as the

injection volume was increased. All subsequent experiments were performed using an

injection volume of 420 nL, at which, efficiencies ranged from $1 \times 10^5$ to $2 \times 10^5$

theoretical plates.

## CITP-UV AND CITP-MS ANALYSIS OF PEPTIDES

Figure 3.13 contains two electropherograms in which the same mixture of nine

peptides was analyzed by CITP, using either UV absorbance detection or MS

detection. The CITP conditions were identical in both cases, with one exception; in the

case of the CITP-MS analysis, the sample was pushed roughly 20 cm using

hydrodynamic pressure after the focusing step. This extra hydrodynamic push step

decreased the analysis time by approximately 9 minutes; of course the pressure induced flow profile reduces the separation efficiency. If this hydrodynamic push step was not used, the CITP-MS analysis time was approximately 30 minutes, a full 10 minutes longer than the same analysis by CITP-UV. Using a shorter capillary would decrease the analysis time; however, the current setup requires a minimum capillary length of 85 cm. In addition, the use of a shorter capillary would reduce the amount of sample injected. This lengthening of the migration time appears to be caused by the use of a sheath liquid as is explained below.

The resolution is considerably lower in the case of the CITP-MS electropherogram. The use of the hydrodynamic push step is not to blame for the large decrease in resolution. When the hydrodynamic push step is omitted, the resolution does not improve significantly. The slow scan rate of quadropole mass spectrometers, 1 Hz in this case, causes some decrease in resolution. An additional source of reduced resolution is the sheath fluid which, in addition to maintaining electrical contact between the capillary and the electrospray needle, serves as the cathodic buffer reservoir. The sheath fluid was 50:50:0.2, $MeOH:H_2O:HOAc$ while the BGE was 35 mM $\beta$ alanine adjusted to pH 3.2 with formic acid. The difference in composition between the anodic and cathodic

buffer reservoirs results in the formation of ionic boundaries in the capillary and causes decreased resolution and increases analysis time as shown by Foret et al.[20] In the study, the authors attribute the decrease in resolution to the larger injection volume in their CE-MS experiments as compared to the CE-UV experiments. However, equal injection volumes were used in this work and decreased resolution was still observed.
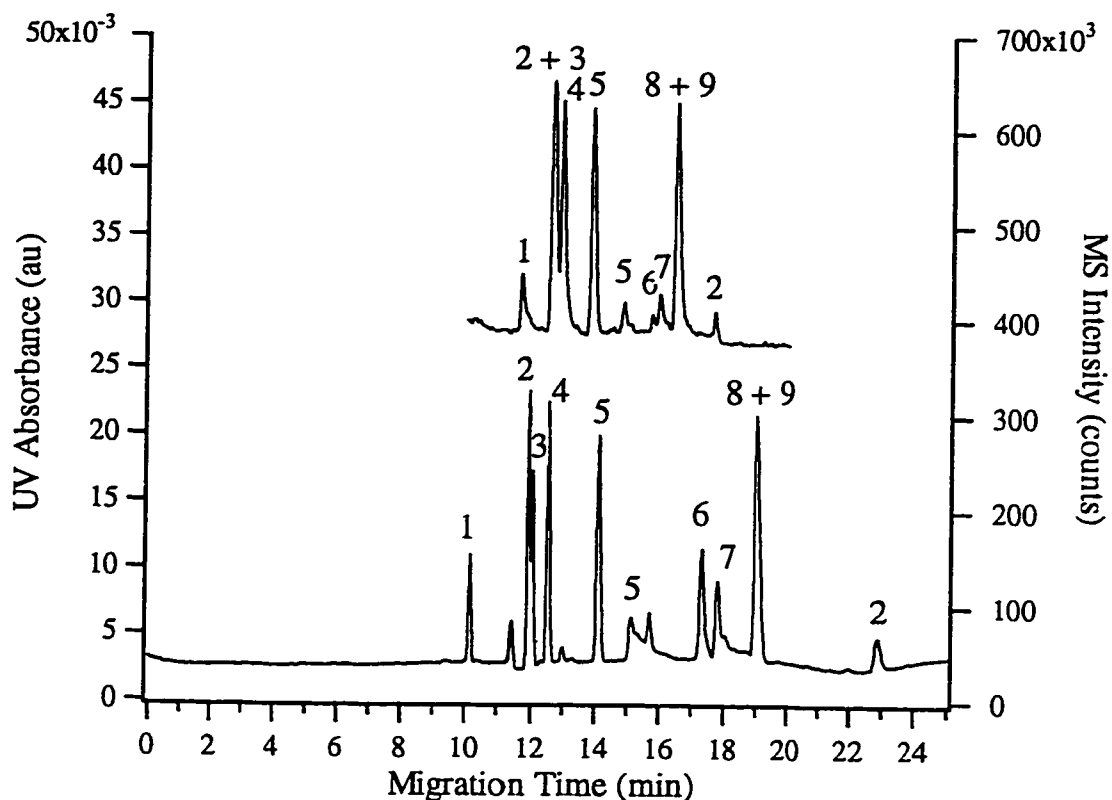
Figure 3.13 - Comparison of CITP-UV (lower trace) and CITP-MS of a mixture of standard peptides. Peak assignments (1) Dynorphin A (2) Angiotensin III (3) Dynorphin B (4) Bradykinin (5) Angiotensin I (6) Somatostatin (7) Substance P (fragment 2-11) (8) Angiotensin II (9) Cholecystokinin (fragment 10-20). CITP and MS conditions: sample concentration 1 μg/ml, injection volume 0.42 μl, other conditions, see experimental section. MS acquisition was started 10 minutes after the CE run voltage.

Clearly, further study of the effects of liquid sheaths is required. Interestingly, Pleasance *et al.* did not find a significant change in efficiency or in analysis time for CE-MS using a bare capillary at a basic pH.[18] However, in their case, the high EOF prevents formation of ionic boundaries in the capillary. In the present work, coated capillaries with negligible EOF were exclusively used.

## DETECTION LIMITS AND RECOVERIES:

Once optimized CITP conditions were established, mass detection limits were measured for CITP-MS in the SIR mode. 9 peptides were analyzed and two ions per peptide were recorded using a dwell time of 30 ms. The detection limits for CITP-MS using an injection volume of 420 nl are given in Table 3.2. The RSD for CITP-MS analysis was 4 %. In this laboratory, typical detection limits for CE-MS are in the low µg/ml range; therefore, the increased sample loading provided by CITP results in a 100-500 fold increase in sensitivity over CZE. However, these detection limits are still approximately 3 orders of magnitude higher than what is required for trace analysis of peptides.

The use of SPE prior to CITP-MS provided a further improvement in the concentration detection limit. Table 3.2 contains the detection limits for SPE-CITP-MS analysis. The RSD for the SPE-CITP-MS process was 13%. The detection limits are 4-5 orders of magnitude lower than those generally obtained by CZE and are suitable for many trace analysis applications. Note that the sample volume for SPE-CITP-MS is 2000 times greater than the sample volume for CITP-MS, therefore, the

mass detection limits of SPE-CITP-MS are higher than the mass detection limits of CITP-MS.

These detection limits are similar to those reported in the literature for analysis of peptides in plasma by SPE-HPLC.[21,22] Crowther *et al* reported detection limits of 2 ng/ml (2 pmol) for off-line SPE followed by HPLC-MS[23]. Tomlinson et al recently reported an improved method for off-line sample loading and cleanup followed by on-line SPE-CITP with MS detection in the full scan mode. They do not report detection limits but do obtain excellent S/N ratios for a peptide mixture at 50 ng/ml (250 fmol loaded).[13]

Table 3.2: Detection Limits for CITP-MS and SPE-CITP-MS analysis

| Peptide | CITP-MS | | SPE-CITP-MS | |
|---|---|---|---|---|
| | ng/ml | fmol | ng/ml | fmol |
| Angiotensin III | 1.7 | 0.77 | 0.02 | 17 |
| Angiotensin I | 2.7 | 0.87 | 0.03 | 18 |
| $Val^4$-$Ile^7$-Angiotensin III | 4.5 | 2.1 | 0.05 | 45 |
| $Asn^1$-$Val^5$-Angiotensin II | 6.0 | 2.4 | 0.05 | 39 |
| Bradykinin | 2.3 | 0.91 | 0.05 | 38 |
| $Sar^1$-$Gly^8$-Angiotensin II | 8.6 | 4.0 | 0.08 | 70 |
| Lys-Bradykinin | 40 | 14 | 0.3 | 130 |
| Dynorphin B | 10 | 2.7 | 0.5 | 250 |

*DL is based on a signal which is equal to $3\sigma_b$. For SPE-CITP-MS, DL is based on sample volume of 800 µl, final volume of 10 µl. For both methods, the injection volume was 420 nl, MS acquisition in SIR mode (2 ions per peptide), 30 msec dwell.

The SPE-CITP-MS detection limits were obtained by using an initial sample volume of 800 μl and a final sample volume of 10 μl. Therefore, the SPE-CITP-MS concentration detection limits should be exactly 80 times lower than the CITP-MS detection limits provided there are no sample losses. However, the recovery of the peptides is not quantitative and varies from peptide to peptide. The recoveries for SPE of 500 and 50 ng/nl peptide mixtures are given in Table 3.3. In general, the recoveries decrease as the peptide concentration decreases. This behavior is similar to that observed by Stausbauch et al. in on-line SPE-CE-UV experiments.[14] The recoveries for the analysis of plasma by SPE-CITP-MS were slightly lower than the recovery obtained for standards. For example, the recovery at a concentration of 20 ng/ml was 65% for angiotensin III in plasma. This decrease is probably due to the extra handling required for the removal of the plasma proteins.

Figure 3.14 contains electropherograms from SPE-CITP-MS analysis of various concentrations of peptides. The variation in relative heights of the peaks results from the variation in recovery among the different peptides. The peak at a migration time of 12 min corresponds to angiotensin I. This peptide has the highest recovery and is also the most acidic peptide (pI = 7.0) in the mixture. Lys-bradykinin (pI = 12.6) is the most basic peptide and has one of the lowest recoveries. Although not explicitly discussed, this behavior is also observed in on-line SPE-CE.[14] The pI and sequence of the peptides are
included in table 3.3.

The recoveries listed above are for SPE performed using a mixture of membranes. However, initial SPE work was performed using only one layer of SDB-XC membrane, in which case the peptide recovery was typically 50-70%. When two SDB-XC membranes were used, the range of recoveries increased to 66-91%. In an

effort to further increase the recovery, adsorbents with different functional groups were combined in one tip. The peptide recovery obtained using these mixed phases was higher that the recovery obtained if only one type of adsorbent was used. The results are shown in figure 3.15. The reason for the improvement in recovery when mixed phases were used is not immediately obvious; perhaps the membranes have complimentary affinities for peptides.

Table 3.3: Physical Properties and Recoveries for Various Peptides

| Peptide | Sequence | pI | % Recovery* 500 ng/ml | 50ng/ml |
|---------|----------|-----|--------------|---------|
| Angiotensin III | RVYIHPF | 10.5 | 107 | 78 |
| Angiotensin I | DRVYIHPFHL | 7.0 | 116 | 89 |
| Val$^4$-Ile$^7$-Angiotensin III | RVYVHPI | 10.5 | 103 | 86 |
| Asn$^1$-Val$^5$-Angiotensin II | NRYYVHPF | 10.3 | 76 | 86 |
| Bradykinin | RPPGFSPFR | 10.1 | 83 | 65 |
| Sar$^1$-Gly$^8$-Angiotensin II | Sar-RVYIHPG | 10.5 | 116 | 108 |
| Lys-Bradykinin | KRPPGFSPFR | 12.6 | 79 | 67 |
| Dynorphin B | YGGFLRRQFKVV | 11.7 | 82 | 63 |
| Average | NA | 10.4 | 95 | 80 |

*Recovery is for SPE using a mixed SDB/C18 tip, n=3 , the RSD for SPE-CITP-MS was ca. 13%

69
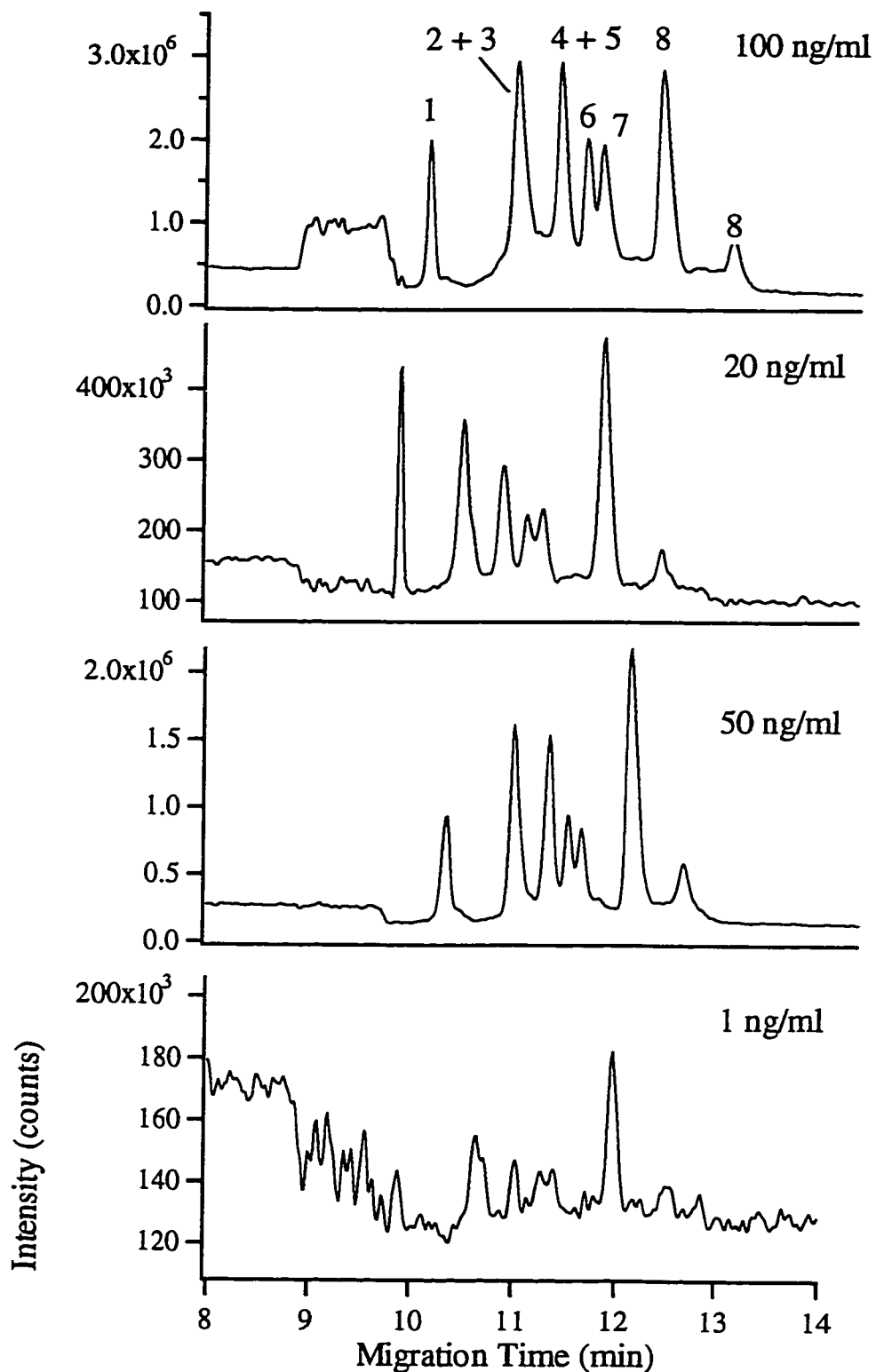
Figure 3.14 - Comparison of SPE-CITP-MS analysis of 100, 50, 20 and 1 ng/ml peptide standards. SPE conditions: SDB-C18 + SDB-XC mixed phase, sample volume 800 ml. Peak assignment: (1) Lys-Bradykinin (2) $Val^4$-$Ile^7$-Angiotensin III (3) $Sar^1$-$Gly^8$-Angiotensin II (4) Angiotensin III (5) Dynorphin B (6) Bradykinin (7) $Asn^1$-$Val^5$-Angiotensin II (8) Angiotensin I.
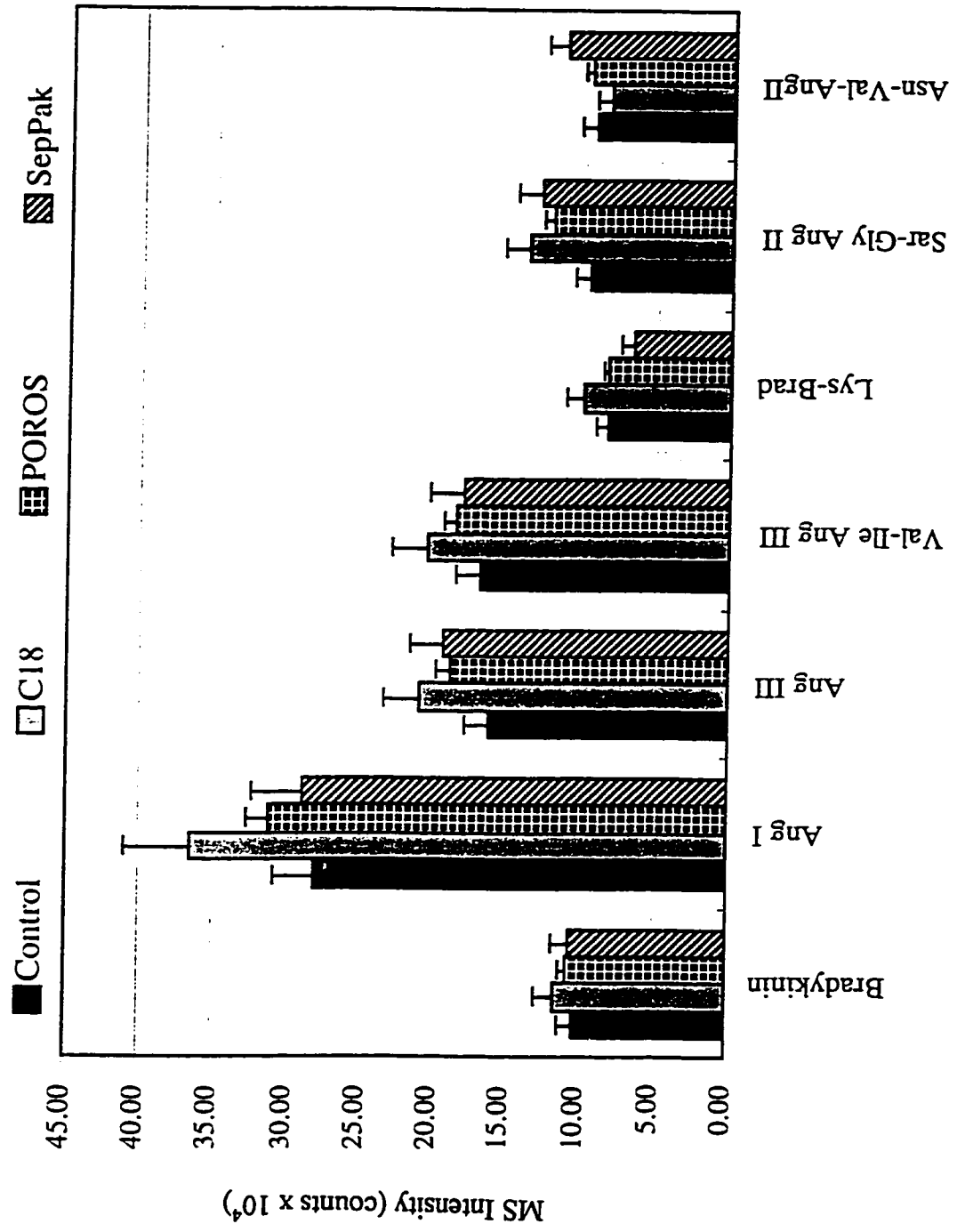
Figure 3.15 - Comparison of recovery for simple and mixed phase SPE.

71

The use of SPE with mixed phase adsorbents increased the sensitivity by approximately two orders of magnitude. This increase is based on a sample size of 1 mL. Greater improvements would be obtained with larger volume samples, albeit at the expense of an increase in analysis time. The improvement in sensitivity is demonstrated in figure 3.16. Figure 3.16 contains electropherograms of a mixture of standard peptides analyzed by CITP-MS and SPE-CITP-MS. This concentration of the peptides is 100 ng/ml in both cases. The figure also contains extracted ion electropherograms (XIE) for four of the peptides. These XIE's aid in comparing the intensities and demonstrate the specificity of MS detection.

## ANALYSIS OF PEPTIDES IN PLASMA BY SPE-CITP-MS:

The analysis of peptide standards is relatively simple and, therefore, useful for initial evaluation of the SPE materials and extraction parameters. In order to demonstrate the usefulness of the technique for the analysis of complex biological samples we analyzed for peptides in human plasma. The analysis of plasma by CZE presents three challenges. The first is overcoming the problems, most notably wall adsorption, encountered when samples containing proteins are analyzed by CZE. The second is to avoid the degradation in efficiency caused by high amounts of electrolytes in the sample matrix. The third is the reduction of the large gap between sensitivity obtained in CZE and the sensitivity required for trace analysis. CZE with absorbance detection provides detection limits in the mid $\mu g/ml$ range; however, endogenous peptides are present at the pg/ml to ng/ml levels.

Plasma contains albumin and globulins at a total concentration of approximately 70 mg/ml. In addition to the well known problem of protein adsorption
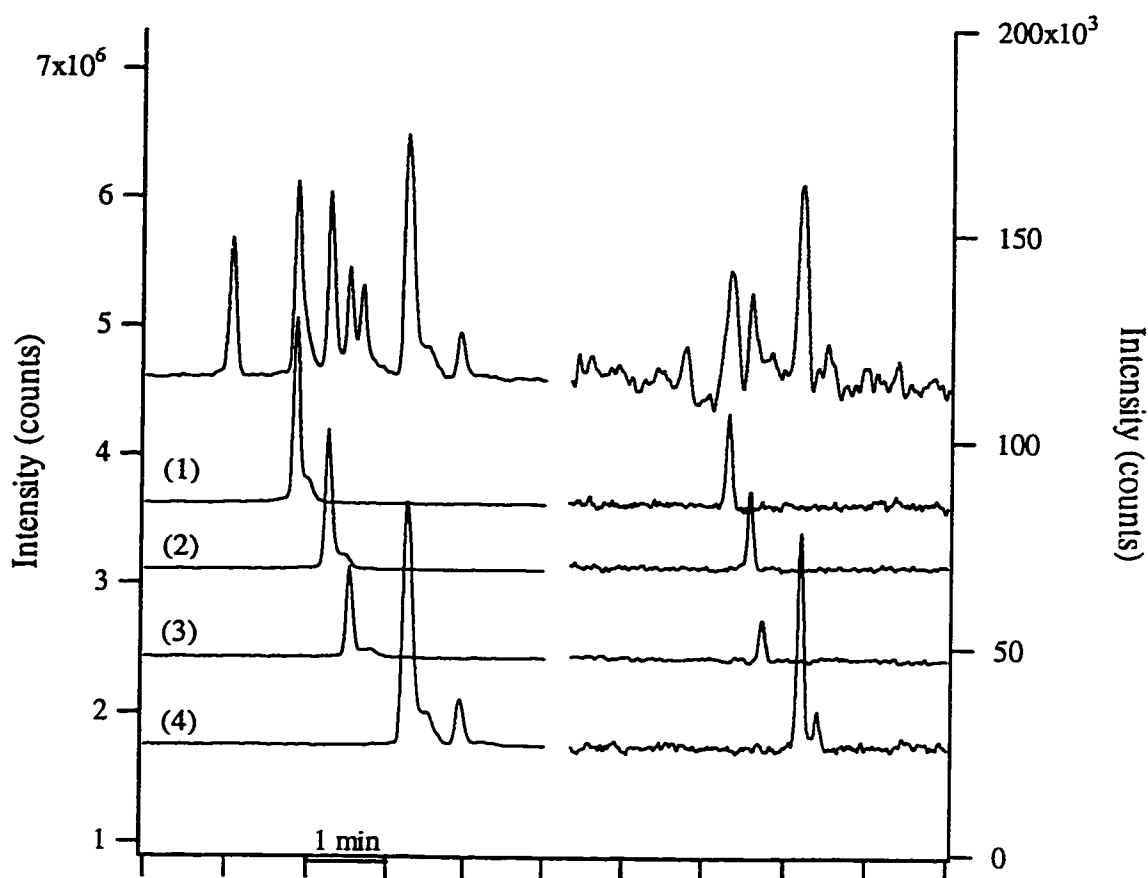
Figure 3.16 - Comparison of sensitivity: (A) 100 ng/ml standard analyzed by CITP-MS & 100 ng/ml standard analyzed by SPE-CITP-MS. (A) and (B) are the SIE for 18 ions. The electropherograms below are extracted ion electropherograms for (1) $Val^4$-$Ile^7$-Angiotensin III, $MH_2^{2+}$, m/z = 442.3 (2) Angiotensin III, $MH_2^{2+}$, m/z = 466.5, (3) Bradykinin, $MH_2^{2+}$, m/z = 531, (4) Angiotensin I, $MH_3^{3+}$, m/z = 433.2

to capillary walls, proteins can also clog SPE materials. The membrane used here is composed of adsorptive beads physically trapped in a polymer mesh support. The manufacturer states that the mean pore size is only 0.08 $\mu$m. Therefore, the plasma proteins would clog such a membrane. Typically 50-100 microlitres of whole plasma could be passed through the membrane before clogging occurred. Therefore, the proteins were removed by precipitation with acetonitrile followed by pelleting by centrifugation. This process removes the majority of the proteins. Clogging of the SPE material did occur if some of the protein pellet was inadvertently collected with the supernatant.

In addition to proteins, plasma contains electrolytes such as $Na^+$, $K^+$, $Cl^-$, $HCO3^-$, at a total concentration of approximately 160 mM. Electrolytes usually interfere with stacking techniques such as CITP. In particular techniques such as field amplification and electroextraction rely on the sample being present in a low ionic strength medium. In this work, where reversed phase membranes were used, electrolytes and other non-adsorbed materials were removed by rinsing the membrane with water after sample application. This process did not remove detectable amounts of peptides.

The use of SPE followed by CITP-MS provides detection limits between 20 and 500 pg/ml using the SIR mode. This level of sensitivity is a $10^4$ fold improvement over typical CE-MS detection limits. Peptides in plasma are present in the low pg/ml range to the high ng/ml range. Obviously, further improvements in sensitivity are desirable, especially if peptide sequencing via MS-MS analysis is desired.

The use of MS detection is critical to the analysis of peptides, or any analyte, in complex samples such as plasma. In figure 3.17, a total ion electropherogram (TIE) for the analysis of plasma by SPE-CITP-MS is given. The complexity of the sample is evident from the figure. Even with the high resolving power of CE and the sample
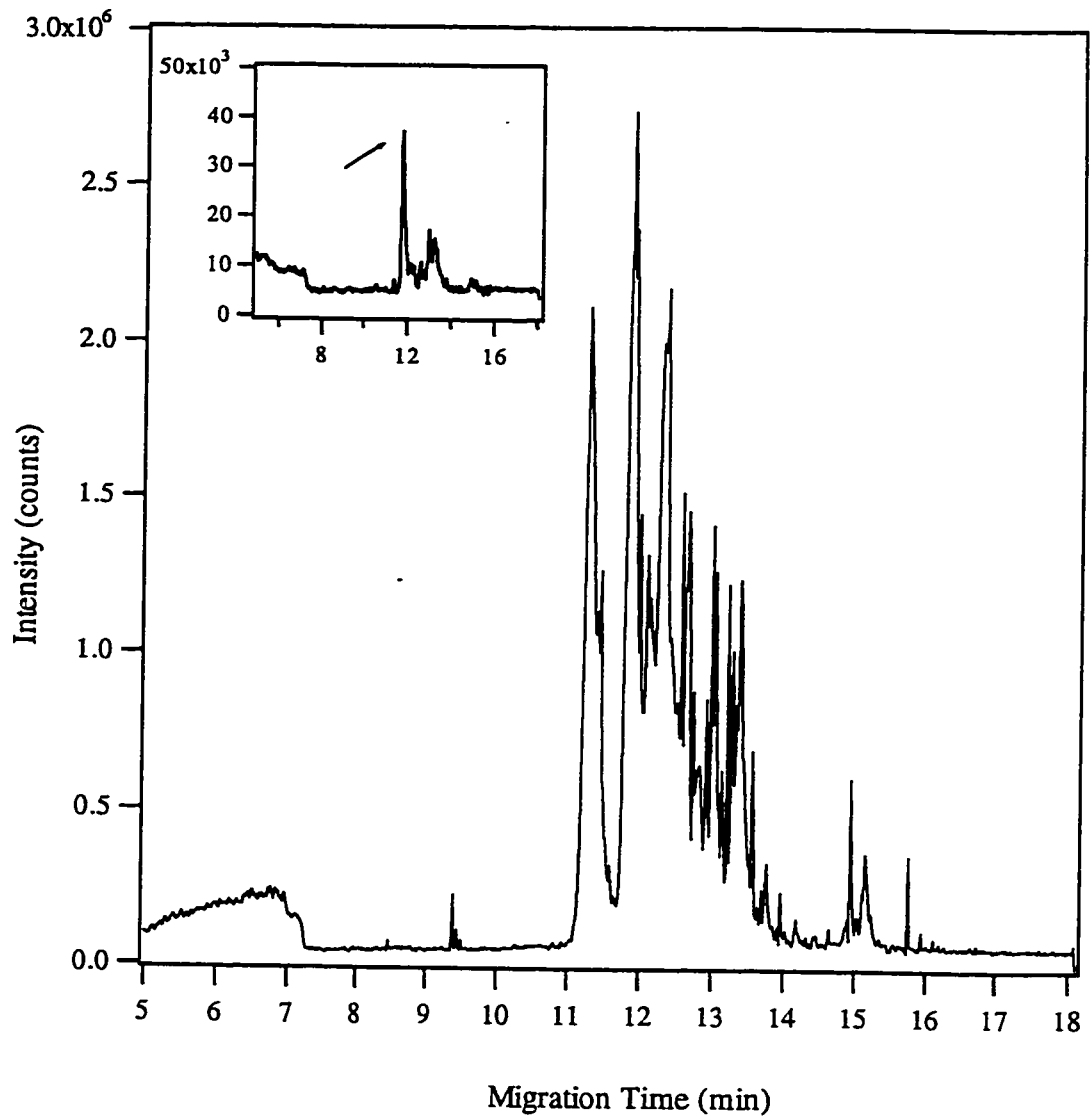
Figure 3.17 - TIE of plasma analyzed by SPE-CITP-MS. Initial sample volume : 1 ml, final volume after SPE: 10 μL. MS Conditions: full scan, m/z = 350-1400, 4 msec dwell. Inset: extracted ion electropherogram for bradykinin.

cleanup via SPE, many of the sample components co-migrate. In the case of plasma analysis by SPE-CITP with UV absorbance detection, the sensitivity was limited by the noise caused by comigrating or poorly resolved components, not by the poor sensitivity of absorbance detection. In such cases MS detection is useful in both a qualitative and quantitative sense as is demonstrated in the inset of figure 3.17. This inset contains a plot of the intensity at m/z = 531, the mass of the $(MH_2)^{2+}$ ion of bradykinin, versus migration time. In the case of MS detection, comigrating components do not interfere with detection, unless of course they are isobaric with the analyte. Even in this case, tandem MS can be used to differentiate the two analytes.

Tandem MS also provides unambiguous confirmation of the peak identity. This ability is demonstrated in figure 3.18, which contains the MS-MS spectrum bradykinin in plasma sample analyzed by SPE-CITP-MS. An MS-MS spectrum of bradykinin standard is included for comparison. These spectra provide unambiguous peak identification and sequence information.
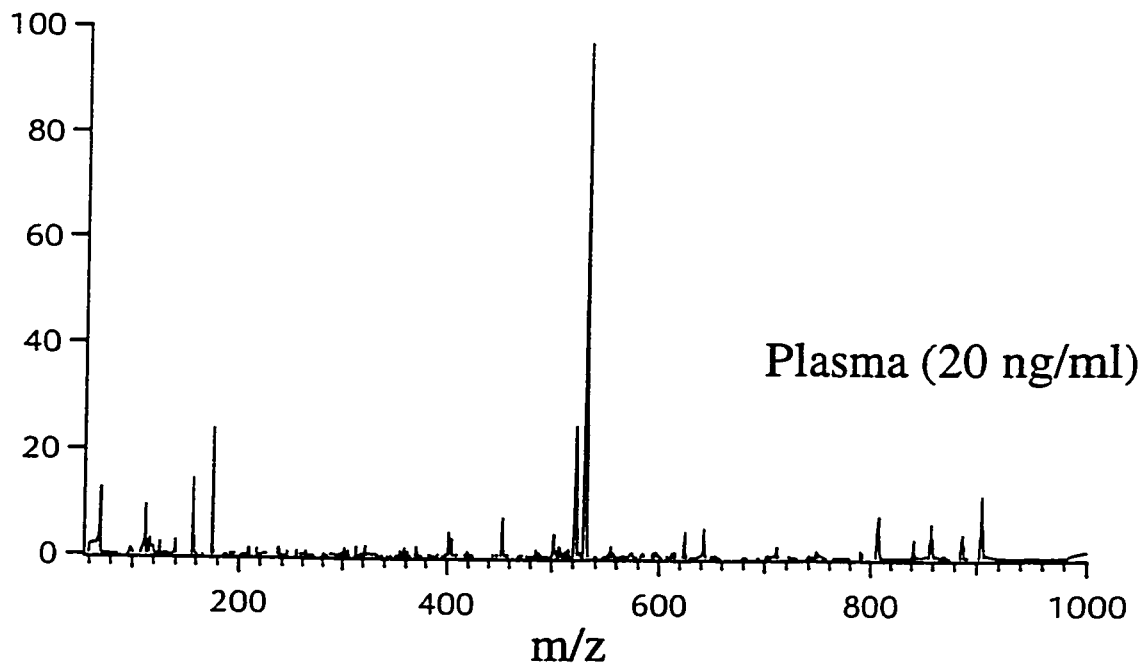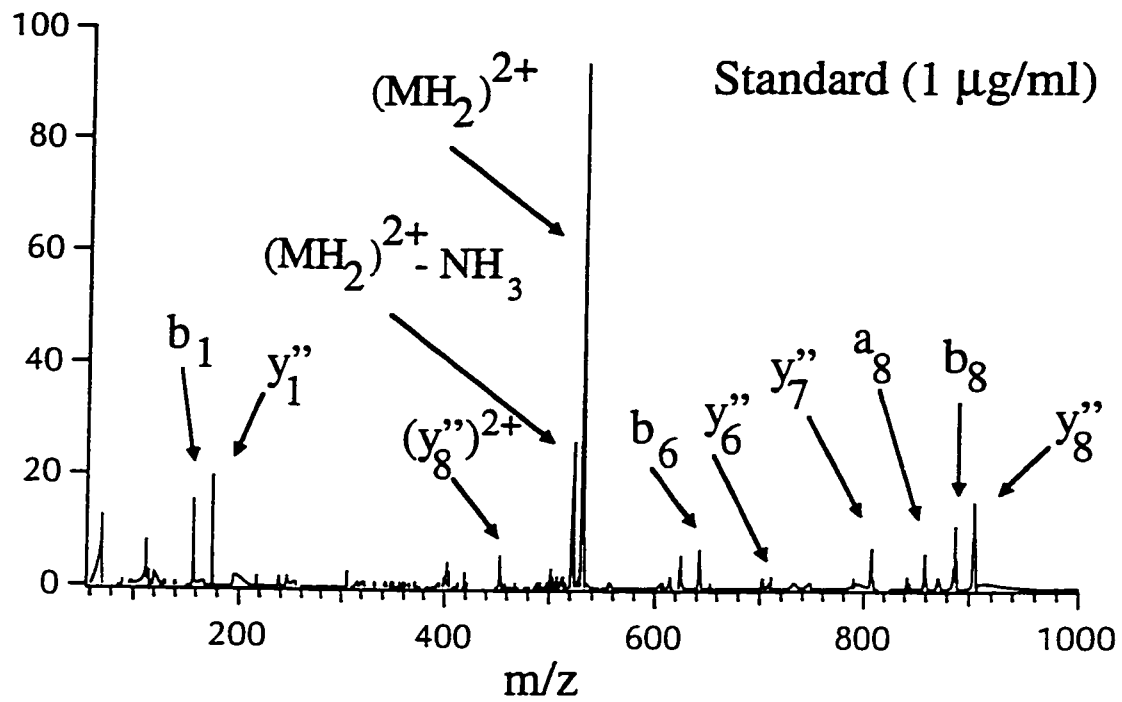
Fig. 3.18    SPE-CITP-MS-MS analysis of bradykinin in plasma

## 3.4 CONCLUSIONS

Techniques such as field amplification and CITP provide a simple method to decrease the concentration detection limits of CE. However, for complex matrices like plasma, coeluting sample components often limit the sensitivity obtained. The use of SPE followed by CITP and MS detection provides both the specificity and sensitivity required for the analysis of complex samples. The concentration sensitivity of the overall SPE-CITP-MS technique is comparable to that of HPLC and the mass detection limits are orders of magnitude lower.

# REFERENCES

[1] Karger, B. L., Szoko, E. and Foret, F., *Electrophor.*, 14, 417, 1993.

[2] van der Vils, E., Mazereeuw, M., Tjaden, U.R., Irth, H., and van der Greef, J., *J. Chromatogr. A.*, 712, 1995, 227-234.

[3] Palmarsdottir, S and Edholm, L.-E., J. Chromatogr. A., 693, 1995, 131-143

[4] Chen, D. Y., and Dovichi, N. J., *J. Chromatogr. B.*, 1994, 265-269.

[5] Lee, T. T.; Yeung, E. S. *J. Chromatogr.* 1992, 595, 319-325.

[6] Chien, R-L and Burgi, D.S., *Anal. Chem.*, (1992), 64 (8): 489A.

[7] CRC handbook of Capillary electrophoresis, pp. 113-116.

[8] Mazereeuw, M., Tjaden, U. R. and Reinhoud, N. J., *J. Chromatogr. Sci.*, 1995, 33, 686-696.

[9] Krishnana, T. R., Ibraham, I, *J. Pharm.Biomed. Anal.*, 1994, 12, 287-294.

[10] Majors, R. E., *LC-GC*, 1995, 13, 542-552.

[11] Hendrikson, T. L., Wilson, G. S., *J. Chromatogr. B.*, 1994, 653(2):147-54.

[12] Tomlinson, A. J., Guzman, N. A., Naylor, S., *J. Cap. Electrophor.*, 1995, 2, 247-255.

[13] Tomlinson, A. J., Benson, L. M., Guzman, N. A., Naylor, S., *J. Chromatogr. A.*, 744, 1996,

[14] Strausbauch, M. A., Landers, J. P., Wettstein, P. J., *Anal. Chem.*, 1996, 68, 306-314.

[15] Tomlinson, A. J., Benson, L. M., Jameson, S., Naylor, S., *Electrophor.*, 1996, 17, 1801-1807.

[16] Chiari, R., Lopez, C. and Righetti, P.G., *Electropho.*, 1996, 18, 127-136.

[17] K. A. Cobb, V. Dolnik, M. Novotny, *Anal. Chem.*, 62, 1990, 2478-2483.

[18] Pleasance, S., Thibault, P., Kelly, J., *J. Chromatogr. A.*, 1992, 591, 325-339.

[19] Reinhoud, N. J., Tjaden, U. and van der Greef, J., *J. Chromatogr. A.*, 1994, 673, 239-253.

[20] Foret, F., Thompson, T. J., Vouros, P., Karger, B. L., Gebauer, P., and Bocek, P., 66, *Anal. Chem.* 1994, 4450-4458.

[21] Monger, L. S., and Olliff, C. J., *J. Chromatogr. A.*, 1992, 577(2), 239-249.

[22] Kukucka, M. A.and Misra, H. P., *J. Chromatogr. B.*, 1994, 653(2), 147-154.

[23] Crowther, J., Adusumalli, Mukherjee, T., Jordan, K, Abuaf, P., Corkum, N., Goldstein, G. and Tolan, J., *Anal. Chem.*, 1994, 66, 2356-2361

# CHAPTER 4

# TRACE ANALYSIS OF PROTEINS BY CAPILLARY ELECTROPHORESIS

## 4.1 INTRODUCTION

The previous chapter mentioned the lack of sensitivity of current methods for peptide analysis by CE. The same is true for protein analysis.[1,2] Unfortunately, concentration detection limits of UV absorbance in capillary electrophoresis often fall in the micromolar range. In biological samples, improved sensitivity is required to analyze most proteins since they are present at nanomolar concentrations.

Techniques developed to decrease the concentration detection limit fall into two major categories: high sensitivity detection and sample enrichment. Examples of the latter include field amplification[3,4] capillary isotachophoresis[5], capillary isoelectric focusing[6], on-capillary concentration using reversed phase adsorbents[7], and on-column concentration using a small-pore plug[8]. These methods improve the concentration detection limit by approximately two orders of magnitude. Examples of high sensitivity detection methods include laser-induced fluorescence (LIF), thermo optical absorbance, and mass spectrometry[9-15]

LIF detection is divided into methods: native fluorescence, which uses UV lasers; and visible fluorescence with uses lasers in the visible region. The UV lasers emit near 250 nm and excite the protein's aromatic amino acids, with tryptophan being the most important. When combined with on-column stacking, native fluorescence has generated subnanomolar detection limits for large proteins such as bovine serum albumin (BSA) and conalbumin.[9] Tryptophan is a relatively rare amino acid, and not all

81 81

proteins will generate useful native fluorescence signals. Also, lasers that operate in the ultraviolet region tend to be expensive and somewhat temperamental in operation. On the other hand, lasers that operate in the visible portion of the spectrum tend to be rugged and relatively inexpensive. However, derivatization of the protein is necessary since they do not posses fluorophores that are excited with visible lasers.

This group recently reported the use of low power lasers with a sheath flow cuvette to achieve a detection limit of 6 molecules of a rhodamine dye and single molecules of the highly fluorescent protein β-phycoerythrin.[16,17] To extend this technology to the analysis of biomolecules, we have developed fluorescent labeling schemes for the analysis of DNA, peptides, sugars, and amino acids.[18-21]

Fluorescent labels such as fluorescein isothiocyanate (FITC) and fluorescamine, have been used for pre-column labeling of peptides.[22,23] Reactions are usually performed with proteins at millimolar concentrations followed by dilution by several orders of magnitude before analysis. However, most fluorescent labeling reagents undergo hydrolysis in aqueous environments. The presence of these competing reactions necessitates the use of high concentrations of labeling reagents, typically in the millimolar range, in order to obtain efficient labeling. Unfortunately, the high background signal from excess fluorescent reagent and hydrolysis products often swamp the fluorescence signal from dilute protein solutions. More problematic, impurities present at the part-per-million level in the fluorescent labeling reagent create a forest of background peaks that inevitably interferes with the protein signal.

An attractive alternative to aqueous-phase labeling is solid-phase labeling. We recently demonstrated that, in the case of a peptide, the use of solid-phase labelling

avoids some drawbacks of pre-column labeling.[18] Several applications of solid-phase labeling using immobilized reagents have been developed. Krull *et al.*, who have performed much of this work, recently published a review of the topic.[24] While attractive for the analysis of small molecules and peptides, solid-phase labeling of proteins has not been demonstrated.

Fluorogenic reagents are an attractive alternative to traditional derivatizing agents for protein labeling.[25] These non-fluorescent reagents form a fluorescent product when they react with primary amines. Unfortunately, fluorogenic reagents also react slowly to form secondary fluorescent products.[21] Nevertheless, the use of a fluorogenic derivatizing reagent in place of a fluorescent reagent reduces the background by orders of magnitude.

Pre-column labeling of proteins can degrade separation efficiency due to the heterogeneity of the reaction products formed from multiple labeling. If amino groups are targeted, then both the n-terminus and lysine ε-amino groups can be labeled. For a protein with $n$ free amino groups (n-terminus plus lysine residues), there are $2^n - 1$ possible products.[26] For ovalbumin, a glycoprotein that has 20 lysine residues plus an n-terminus, there are 1,048,575 possible reaction products. If each product has a different mobility, the resulting electropherogram is far too complex to be useful. In practice, multiple labeling results in broad peak profiles and low plate counts.[9,22]

Our group reported a method for eliminating multiple labeling in peptides based on the use of phenyl isothiocyanate to block lysine's ε-amino group.[26] Unfortunately, the reaction chemistry is cumbersome. Post-column labeling is another method designed to take advantage of the sensitivity of LIF detection.[27] However, the

mixing of the capillary eluent and the labeling reagent can result in severe degradation of separation efficiency.

This chapter presents an improved method for pre-column labeling for the analysis of proteins at picomolar concentrations. We also demonstrate that optimization of reaction and separation conditions minimizes band broadening due to multiple labeling. The separation efficiencies are comparable to those of CZE of non-derivatized proteins.

## 4.2 EXPERIMENTAL

### 4.2.1 Instrumentation

Experiments were carried out using either a Waters Quanta 4000 CE instrument with a UV absorbance detector, a Beckman 5010 P/ACE instrument with an on-column LIF detector, or an in-house constructed CE-LIF instrument with a detector based on a sheath flow cuvette as previously described.[28,29] Unless otherwise stated, 50 cm × 50 μm (i.d.) bare fused-silica capillaries (Polymicro Technologies, Phoenix, AZ) were used. The 488-nm line from an argon-ion laser and a 615DF45 interference filter were used in the Beckman CE instrument. Absorbance measurements were at 214-nm.

The in-house instrument used a 0-30 kV DC power supply (CZE1000, Spellman, Plainview, NY). For the sheath-flow cuvette detector, excitation was provided by the 488-nm line of an argon-ion laser operated at 12 mW (Model 2211-15SL, Uniphase, San Jose, CA or Model Innova 90-4, Coherent, Mountain View, CA), which was focused approximately 30 μm from the tip of the capillary with a 6.3 × objective (Melles Griot, Nepean, ON, Canada). Fluorescence was collected by a 60

x, 0.7 NA microscope objective (MO-0060LWD, Universe Kokagu, Oyster Bay, NY),

filtered with a spatial filter to remove stray light and either a 615DF45 or a 630DF30

bandpass filter (Omega Optical, Brattleboro, VT) to remove scattered light, and

imaged onto a photomultiplier tube (R1477, Hamamatsu, Middlesex, NJ) biased at

either 1.0 or 1.2 kV. The photocurrent was passed through a current to voltage

converter and a low pass filter

(RC = 47 ms) and then digitized with a 16 bit data acquisition board (NB-MIO16XH-

18, National Instruments, Austin, TX) connected to a Macintosh computer.

The critical micellar concentration (CMC) of SDS in borax buffer was

determined using a Model 1650-A impedance bridge from General Radio Company

(Boston, MA). The DC conductivity of the solution was measured as SDS was added

to 2.5 mM borax, pH 9.5 at 24°C. The measurement was made for SDS concentrations

ranging from 0 to 15 mM and the CMC was determined graphically.


## 4.2.2 Reagents

Sodium tetraborate (borax) and sodium dodecyl sulfate (SDS) were purchased from

BDH (Toronto, ON, Canada). Enzyme grade 4-(2-hydroxyethyl)-1-

piperazineethanesulfonic acid (HEPES) was purchased from Fisher Scientific (Fair

Lawn, NJ). 2-mercaptoethanol was purchased from Caledon Laboratories ltd.

(Edmonton, AB, Canada). Tricine was purchased from Sigma (St. Louis, MO).

Preconcentration spin-tubes were purchase from Centricon (Andover, MA). For most

CZE experiments the running and sheath flow buffers were 2.5 mM borax and 5 mM

SDS. For some CZE experiments, 25 mM Tricine (pH 8.0) was used as the running

buffer. The running and sheath flow buffer for CGE experiments was 5 mM HEPES and 5 mM SDS. All buffers were made with Milli-Q deionized water and were filtered using a 0.2-μm filter. Proteins were used as received from Sigma (St. Louis, MO) and dissolved in 2.5 mM borax pH 9.4. Derivatizing reagents, 5-furoylquinoline-3-carboxaldehyde (FQ) and potassium cyanide (KCN), were purchased from Molecular Probes (Eugene, OR). KCN was dissolved in 2.5 mM borax buffer at a concentration of 25 mM. A stock solution of 10 mM FQ was prepared in methanol, 10-μL aliquots were then placed into 500-μL microcentrifuge tubes and the solvent removed under vacuum using a Speed Vac (Savant Instruments Inc., Farmingdale, NY). The dried FQ aliquots were stored at -20 °C. These precautions were necessary since FQ degrades slowly in solution, even if the solutions are stored at -20 °C. Degradation is particularly prominent during repeated freeze-thaw cycles.

4.2.3 Capillary Zone Electrophoresis

Derivatization was typically performed by adding 9 μL of protein solution and 1 μL of 25 mM KCN to a vial containing 100 nmol of previously dried FQ. Reaction times between 10 s and 1 hr were used. Reaction vials were protected from light as much as possible.

Separations were performed in uncoated capillaries at electric fields ranging from 400 V/cm to 700 V/cm. To reduce the background signal, the polyimide coating was removed from the last few millimeters of the capillary using a gentle flame. Samples were introduced electrokinetically.

### 4.2.4 Denaturing gel electrophoresis

Denaturing gel electrophoresis was performed with 10 μl of solution containing ovalbumin, BSA, conalbumin, myoglobin, carbonic anhydrase, all at a concentration of

$10^7$ M. The sample was prepared in 2.5 mM borax buffer, pH ~9.4, containing 50 mM SDS and 1% 2-mercaptoethanol, and was heated at 95 °C for five minutes to denature the proteins. This denatured protein solution was derivatized by mixing 7 μL of the solution with 100 nmol dry FQ and 3 μL of a 5 mM KCN solution. The mixture was incubated for 10 min at room temperature. The solution was then diluted to 100 μL with deionized water. The same procedure was used for the blank except 2.5 mM borax was substituted for the protein solution.

The mixture was separated in a 7.5% dextran (molecular weight = $2 \times 10^6$) solution that was prepared in a buffer made from 5 mM HEPES (pH = 8.0) and 5 mM SDS. The capillary was coated with 3% polyacrylamide on a vinyl sublayer according to the method of Cobb *et al.*[30] The capillary was equilibrated with the HEPES/SDS running buffer by applying a 1 kV/cm electric field for 10 min. The sample was injected for 5 s at 1 kV/cm; separation was also at 1kV/cm. The dextran was replaced between each run.

### 4.3 RESULTS AND DISCUSSION

This section presents a method for labelling and analysis of proteins by CE-LIF. The success of the method relies on the use of sodium dodecyl sulphate (SDS) as a buffer additive; therefore, the behaviour of SDS in solution and SDS-protein

interaction are discussed first. Examples of labelled protein separations by sub-micellar CE and capillary gel electrophoresis are then presented followed by a discussion of optimal labelling conditions. This section concludes with a comparison of CE-LIF with other detection schemes for protein analysis by CE.

### 4.3.1 Behaviour of SDS in aqueous solution

The ambiphilic nature of the SDS results in complex solution behaviour. At low concentrations, SDS is presented as individual, solvated molecules. Above a certain concentration, called the critical micelle concentration (CMC), SDS is presents as individual molecules and spherical micelles. In aqueous solutions, the anionic sulphate groups are at the surface of the micelle whereas the hydrophobic $C_{12}$ tails align towards the sphere's core.

Figure 4.1 contains the data used to calculate the CMC. There are two major regions in the graph. At low concentrations, the SDS is present as monomers and at SDS concentrations above the CMC, which is 6.4 mM, there are both micelles and monomers present. In the gradual transition between these two regimes, SDS monomers and portions of micelles, but no full micelles, are present. The SDS concentration used for most experiments was 5 mM, which is in this transition region.

### 4.3.2 Separation of labelled proteins

SDS is essential for the separation of labelled proteins. As mentioned, labelling of analytes that posses multiple sites for labelling produces a mixture of products. This problem is called multiple labelling. In the absence of SDS, multiple

labelling causes excessive band broadening. In this section, the role of SDS in protein separations is discussed simultaneously with the labelling process.

The behaviour of proteins in the presence of SDS appears to depend on the phase(s) of SDS present. Specifically, two regimes are present; sub-micellar, and micellar. Ovalbumin, since it consists of several glycoforms with similar mobility, is a useful model protein to study both the effects of SDS and the effects of multiple labelling. This section begins with analysis of labelled ovalbumin in free solution, i.e. in the absence of SDS, followed by analysis in sub-micellar and micellar regimes. A discussion of the behaviour of native BSA and native ovalbumin in the three regimes follows.

Free solution separations

Ovalbumin's glycoforms are resolved by free solution electrophoresis. Curve A in Figure 4.2 represents the free solution electropherogram of ovalbumin labeled with FQ using a 60 s reaction time, and is compared to a UV absorbance electropherogram of unlabeled ovalbumin, curve B. The profiles are similar; the partially resolved peaks are glycoforms of ovalbumin.[31,32] The similarity in profile between electropherograms A and B demonstrates that broadening due to multiple labeling is not significant for the short reaction time.

When the reaction time is increased to 10 min, broadening associated with multiple labeling increases and the glycoforms are no longer distinguishable, curve C of Figure 4.2. Presumably, the complex mixture of reaction products generates a broad envelope under electrophoretic analysis. In this buffer system, which does not contain SDS, an increase in reaction time causes a loss of separation efficiency.
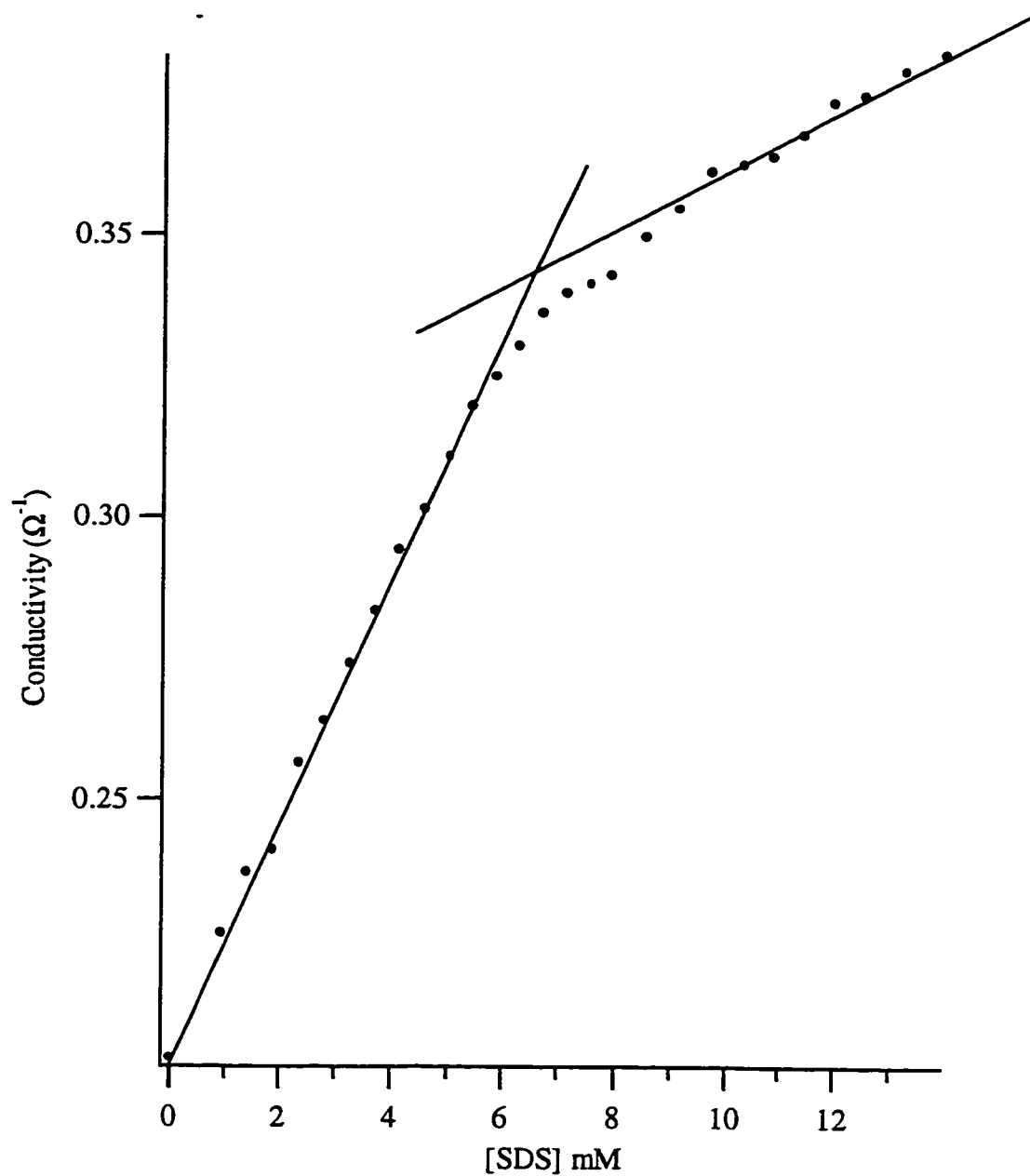
Figure 4.1 - Determination of the critical micellar concentration (CMC) of SDS in 2.5 mM borax at room temperature.
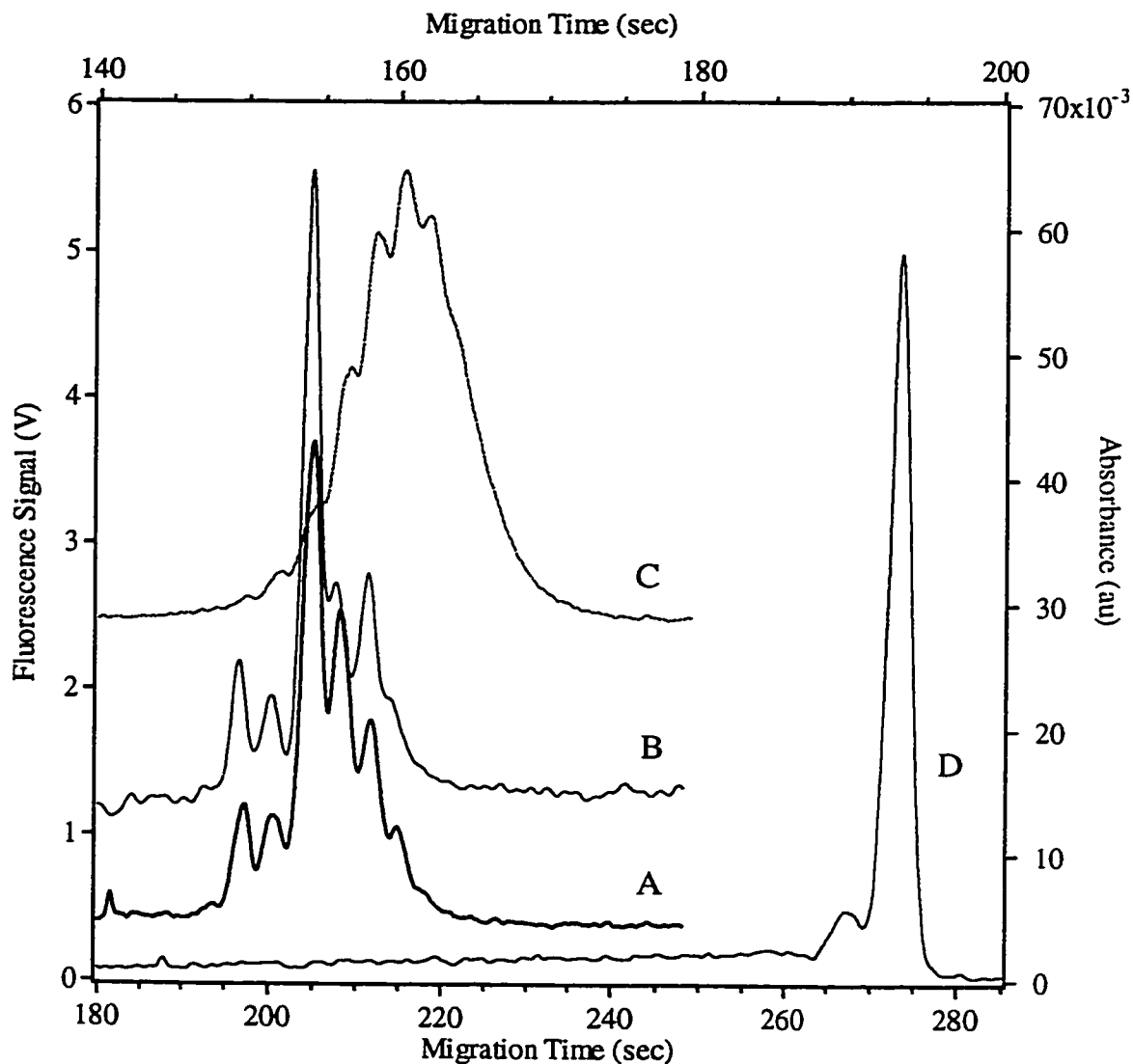
Figure 4.2 - Comparison of ovalbumin analyzed under various conditions. Running buffer: (A)-(C): 25 mM Tricine, pH = 8.0 (D) 25 mM tricine + 5 mM SDS
(A) FQ-labeled ovalbumin, 15 s reaction, LIF detection; $t_m$ = 205.2 s
(B) Unlabeled ovalbumin, UV absorbance detection, $t_m$ = 150.8 s
(C) FQ-labeled ovalbumin, 10 min. reaction, LIF detection; $t_m$ = 215.5 s
(D) FQ labeled ovalbumin, 1 min reaction, LIF detection, $t_m$ = 272.6 s.
Note that electropherogram (B) is plotted versus top x-axis and right y-axis.
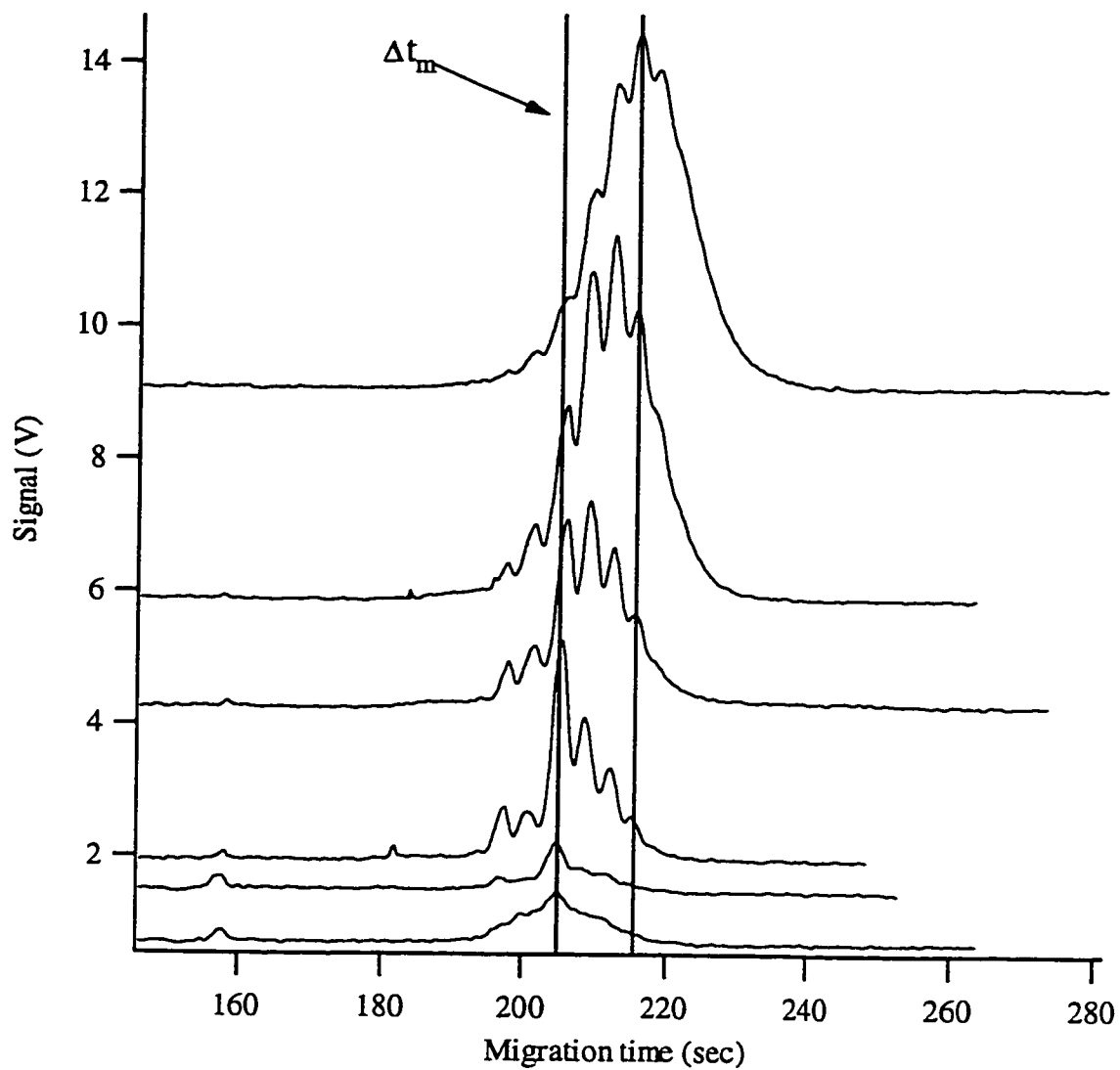
Figure 4.3 - Labelling of Ovalbumin with FQ. Reaction times were, from bottom to

top, 0.12, 0.25, 1, 2.5, 5 and 10 minutes. CE conditions: see Fig. 1. $\Delta t_m = 5$ s.

Figure 4.3 contains electropherograms generated from a sequence of reaction times. The conversion of the cationic lysine residues to neutral FQ labelled lysine residues causes the shift to longer migration times as the reaction proceeds. The electropherograms for the first two stages of the reaction do not resemble the electropherogram of unlabelled ovalbumin. Perhaps, the short reaction time results in a highly heterogeneous product.

This data demonstrates that a short reaction time of 1 min is useful for preserving efficiency. However, these short reaction times do not provide high sensitivity, which is why fluorescence labelling was used in the first place. Therefore, a technique that preserves separation efficiency at long reaction times is required.

Sub-micellar separation

The high efficiency separation at long reaction times is recovered by the addition of 5 mM SDS to the buffer, curve D in Figure 4.2. All information on glycosylation status is eliminated, and the complex and broad envelope of peaks collapses to a single, narrow peak. The surfactant interacts with sugars,[31] which apparently counteracts the mobility difference induced by the sugars. The addition of SDS to the running buffer generated a similar improvement in efficiency for all proteins studied. For example, Figure 4.4 contains the electropherograms for the analysis of FQ labelled BSA in a sub-micellar regime and the separation of unlabelled BSA in free solution. The peak efficiency of the FQ-BSA in the free solution analysis, at only 4000 theoretical plates, reflects the significant broadening caused by multiple

labelling. The addition of 5 mM SDS to the running buffer increases the efficiency to 125,000 plates, which is twice the efficiency obtained for the unlabelled BSA.

The interactions between SDS and proteins are complicated. SDS, present at high concentrations, complexes with denatured proteins in polyacrylamide gel electrophoresis (SDS-PAGE). The interactions occur between the protein's hydrophobic regions and the long alkane chain of SDS. In addition, the anionic sulfate group of SDS interacts with positively charged side chains of unlabeled lysine residues. Oakes demonstrated that, in the case of BSA, the binding of the first 20 SDS molecules occurs mainly through the anionic sulfate group of SDS.[31] The protein is not denatured at this concentration of SDS.[31] The conversion of a lysine residue to a covalent FQ-lysine moiety or an ionic SDS-lysine moiety results in approximately the same increase in mass, 242 amu or 283 amu respectively. Lysine is converted from positively charged to neutral in both cases. Therefore, the presence of SDS masks the mobility differences of the various products of the FQ ovalbumin labeling reaction.
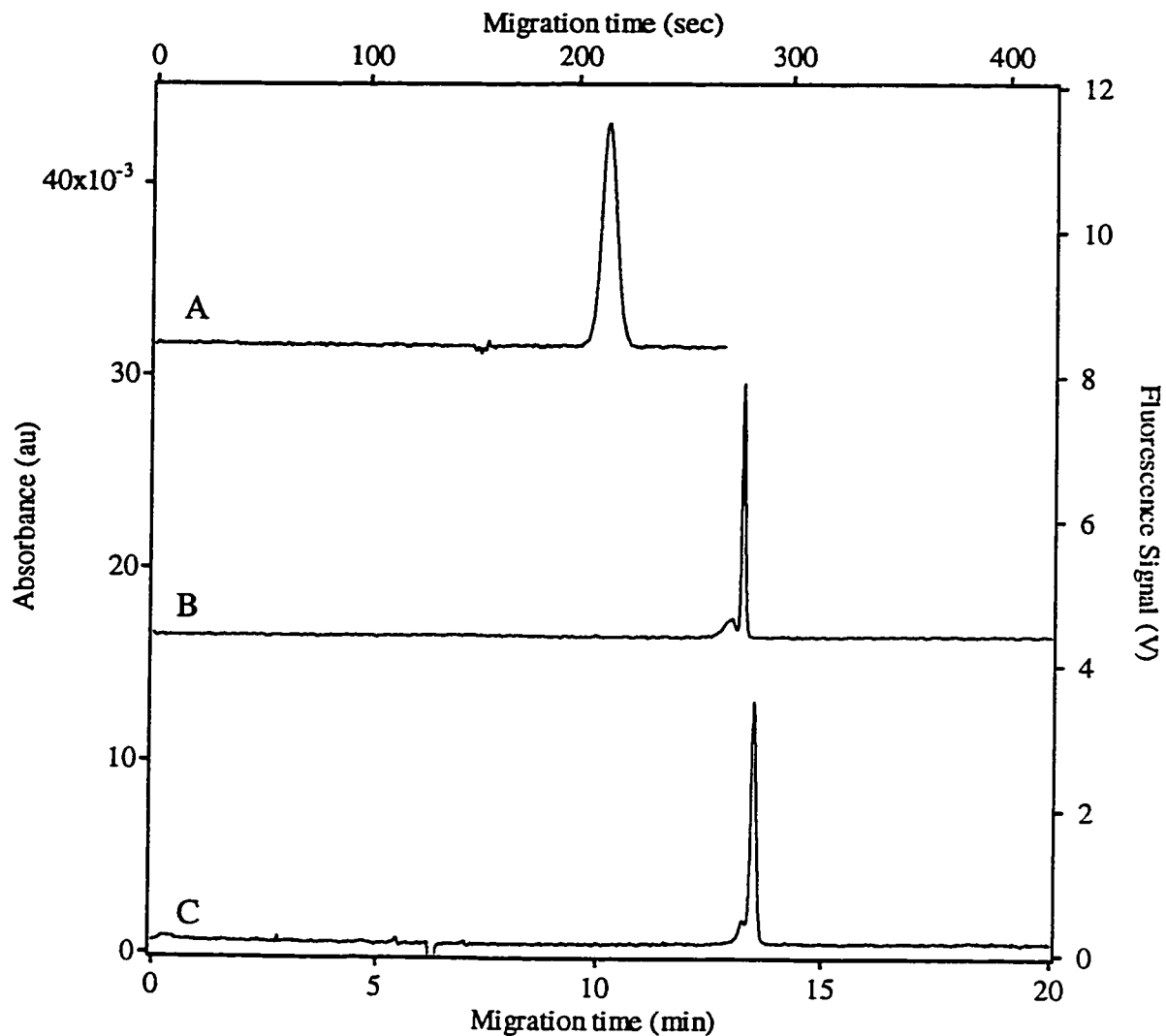
Figure 4.4 - The analysis of FQ labelled BSA analysed by (A) free solution and (B) sub-micellar CE-LIF. (C) The analysis of native BSA by free solution electrophoresis with UV detection is given for comparison. CE conditions: (A) and (B) see Figure 1A and 1D respectively, (C) polybrene coated capillary, BGE: 0.5 M HCOOH, BSA dissolved in water.

Micellar separation

There is a gradual loss of separation efficiency as the surfactant increases above the CMC. The theoretical plate count for the separation with a 5 mM SDS concentration, 75,000 plates, is seven times larger than the plate count for the separation with 20 mM SDS concentration.

Complexation between the protein and surfactant molecules determines the quality of the separation at sub-micellar concentrations. On the other hand, the much larger micelles will interact with the cationic lysine groups on the protein, creating a complex that is much larger than the FQ-lysine derivative.[32] Micellar separations are not efficient in masking mobility differences due to multiple labeling.

## 4.3.3 ANALYSIS OF NATIVE PROTEINS

The analysis of native ovalbumin and native BSA in the presence of various concentrations of SDS illustrates the complexity of the SDS-protein interaction. The results are contained in Figures 4.5 to 4.7. In Figure 4.5, the migration time of the proteins increases with the SDS concentration. This is the expected behavior; upon
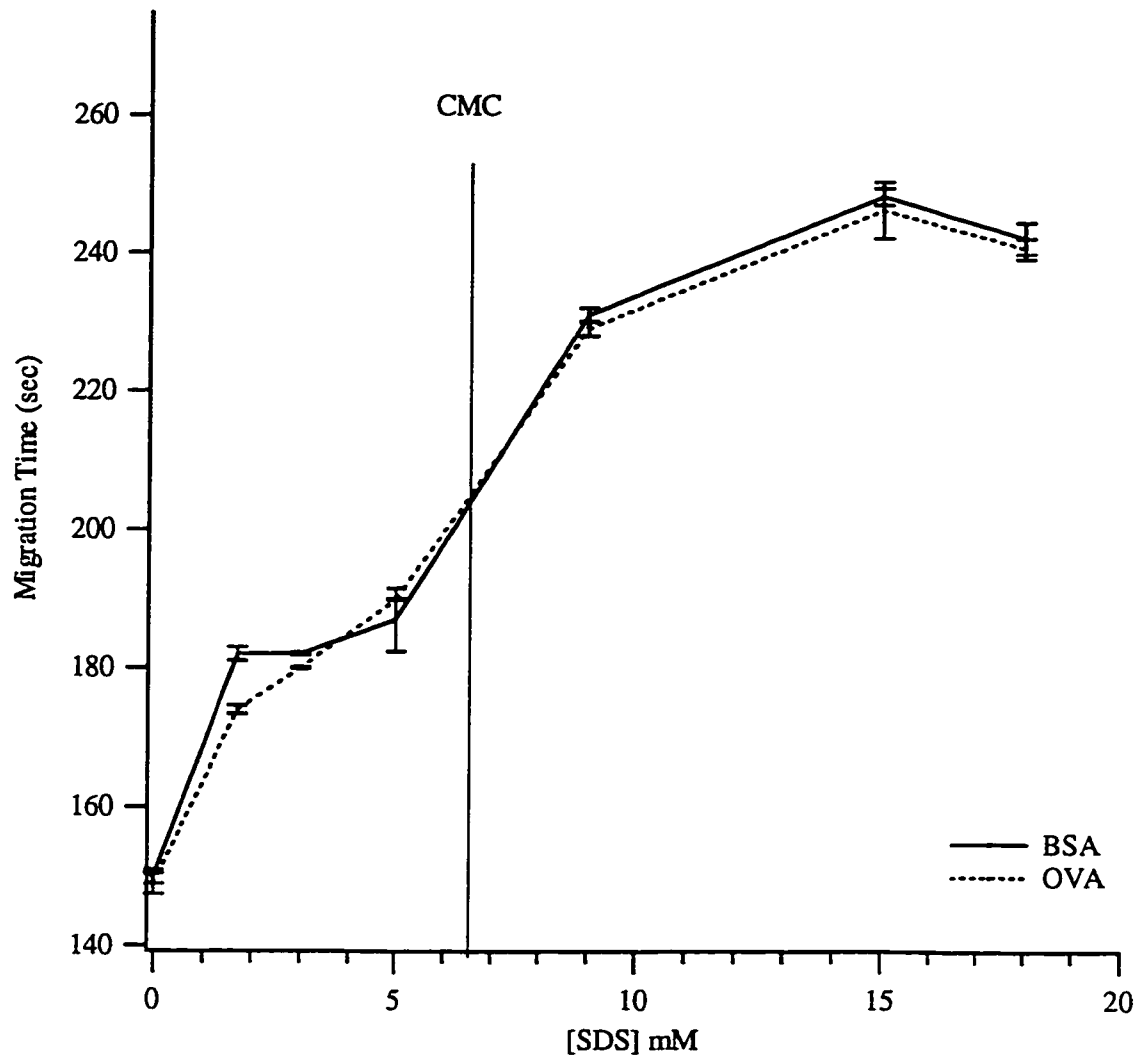
Figure 4.5 - The effect of SDS on the migration time of ovalbumin and BSA. The
average migration time is plotted in cases where the proteins exhibited multiple peaks.
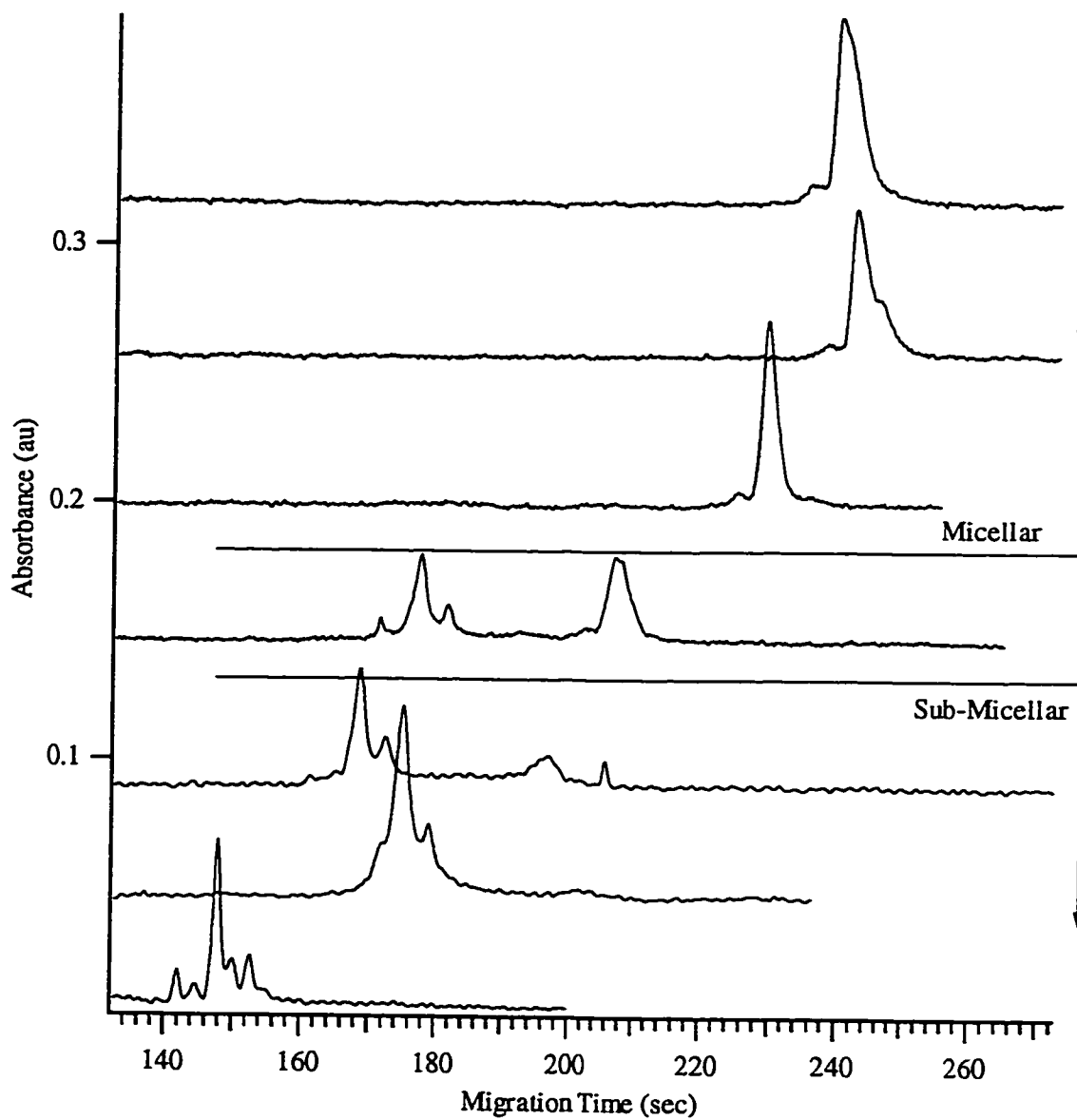
Figure 4.6 - The effect of SDS on the analysis of native ovalbumin by CE. The concentration of SDS was, from bottom to top, 0, 1.7, 3, 5, 9, 15 and 18 mM.
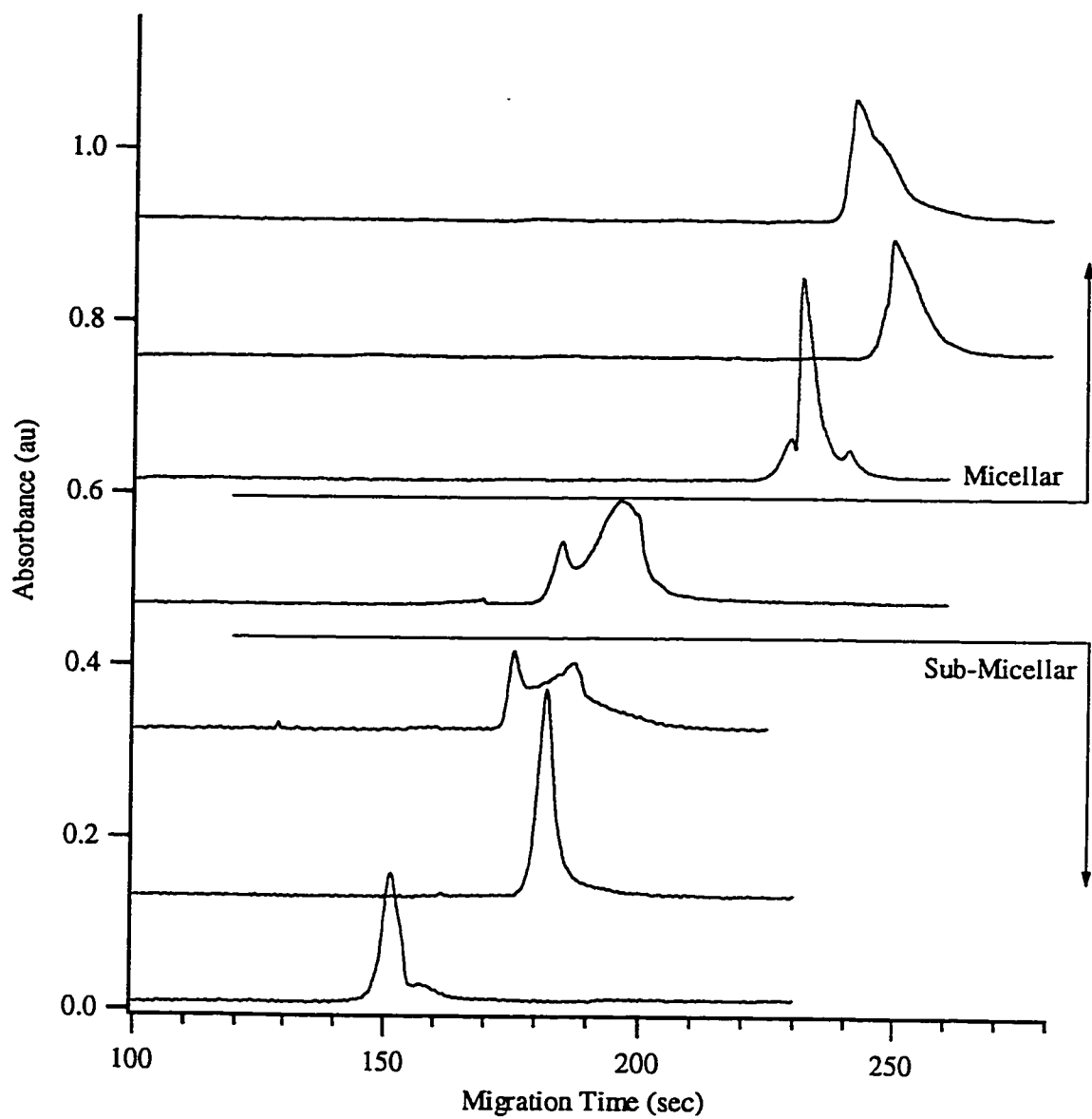
Figure 4.7 -The effect of SDS on the analysis of native BSA by CE. The

concentration of SDS was, from bottom to top, 0, 1.7, 3, 5, 9, 15 and 18 mM.

binding to the protein, SDS reduces the protein's charge, and consequently its mobility. The nature of the protein-SDS interaction depends of the phase of SDS present. The peak shape in the SDS monomer and SDS micelle regimes varies greatly, as can be seen in Figures 4.6 and 4.7. In particular, both proteins exhibit peak splitting in the intermediate regime between monomers and micelles.

The behavior of the unlabelled proteins in the presence of SDS is included here for comparison. At all SDS concentrations, only one peak was observed and the peak shape was Gaussian. The peak width varied considerably with the concentration of SDS as is depicted in Figure 4.8. The peak width was optimal at sub-micellar concentrations of SDS.

## 4.3.4 ANALYSIS OF PROTEIN MIXTURES IN SUB-MICELLAR SEPARATIONS

The use of sub-micellar concentrations of SDS masks the differences in the electrophoretic mobility of multiply labeled proteins and different glycoforms of a protein. However, the addition of SDS does not degrade the separation of mixtures of proteins. Figure 4.9 shows the electropherogram of a mixture of FQ labeled BSA, β-lactoglobulin, and α-lactalbumin labeled at 5 nM, 10 nM and 15 nM respectively. The resolution obtained is similar to that obtained by Saz *et al.* for the analysis of the native proteins.[12]

Our analysis took 2.5 min, 1 min for derivatization and 1.5 min for separation and detection. The speed of the labeling process is important because the need for lengthy reactions is a common criticism of pre-column labeling. We use a 10 s reactions for concentrations of ovalbumin greater than $10^{-8}$ M. Reactions lasting less
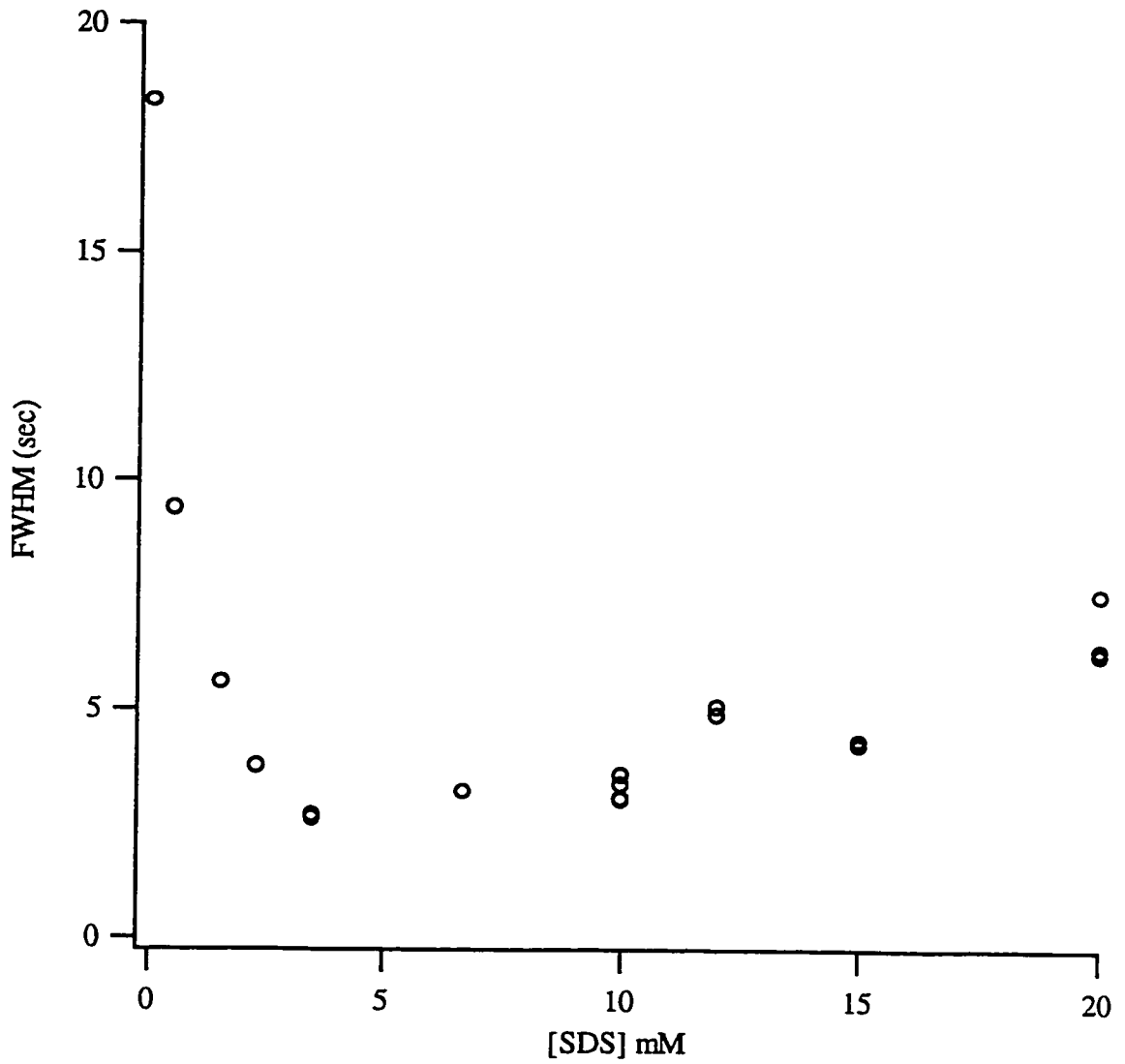
Figure 4.8 - The effect of the SDS concentration in the running buffer on the peak width of FQ-labelled ovalbumin. The concentration of borax was constant at 2.5 mM.
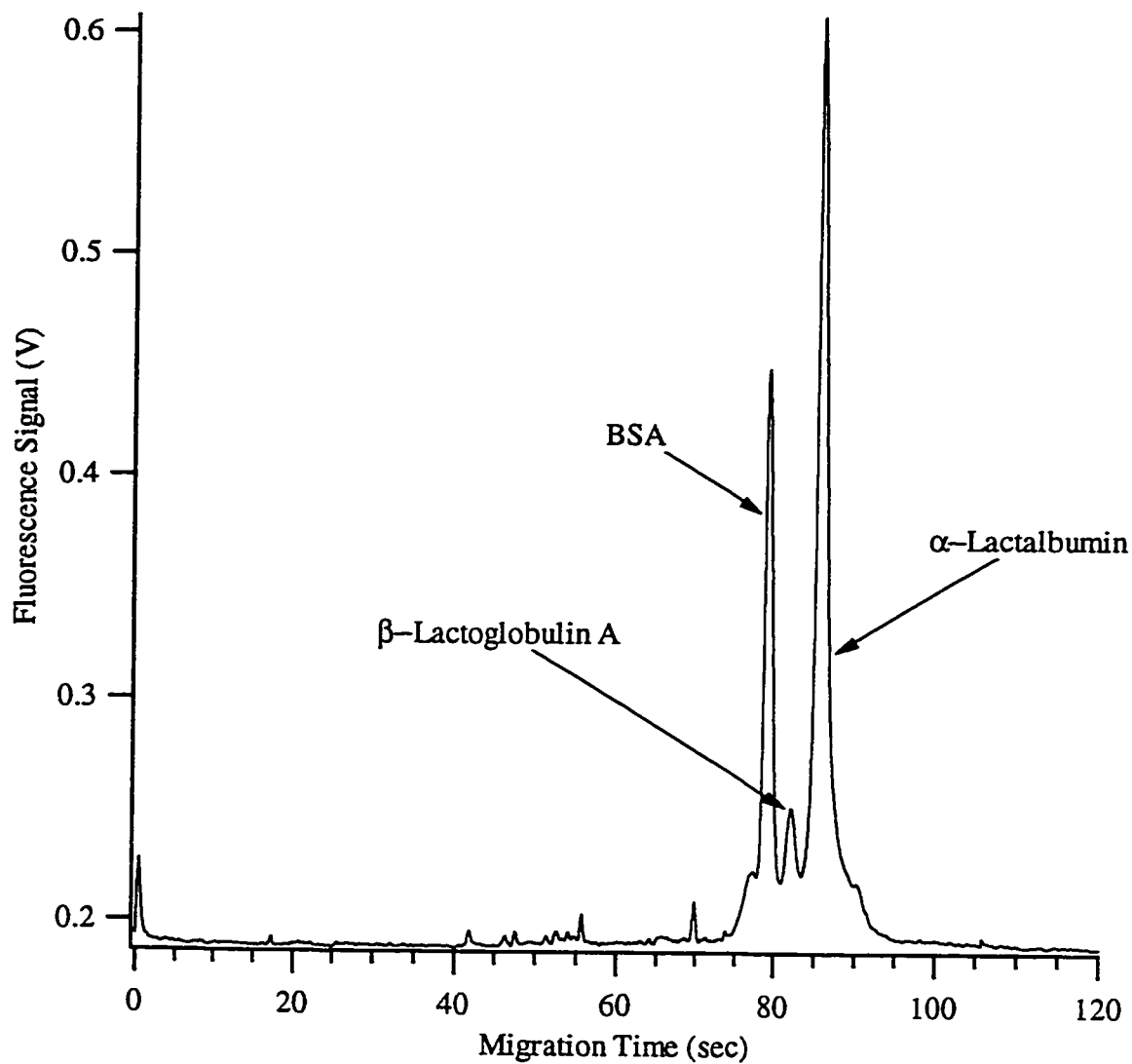
Figure 4.9 - Separation of FQ labeled bovine serum albumin, β -lactoglobulin, and α-lactalbumin labeled at a concentration of 5 nM, 10 nM and 15 nM respectively. 60 s reaction time, 5 s × 2 kV injection, 20 cm × 50 μm (i.d.) capillary, E = 700 V/cm, running buffer: 2.5 mM borax + 5 mM SDS.

than 10 s should be possible but are difficult to perform manually. A capillary length of 20 cm and an electric field of 700 V/cm were used to obtain the electropherogram. With such short analysis times, the methods developed here should be useful for analyzing large number of samples for screening purposes.

Separations performed in buffer filled capillaries, instead of gel filled capillaries, are advantageous when rapid and rugged separations are required. However, in our experience, many proteins have similar mobilities in zone electrophoresis despite the large differences in mass between the proteins. An example of this problem is given in Figure 4.10. Here, BSA and OVA are labelled with FQ and then analyzed in sub-micellar regime. The resolution obtained is 0.8, which indicates that the proteins have similar size-to-charge ratios despite their large differences in mass.

## 4.3.5 DENATURING CAPILLARY GEL ELECTROPHORESIS OF PROTEINS

Free solution electrophoresis of proteins is a very simple technique. However, it is not possible to calculate the molecular weight of a protein based on its free solution mobility. Denaturing gel electrophoresis of unlabeled proteins produces a separation where the logarithm of molecular weight is proportional to the logarithm of migration time. The following data demonstrates similar behavior for fluorescently labeled proteins.

In denaturing capillary gel electrophoresis (dCGE), proteins are extensively denatured and treated with high concentration of SDS. The surfactant forms a complex with the protein, creating molecules with roughly identical size-to-charge
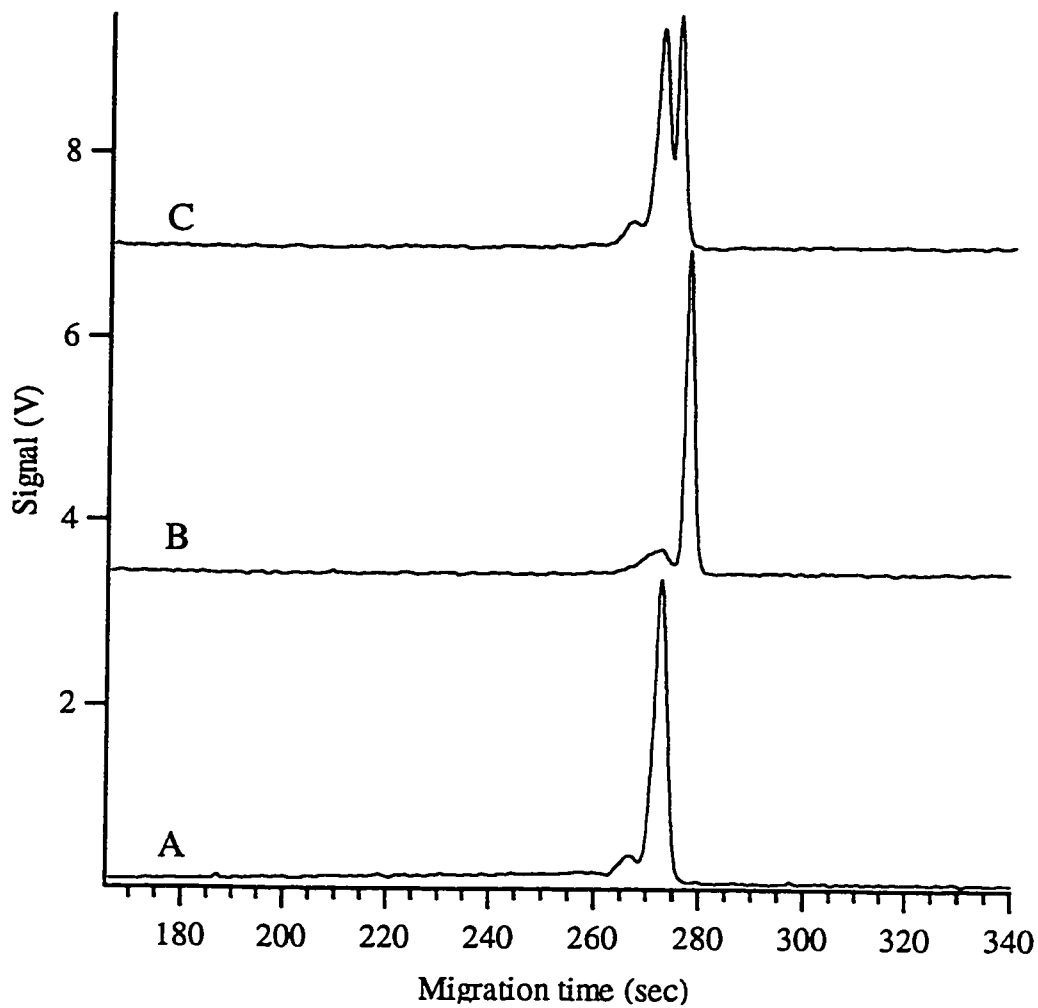
Figure 4.10 - Analysis of (A) FQ-Ovalbumin and (B) FQ-BSA as well as a mixture of

both (C) in a submicellar SDS/Tricine buffer. BGE: 25 mM tricine (pH 7.35) + 5 mM

SDS. Samples were labelled with FQ for 1 minute,
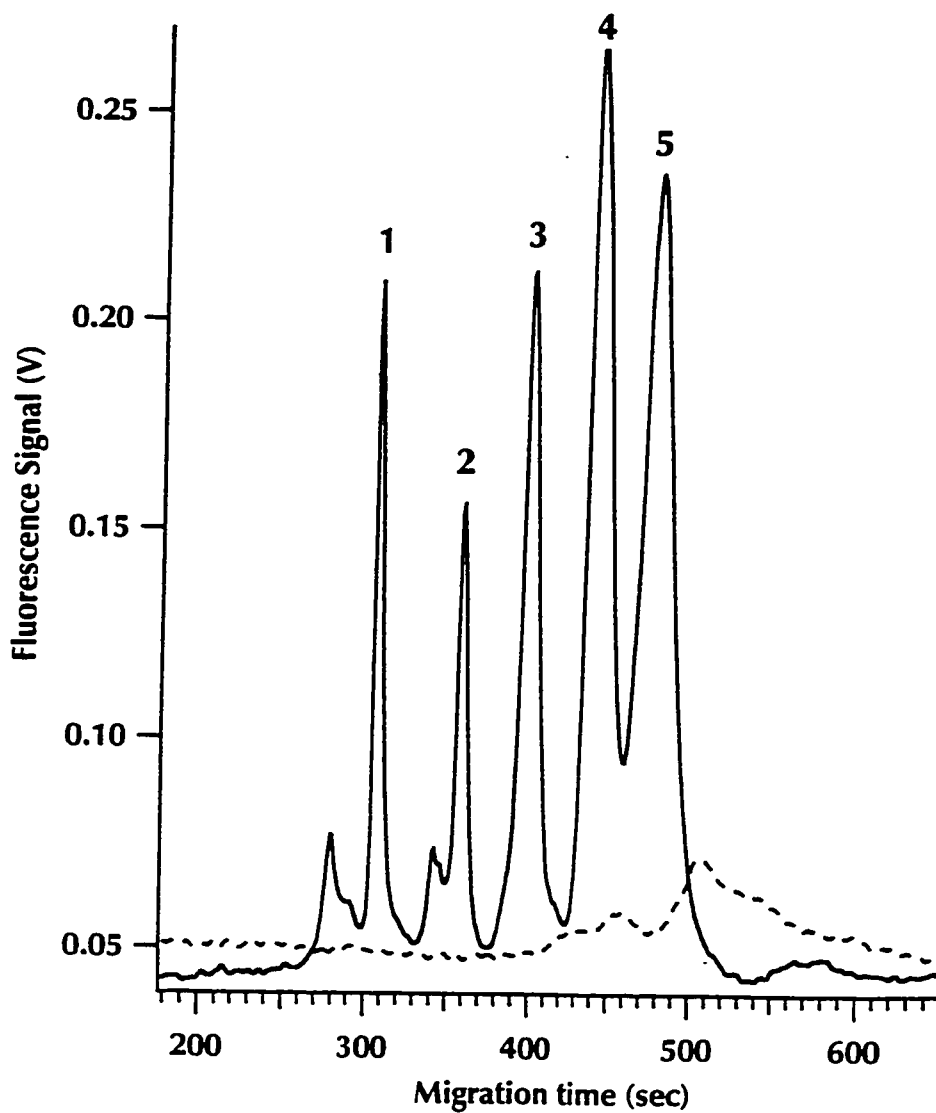
Figure 4.11 - dCGE-LIF analysis of (1) myoglobin, (2) carbonic anhydrase, (3) ovalbumin,

(4) BSA and (5) conalbumin labeled at a concentration of $10^{-7}$ M with FQ. Solid trace:

sample; dashed trace: blank. CE was performed on a 25 cm × 50 μm capillary coated with

3% polyacrylamide and filled with 7.5 % dextran (MW = 2 × $10^6$), E = 1 kV/cm.

ratio. The proteins are labeled, diluted ten-fold and then separated in a dextran filled

capillary that contains 5 mM SDS. Dextran acts as a sieving medium that separates the

proteins based on size. Figure 4.11 shows the dCGE separation of, in order of elution,

myoglobin, carbonic anhydrase, ovalbumin, BSA and conalbumin labeled with FQ. A

plot of log(migration time) versus log(molecular weight) was linear. The slope was

0.282 and the correlation coefficient ($R^2$) was 0.990.

## 4.3.6 OPTIMIZATION OF REACTION CONDITIONS

This section presents the effects of reaction time, the derivatizing reagent

concentration, and the presence of organic solvents in the reaction mixture.

Organic solvents are detrimental to separation efficiency. The instability and

low solubility of many derivatizing reagents in aqueous solution necessitates the use

of organic solvents. Most manufacturers' protocols, suggest that stock solutions be

prepared using neat organic solvents, methanol in the case of FQ, and that aliquots be

added to aqueous sample solutions. The presence of methanol in the derivatization

step results in an additional, small, broad and partially resolved peak prior to the main

peak, Figure 4.12. With the elimination of methanol from the reaction mixture, the

broad peak was all but eliminated and efficiency increases from 30,000 plates

(electropherogram A) to 190,000 plates (electropherogram C).

Reaction time plays a critical role in optimizing sensitivity and

efficiency (Figure 4.13). The signal-to-noise ratio and the peak efficiency reach a

plateau after ~30 min. the same behavior is obtained for other proteins such as $\alpha$-

lactalbumin, Figure 4.14. This increase in efficiency with reaction time is only

observed with buffers that contain SDS near the CMC. If SDS is omitted,
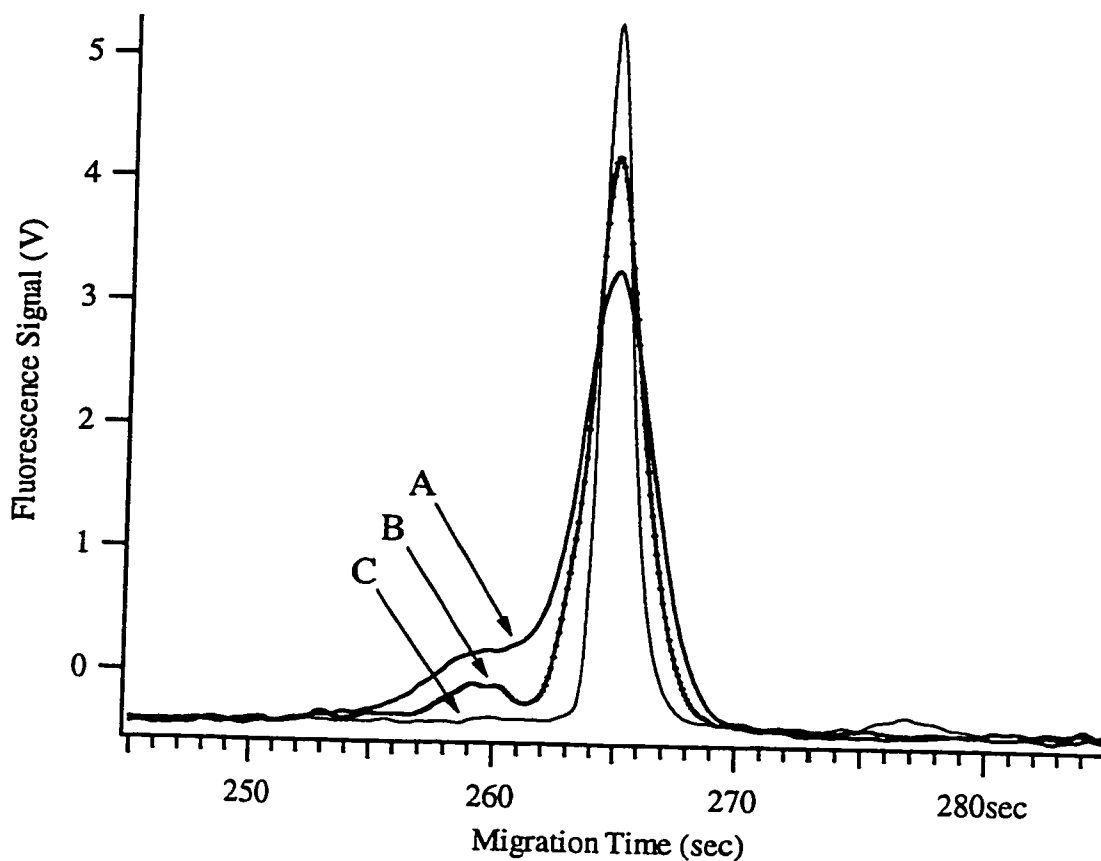
Figure 4.12 - Effect of the presence of methanol of peak efficiency. Reaction conditions: (A) & (B); $10^{-5}$ M ovalbumin, 1 min reaction, 1:20 dilution in running buffer, 5 s × 3 kV injection. (C) $10^{-8}$ M ovalbumin, 26 min. reaction, 5 s × 5 kV injection. % MeOH in reaction (A) 75 %, (B) 2.5% (C) 0%. Peaks offset slightly for clarity, actual migration times were 264.6 s in A, 263.7 s in B and 259.5 s in C. CE conditions for all runs: running buffer; 2.5 mM borax + 5 mM SDS; E = 400 V/cm, capillary: 50 μm (i.d.) x 145 μm (o.d.) x 50 cm (l).
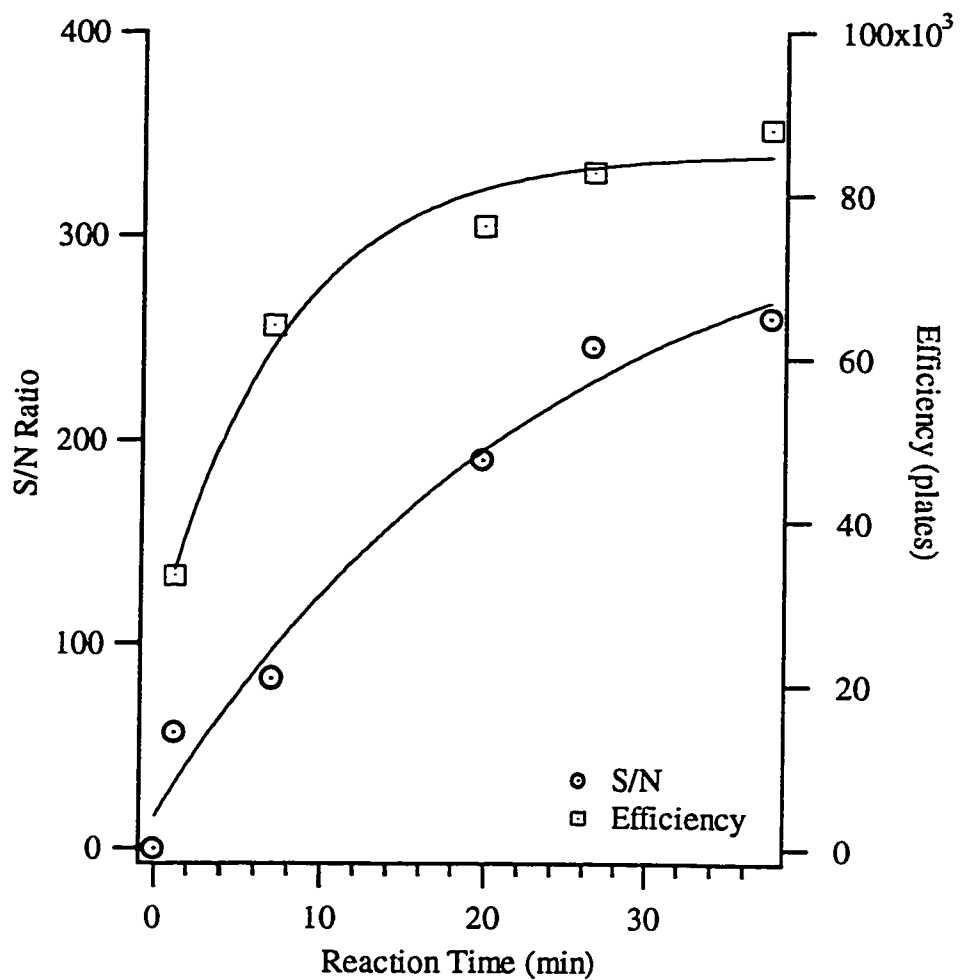
Figure 4.13 - Dependence of signal to noise ratio (o) and peak efficiency (≤) on reaction time. Reaction conditions: 14.4 µL × $10^{-8}$ M ovalbumin + 1.6 µL × 25 mM KCN + 80 nmol FQ, 5 s × 5 kV injection, 48 amol injected. CE conditions: same as Fig. 4.12.
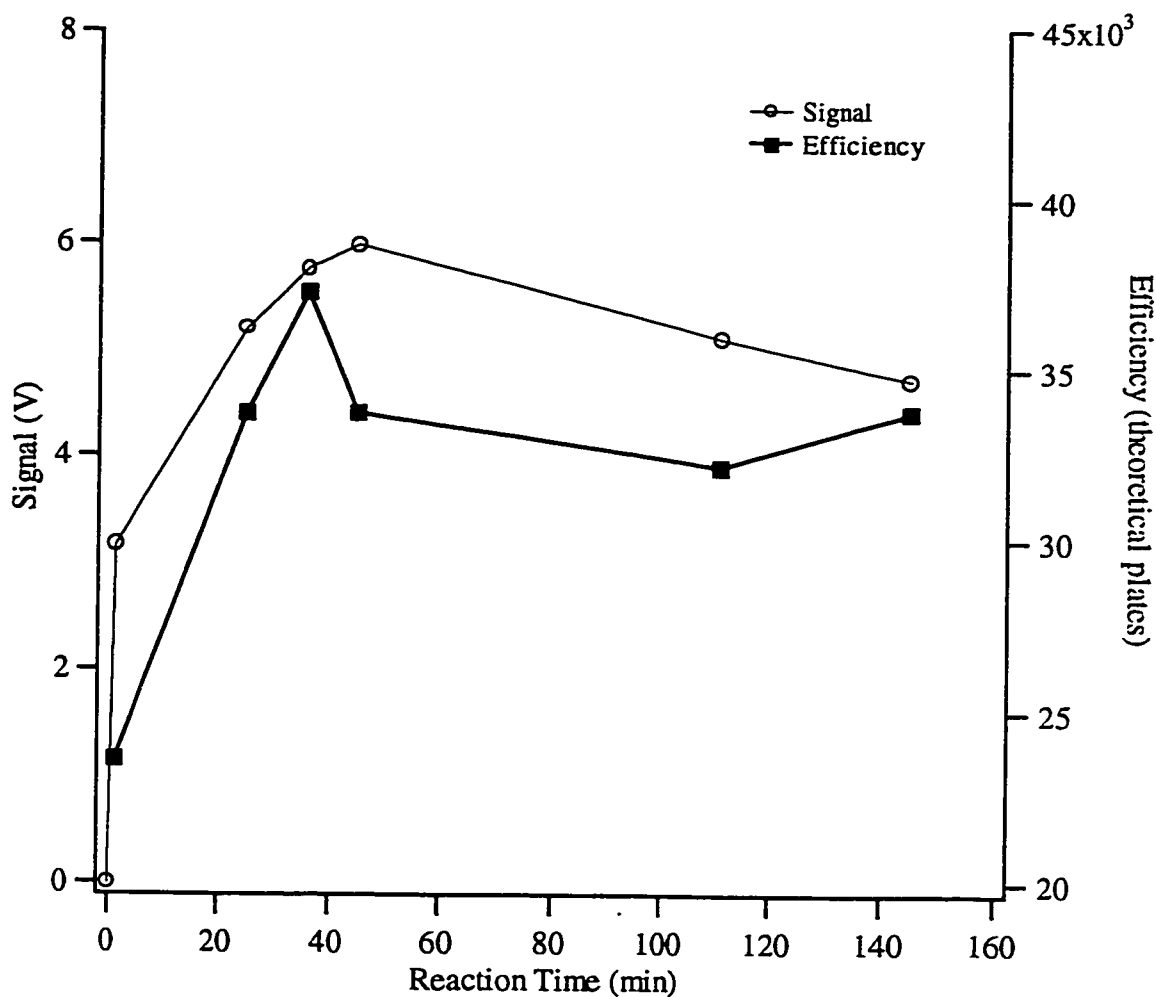
Figure 4.14 - Dependence of signal to noise ratio (o) and peak efficiency (') on

reaction time. Reaction conditions: 16 μL × 10$^{-7}$ M α-lactalbumin ovalbumin + 1 μL ×

21 mM KCN + 170 nmol FQ, 5 s × 5 kV injection, 48 amol injected. CE conditions:

same as Fig. 4.12.
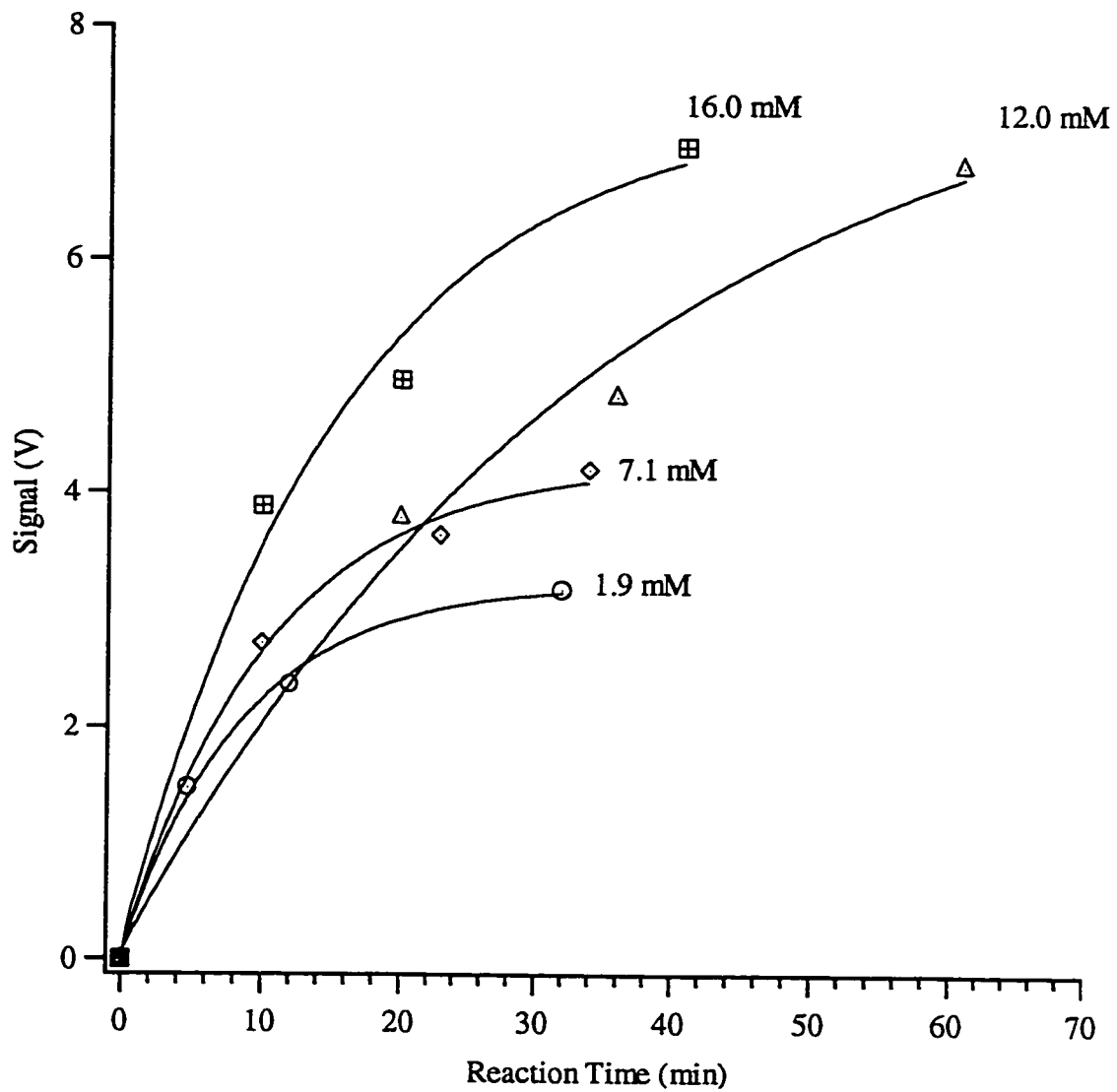
Figure 4.15 - The effect of FQ concentration on the signal of FQ-labelled ovalbumin.

the broadening due to multiple labelling increases with reaction time.

The concentration of the derivatizing reagent does, to a point, influence the sensitivity and efficiency obtained. Figure 4.15 contains a plot of the signal as a function of reaction time for various FQ concentrations. The signal intensity increases with increasing FQ concentration. The increase in signal is due to an increase in the number of lysine groups labelled. There are two drawbacks to using high concentrations of FQ.

Firstly, FQ is not readily soluble in aqueous solutions so a precipitate rapidly forms once the FQ concentration reaches 10 mM. The precipitate can degrade the capillary surface and can also interfere with the detection. Secondly, the increase in FQ concentration is accompanied by an increase in peak width, Figure 4.16.

## 4.3.7 DETECTION LIMIT

It is important to distinguish between assay and instrumental detection limit. The assay detection limit refers to the total assay and represents the minimum amount of *unlabeled* protein required for the assay. The instrumentation detection limit refers to the detection of labeled protein and ignores difficulties in labeling dilute solutions of proteins.

Fluorogenic derivatizing reagents tend to produce low background signals. Figure 4.17, curve B presents the sub-micellar electropherogram of a reagent blank. The blank generated several peaks with a migration time of ~180 s. The background signal appears to be due to trace impurities in the derivatizing reagent. The shape of the background signal changes from lot-to-lot of reagent, presumably due to
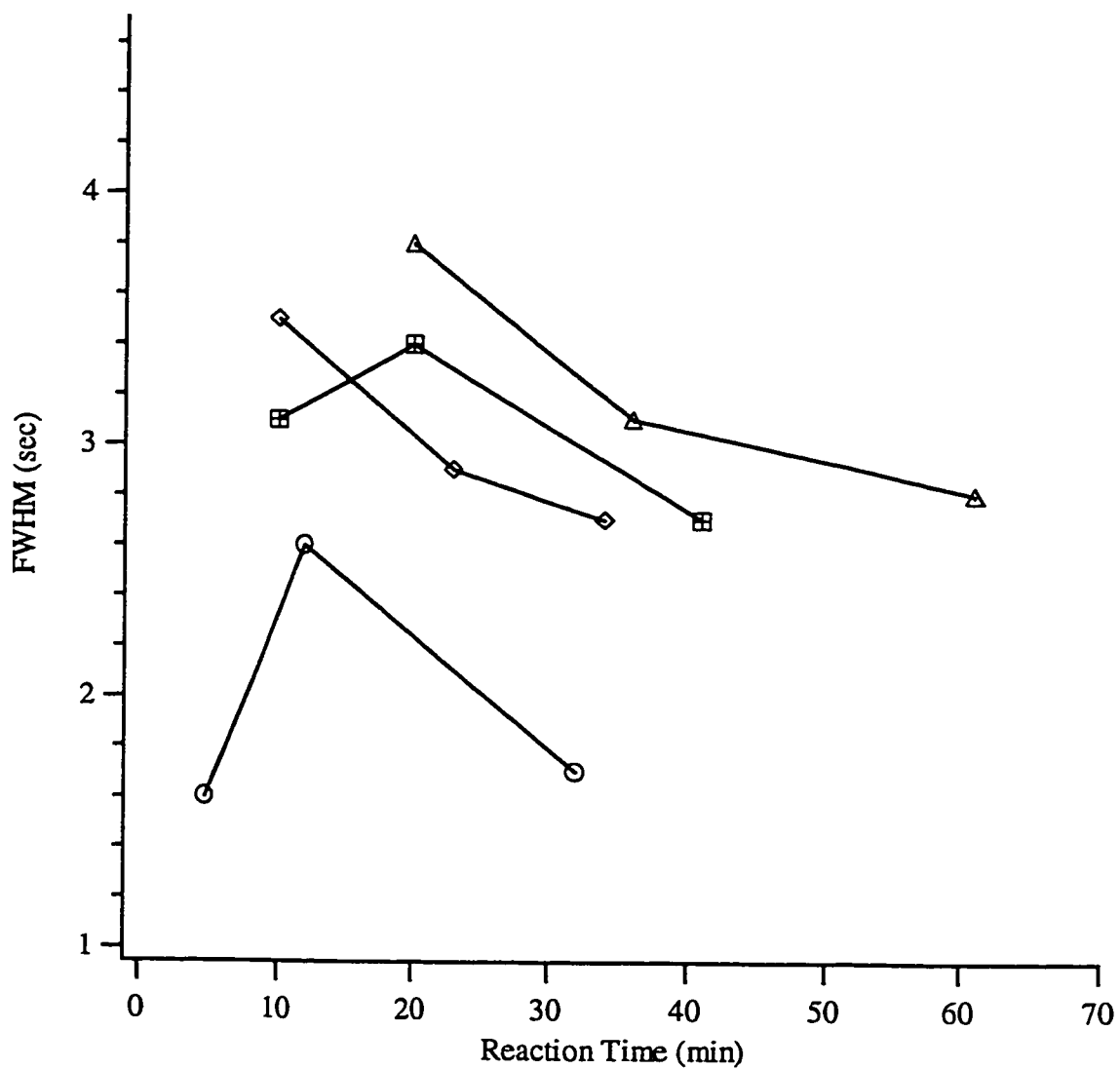
Figure 4.16 - The effect of FQ concentration of peak width of FQ-labelled ovalbumin.
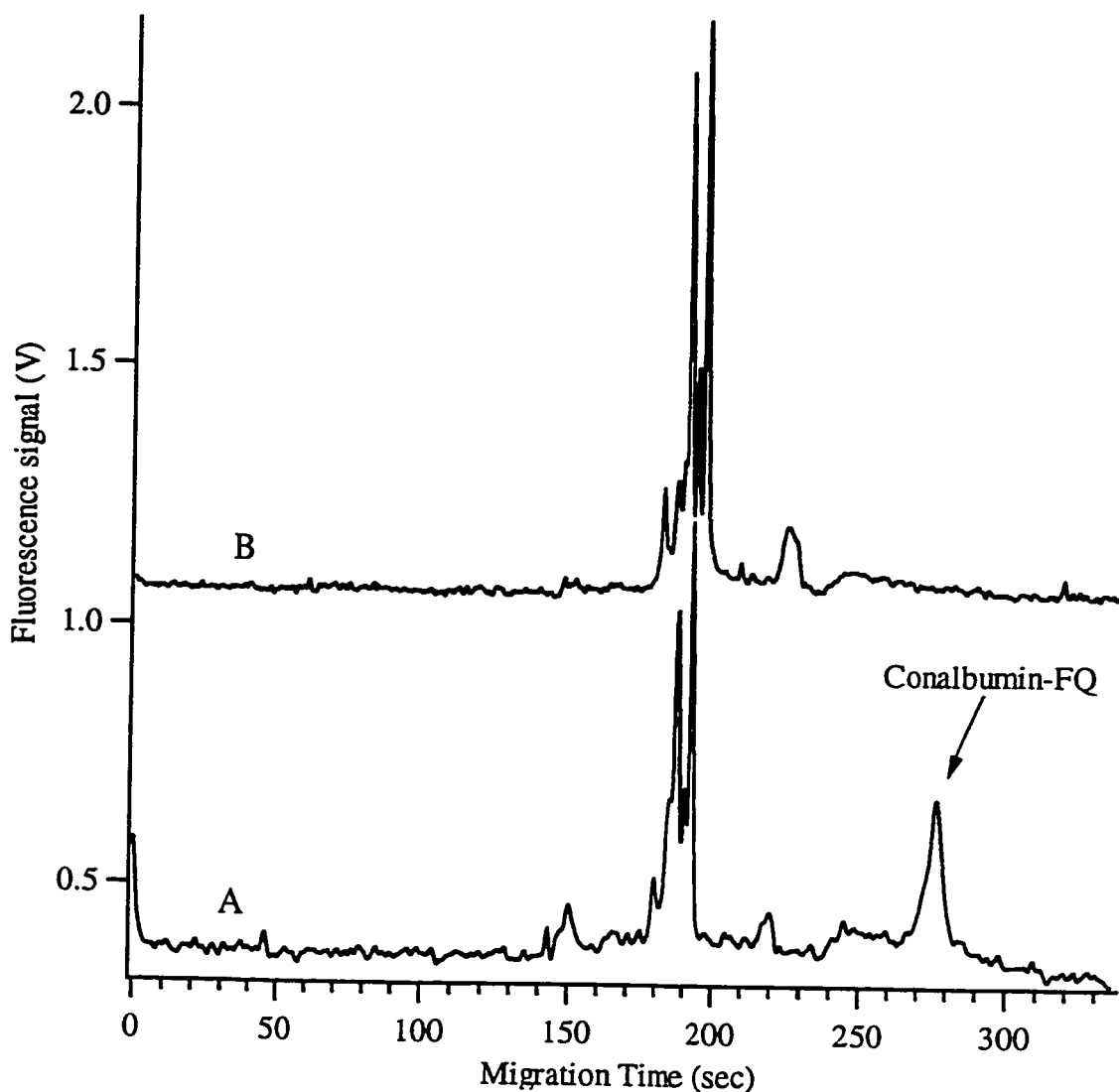
Figure 4.17 - Picomolar analysis of conalbumin and blank. (A) Sample reaction conditions: 2 µL × $10^{-10}$ M conalbumin + 1 µL × 10 mM KCN + 2 µL × 10 mM FQ, 17.5 min reaction, 5 s × 5 kV injection. (177 zeptomoles injected) S/N = 51. FQ-conalbumin peak indicated with asterisk, other peaks due to secondary reaction products. (B) Blank reaction conditions: 2 µL × 2.5 mM borax + 1 µL × 10 mM KCN + 2 µL × 10 mM FQ, 17 min reaction, 5 s × 10 kV injection. CE Conditions: same as Fig. 4.12

slight differences in the composition of these impurities. Fortunately, none of the proteins that we have analyzed co-migrates with these background peaks.

FQ may be used to assay picomolar concentrations of protein. An electropherogram of conalbumin *derivatized* at a concentration of $10^{-10}$ M is shown in Figure 4.17. The assay detection limit ($3\sigma$) for unlabeled conalbumin is $1 \times 10^{-11}$ M, Table 4.1. These are among the lowest reported mass and concentration detection limits for a native protein using any detection scheme for CE. These detection limits are for the assay, which reflects both the instrumental detection limits along with the reaction efficiency, impurity production, adsorption losses to the vessel walls, etc.

The assay detection limits can be no lower than the instrumental detection limits. To estimate the instrumental detection limit, 1.0 μM conalbumin was labeled with FQ for 55 minutes and then diluted to 83 pM with running buffer. The mass detection limits was 560 molecules (930 ymol) of FQ-labeled conalbumin injected onto the capillary in an injection volume of 2.9 nL and assuming 100% labeling efficiency. The instrumental detection limit is $3.3 \times 10^{-13}$ M. The instrumental detection limit of FQ labeled protein is 30 times lower than the assay detection limit of unlabeled protein.

Preconcentrating the protein with a size-exclusion spin-tube prior to labelling can reduce the concentration detection limit. Figure 4.18 contains an electropherogram from the preconcentration and analysis of 1 ml of 0.1 nM BSA. In this case, the sample is spun though a membrane with a molecular weight cutoff of 10 kDa. The membrane is inverted and any sample components retained by the membrane are collected into a fresh vial, labelled with FQ and analyzed. This technique increases the
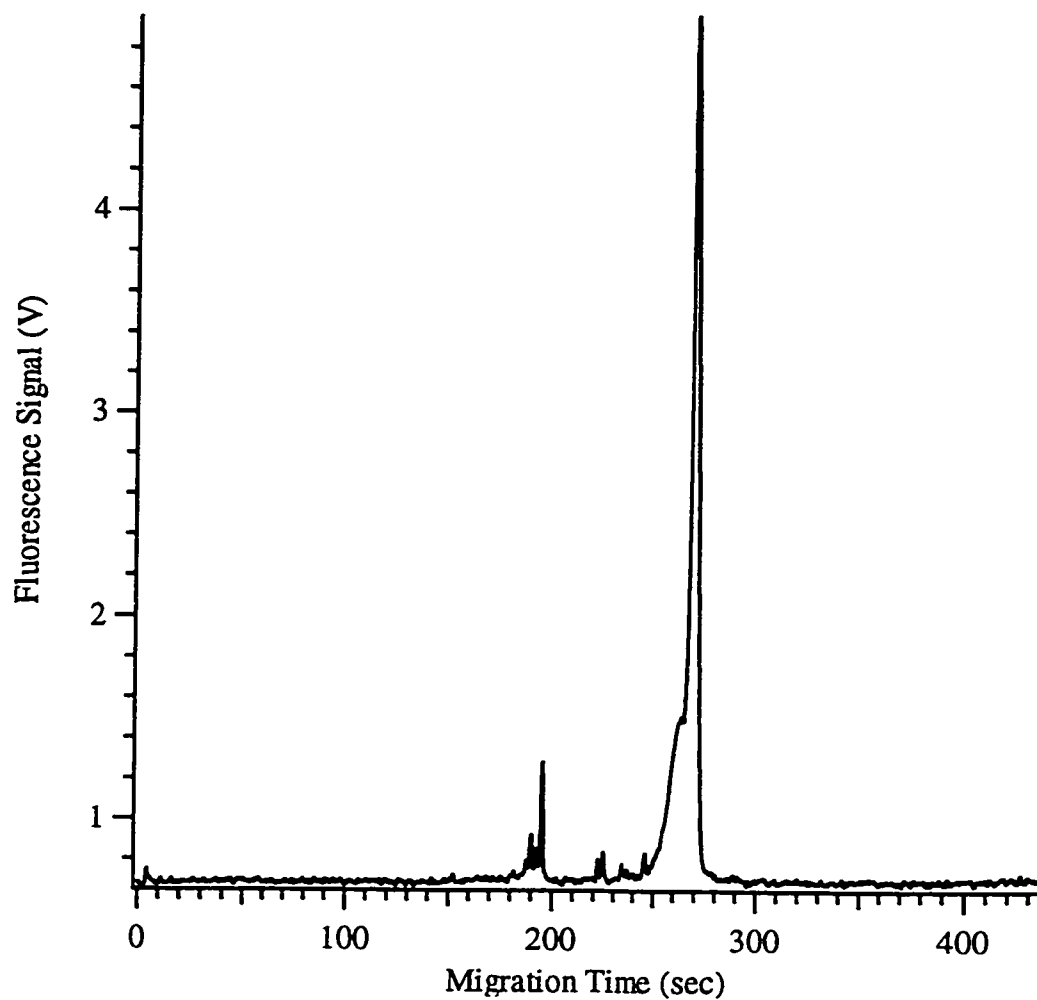
Figure 4.18 - Preconcentration of 1.0 mL of 0.1 nM BSA using a size exclusion membrane. After preconcentration, the BSA was labelled with FQ for 20 min and injected for 5s at 1 kV. CE conditions: see Figure 4.12
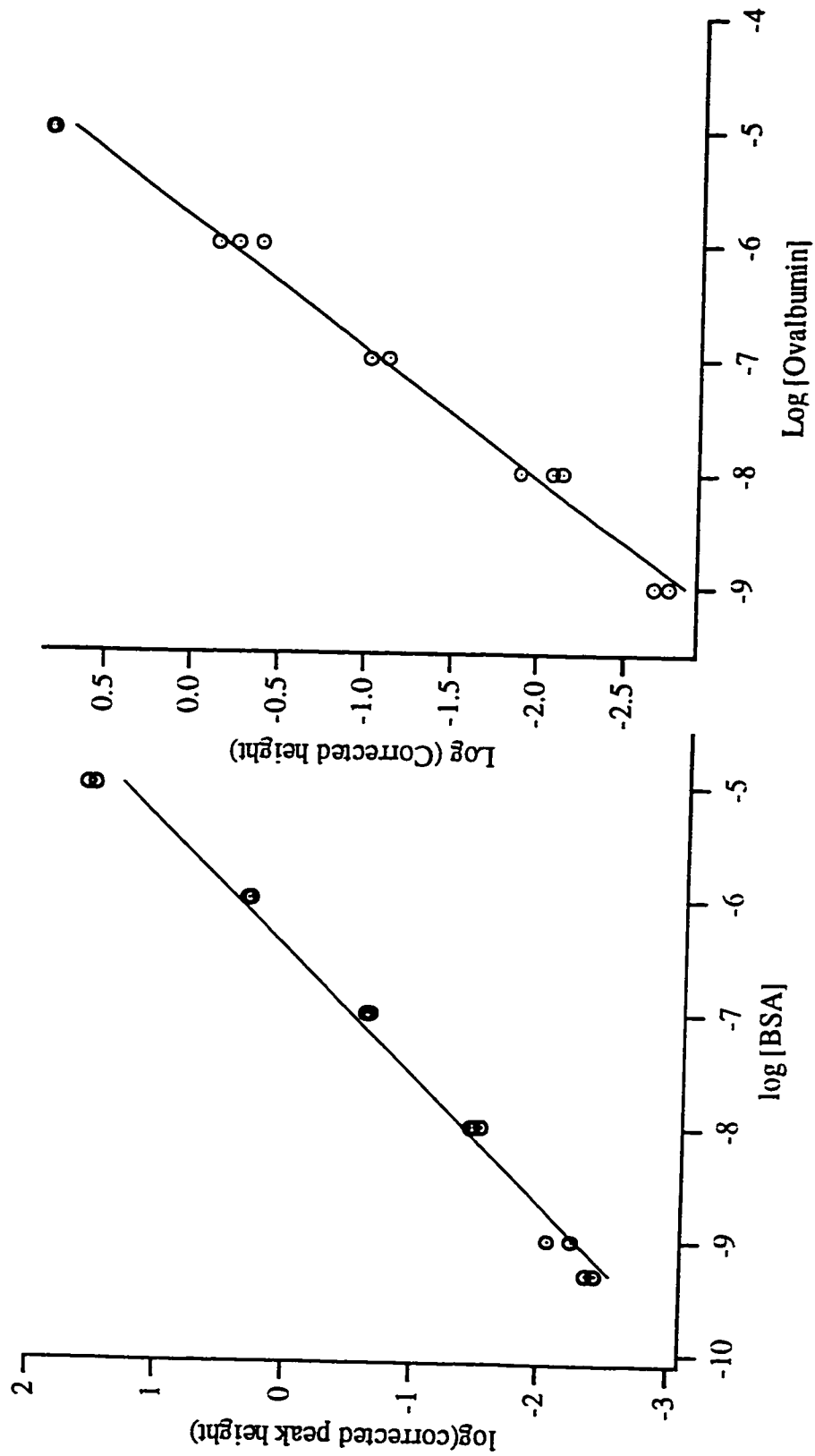
Figure 4.19 - Calibration curves for the analysis of FQ-labelled BSA and FQ-labelled ovalbumin

sensitivity roughly 50 times. Unfortunately, the technique was highly variable presumably due to irreversible losses of protein on the membrane and was not pursued further.

### 4.3.8 Linear Dynamic Range

Figure 4.19 contains a log-log calibration curve for the assay of BSA, which was generated over a concentration range from $5 \times 10^{-10}$ M to $1 \times 10^{-5}$ M using a 30 minute reaction time. The curve was linear over five and a half orders of magnitude, with slope of $1.11 \pm 0.06$ and correlation coefficient of 0.9994. At concentrations below $5 \times 10^{-10}$ M, insufficient product was formed to permit detection. This detection limit for BSA is five-fold poorer than that observed for conalbumin. The two proteins have nearly the same number of lysine residues; therefore, the difference in detection limit must result from differences in reaction efficiencies of the two molecules. Apparently, BSA does not have a large number of lysine residues that are readily accessible to the derivatizing reagent.

At concentrations equal to or higher than $10^{-4}$ M, the calibration curve deviated from linearity. At a BSA concentration of $10^{-4}$ M, the FQ/lysine ratio is only 1.7 and the CN/lysine ratio is only 0.42. Therefore, the concentration of both derivatizing reagents decreases significantly during the reaction causing a negative deviation from linearity. The solubility of FQ limits the use of higher concentrations in aqueous solutions. The increased production of background peaks prevents the use of higher concentrations of cyanide.
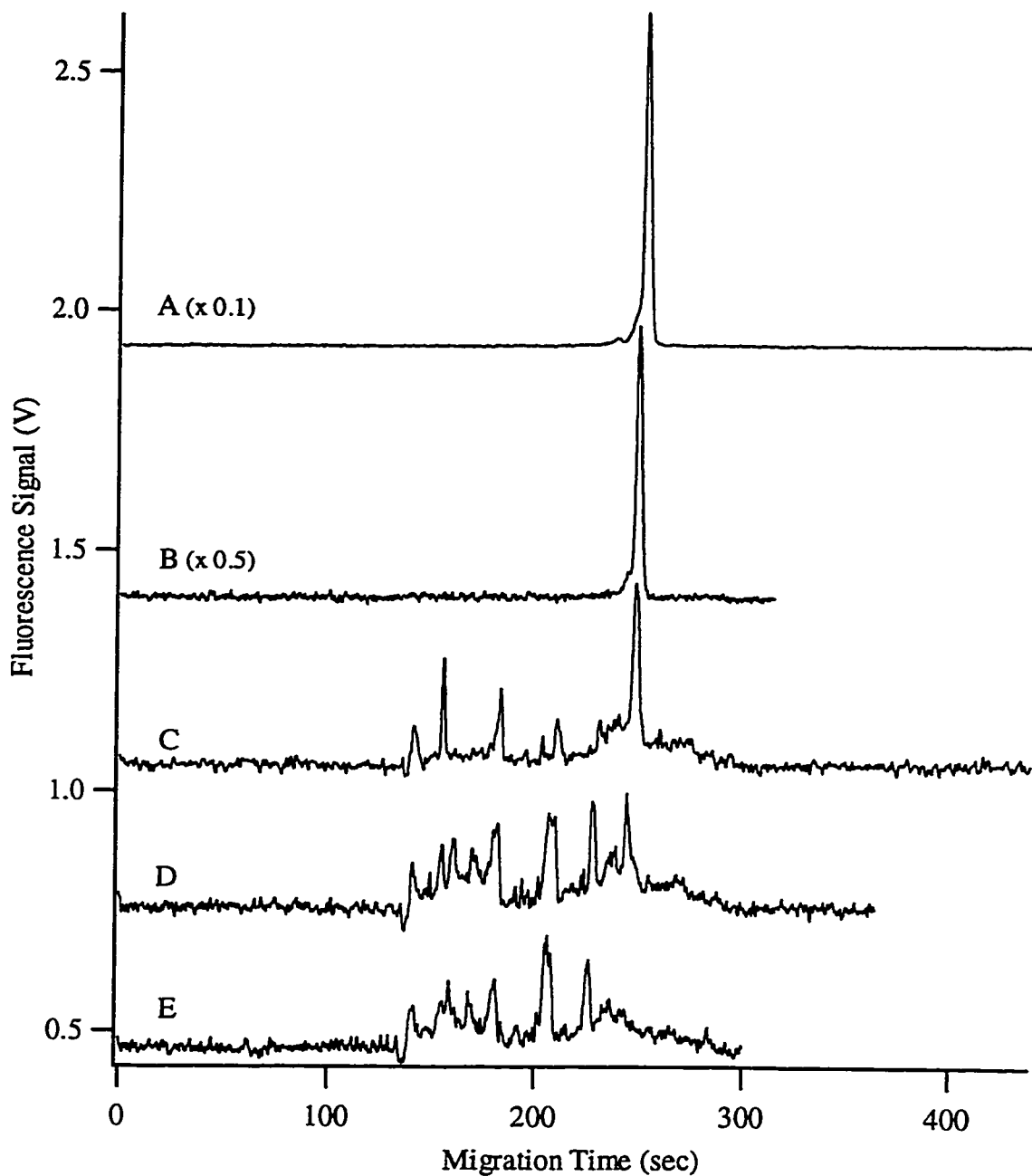
Figure 4.20 - FQ labelling of Ovalbumin. The ovalbumin concentration was (A) $10^{-6}$ M, (B)$10^{-7}$ M, (C) $10^{-8}$ M and (D) $10^{-9}$ M and (E) 0 (reagent blank). All reaction were carried out for 1 min. Samples D and E were injected undiluted, whereas, samples A, B and C were diluted 1:20, 1:20 and 1:3 with running buffer before injection respectively.

118
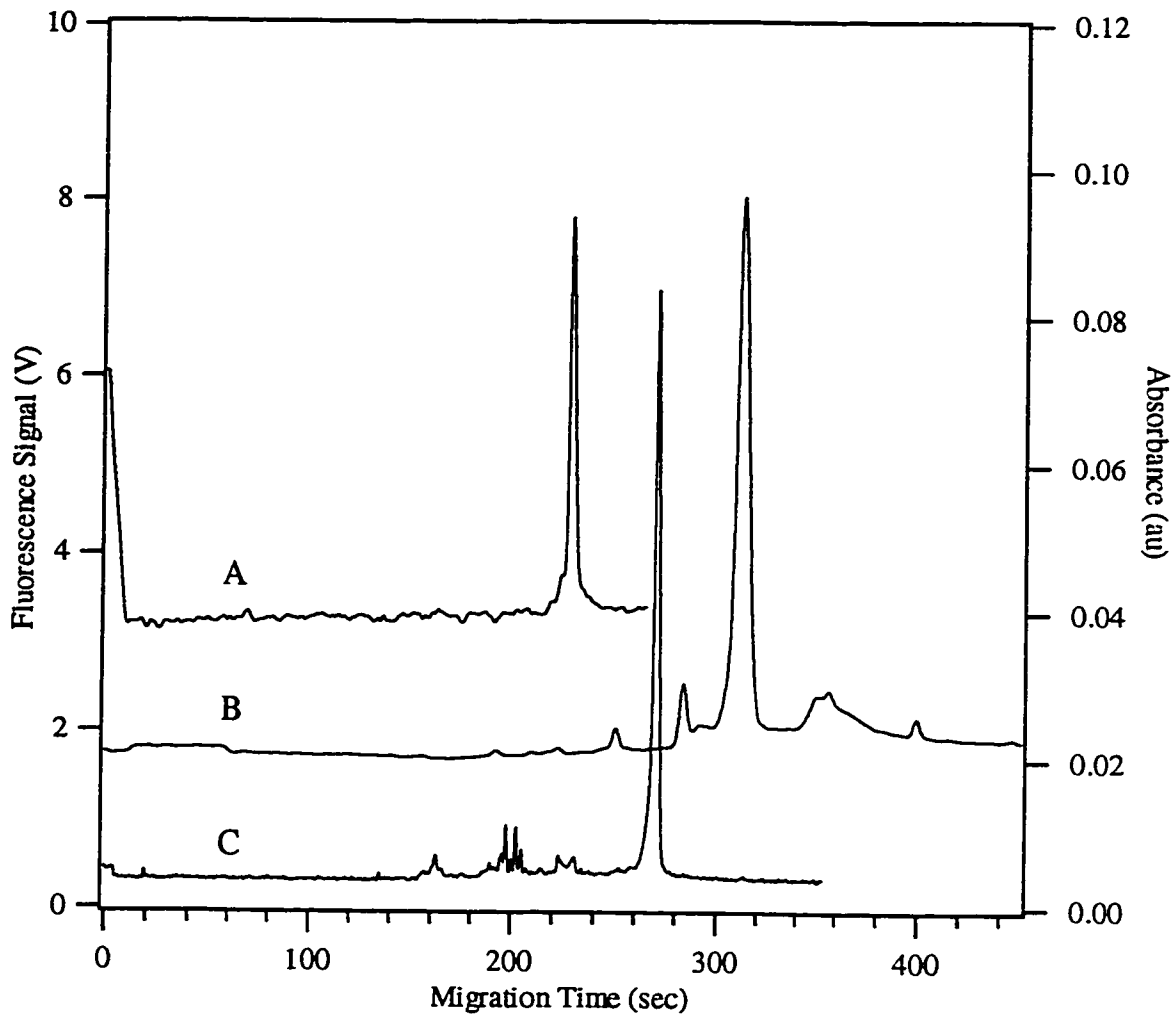
Figure 4.21 - CE analysis of ovalbumin. (A) UV absorbance detection [ovalbumin] = $10^{-4}$ M, 48.1 cm × 50 μm (i.d.) capillary, 5 s × 1 kV injection, (B) on-column CE-LIF detection, [ovalbumin] = $10^{-6}$ M, 57 cm × 75 μm (i.d.) capillary, 5 s × 1.5 kV injection, and (C) sheath flow CE-LIF detection, [ovalbumin] = $10^{-8}$ M, 50 cm × 50 μm (i.d.) capillary, 5 s × 5 kV injection. Electropherogram A is plotted vs. the right hand axis and electropherograms B and C are plotted versus the left-hand axis.

The results were similar for other proteins. Ovalbumin was labelled over a concentration range of $10^{-9}$ M to $10^{-5}$M. The curve had a slope of $0.89 \pm 0.03$ and correlation coefficient of 0.993, Figure 4.19. Figure 4.20 contains electropherograms from each of the concentrations analyzed. This data may appear redundant at first but is given to demonstrate the advantage of using a fluorogenic reagent. At the lower concentrations of protein, the background peaks become significant in height relative to the protein peak. Nevertheless, the background is orders of magnitude lower than that produced by traditional fluorescent derivatizing reagents such as fluorescein isothiocyanate.

## 4.3.8 COMPARISON OF HIGH-SENSITIVITY DETECTORS

The electropherograms shown in Figure 4.21 compare the signal-to-noise ratio of LIF and UV-absorbance detection. The protein was derivatized with FQ in the case of LIF detection. Relative signal-to-noise ratios were calculated for the three detection methods after correcting for the different amounts injected, Table 4.1. Sheath-flow LIF detection provides the highest signal-to-noise ratio and is assigned a relative value of 1. The signal-to-noise of on-column LIF detection is 80 times poorer than that of sheath-flow LIF detection while the signal-to-noise of UV absorbance detection is 30,000 times poorer than the sheath flow LIF detector.

## TABLE 4.1: COMPARISON OF UV AND LIF DETECTION

| Detection Method | Ovalbumin Conc. | Amount Injected (amol) | Relative S/N | Efficiency (plates) |
|---|---|---|---|---|
| On-Column UV abs | $10^{-4}$ M | $1.1 \times 10^5$ | 0.000033 | 28,000 |
| On-Column LIF | $10^{-6}$ M | 670 | 0.012 | 20,000 |
| Sheath-flow LIF | $10^{-8}$ M | 41 | 1.0 | 52,000 |

Table 4.2 contains the concentration detection limits obtained for various proteins using sheath flow LIF detection as well as literature values for thermo-optical absorbance detection (TOAD)[12] and native LIF detection,[9] all data converted to S/N = 3. In the TOAD study, the samples were dissolved in water. Therefore, the TOAD detection limits were enhanced due to on-column stacking. The authors of the native fluorescence study lowered their detection limits to 3 pM for conalbumin and 11 pM for BSA by using stacking; however, they also reported results for analysis without stacking that are listed in Table 4.2.[9] The detection limits reported here are 10 to 10,000 times lower than other detection schemes for the CE analysis of proteins, at least in the absence of stacking. It should be mentioned that for pre-column labeling, stacking only improves detection limits if the analyte and background species do not co-migrate since stacking also concentrates the background species.

## TABLE 4.2: COMPARISON OF LIMITS OF DETECTION (LOD'S)

| Protein | M.Wt.(x10³) | Lys/Trp/Tyr/Phe (Residues) | Concentration LOD's (x10⁻⁹ M) | | |
|---------|-------------|----------------------------|------------------------------|---------|-----------|
| | | | Multiple-Label[c] LIF | TOAD[a] | Native[b] LIF |
| Trypsin Inhibitor | 7.5 | 10-2-4-9 | 1 | 27,000 | — |
| α-Lactalbumin | 14.2 | 12-4-4-4 | 0.5 | 3,700 | — |
| Myoglobin | 17.2 | 19-2-3-6 | 0.5 | 63 | — |
| β-Lactoglobin A | 19.9 | 15-2-4-4 | 1 | 4000 | — |
| Carbonic Anhydrase | 31 | 20-6-10-11 | 0.5 | 100 | — |
| Ovalbumin | 45 | 20-3-10-20 | 0.2 | — | — |
| Bovine serum albumin | 66.5 | 60-3-21-30 | 0.05 | 10 | 0.3 |
| Conalbumin | 77.8 | 59-11-21-27 | 0.01 | — | 0.15 |

[a]See Ref. 12 (detection limits were converted to signal-to-noise ratio of 3)

[b] See Ref. 9 (detection limits were converted to signal-to-noise ratio of 3)

[c] This Work (detection limits are at a signal-to-noise ratio of 3)

— = not given.

The proteins' molecular weight and the number of lysine (Lys), tryptophan (Trp), tyrosine (Tyr), and phenylalanine (Phe) residues[33,34] are essential in understanding the differences in sensitivity between the techniques. The absorption of light, and its conversion to heat, is the basis of TOAD. High sensitivity is only obtained for proteins that have a large number of the three highly absorbing residues, namely, Phe, Tyr and Trp. The molar absorptivities for Phe, Tyr and Trp are 197, 450 and 3500 $M^{-1}cm^{-1}$ respectively for the free amino acids at 257 nm, which is the wavelength used in the TOAD study.[35]

Tryptophan fluorescence is the basis of native LIF detection, although tyrosine fluorescence is sometimes important. Tyrosine only fluoresces in the absence of tryptophan and even then only with a low quantum yield.[36] Small species, such as $O_2$, $I^-$ and acrylamide quench tryptophan's fluorescence. Also, tryptophan's quantum yield decreases by two-thirds when the residue is in a hydrophobic environment as compared to the quantum yield of tryptophan residues in a hydrophilic environment.[37] In proteins, approximately a third of the tryptophan residues are located in the hydrophobic regions.[38] Also, tryptophan's low abundance, at only 1.3 per 100 residues,[39] indicates that many small proteins would escape detection by native fluorescence. The detection limits based on native fluorescence shown in Table 4.2 correspond to two proteins that have a large number of tryptophan residues and are thus particularly suited to this detection scheme.

Finally, in the case of precolumn derivatization, detection is based on fluorescence of FQ labeled amino groups, either the ε-amino group of lysine or the α-amino group of the n-terminal amino acid. Lysine, whose abundance is 5.7 per 100 residues, is one of the more abundant amino acids.[39] Highest sensitivity is obtained for proteins that have a large number of lysine residues such as conalbumin, which has 59 lysine residues.

In addition to sensitivity, the universality of the detection scheme and the cost of the detector are important. The universality and limitations of TOAD, native LIF and multiple-label LIF are largely based on the ratios of the four residues. The average ratio of Lys/Trp/Tyr/Phe residues in eukaryotic proteins is 4.4/1/2.5/3.[39] Therefore, of the three detection schemes, multiple-label LIF detection should be the

most universal. Practically, the deep-UV argon-ion lasers used in the native fluorescence and thermo-optical studies cost many tens of thousands of dollars, require water cooling, require three-phase 220 V electrical power, and have a relative short lifetime. The argon-ion laser used in this study costs less than US$10,000, is air-cooled, operates from 110 V, and has a long lifetime.

## 4.4 CONCLUSIONS

The methods and discussions presented in this chapter demonstrate that protein labelling is a viable and highly sensitive method for the analysis of proteins. The success of the technique relies on the development of appropriate labelling and separation conditions. These results contrasted with the previous example of protein labelling where the techniques appropriate for small molecules where applied to proteins.[10]

The techniques developed in this chapter will be expanded upon in Chapter 5, where the labelling and separation conditions are combined with on-capillary reaction and stacking techniques.

# REFERENCES

[1] Novotny, M. V.; Cobb, K. A.; and Liu, J. *Electrophor.* 1990, 11, 735-749.

[2] Schoneich, C.; Huhmer, A. F. R.; Rabel, S. R.; Stobaugh, J. F.; Jois, S. D. S.; Larive, C. K.; Siahaan, T. J.; Squier, T. C.; Bigelow, D. J.; and Williams, T. D. *Anal. Chem.* 1995, 67, 155R-181R.

[3] Chen, F.-T. A.; and Sternberg, J. C. *Electrophor.* 1994, 15, 13-21.

[4] Burgi, D. S. *Anal. Chem.* 1993, 65, 3726-3729.

[5] Foret, F.; Szoko, E.; and Karger, B. L. *Electrophor.* 1993, 14, 417-428.

[6] Zhu, M.; Rodrigyez, R.; and Wehr, T. *J. Chromatogr.* 1991, 559, 479-488.

[7] Tomlinson, A. J.; and Naylor, S. *J. High Res. Chromatogr.* 1995, 18, 384-386.

[8] Liao, J.-L.; Zhang, R., and Hjerten, S. *J. Chromatogr. A* 1994, 676, 421-430.

[9] Lee, T. T.; and Yeung, E. S. *J. Chromatogr.* 1992, 595, 319-325.

[10] Swaile, D. F.; and Sepaniak, M. J. *J. Liquid Chromatogr.* 1991, 14, 869-893.

[11] Craig, D. B.; Wong, J. C. Y.; and Dovichi, N. J. *Biomed. Chromatogr.*, in press.

[12] Saz, J. M.; Krattiger, B.; Bruno, A. E.; Diez-Masa, J. C.; and Widmer, H. M. *J. Chromatogr. A* 1995, 699, 315 322.

[13] Waldron, K. C.; and Dovichi, N. J. *Anal. Chem.* 1992, 64, 1396-1399.

[14] Kelly, J. F.; Locke, S. J.; Ramaley, L.; and Thibault, P. *Anal. Chem.* 1994, 62, 1359.

[15] Amankwa, L. N.; Harder, K.; Jirik, F.; and Aebersold, R. *Protein Science* 1995, 4, 113-125.

[16] Chen, D. Y.; Adelheim, K.; Cheng, X. L.; and Dovichi, N. J. *Analyst* 1994, 119, 349 -352.

[17] Chen, D.; and Dovichi, N. J. *Anal. Chem.* 1996, 68, 690-696.

[18] Pinto, D. M.; Arriaga, E. A.; Sia, S.; Li, Z.; and Dovichi, N. J. *Electrophor.* 1995, 16, 534 540.

[19] Zhang, Y.; Arriaga, E.; Diedrich, P.; Hindsgaul, O.; and Dovichi, N. J. *J. Chromatogr. A* 1995, 716, 221-229.

[20] Starke, H. R.; Yan, J. Y.; Zhong, Z. J.; Muhlegger, K.; Effgen, K.; and Dovichi, N. J. *Nucleic Acids Research* 1994, 22, 3997-4001.

[21] Arriaga, E. A.; Zhang, Y.; and Dovichi, N. J. *Anal. Chim. Acta* 1995, 299, 319-326.

[22] Szulc, M. E.; and Krull, I. S. *J. Chromatogr. A* 1994, 659, 231-245.

[23] Boppana, V. K.; Miller-Stein, C.; Politowski, J. F.; and Rhodes, G. R. *J. Chromatogr.* 1991, 548, 319-327.

[24] Szulc, M. E. and Krull. I. S. *J. Chromatogr.* 1994, 231-245

[25] Beale, S. C.; Hsieh, Y.-Z.; Wiesler, D.; and Novotny, M. *J. Chromatogr.* 1990, 499, 579-587.

[26] Zhao, J. Y.; Waldron, K. C.; Miller, J.; Zhang, J. Z.; Harke, H.; and Dovichi, N. J. *J. Chromatogr.* 1992, 608, 239-242.

[27] Gilman, S. D.; Pietron, J. J.; and Ewing, A. G. *J. Microcol. Sep.* 1994, 6, 373-384.

[28] Wu, S.; and Dovichi, N. J. *J. Chromatogr.* 1989, 480, 141-155.

[29] Cheng, Y.F.; and Dovichi, N.J. *Science* 1988, 242, 562-564.

[30] Cobb, K. A.; Dolnik, V.; and Novotny, M. *Anal. Chem.* 1990, 62, 2478-2483.

[31] Oakes, J. *Trans Faraday Soc.*, 1974, 70, 2200-2209.

[32] Yamasaki, M.; and Yano, H. *Int. J. Biol. Macromol.* 1992, 14, 305-312.

[33] http://expasy.hcuge.ch/sprot/sprot-top.html.

[34] Mathews, C.K.; and van Holde, K.E. *Biochemistry* The Benjamin/Cummings

Publishing Company: Redwood City, 1990, Chapter 5.

[35] Wetlaufer, D. B. *Advances in Protein Chemistry* 1962, 17, 303-390.

[36] Teale, F. W. J. *Biochemistry Journal* 1960, 76, 381-388.

[37] Konve, S. V. *Fluorescence and Phosphorescence of Proteins and Nucleic Acids*;

Plenium Press: New York, 1967.

[38] Chothia, C. *J. of Molec. Biol.* 1976, 105, 1-14.

[39] McCaldron, P.; Argon, P. *Proteins* 1988, 4, 99-122.

# CHAPTER 5

# TRACE ANALYSIS OF PROTEINS BY ELECTROPHORETICALLY MEDIATED MICROCHEMICAL ANALYSIS

## 5.1 INTRODUCTION

This chapter presents a method for the analysis of proteins at picomolar

concentrations. The method expands on the concepts and techniques introduced in

Chapter 4. The method is called electrophoretically mediated microanalysis

(EMMA)[1,2]. EMMA has been used to determine calcium, in the enzymatic analysis of

ethanol and in the photometric analysis of ions.[3,4,5] The labelling occurs in the

capillary, as opposed to pre-capillary labelling where the reagents react in a vial and

are injected after the completion of the reaction. The EMMA method provides greater

control over the reagents than the pre-capillary method resulting in increased

sensitivity and separation efficiency, and decreased reagent consumption.

The EMMA technique uses electrophoresis to control the reaction. The

reagents and sample are introduced in order of increasing mobility where, under the

influence of an electric field, the reagents mix, react, and form a product. The time

during which the reagent zones overlap determines the reaction time. Longer reactions

are obtained by stopping the electric field after the reagent zones mix. After the

reaction is complete, the product is separated from the reagents using zone

electrophoresis. Electroinjection analysis is a variant of EMMA in which the reagents

are introduced from opposite ends of the capillary.[6] These methods show great

promise for microscale-based analysis and detection.

## 5.2 EXPERIMENTAL

### 5.2.1 Reagents

Sodium tetraborate (borax) and sodium dodecyl sulfate (SDS) are from BDH

(Toronto, ON, Canada). All buffers were made with Milli-Q deionized water and are

filtered using a 0.2-µm filter. Sinapinic acid (SA), acetone and all proteins are from

Sigma (St. Louis, MO). The proteins were used as received and dissolved in 2.5 mM

borax pH 9.4. Derivatizing reagents, 5-furoylquinoline-3-carboxaldehyde (FQ) and

potassium cyanide (KCN), are from Molecular Probes (Eugene, OR). KCN is

dissolved in water (100 mM). A stock solution of 100 mM FQ is prepared in

methanol, 10 µL aliquots are placed into 500 µL microcentrifuge tubes and the solvent

removed under vacuum using a Speed Vac (Savant Instruments Inc., Farmingdale,

NY). The dried FQ aliquots are stored at -20 °C. The dried FQ is dissolved in running

buffer, 2.5 mM borax and 5 mM SDS at pH 9.3, to a final concentration of 5 mM

unless stated otherwise. Protein solutions are prepared daily in 2.0 mM borax, 4 mM

SDS, 5 mM KCN. The final concentration of proteins varies from $10^{-8}$ M to $10^{-12}$ M.

All solutions were kept on ice.

### 5.2.2 Instrumentation

The CE-LIF instrument was built in-house and is based upon a post-capillary

LIF detector as described in chapter 4.

Matrix-assisted laser desorption/ionization-time of flight (MALDI-TOF)

experiments were performed using a Hewlett Packard linear TOF mass spectrometer.

The labeled protein sample was diluted tenfold in matrix solution (13 mg/ml SA in

129

acetonitrile:H$_2$O, 45:55) and 0.5 μL was deposited onto the sample probe. Prior to the application of the sample, 0.5 μl of saturated SA in acetone was applied to the MALDI probe to provide a sublayer. The spectra consist of the sum of approximately 50 scans.

5.2.3 Labelling reaction and capillary electrophoresis

The procedure for EMMA labelling with FQ is shown schematically in Figure 5.1. Typical conditions are as follows. The protein/KCN solution is injected at 50 V/cm for 5 s in step 1. The capillary tip is washed twice with running buffer to minimize contamination. The FQ solution is electrokinetically injected at 50 V/cm for 5 s in step 2. The capillary tip is immersed in a heated vial of running buffer in step 3. After the reaction, the capillary is immersed in running buffer at room temperature. The CE separation is carried out at 400 V/cm in step 4. For all experiments, a 50 μm i.d. x 150 μm o.d. capillary with a length of either 35 or 40 cm is used.

The heated vial used in step 3 begins to cools as soon as it is removed from the dry bath incubator (11-718, Fisher Scientific, Edmonton, AB), therefore, the median temperature is given. For the temperatures in the dry bath incubator, 35.5, 46, 57 and 67.5 °C, the temperature in the vial at the end of the 30 s reaction is 34.5, 44, 53, and 62.5 °C respectively. Unless otherwise stated, the reaction temperature is 23 °C.

5.2.4 End-labelled free solution electrophoresis

Separation were performed in 50 μm x 50 cm capillaries whose inner surface was coated with linear polyacrylamide according to the method of Hjerten.[7] The running buffer was 1X TBE (0.54 g of Tris, 0.275 g of boric acid and 0.10 mmol of

disodium EDTA in 50 mL of deionized water). All DNA samples were labelled with biotin and fluorescein as previously described.[16]

## 5.3 RESULTS AND DISCUSSION

This section begins with a detailed description of the EMMA reaction parameters. As in the previous chapter, ovalbumin serves as the model protein. Following this, the detection limits and separations obtained using EMMA are presented. The next section consists of the use of mass spectrometry to study the labelling process. The mass spectra of labelled ovalbumin provide insight into the labelling process. In particular, the extent of multiple labelling is quantified. This data permits a discussion of the role of multiple labelling in separation efficiency as well as a general discussion of separation efficiency in protein analysis. The mass spectra of unlabelled proteins raises the question of the role of protein heterogeneity in determining separation efficiency. In the course of this last discussion, a brief digression into the separation of protein-DNA complexes is taken.

### 5.3.1 REACTION PARAMETER OPTIMIZATION

Several parameters must be optimized in the EMMA technique. Of particular importance was the use of a high reaction temperature and a discontinuous buffer that induces sample stacking. This section presents a detailed discussion of the reaction parameters. Table 1 summarizes the results obtained. Critical parameters, as well as parameters which indicate the mechanism occurring in the EMMA method, are discussed below.
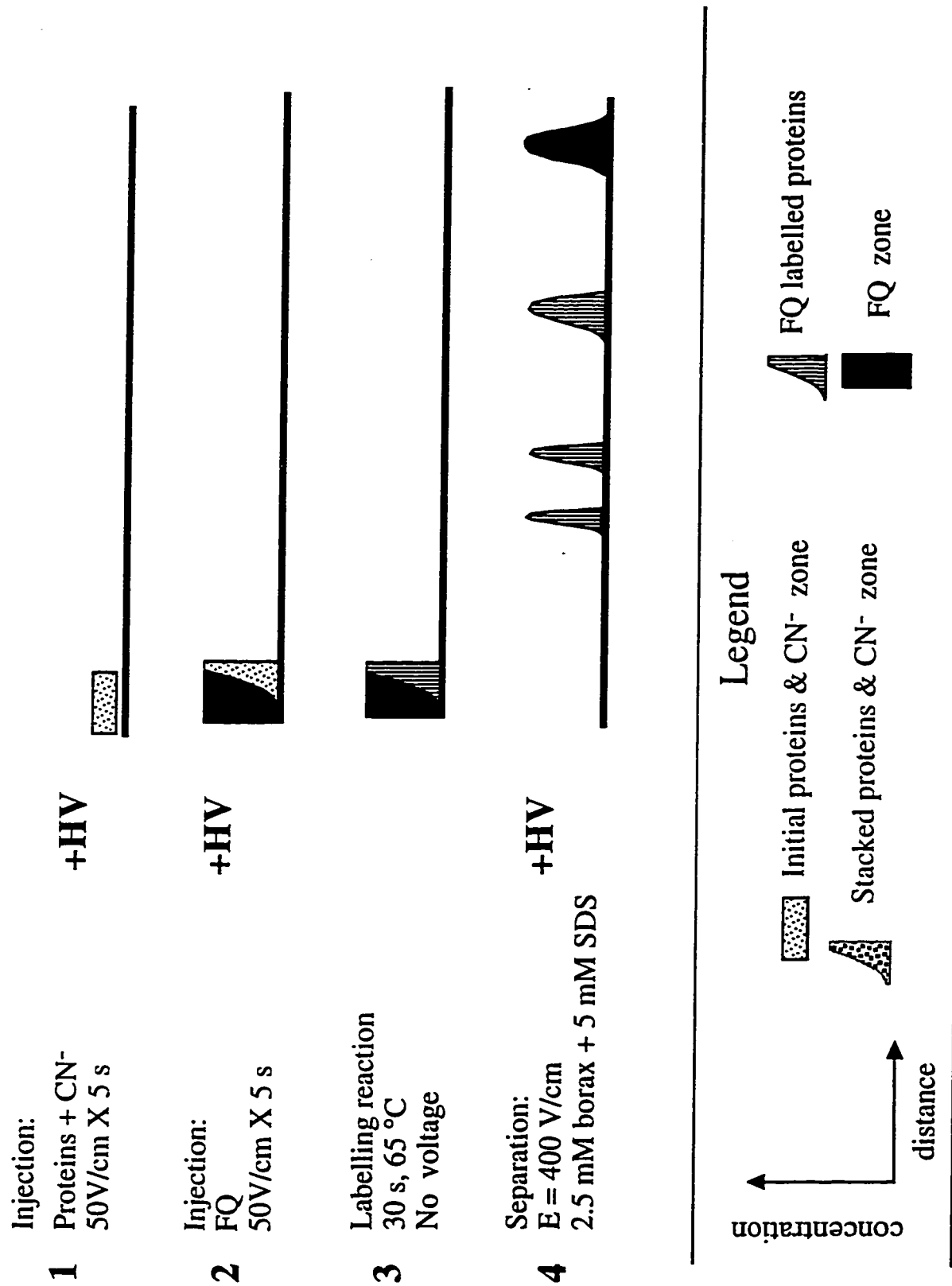
1 Injection:
Proteins + CN-
50V/cm X 5 s

+HV

2 Injection:
FQ
50V/cm X 5 s

+HV

3 Labelling reaction
30 s, 65 °C
No voltage

4 Separation:
E = 400 V/cm
2.5 mM borax + 5 mM SDS

+HV

Legend

Initial proteins & CN- zone

Stacked proteins & CN- zone

FQ labelled proteins

FQ zone

concentration

distance

Figure 5.1 Schematic of the EMMA labelling procedure

## TABLE 5.1: REACTION PARAMETER OPTIMIZATION

| Parameter* | Range | Effect On | |
|---|---|---|---|
| | | *Efficiency (N x10³) | Peak Height |
| Electrokinetic mixing | 0-10 s @ 400 V/cm | No effect | 0.68 – 0.42 |
| FQ concentration | 0.1-5 mM | 180 – 75 | 4.4 - 6.4 |
| | 5-25 mM | No effect | no effect |
| FQ injection | 5 s @ 25-125 V/cm | No effect | 0.9-1.2 |
| Protein/CN injection | 5 s @ 25-125 V/cm | 46 - 36 | 1.3 to 2.1 |
| Reaction time (T = 23 °C) | 0.5 - 9 min | 50 - 95 | 0.12-1.74 |
| Reaction Temp. (30 s rxn) | 23°C - 65°C | 40 - 300 | 0.12 – 5.8 |

*Except for the parameter under study, the following conditions were used: step 1; $10^{-7}$ M ovalbumin & 5 mM CN⁻ injection for 5 s at 1 kV; step 2: 5 mM FQ injection at 1 kV for 5 s; step 3: 30 s reaction @ 23 C; step 4: separation @ 400 V/cm, 50-μm (i.d.) x 40-cm (l) capillary.

*The separation efficiencies were calculated using the following equation, which based on an exponentially-modified Gaussian peak shape.[8] The symbols are defined in Figure 5.2.

$$N = \frac{41.7\left(\dfrac{t_r}{w_{0.1}}\right)^2}{B\big/A + 1.25}$$

In EMMA, reagent mixing occurs through electrophoretic movement; therefore, the relative mobilities of the reagents should be known. FQ, being neutral, has a net mobility equal to the electroosmotic mobility of 6.7 x $10^{-4}$ cm²/V-s. At a pH of 9.3, the net mobilities of ovalbumin and cyanide are 5.1 x $10^{-4}$ cm²/V-s [9] and 2.8 cm²/V-s respectively.[10] Given this data, CN⁻ should be injected first followed by OVA and finally FQ. To reduce the number of injections to two, the protein and cyanide are mixed prior to the analysis. In principle, CN⁻ and FQ could be mixed before injection; however, they react and form fluorescent impurities that interfere with the analysis.
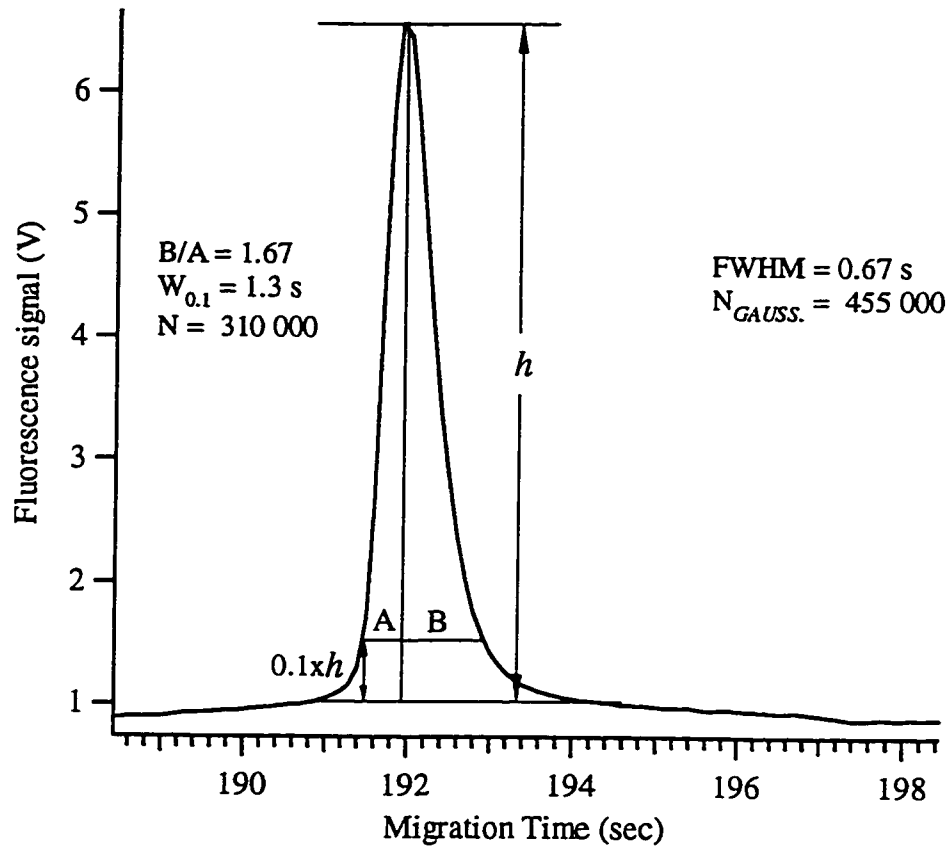
Figure 5.2 - Parameters for calculating N for exponentially-modified Gaussian peaks. Note the error in N if the peak shape is assumed to be Gaussian.

Ovalbumin was analyzed by injecting the protein/CN⁻ solution followed by the FQ solution and by reversing the order. The data in Figure 5.3 demonstrates that a peak for labelled ovalbumin is observed regardless of the injection order. However, the signal and efficiency are 23 and 1.5 times smaller respectively if the reverse order is used. This result indicates that electrophoretic mixing is the major source of mixing but that diffusional mixing does play a minor role in the mixing process.

In an effort to increase sensitivity, an additional electrokinetic mixing step was used after the FQ injection step. Instead of the signal increasing due to improved reagent mixing, the signal decreased by 20% (see Figure 5.4). This decrease in signal indicates that the reagent zones are already in an optimal position after the FQ injection. Additional electrokinetic mixing probably begins to separate the reagents; in other words, a CE separation of the reagents begins.

The reaction time plays a critical role in the sensitivity and efficiency obtained. FQ reacts with more lysine residues as the reaction time increases, see Figure 5.5. However, in the interest of throughput, a reaction time of 30 seconds was used for further experiments. The migration time of the FQ-labelled ovalbumin increases by approximately 5 seconds over the course of the reaction. The conversion of lysine residues from cations to neutral FQ-lysine moieties causes this reduction in mobility.

The sensitivity increases with the FQ concentration (Figure 5.6). Unfortunately, FQ precipitates at concentrations above 10 mM resulting in decreased reproducibility. The decrease in efficiency is another drawback of using high concentrations of FQ. Presumably, the heterogeneity of the reaction products increases
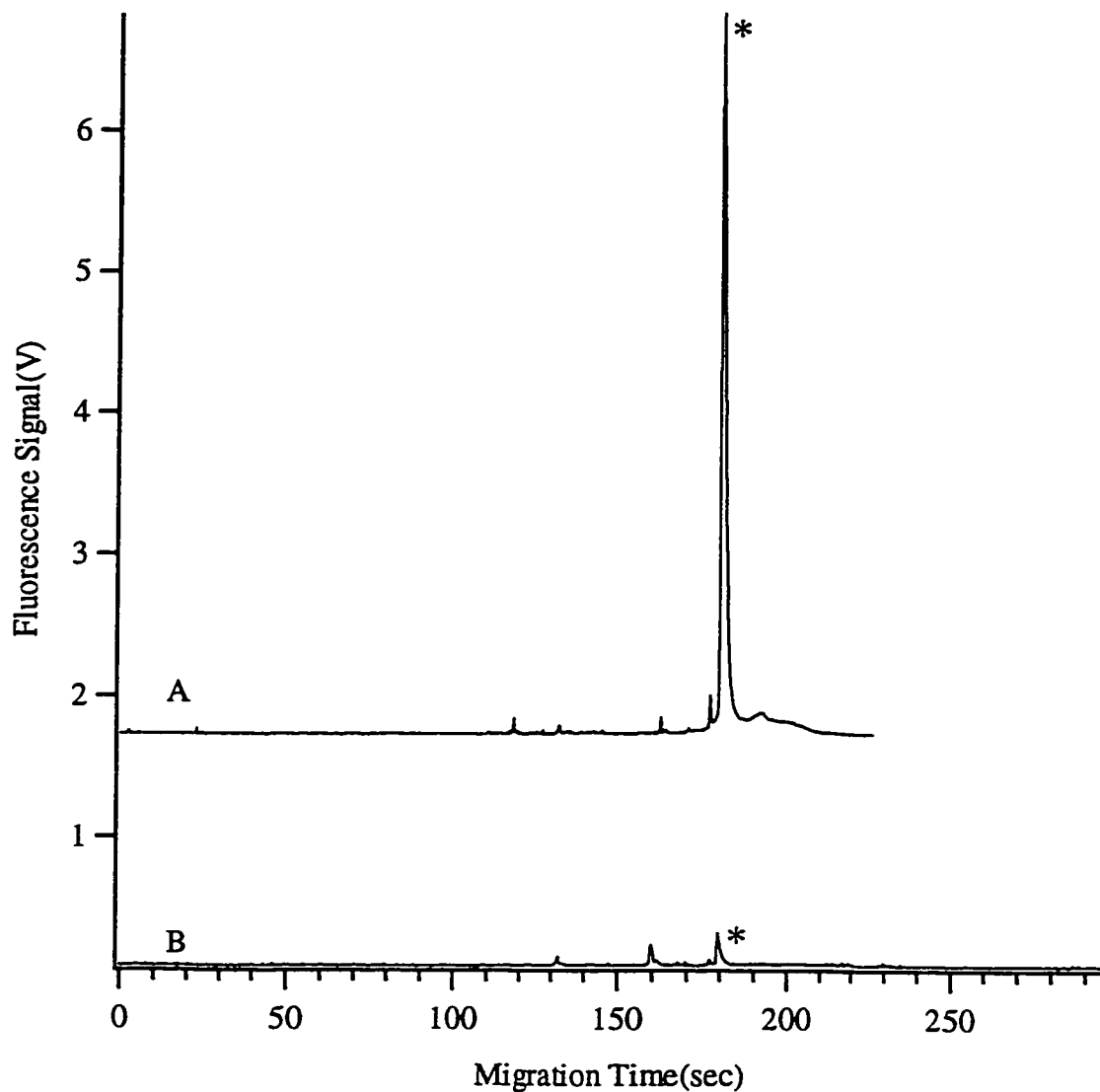
Figure 5.3 - Effect of injection order on EMMA labeling of ovalbumin. The asterisk indicates the peak for FQ labeled ovalbumin. (A) Step 1: $10^7$ M ovalbumin & 5 mM injection for 5 s at 1 kV; step 2: 5 mM FQ injection at 1 kV for 5 s; step 3: 30 s reaction @ 65 C; step 4: separation @ 400 V/cm, 50-μm (i.d.) x 40-cm ($l$) capillary.
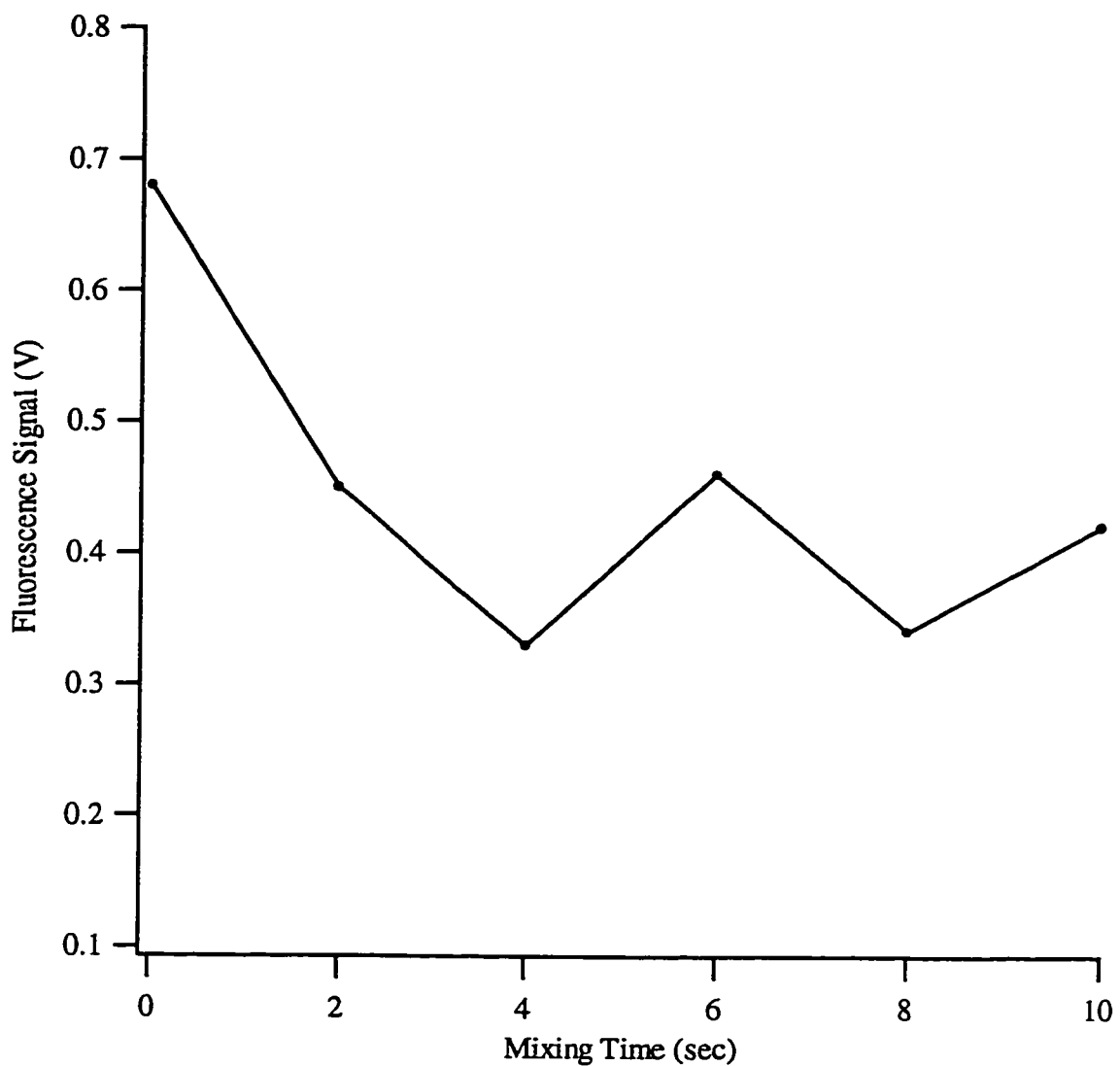
Figure 5.4 - The effect of electrokinetic mixing on the signal in EMMA analysis of ovalbumin. The conditions were the same as in Figure 5.3 except that the reaction was performed at room temperature and the mixing step was inserted between steps 2 and 3.
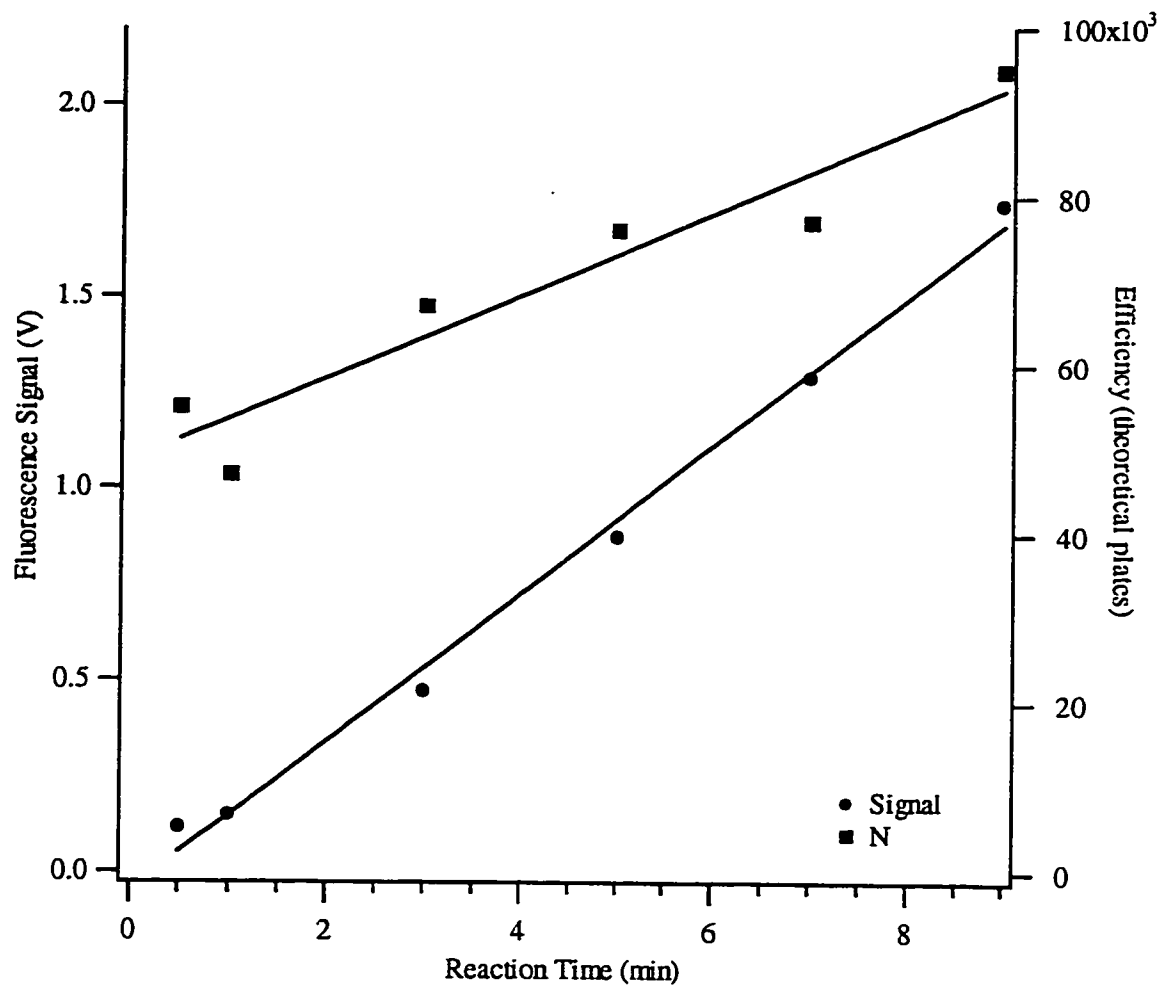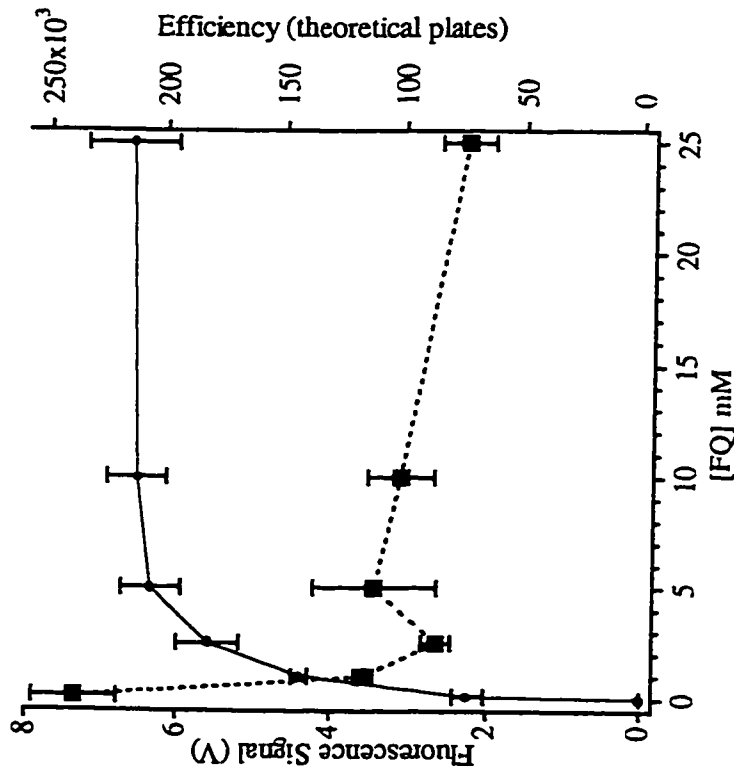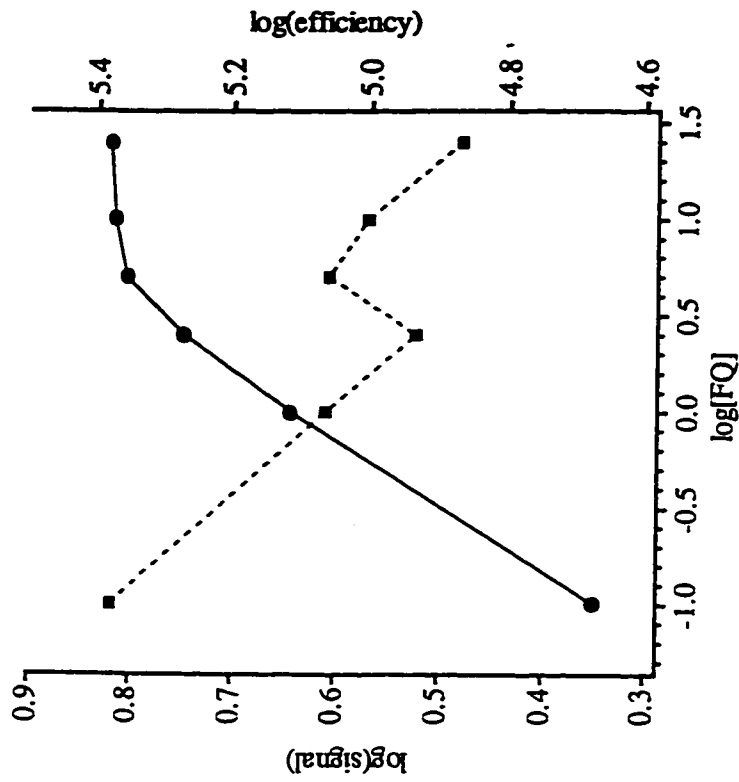
Figure 5.5 -The effect of reaction time on sensitivity and efficiency. The experimental

conditions were the same as in Figure 5.4. The average RSD for the signal and

efficiency was 12 and 30% respectively, n = 3.

Figures 5.6A and 5.6B: The effect of derivatizing regent concentration on signal ( ) and separation efficiency (Y).

Reaction conditions: Step 1: 10^-7 M ovalbumin injection for 5 s @ 2 kV. Step 2: FQ injection for 5 s @ 2 kV. Step 3:

Reaction @ 65 °C for 40 sec. Step: 4 separation @ 400 V/cm. Capillary: 50 μm (i.d.) x 35 cm (*l*). Error bars are ± one

standard deviation (n=3)

with the number of FQ labels attached. This data is consistent with the data obtained for pre-capillary labelling.

The final, and most important, parameter studied was the reaction temperature. Raising the reaction temperature from 23 °C to 65 °C increases the peak height 48 times and the peak efficiency 6 times. Figure 5.7 contains the plots of the fluorescence signal and separation efficiency as a function of reaction temperature. Ovalbumin has 20 lysine residues. The reaction rate is expected to increase with temperature resulting in an increase in the number of labels attached during the 30 s reaction. The signal should increase linearly with the number of fluorescent labels attached.

In summary, the following conditions provided high sensitivity, high efficiency and high throughput: the sample, dissolved in 2 mM borax + 4 mM SDS, pH 9.4, is injected for 5 s at 2 kV (57 V/cm); then 10 mM FQ, dissolved in running buffer (2.5 mM borax and 5 mM SDS), is injected for 5 s at 2 kV; the capillary tip is immersed in 65 °C running buffer for 30 s; the capillary is immersed in running buffer and the separation is carried out at 400 V/cm.

## 5.3.2 DETECTION LIMITS, LINEARITY AND MIXTURE ANALYSIS USING EMMA

The optimized reaction conditions were used to obtain calibration curves, calibration curves and detection limits for ovalbumin and conalbumin. Figure 5.8 contains electropherograms from the analysis of ovalbumin from $10^{-8}$ M to $10^{-11}$ M. At the lowest concentration, only 25 zeptomole (1 femtogram) was injected. The
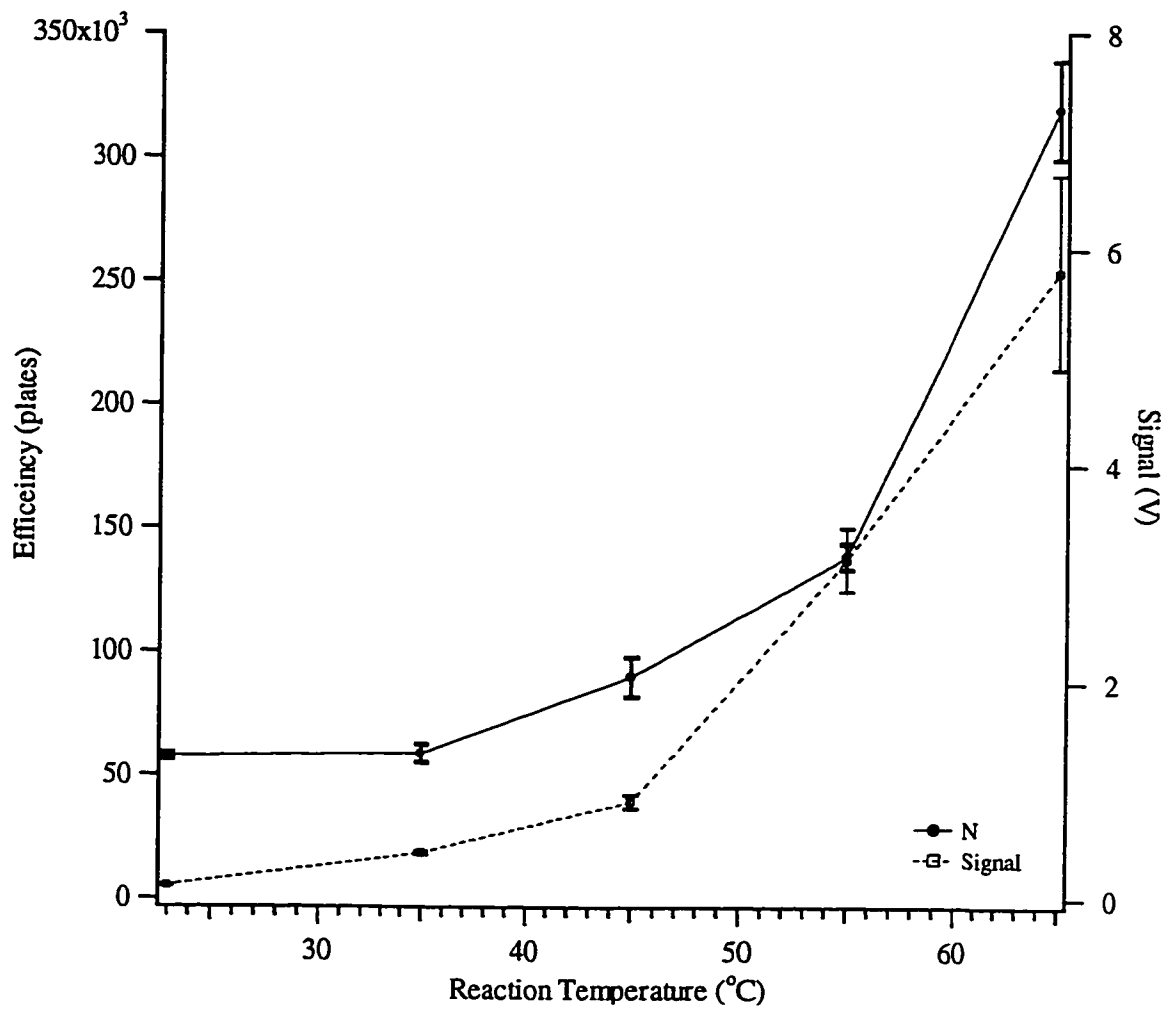
Figure 5.7 - The effect of reaction temperature on signal and efficiency. All reaction were performed for 30 sec. For the remaining conditions, see Figure 5.6.
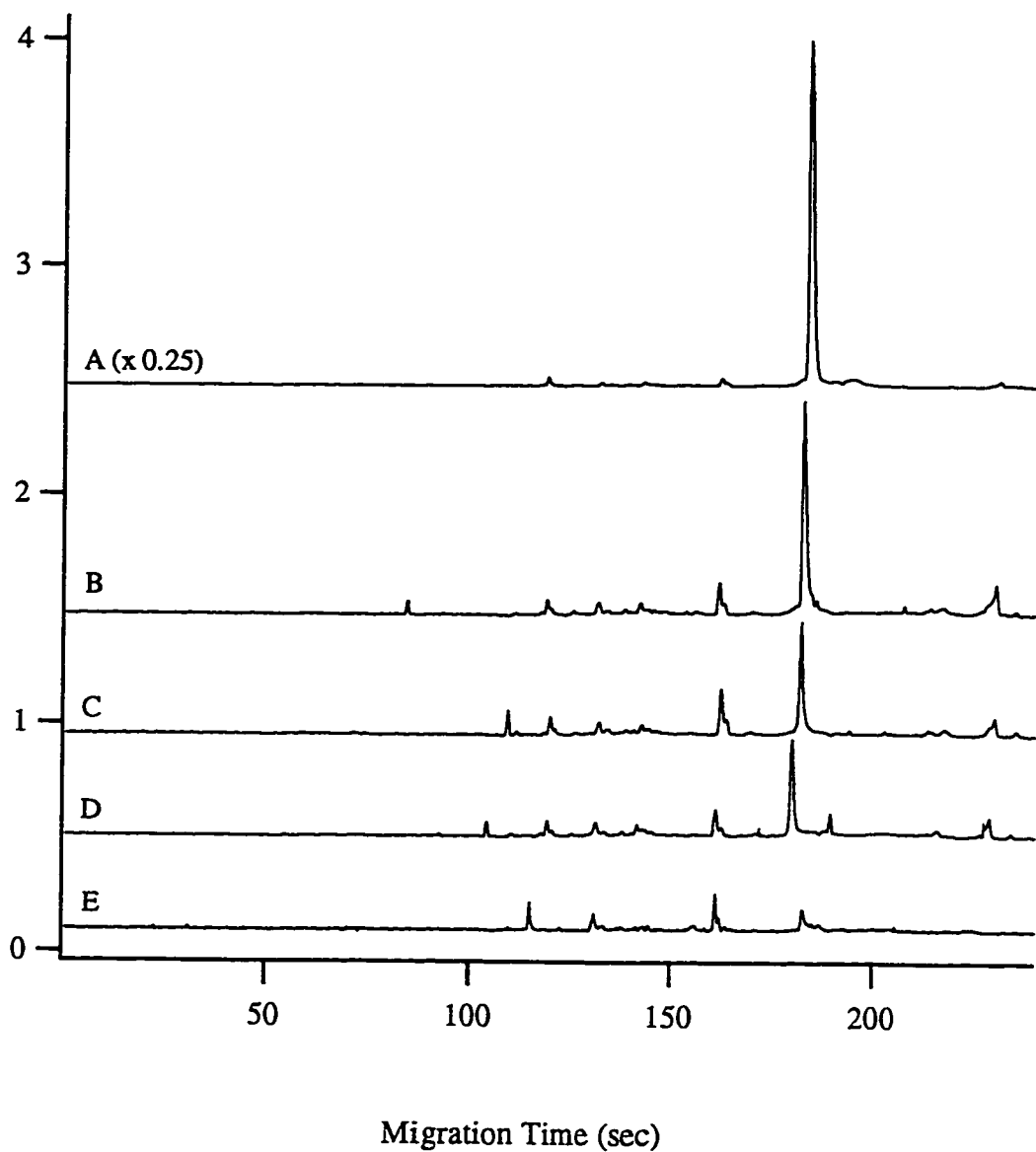
Migration Time (sec)

Figure 5.8 - Trace analysis of ovalbumin by EMMA. The concentration of ovalbumin was (A) $10^{-8}$, (B) $10^{-9}$, (C) $10^{-10}$, (D) $10^{-11}$ and (E) 0 (reagent blank). EMMA conditions: Step 1: sample & KCN injection for 5 s at 2 kV (57 V/cm); Step 2: 10 mM FQ injection for 5 s at 2 kV; step 3: reaction at 65 °C for 30 s, Step 4: separation at 400 V/cm.
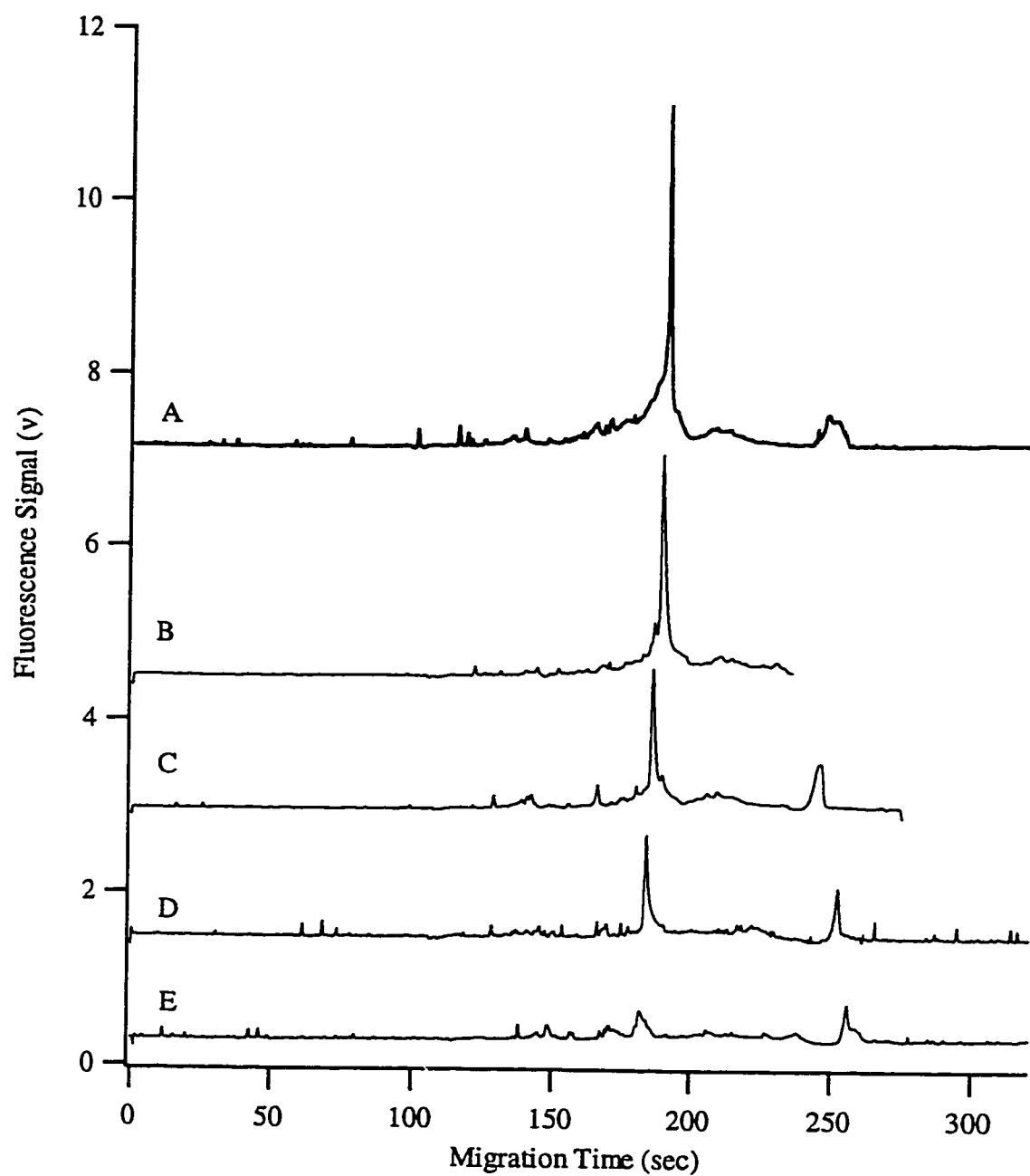
Figure 5.9 - Trace analysis of conalbumin by EMMA. The concentration was (A) $10^{-10}$, (B) $5 \times 10^{-11}$, (C) $10^{-11}$, (D) $5 \times 10^{-12}$ and (E) 0 (reagent blank). EMMA conditions: see fig. 5.8.
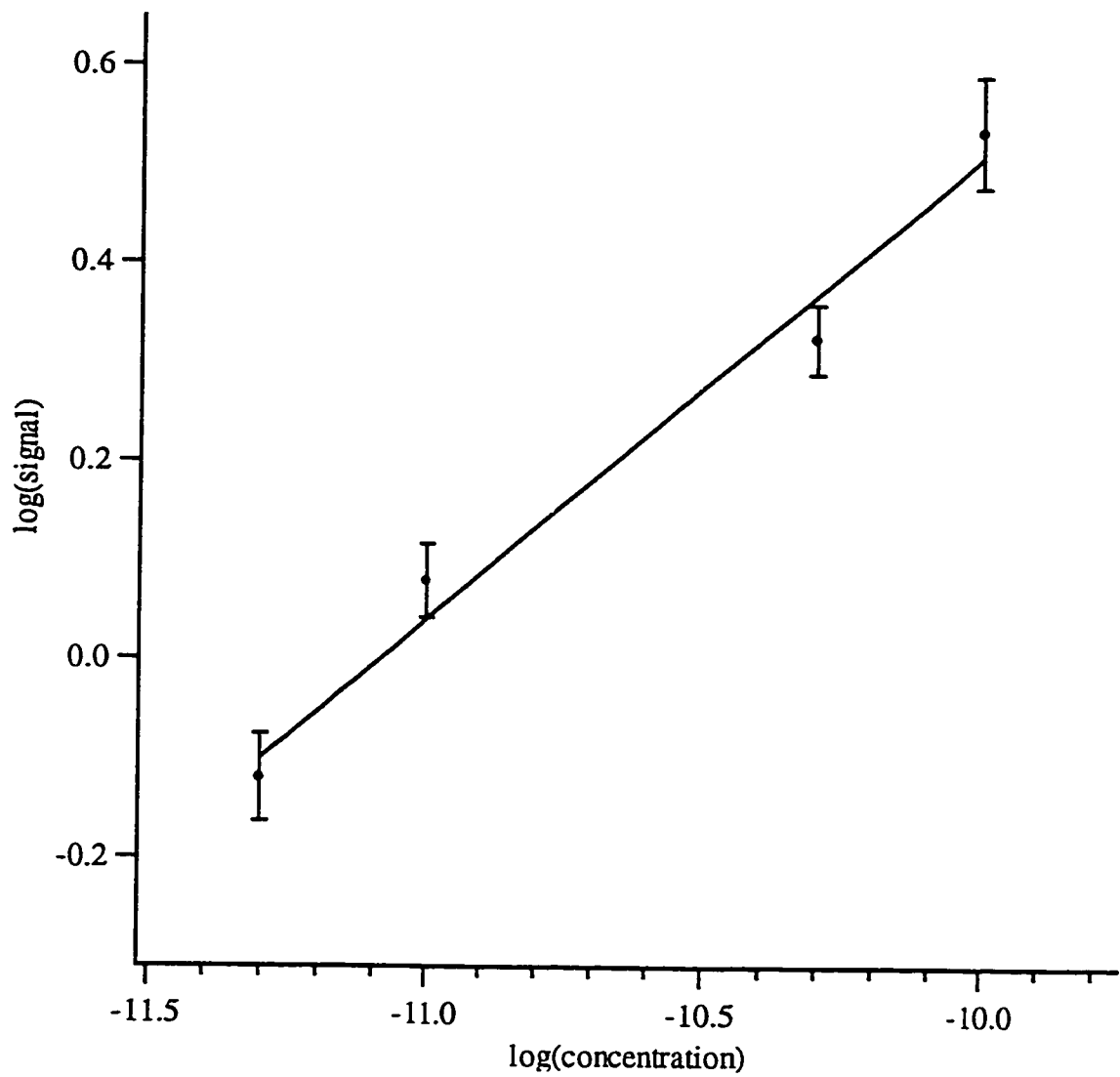
Figure 5.10 – Calibration curve for the analysis of conalbumin at trace levels. The curve fits the following equation: log(signal) = 5.2 ± 0.5 + (0.47 ± 0.05)log[conalbumin]

detection limit was $5 \times 10^{-12}$ M. The sensitivity is higher for conalbumin, a protein with 59 possible sites for FQ labelling (Figure 5.9). The lowest concentration analyzed was $5 \times 10^{-12}$ M, which corresponds to 28 zeptomoles injected. The detection limit for conalbumin is $3 \times 10^{-13}$ M.

The slope of the log-log calibration curve in Figure 5.10 is 0.5, within experimental error, which indicates a square root relationship between signal and concentration. This non-linearity is likely a result of the use of sample stacking.

The only other methods that approach the sensitivity of the EMMA method are native fluorescence and the pre-capillary labelling method presented in chapter 4. The conalbumin detection limit is 33 times lower than the detection limit obtained for pre-capillary labelling, and 10 times lower than the detection limit obtained for native fluorescence detection under stacking conditions.[11] The EMMA detection limit for ovalbumin is 40 times lower than the detection limit obtained using the pre-capillary method. Figure 5.10 illustrates these improvements. Despite the 100 fold lower concentration, the S/N ratio in the EMMA analysis was ten times higher than the S/N ratio in the pre-capillary method. The efficiency in the EMMA method was 75,000 theoretical plates as opposed to an efficiency of 40,000 plates in the pre-capillary method.

In the EMMA analysis, co-migrating peaks from reactions between FQ and $CN^-$ produce chemical noise. The chemical noise limits the sensitivity and is approximately ten times higher than the next major source of noise, shot noise from scattered light.
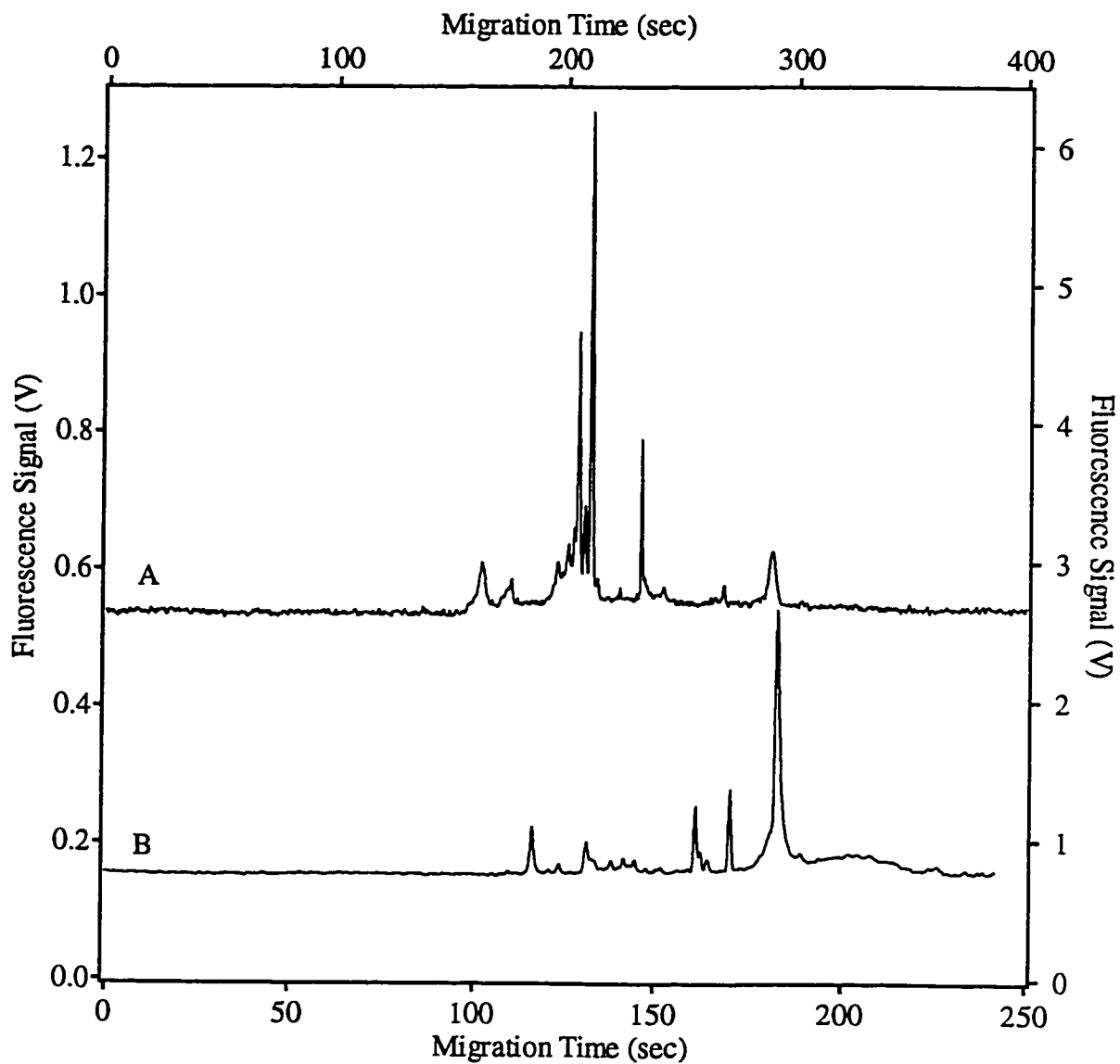
Figure 5.10 Comparison of (A) pre-capillary and (B) EMMA labelling of ovalbumin. The ovalbumin concentration was $10^9 M$ in (A) and $10^{11} M$. The pre-capillary labelling was performed at room temperature for 16.5 min & the EMMA labelling was performed at 65 °C for 30s.
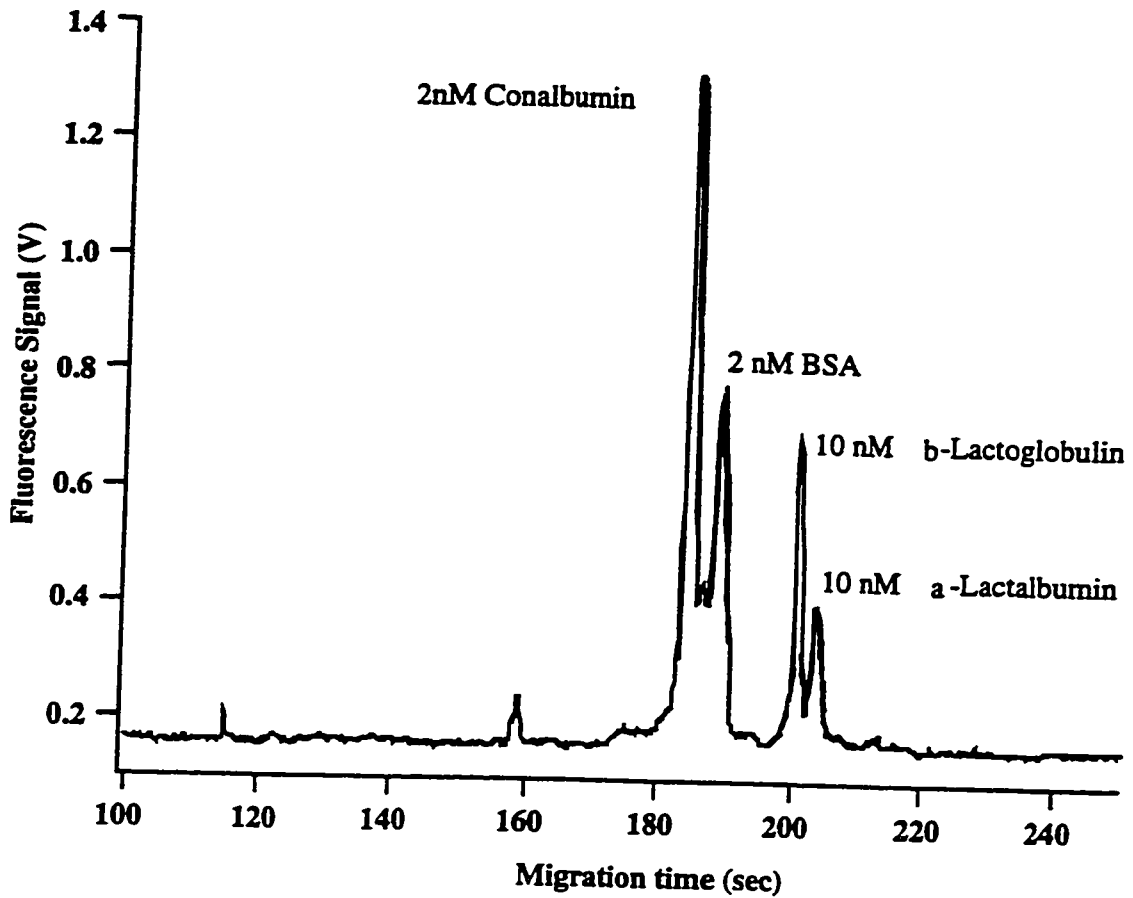
Figure 5.11 - Separation of protein mixtures after EMMA labeling. In step 1, protein concentrations are 2 nM conalbumin, 2 nM BSA, 10 nM β-lactoglobulin, and 10 nM α-lactalbumin. Other reaction steps and conditions are the same as in Figure 2. Peak assignments: (1) conalbumin, (2) BSA, (3) β-lactoglobulin, (4) α-lactalbumin.

Mixture of proteins at trace levels can be analyzed using EMMA. Figure 5.11

contains an electropherogram resulting from the EMMA analysis of a mixture

containing 2 nM conalbumin, 2 nM BSA, 10 nM $\beta$-lactoglobulin, and 10 nM $\alpha$-

lactalbumin. In the previous chapter, a similar mixture was labeled off-line and then

separated under similar conditions. The resolution between $\beta$-globulin and $\alpha$-

lactalbumin is similar in both cases. BSA and $\beta$ -lactoglobulin were better separated in

on-capillary labelling than in pre-capillary labelling.

## 5.3.3 The use of MALDI-TOF-MS to study the labelling reaction

CE-LIF does not posses the ability to discretely monitoring the labelling of

lysine residues since the signal is the sum of the fluorescence from all the FQ labels.

To a certain extent, time-of-flight mass spectrometry (TOF-MS) allows us to

discretely monitor the labelling process. TOF-MS, when coupled with matrix-assisted

laser desorption and ionization (MALDI), is nearly ideal for protein analysis. The MS

data compliments the discussion of the optimization of reaction conditions previously

presented

In this section, a discussion of the reaction kinetics will precede a discussion of

the reaction heterogeneity.

Before begin these two discussions, a few points on MALDI-TOF-MS spectra

are presented. Figure 5.12 contains the MS spectra from the analysis of native and

labelled ovalbumin at various reaction times. The intensity varies with the sample

preparation and data acquisition parameters; therefore, the intensity does not correlate

with any parameter of the labelling reaction. The peak width, however, is mainly
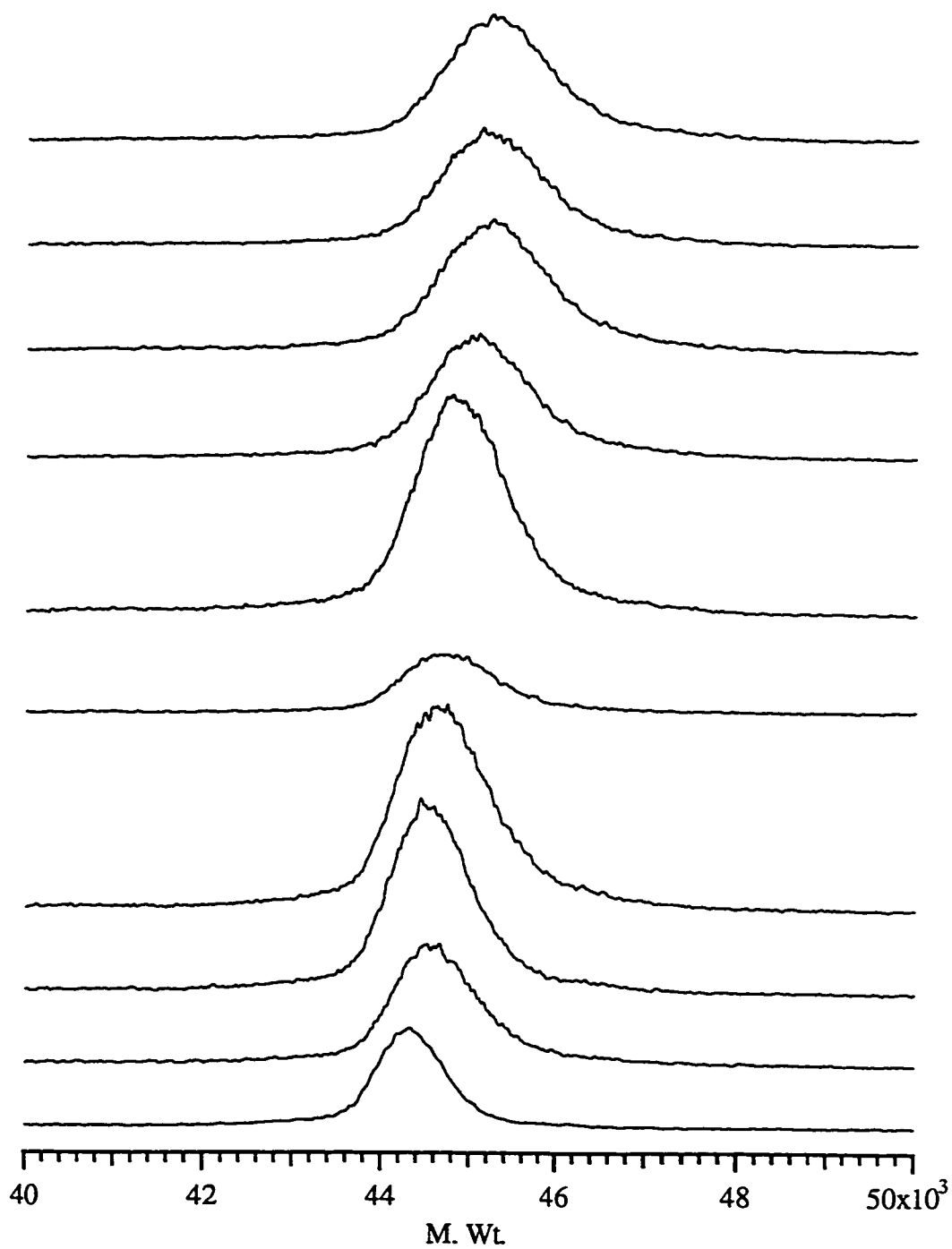
148

Figure 5.12 - MALDI-TOF-MS spectra from the analysis of unlabelled and FQ labeled ovalbumin. The bottom trace corresponds to unlabelled ovalbumin. The remaining traces, from top downwards are for reaction times of 30, 25, 20, 13, 6.0, 3.0, 1.0 0.50 and 0.25 min
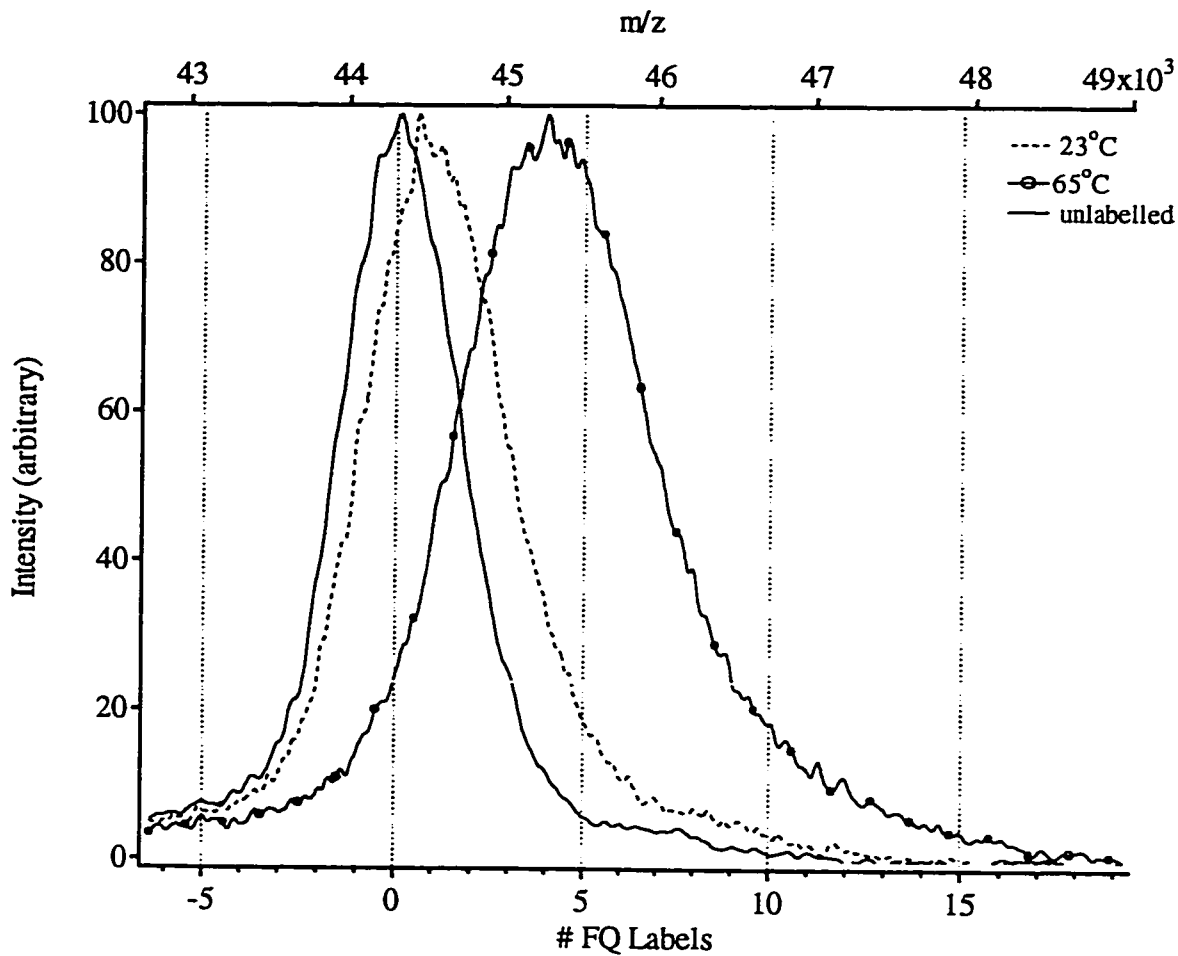
149

Figure 5.13 - MALDI-TOF-MS analysis of unlabelled ovalbumin and ovalbumin labelled for 30 s. The spectra are for the singly charged ions, therefore, the molecular weight and the m/z ratio are equivalent. The intensities were normalised to facilitate comparison.

determined by the inherent protein heterogeneity and the heterogeneity of the labelling process. To a lesser degree, the instrument's resolution affects the width. The peak width measurement is reproducible; the RSD is less than 1%.

Reaction kinetics

Figure 5.13 contains the MS spectra for unlabelled ovalbumin and ovalbumin labelled for 30 s at either 23 °C or 65 °C. The increase in temperature results in an increase in the average number of FQ labels from 0.8 to 4.6, a factor of 5.6. The increase in temperature also increases the maximum number of FQ labels attached. For example, significant amounts of ovalbumin have 8 FQ labels at the higher temperature whereas at room temperature, the maximum number of FQ labels is approximately 2.

The increased reaction temperature, in addition to increasing sensitivity, results in a decrease in analysis time. Figure 5.14 contains the kinetic curves for the two temperatures. The faster reaction at the higher temperature allowed for the reaction time to be decreased to 30 s from 9 min. Note that the majority of ovalbumin's 20 lysine residues remain unlabelled at both temperatures.

Figure 5.15 contains a comparison of the kinetic curves from CE-LIF and MS analysis. This data shows that the fluorescence signal increases linearly with the number of FQ labels. Furthermore, for reactions performed at 23 °C, the average number of FQ labels reaches a maximum after 30 minutes and does not approach the number of labels at 65 °C. This indicates that the higher temperature renders more lysine residues accessible to contact with FQ. This increase is likely due to partial denaturation of the protein.
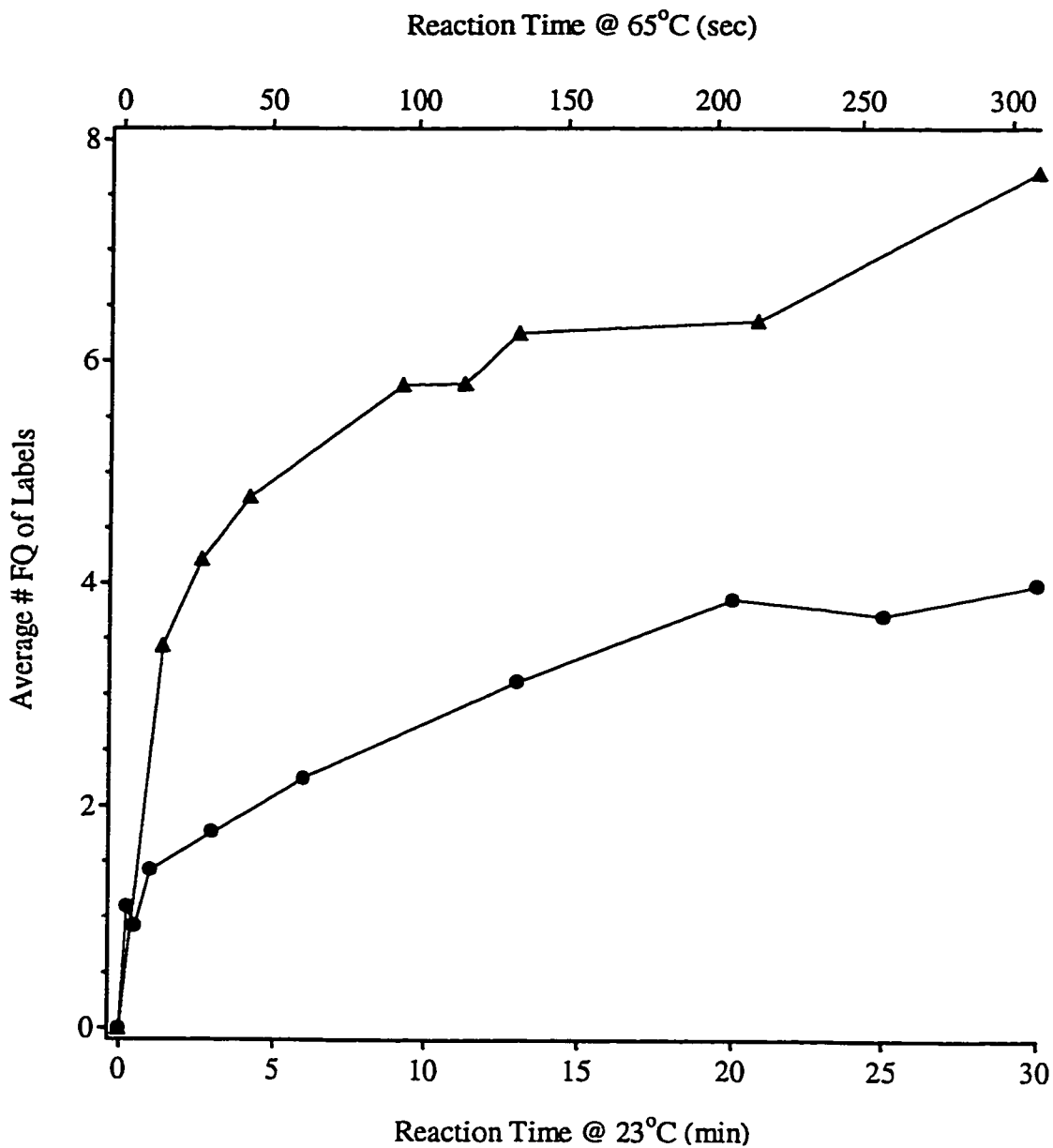
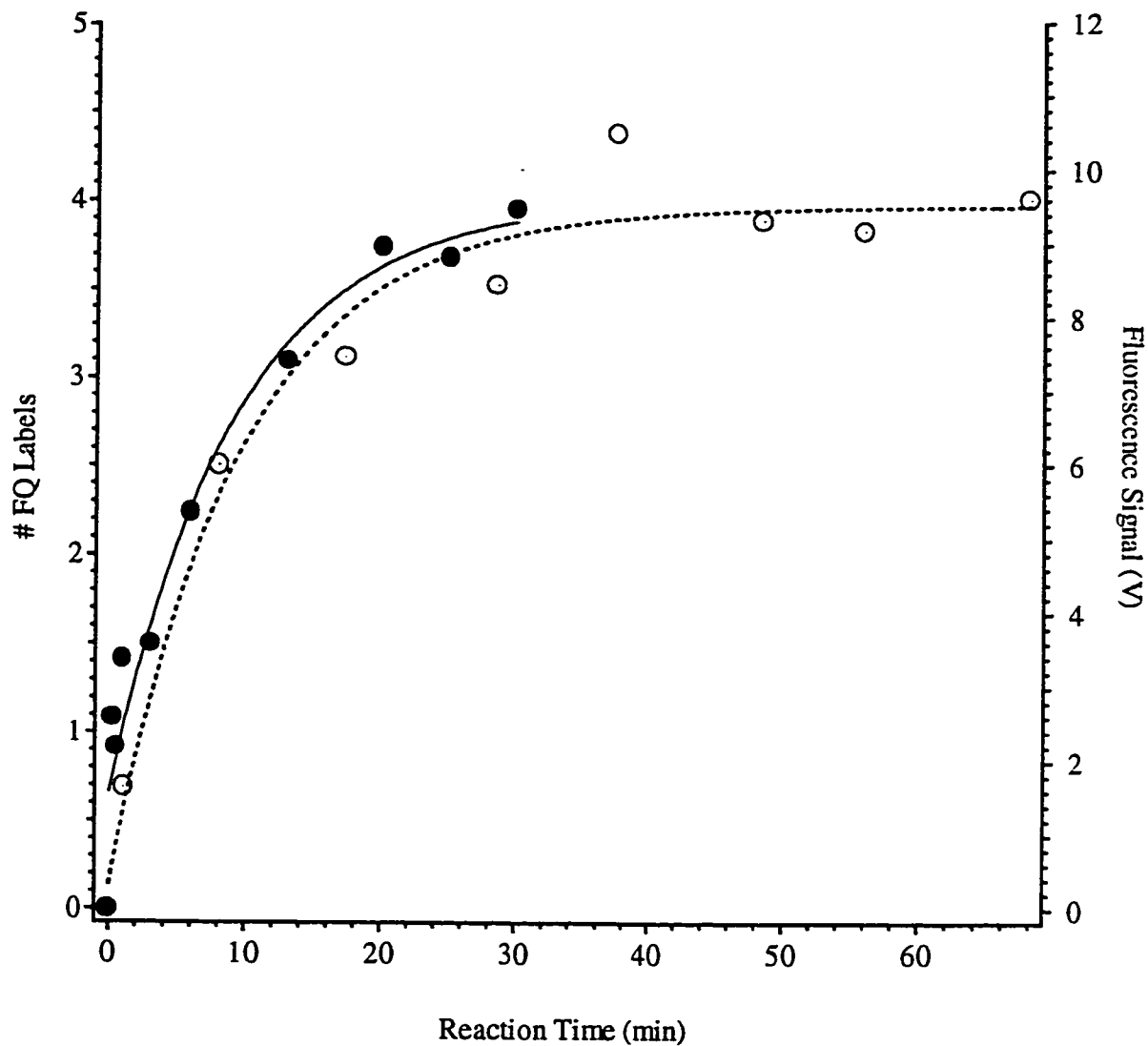Figure 5.14 - kinetics for the labelling of ovalbumin with FQ at 23 °C (●) and 65 °C (▲).

Figure 5.15 - Comparison of labelling of ovalbumin with FQ. The reaction was

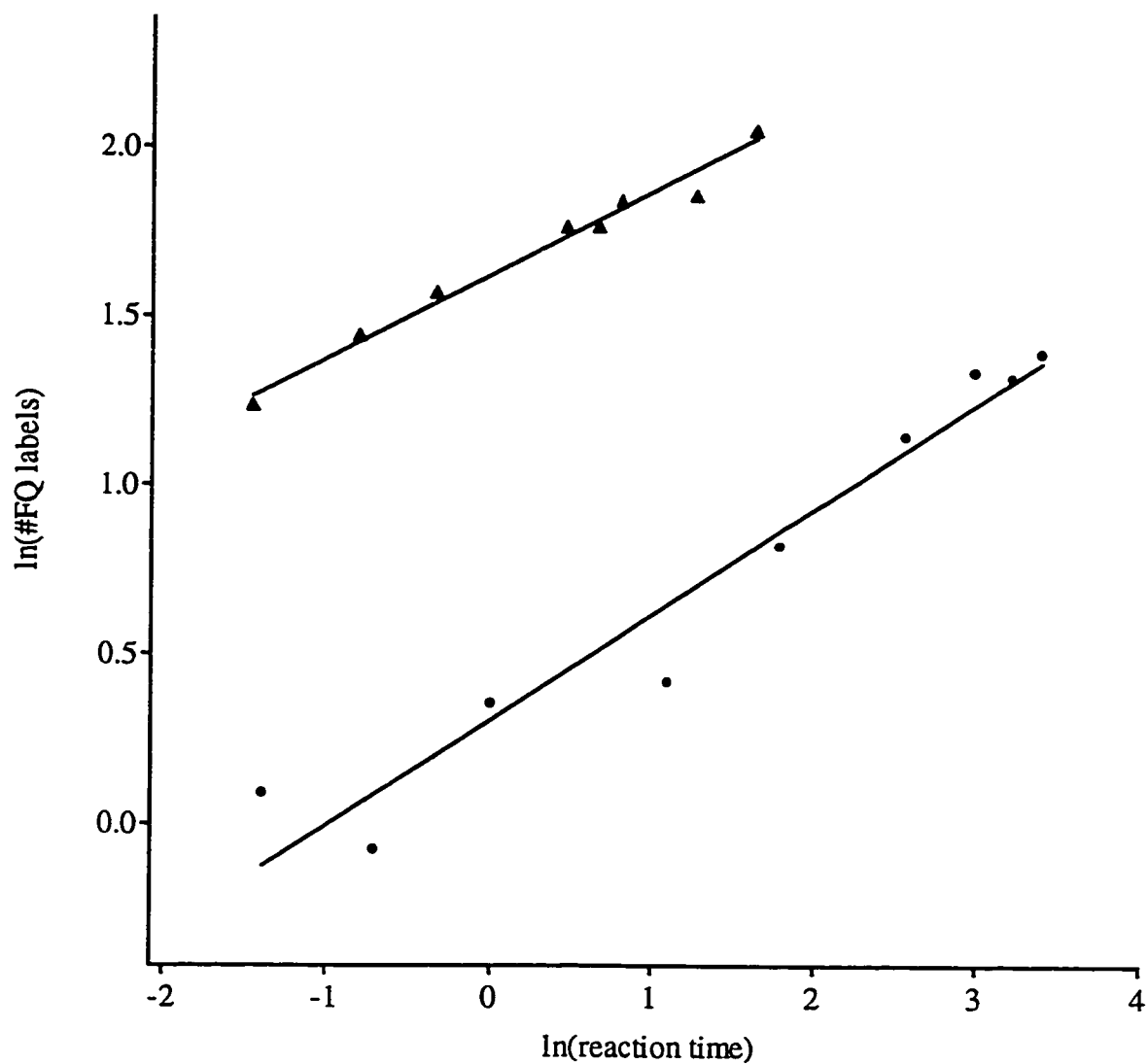monitored by MALDI-TOF-MS (●) and CE-LIF (O). Labelling was done off-line in

both cases.

Figure 5.16 - Reaction kinetics at 65 °C (▲) and (B) 23 °C (●). The intercepts and slopes, respectively, of the lines are 1.6 ± 0.1, 0.24 ± 0.01 at 65 °C and 0.30 ± 0.06, 0.31 ± 0.03 at 23 °C.

The plots of log(#FQ labels) versus log(reaction time) was linear for both temperatures, as seen in Figure 5.16. Data for the progress of a reaction at different temperatures lends itself to the study the temperature dependence of the rate constant according to the Arrhenius equation. Here, however, the data does not reflect the behavior of a single reaction since there are several unique lysine residues reacting at the same time.

Reaction heterogeneity

As mentioned in the previous chapter, analytes with $n$ reactive sites can produce $2^n - 1$ reaction products. These heterogeneous products cause band broadening in CE separations.

MALDI-TOF-MS was used to quantify the heterogeneity caused by the labelling process. The FWHM was measured for FQ labelling of ovalbumin at 23 °C and 65 °C. The FWHM prior to labelling was 800 Da. This width is a combination of the instrument's resolution and the natural variation in molecular weight due to variations in glycosylation. After conducting a 30 s labelling reaction, the FWHM increases to approximately 1100 Da and 1500 Da for reaction at 23 °C and 65 °C respectively.

The peak variance is also a useful measure of the heterogeneity due to labelling. The equation below describes the total variance ($T$) of the MS peak as the sum of the variance due to the instrumental resolution ($MS$), the inherent heterogeneity of the protein ($OVA$) and the heterogeneity of the labelling process ($FQ$).
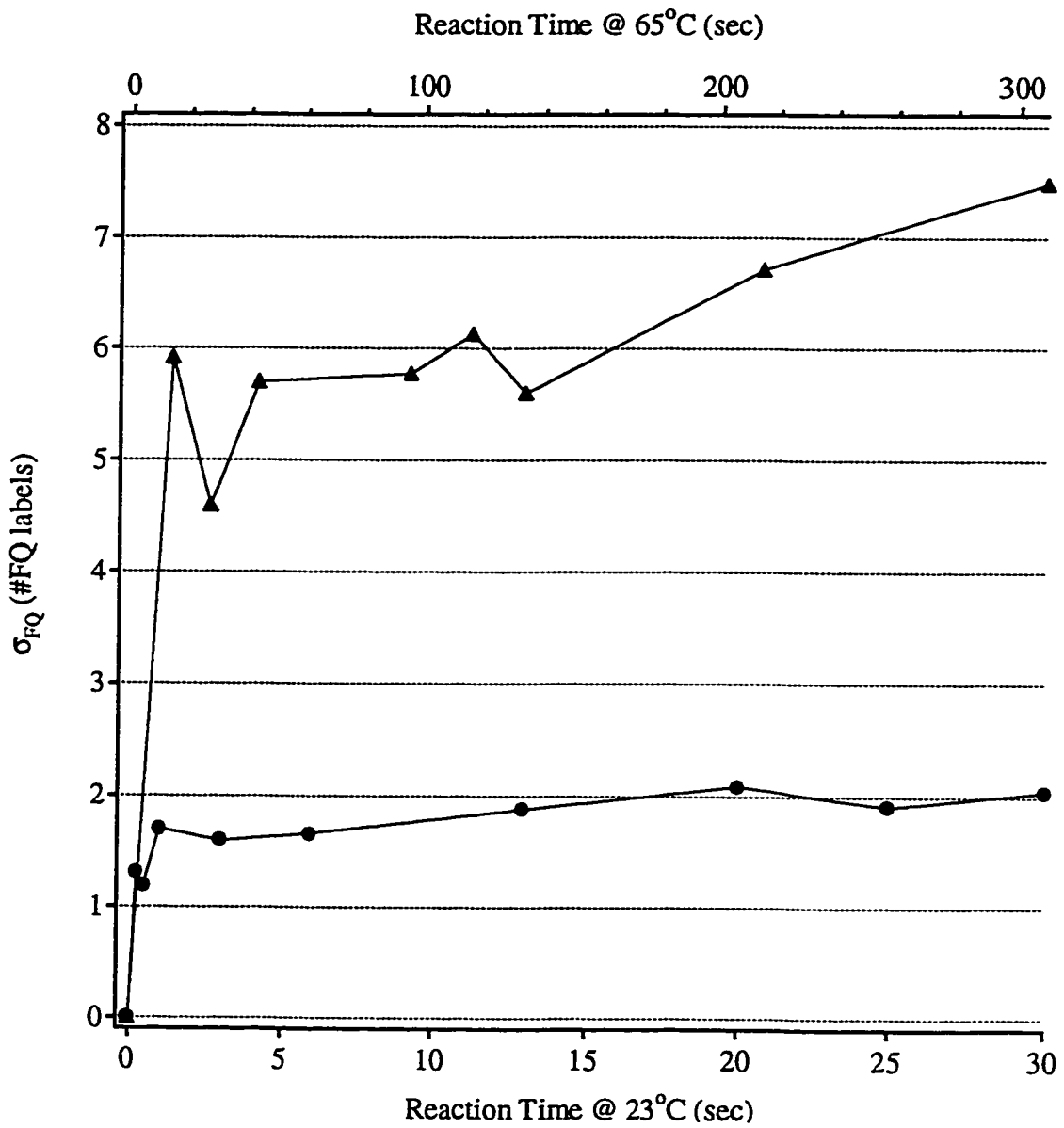
Figure 5.17 - The standard deviation due to labelling with FQ. The reaction

temperature was 23 °C (●) and 65 °C (▲).

156

$$\sigma_T^2 = \sigma_{MS}^2 + \sigma_{OVA}^2 + \sigma_{FQ}^2 \qquad\qquad (5.1)$$

The MS spectra of unlabelled ovalbumin provides the first two terms on the right

since the variance due to labelling is zero for unlabelled ovalbumin. The MS peak

shapes for the reaction performed at 23 °C were Gaussian, therefore, the total variance

is easily measured from the MS spectra. In the case of the reaction performed at 65 °C,

the peak shapes were far from Gaussian; therefore, the total variance was calculated

using the method of Kirkland et al.[12] Figure 5.17 contains the standard deviation due

to labelling as a function of reaction time.    The range of FQ labels is a useful

measure of the heterogeneity due to labelling. Figure 5.18 contains the range of FQ

labels as a function of time. The intervals contain 95% of the range. Due to the

asymmetry of the peaks for the reaction performed at 65 °C, this range was measured

manually measured from the MS spectra. In the case of the data for the reaction at 23

°C, the range is simply the average $\pm$ 2$\sigma$. The data clearly shows that the heterogeneity

increases with both reaction temperature and reaction time.

Figure 5.19 compares FQ labelled BSA and commercial FITC-labelled BSA.

The standard deviation due to labelling with FITC and FQ was 1600 Da and 740 Da,

respectively. If we factor in the relative molecular weights, the standards deviation

due to labelling is 1.6 times higher in the case of FITC. The separation efficiency

obtained with the FQ-labelled BSA was approximately twice that obtained with FITC-

labelled BSA.

## 5.3.4 SEPARATION EFFICIENCY IN PROTEIN SEPARATIONS

Role of multiple labelling & protein-wall interactions

Based on the MS data, the separation efficiency should decrease if either the reaction time or the reaction temperature is increased. The opposite is actually observed. This observation demonstrates that broadening due to multiple labelling is not a major source of band broadening and is consistent with results obtained for pre-capillary labelling.

Perhaps then, the strength of the protein-wall is the main contribution to band broadening. Protein-wall interactions arise from interactions between the capillary's anionic silanol groups and the cationic amine groups at the end of lysine and arginine side chains. Therefore, labelling lysine groups with hydrophobic FQ labels reduces protein-wall interactions. The lysine groups on the outside of the protein are the ones that are most likely being labeled and these lysine residues are also the most likely to interact with the capillary walls. More of the lysine residues react with FQ at higher temperature. This explains why the efficiency increases as the temperature or reaction time increases despite the increase in heterogeneity due to multiple labelling.
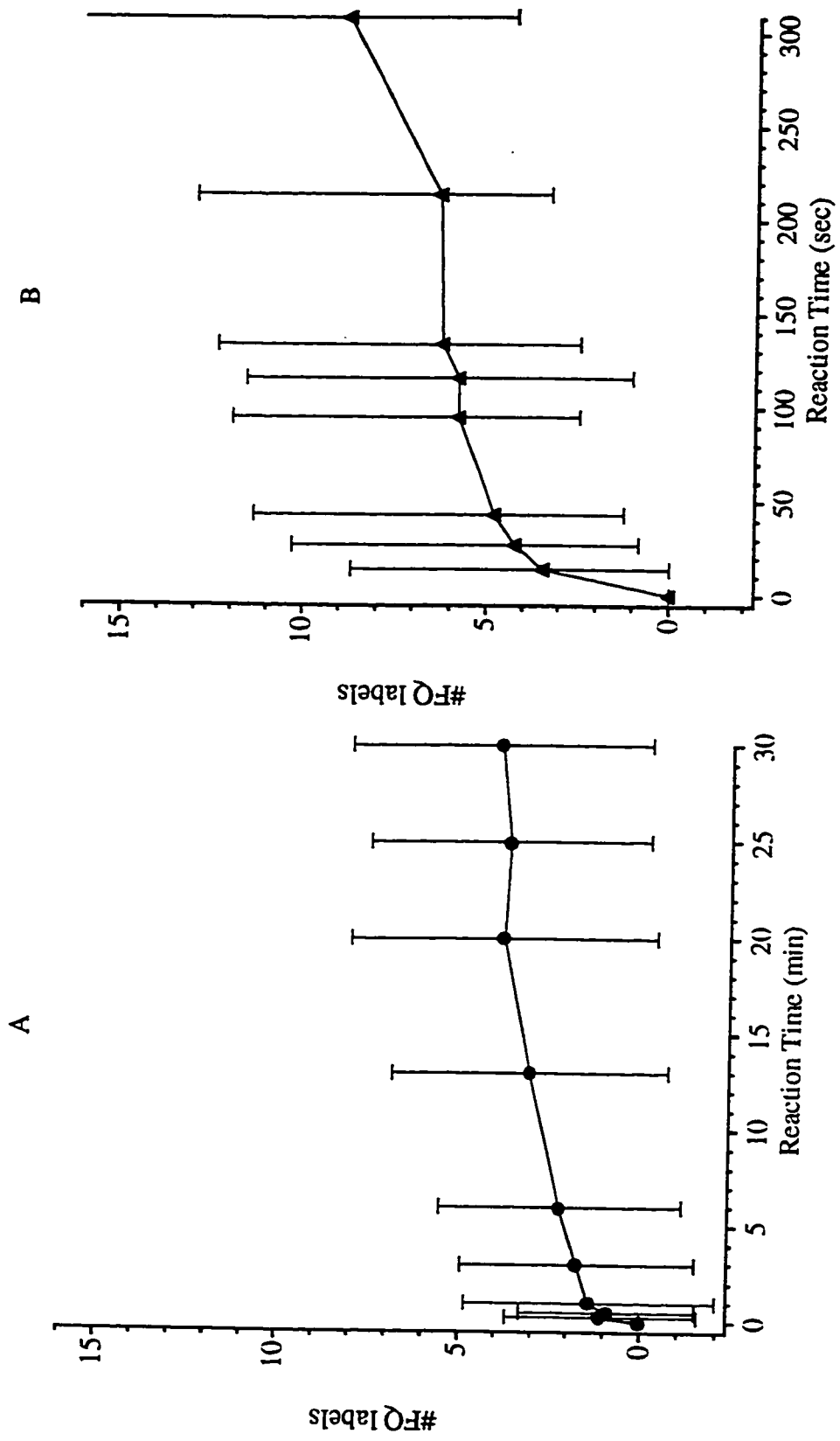
Figure 5.18 - The increase in heterogeneity of ovalbumin due to labelling with FQ at (A) 23 °C and (B) 65 °C. The data correspond to the average and the range which contains 95 % of the peak area.
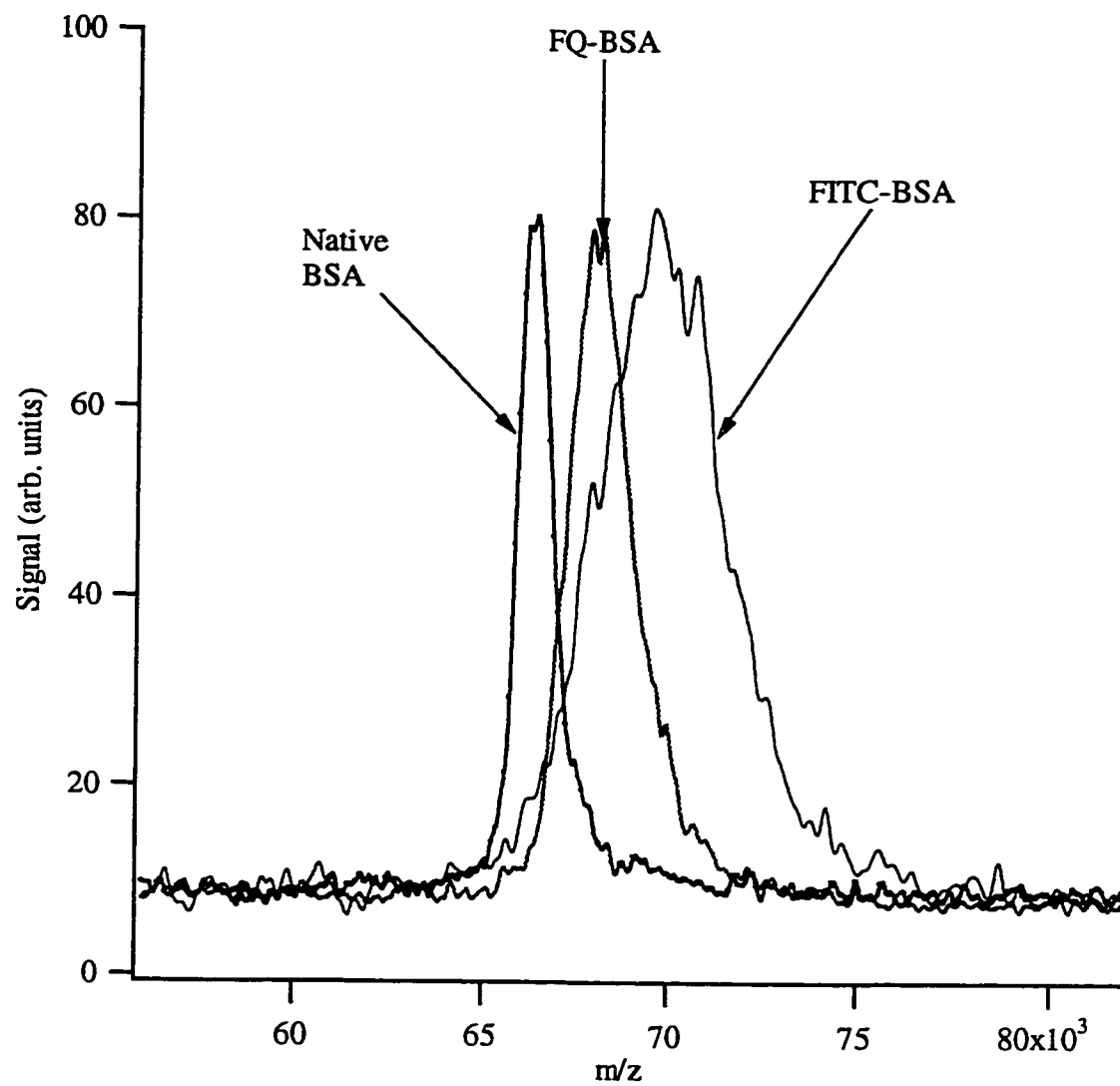
Figure 5.19 - MALDI-TOF-MS analysis of native BSA, FQ-labelled BSA and FITC-BSA form Sigma. The FQ labelling was performed at room temperature for 3 min.

Role of sample stacking

The separation efficiency in the initial EMMA experiments was equal to the efficiency obtained under similar conditions in the pre-capillary method. However, by modifying the composition of the sample buffer, the separation efficiency tripled.

The increase in efficiency is due to the use of sample focusing. Sample focusing converts an initially long sample zone into a narrow zone, thereby increasing both efficiency and sensitivity. Ideally, the contribution of initial zone width to band broadening is negligible after sample focusing.

The optimal buffer for focusing, determined empirically, was 2.0 mM borax, 4 mM SDS and 5 mM KCN. The buffer's in ionic strength is similar to that of the running buffer (2.5 mM borax, 5 mM sodium SDS); therefore, field enhancement, the technique discussed in chapter 3, is not the mechanism responsible for the focusing. The sample focusing is due to the self-stacking induced by the $CN^-$ in the sample plug. This conclusion is supported by the variation in stacking that occurred as the $CN^-$ concentration was varied and by the peak tailing observed. Peak tailing can be due to stacking or to analyte-wall interactions. In this case, the tailing is not due to analyte-wall interactions since there was no tailing under CZE conditions.

Self-stacking is similar to isotachophoresis and can occur when the sample zone contains an ion that is not present in the running buffer.[13] The ion's mobility and concentration must be correct for self stacking to occur, however, a concentration that is too high prevents the transition from a CITP regime to a CZE regime. In the present case, a $CN^-$ concentration above 12 mM prevented the transition resulting in poor

resolution whereas no stacking was observed if the CN⁻ concentration fell below 3 mM.

A separation regime based on focusing followed by CZE often provides higher efficiency than CZE alone. When the protein is in the focusing regime, there is no diffusional band broadening due to the self-corrected nature of focusing[14]. Therefore, sample introduction under self-stacking conditions provides higher efficiency than that provided by conventional sample injection. In stacking, the difference in conductivity between the sample and buffer zone causes band broadening, a source of band broadening absent in CZE.

Despite the high plate counts obtained here, the efficiency is still lower than the maximum value predicted by Jorgensen and Lukas. They predicted that plate counts for protein separations would exceed $10^6$ theoretical plates if capillary coatings that eliminate protein-wall interactions were developed.[15] This prediction, which is based on longitudinal diffusion being the major source of band broadening, is used as a benchmark by many authors to gage the quality of capillary coatings. However, this prediction ignores the contribution of protein heterogeneity to bandbroadening. This topic will now be discussed.

Protein heterogeneity as a source of band broadening

Post-translational modifications, such as the glycosylation of ovalbumin, are the main source of protein heterogeneity. Glycosylation is the process where oligosaccharides are attached to a protein. Ovalbumin has two amino acid sites that are glycosylated; several oligosaccharides can be attached to these sites. Therefore,

from the point of view of analytical chemistry, ovalbumin should be viewed as a complex mixture of analytes. An electropherogram of the CZE separation of ovalbumin is given in Figure 5.20. The various peaks correspond to different glycoforms of ovalbumin. If, as is usually the case, ovalbumin is regarded as one analyte, than it is clear than protein heterogeneity is the major source of band broadening.

Another illustration of the effects of protein heterogeneity is the separation of DNA using end-labelled free solution electrophoresis (ELFSE). In this technique, a protein is attached to DNA to enable its separation by CZE. The charge to friction ratio of DNA does not vary with the length of the DNA strand. Therefore, if analyzed by CZE, a strand of DNA 5 bases co-migrates with a strand that is fifty bases long. However, if a friction-generating molecule is attached to the DNA, the mobility increases with length and DNA can be separated by CZE. The separation of DNA by CZE would be superior to traditional size based separation in many respects.[16]

A requirement of the ELFSE technique is that the friction-generating molecule is homogeneous. Therefore, using *E. Coli.* streptavidin, a highly heterogeneous protein, as the friction-generation molecule appears to be an obvious mistake. However, streptavidin was a convenient choice since it binds strongly to biotin-labelled DNA and bears no net charge at neutral pH. Biotin labelled DNA is easily prepared by standard DNA sequencing methods.

The first ELFSE experiments, performed with streptavidin from *E. coli.*, exhibited poor separation efficiency (Figure 5.21). CZE and by MALDI-TOF-MS
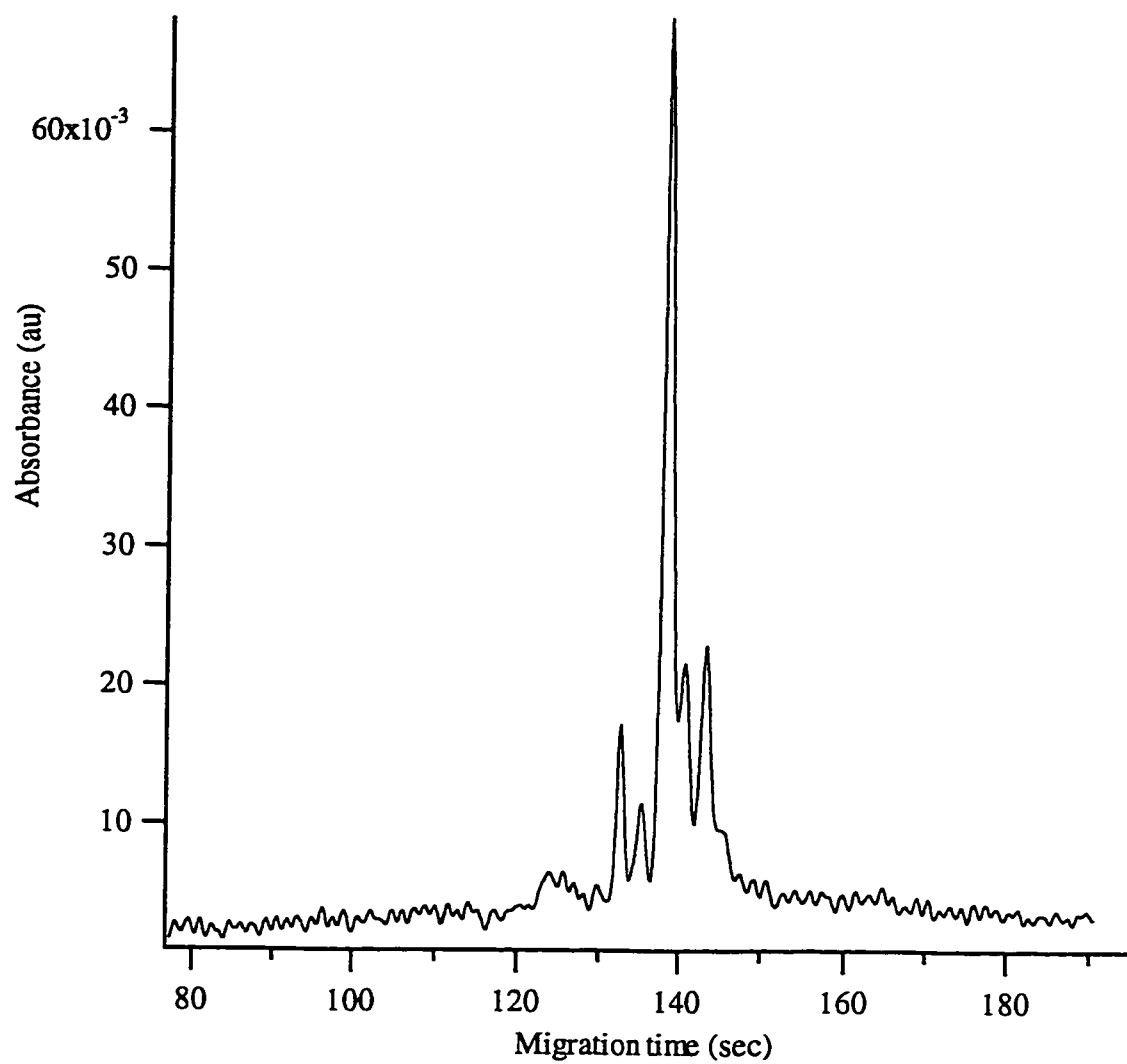
Figure 5.20 - Analysis of unlabelled ovalbumin by CE-UV. Sample 0.1 mM

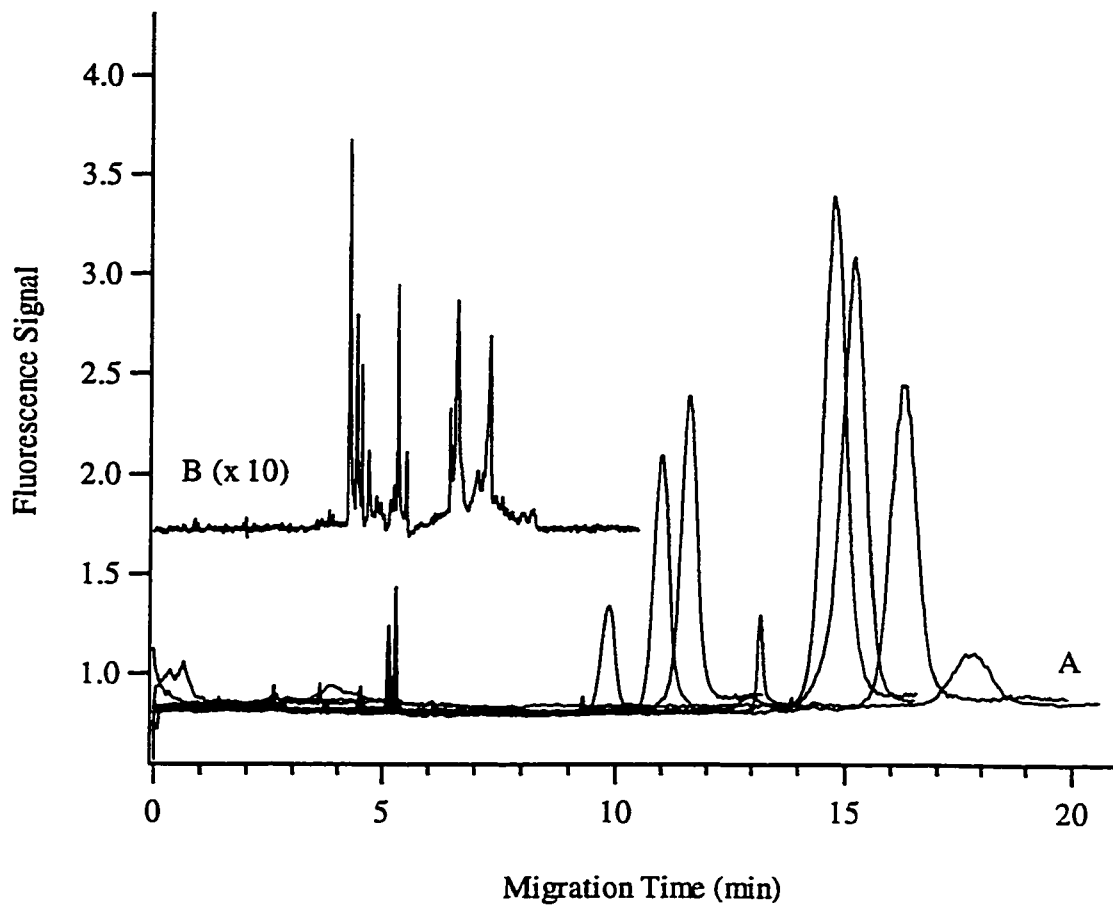ovalbumin, running buffer: 2.5 mM borax, capillary 50 μm x 35 cm (to detector), E =

400 V/cm.

Figure 5.21- ELFSE separation of dsDNA fragments. The friction-generating

molecule used was (A) streptavidin from E. Coli or (B) recombinant streptavidin. The

fragments were injected separately in A. Two unique sets of DNA fragment length

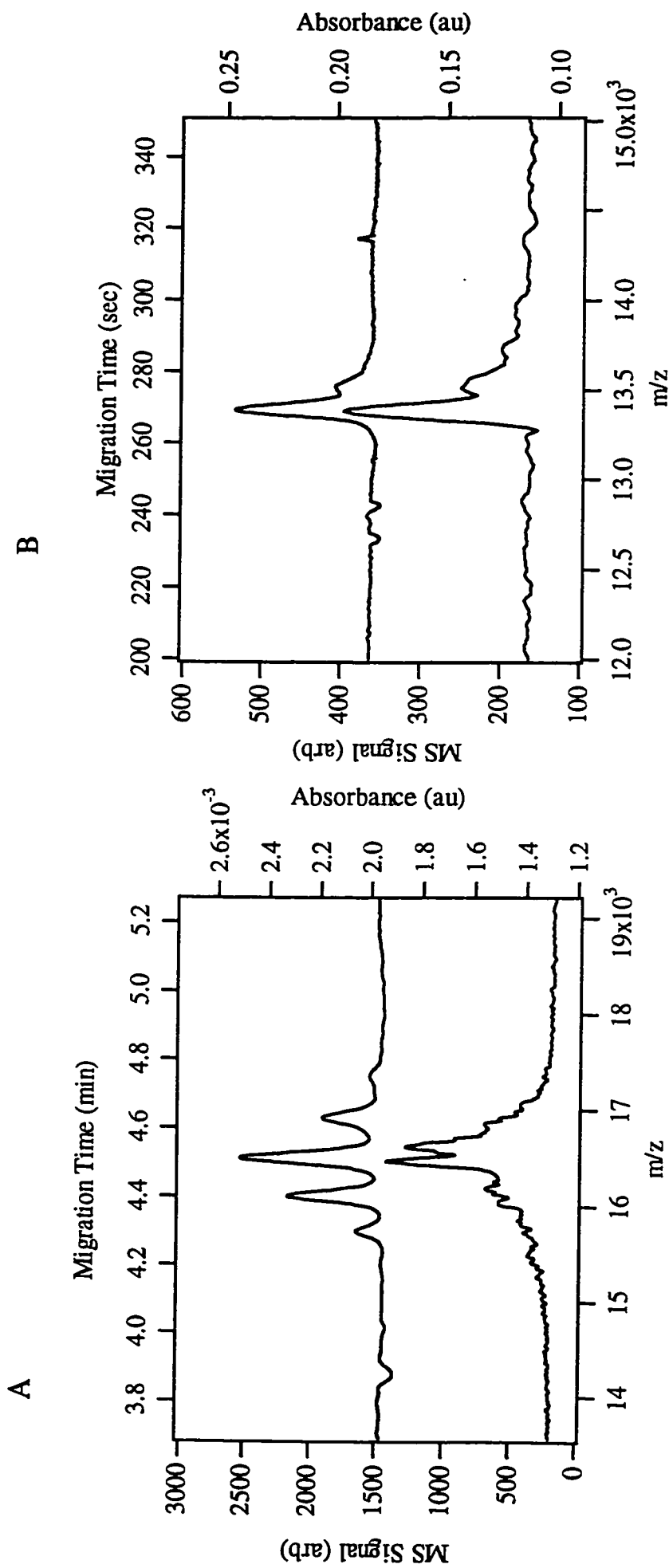were used, however, the range of fragments was 30-500 base pairs in both cases.

Figure 5.22 - Analysis of (A) *E. Coli* streptavidin and (B) recombinant streptavidin. The lower traces are the MALDI-TOF-MS spectra and the upper traces are the CE-UV electropherograms.

166

analysis revealed that the *E. coli* streptavidin is highly heterogeneous (Figure 5.22A). This heterogeneity is the major source of

band broadening in the DNA analysis. Recombinant streptavidin, which is designed to be more homogeneous than the E. coli streptavidin, was used in an effort to improve efficiency. The data in Figure 5.22B shows that this is so. There are still at least two species present in the recombinant streptavidin; however, its use improves the efficiency 20 times.

These examples demonstrate the effects of protein heterogeneity in protein separations. The heterogeneity can be considered as an important source of band broadening. However, this classification is misleading since sources of band broadening are regarded as impediments to efficient separations and, as such, something to be eliminated. Alternatively, protein heterogeneity is a source of valuable information in areas such as protein function, protein folding and the role of proteins in aging.

## 5.4 CONCLUSIONS

The EMMA method presented here is the most sensitive method available for protein analysis by CE. The EMMA method is simple; it used a commercially available fluorogenic reagent, bare fused-silica capillaries and a detection system that is similar to commercially available LIF detectors. EMMA provides higher efficiency, reduced sample handling, and higher sensitivity than pre-capillary labelling method presented in chapter 4. To our knowledge, EMMA labelling followed by CE-LIF is the only CE technique capable of analyzing picomolar levels of proteins.

The use of MALDI-TOF-MS provided insight into the labelling process. Perhaps, the most useful insight is that contrary to popular belief, the heterogeneity of the labelling process does not degrade separation efficiency.

Finally, this chapter demonstrates the variety of factors that contribute to separations efficiency of proteins, a topic that is receiving continued attention.

# References

[1] Bao J.; Regnier, F.E. *J. Chromatogr.* 1992, 608, 217-24.

[2] deFrutos, M.; Paliwal, S.K.; Regnier, F.E. *Anal. Chem.* 1993, 65, 2159-2163.

[3] Harmon, B. J., Patterson, H., Regnier, F. E., *J. Chromatogr. A.*, 1993, 657, 429-434.

[4] Harmon, B. J., Leesong, I., Regnier, F. E., *Anal. Chem.*, 1994, 66, 3797-3805.

[5] Patterson, H. D., Harmon, B. J. Regnier, F. E., *J. Chromatogr. A.*, 1994, 662, 389-395.

[6] Andreev, V. P., Kamenev, A. G., Popov, N. S., *Talanta*, 1996, 43, 909-914.

[7] Hjerten, S. J., *J. Chromatogr.*, 1985, 347, 191-198.

[8] J. P. Foley and J. G. Dorsey, *Anal. Chem.*, 1983, 55, 730.

[9] [Cobb, 1990 #128]

[10] [, 1989-1990 #138]

[11] Lee, T. T.; Yeung, E. S., *J. Chromatogr.*, 1992, 595, 319-325.

[12] Kirkland, J., Yau, W., Stoklosa, H. and Dilks Jr., C., *J. Chromatogr. Sci.*, 1977, 15, 303-315.

[13] Gebauer, P., Thormann, W. and Bocek, P., *J. Chromatogr. A.*, 1992, 608, 47-57.

[14] CRC handbook of Capillary Electrophoresis: A Practical Approach, pp. 113-116.

[15] Jorgensen, J. W. and Lukas, K. D., *Anal. Chem.* 1981, 53, 1298-1302.

[16] Drouin, G., Heller, C., Slater, G., Viovy, J-L, Pinto, D. M. and Dovichi, N. J., *J. Chromatogr. A.*, in press.

# FQ⁻ LABELLING MECHANISM



FQ

RESIDUE

Fluorescent Product
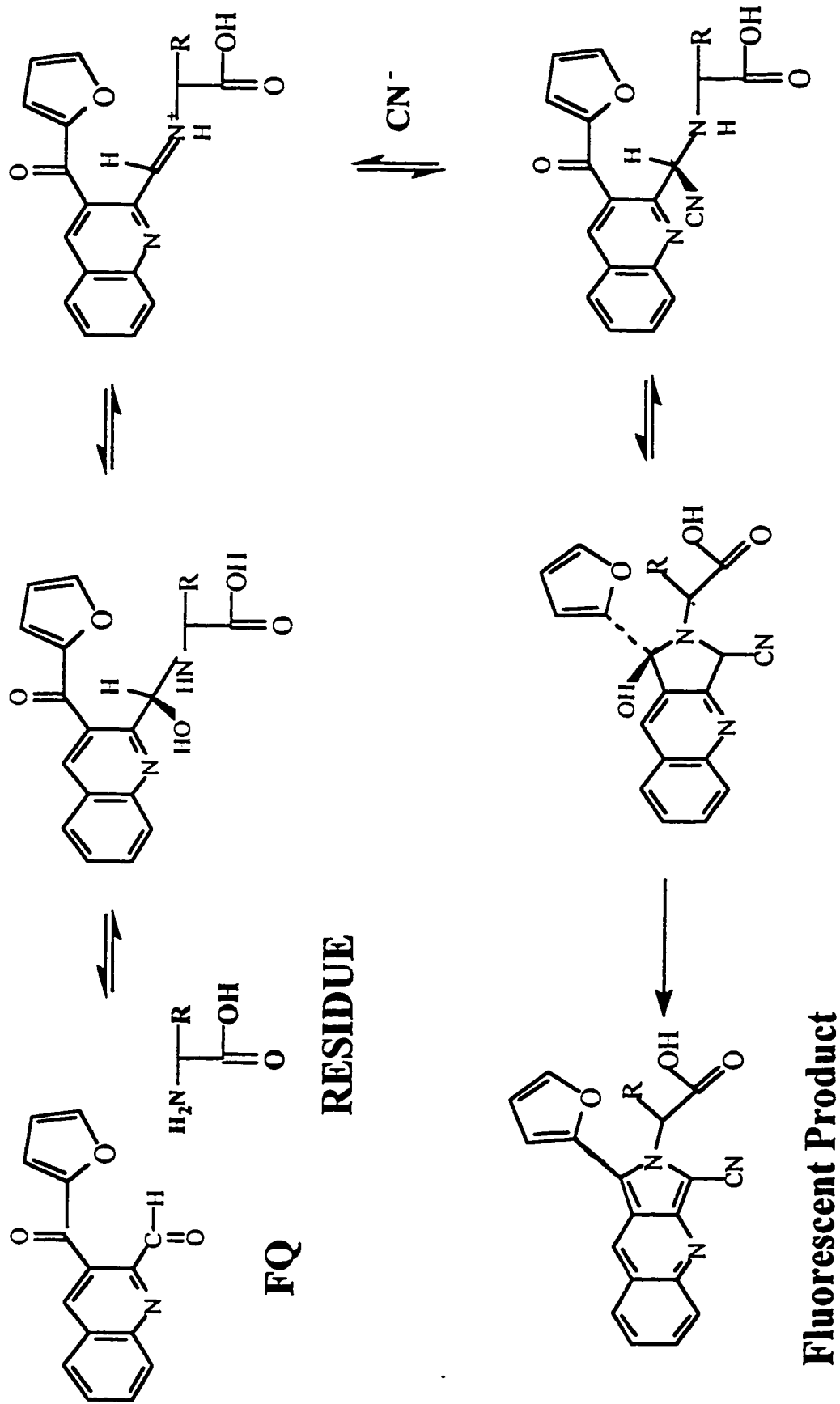
# Appendix 2 - Publications derived from this thesis

Lee, I. H., Pinto, D. M. Arriaga, E. A. and Dovichi, N. J., Electrophoretically mediated microchemical analysis of proteins by capillary electrophoresis with laser-induced fluorescence detection, Anal. Chem., in press.

Heller, C., Viovy, J-L., Slater, G., Dovichi, N. J., Pinto, D. M. and Drouin, G., End-labelled free-solution electrophoresis of DNA, J. Chrom. B., in press.

Pinto, D. M., Arriaga, E. A., Craig, D., Sharma, N., Angelova, J., Boulet, C., Ahmedazedeh, H. and Dovichi, N. J. Picomolar assay of native proteins by capillary electrophoresis – pre-column labelling sub-micellar separations, and laser-induced fluorescence detection, Anal. Chem., 1997, 69(15), 3015-3021.

Pinto, D. M., Arriaga, E. A., Sia, S., and Dovichi, N. J., Solid-phase labelling of picomole amounts of insulin chain B and its analysis by capillary electrophoresis with laser-induced fluorescence detection, Electrophoresis, 1995, 16, 534-540.

Pinto, D. M., Arriaga, E. A., Sia, S., and Dovichi, N. J., Use of a solid phase to label toxins with fluorescent labels and ultrasensitive determination based in capillary-tube electrophoresis with laser-induced fluorescence detection, Ing. Cienc. Quim., 16, 1996, 28-29.

Pinto, D. M., Thibault, P., Bateman, K. P. Locke, S. and Dovichi, N. J., Trace analysis of peptides by solid-phase extraction followed by capillary electrophoresis mass spectrometry, submitted, J. Chrom. B.

Capillary electrophoresis and laser-induced fluorescence in environmental chemistry, Dovichi, N. J., Le, X. C., Arriaga, E. A. and Pinto, D. M., In *Environmental measurement and analysis*, Koizumi, H. ed., pp. 102-104. Japan science and technology corporation, 1997

# IMAGE EVALUATION
## TEST TARGET (QA-3)

150mm

6"
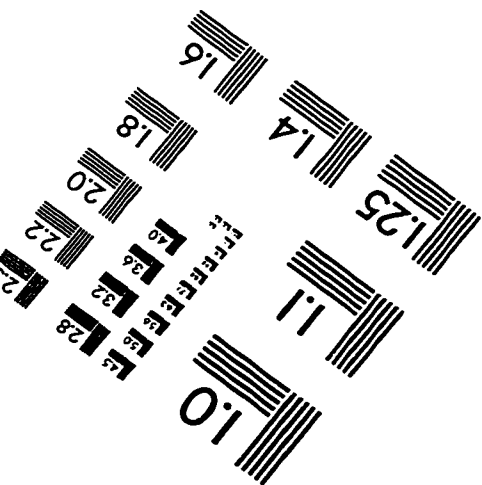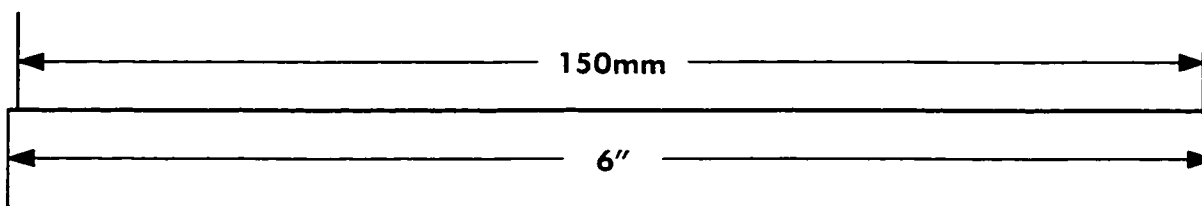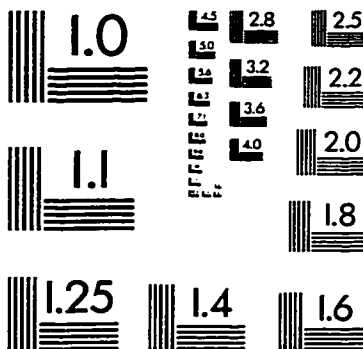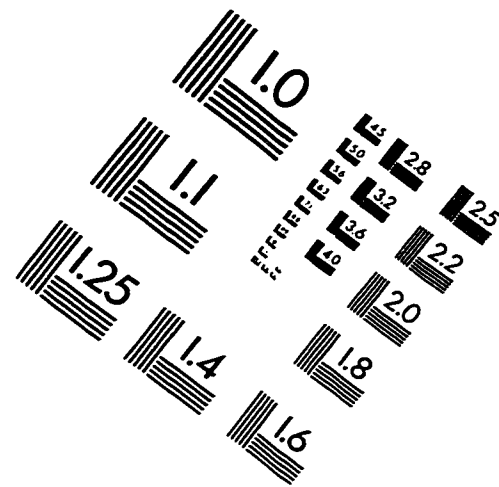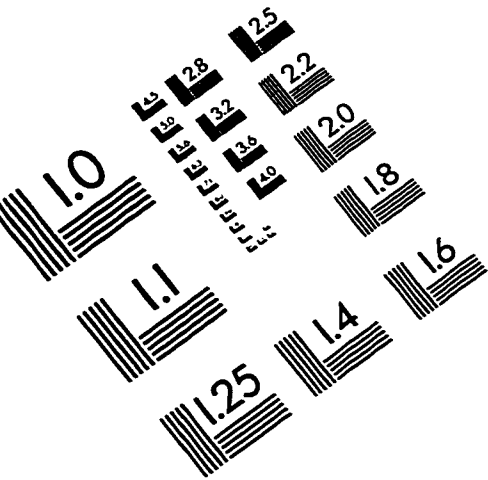
APPLIED IMAGE, Inc
1653 East Main Street
Rochester, NY 14609 USA
Phone: 716/482-0300
Fax: 716/288-5989